R-01-52

Methodology study of Posiva difference flow meter in borehole KLX02 at Laxemar

Jan-Erik Ludvigson, Kent Hansson
Geosigma AB

Pekka Rouhiainen
PRG-Tec Oy

February 2002

Svensk Kärnbränslehantering AB
Swedish Nuclear Fuel
and Waste Management Co
Box 5864
SE-102 40 Stockholm Sweden
Tel 08-459 84 00
+46 8 459 84 00
Fax 08-661 57 19
+46 8 661 57 19

ISSN 1402-3091
SKB Rapport R-01-52

Methodology study of Posiva difference flow meter in borehole KLX02 at Laxemar

Jan-Erik Ludvigson, Kent Hansson
Geosigma AB

Pekka Rouhiainen
PRG-Tec Oy

February 2002

Keywords: Difference flow logging (DIFF), Transmissivity, hydraulic head, flowing fracture, conductive fracture

Foreword

The methodology study of the Posiva Flow Log/Difference Flow Meter in borehole KLX02 is part of a joint venture between SKB and POSIVA. The preparation of this report is a co-operation between GEOSIGMA and PRG-TEC.

In the present report, GEOSIGMA prepared drafts of Chapters 1, 3, 4, part of 5, 8 and 9 while PRG-TEC prepared drafts of Chapters 2, part of 5, 6, 7 and 10. All chapters were then mutually reviewed by both organisations and modified.

After comments from SKB and POSIVA the report was finalised as teamwork. In particular, Section 4.7 and Chapter 7 was updated by PRG-TEC while GEOSIGMA updated Chapters 1 and 3 and prepared Section 8.4 and completed the report with Abstract, Sammanfattning etc. Both organisations reviewed and concluded Chapters 9 and 10.

Finally, the report has been extensively reviewed within the SKB-group for "Hydrogeological methodology studies for PLU".

Abstract and summary

As a co-operative work between SKB and Posiva, the Posiva Flow Log/Difference Flow Meter was tested in borehole KLX02 at Laxemar. Two field campaigns were carried out, Campaign 1 in February–March 2000 and Campaign 2 in May–June 2000. In both Campaigns, the borehole interval 200–1,400 m in borehole KLX02 was measured.

Conventional borehole flow meters measure the cumulative flow along a borehole. However, the <u>changes</u> of flow with depth are generally more interesting and useful. The name "Difference Flow Meter" is due to that the flow meter directly measures these changes of flow along the borehole.

The main measurement methods of difference flow logging are sequential and overlapping flow logging, respectively. In Finland, where the method is developed, the terms normal mode and detailed mode, are used for sequential and overlapping flow logging, respectively. In sequential logging, both the thermal pulse- and thermal dilution methods are used to measure flow, which results in a lower measurement limit of flow. In overlapping flow logging, only the thermal dilution method is used to speed up the measurement but at a higher measurement limit. The faster measurement rate allows for shorter test sections, i.e. a more detailed screening of the flow differences along a borehole.

The first task of Campaign 2 was performing overlapping flow logging along the hole during pumping. The second task of Campaign 2 was to test combined overlapping flow logging together with measurements of the electric conductivity of the water in the fractures. In conjunction with Campaign 2, a special methodology study was made in the interval 200–400 m in KLX02. This interval was chosen to avoid any disturbances of rising, saline water in the borehole which was the case during Campaign 1.

The main purposes of the methodology study were firstly, to investigate the capability of the Posiva Difference Flow Meter to determine the transmissivity and undisturbed freshwater head of the identified flowing fractures. A large number of repeated flow-logging sequences with different measurement methods, section- and step lengths were carried in this borehole interval at different drawdowns in the hole. The aim of the latter measurements was also to propose relevant testing programme for difference flow logging in site investigations.

Most of the measurements in the methodology study were carried out using overlapping flow logging (only thermal dilution) in 0.5-m sections moved in 0.1-m steps for detailed localisation of flowing fractures. Several flow logging sequences were carried out at different drawdowns for comparison (0, 1, 2, 4, 8 and finally at 22 m drawdown). The quality of data obtained from the difference flow logging was regarded as good. The consistency between measured flows at different drawdowns was generally good. Good linearity was also found between the measured flows at the anomalies and the drawdown applied in the hole in most cases.

In total, 59 flowing fractures were interpreted from the difference flow logging in the borehole interval 200–400 m. The number of interpreted flowing fractures increased significantly when the drawdown in the hole was increased from 0 to 1-m. On the other

hand, increased drawdowns between 1–8 m only resulted in a slight increase of the number of interpreted flowing fractures. However, at a drawdown of 22 m, the number of identified flowing fractures decreased. This depends on an increased base-flow level due to a noise appearing in the flow logging at 22-m drawdown, which masked small flow anomalies. The noise did not appear at lower drawdowns.

The source of the noise of the base-flow level is not clear. Possible reasons are gas bubbles in the water at the flowing fractures or drilling debris in the water in the borehole. In addition, another potential source of noise may be due to the significant differences of the chemical and physical composition (e.g. density and viscosity) of waters in fractures and in the borehole. Most depths, at which sharp changes in the base-flow occurred, correspond to high-conductivity fractures with large inflows to the borehole. At most of these depths, crush zones are interpreted in the core logging.

The methodology study has shown that it is possible to determine the transmissivity of interpreted conductive fractures by different combinations (pairs) of data from overlapping flow logging at different drawdowns applied in the hole. Good consistency of calculated transmissivities from different drawdown combinations was generally obtained. In addition, in KLX02, the specific flow rate (Q/s) at each logging sequence was found to be a good estimator of transmissivity. However, this may not be the case in boreholes where large head variations occur along the hole.

This study has also shown that the undisturbed freshwater head of the interpreted conductive fractures also may be calculated from the difference flow logging sequences by using relevant drawdown combinations (pairs). It was found that one of the sequences should be at zero (or small) drawdown to get reliable head values.

A potential uncertainty in the difference flow logging may be leaking rubber discs of the flow tool at very fractured borehole intervals, e.g. fracture zones and in other intervals of bad condition, e.g. cavities. This fact may cause that the recorded flow in such intervals may be significantly underestimated or missed completely. Another potential uncertainty may arise from changing salinity and density conditions along the hole, particularly at pumping. This fact may cause that the hydraulic head conditions along the borehole are significantly changed with time, which will thus affect both the determinations of transmissivity- and undisturbed head.

Finally, the estimated measurement limits and relevant measurement programmes for difference flow logging in site investigations are discussed and proposed both for hydrochemistry-prioritised boreholes and other boreholes.

Sammanfattning

Som ett samarbete mellan SKB och Posiva testades Posivas Differensflödeslogg i borrhål KLX02 på Laxemar. Två fältmätningskampanjer utfördes, kampanj 1 i februari–mars 2000 och kampanj 2 i maj–juni 2000. I båda kampanjerna mättes intervallet 200–1,400 m i KLX02.

Konventionella borrhålsflödesmätare mäter det kumulativa flödet längs ett borrhål. Emellertid är flödets variation mot djupet vanligen mer intressant och användbart. Namnet ”differensflödesmätare” härrör från det faktum att flödesmätaren direkt mäter denna flödesvariation längs borrhålet.

De huvudsakliga mätmetoderna för differensflödesloggning är sekventiell respektive överlappande flödesloggning. I Finland, där metoden utvecklats, används benämningen normal mode och detailed mode för sekventiell respektive överlappande flödesloggning. Vid sekventiell loggning används både termisk puls- och termisk utspädningsmetoderna för att mäta flöde vilket resulterar i en lägre mätgräns. Vid överlappande flödesloggning används bara termisk utspädningsmetoden för att snabba upp mätningarna men till priset av en högre mätgräns. Den snabbare mäthastigheten tillåter kortare testsektioner, dvs. en mer detaljerad kartläggning av flödesändringarna längs borrhålet.

Den första uppgiften i mätkampanj 2 var att utföra överlappande flödesloggning längs hålet under pumpning. Den andra uppgiften i mätkampanj 2 var att testa överlappande flödesloggning i kombination med mätningar av den elektriska ledningsförmågan för vattnet i sprickorna. I samband med kampanj 2 gjordes en speciell metodstudie i intervallet 200–400 m i KLX02. Detta intervall valdes för att undvika störningar av stigande salt vatten i borrhålet vilket var fallet under kampanj 1.

Det huvudsakliga syftet med metodstudien var för det första att undersöka möjligheten av att bestämma transmissiviteten och den ostörda trycknivån i de identifierade flödande sprickorna med Posiva differensflödesmätare. Ett stort antal upprepade mätningar med olika mätmetoder, sektions- och steglängder utfördes i detta borrhålsintervall vid olika avsänkningar i hålet. Syftet med de senare mätningarna var också att föreslå relevanta tekniska mätprogram för differensflödesloggning för platsundersökningar.

De flesta av mätningarna i metodstudien utfördes som överlappande flödesloggning (bara termisk utspädning) i 0.5-m sektioner som förflyttades i 0.1-m steg för detaljerad lokalisering av flödande sprickor. Flera flödesloggningssekvenser utfördes vid olika avsänkningar för jämförelse (0, 1, 2, 4, 8 och 22 m avsänkning). Datakvaliteten som erhölls från differensflödesloggningen bedömdes som bra. Överensstämmelsen mellan mätta flöden och vid olika avsänkningar var vanligen god. God linjäritet befanns också i de flesta fall mellan de mätta flödena vid anomalierna och avsänkningen som applicerades i hålet.

Ett antal av totalt 59 flödande sprickor tolkades från differensflödesloggningen i borrhålsintervallet 200–400 m. Antalet tolkade sprickor ökade avsevärt när avsänkningen i hålet ökades från 0 till 1-m. Å andra sidan resulterade ökade avsänkningar mellan 1–8 m endast i en liten ökning av antalet tolkade flödande sprickor. Vid en avsänkning av 22-m minskade emellertid antalet identifierade flödande sprickor. Detta beror på en ökning av basflödesnivån på grund av ett brus som uppträdde vid flödes-

loggningen vid 22-m avsänkning, vilket maskerade små flödesanomalier. Bruset uppträdde inte vid lägre avsänkningar.

Källan till bruset i basflödesnivån är inte känd. Möjliga orsaker är gasbubblor i vattnet vid de flödande sprickorna eller borrkax i vattnet i borrhålet. En annan möjlig källa till brus kan orsakas av de väsentliga skillnaderna i den kemiska och fysikaliska egenskaperna (t ex densitet och viskositet) av vattnet i sprickor och i borrhålet. De flesta djup, där skarpa ändringar i basflöde inträffade, motsvarar högkonduktiva sprickor med högt inflöde till borrhålet. Vid de flesta av dessa djup har krosszoner tolkats vid kärnkarteringen.

Metodstudien har visat att det är möjligt att bestämma transmissiviteten på tolkade konduktiva sprickor genom olika kombinationer (par) av data från överlappande differensflödesloggning vid olika applicerade avsänkningar i hålet. God överensstämmelse av beräknade transmissiviteter erhölls vanligen för olika avsänkningskombinationer. För övrigt befanns det specifika flödet (Q/s) för varje loggningssekvens vara en god estimator på transmissivitet. Detta behöver emellertid ej vara fallet i borrhål där stora variationer i tryck förekommer längs hålet.

Denna studie har också visat att det ostörda trycket i tolkade konduktiva sprickor också kan beräknas från differensflödesloggning genom att använda loggningssekvenser med relevanta avsänkningskombinationer (par). Det befanns att ett värde i paret bör vara vid ingen (eller liten) avsänkning för att erhålla pålitliga värden på det naturliga trycket.

En potentiell osäkerhet i differensflödesloggningen kan vara läckande gummidiskar vid flödesmätningssonden i mycket uppsprucknа borrhålsintervall, t.ex. sprickzoner och i andra intervall i dåligt skick, t ex kaviteter. Detta kan orsaka att det mätta flödet i sådana intervall kan vara betydligt underskattat eller missas helt. En annan möjlig osäkerhet kan härröra från ändrade salinitets- och densitetsförhållanden längs hålet, speciellt vid pumpning. Detta kan orsaka att tryckförhållandena längs borrhålet ändras väsentligt med tiden, vilket påverkar både bestämningen av transmissivitet och ostört tryck.

Slutligen diskuteras mätgränserna för metoden och relevanta mätprogram för differensflödesloggning för platsundersökningar föreslås, både för hydrokemi-prioriterade borrhål, och övriga borrhål.

Contents

APPENDICES

1 Introduction

1.1 Background

As a co-operative work between SKB and Posiva, the Posiva Flow Log/Difference Flow Meter was tested in KLX02 at Laxemar. Two field campaigns were carried out, Campaign 1 in February–March 2000 and Campaign 2 in May–June 2000. In both Campaigns, the borehole interval 200–1,400 m in KLX02 was measured. The results of both measurement campaigns are reported in Rouhiainen (2000).

The Posiva difference flow meter can be used in several ways. The main measurement modes are sequential and overlapping flow logging, respectively. In Finland, where the method is developed, the term normal mode and detailed mode, respectively are used for the corresponding types of flow logging. In sequential flow logging, both the thermal pulse- and the thermal dilution measurement methods for flow are used, which results in a lower measurement limit for flow. In overlapping flow logging, only the thermal dilution method is used to make the measurement faster but at the price of a higher measurement limit. Sequential flow logging is generally carried out in longer borehole sections whereas overlapping flow logging allows identification of individual flowing fractures within shorter sections, which are successively moved in short steps along the hole.

The main tasks of Campaign 1 were sequential flow logging in 3-m sections together with fresh water head measurements along the hole, both under natural and pumped conditions, respectively. The main task of Campaign 2 was overlapping flow logging during pumping. Furthermore, to investigate if the transmissivity of individual fractures could be determined from the overlapping flow logging in 0.5-m sections moved in 0.1-m steps along the hole. The second task of Campaign 2 was to test combined overlapping flow logging together with measurements of the electric conductivity, both of the borehole fluid and of the water in fractures.

1.2 Objectives

In conjunction with Campaign 2, a special methodology study was carried out in the interval 200–400 m in KLX02. This interval was chosen to avoid disturbances of rising, saline water in the borehole which was the case during Campaign 1. The main purpose of the methodology study was firstly, to investigate the capability of the Posiva Flow Log/Difference Flow Meter to determine the transmissivity and the in situ freshwater head of the identified flowing fractures.

Secondly, a number of repeated measurements with different measurement modes, section- and step lengths and drawdowns were carried in this borehole interval. The aim of the latter measurements was to work out an "optimal" technical testing programme for difference flow logging in site investigations.

Most of the measurements in the methodology study were carried out by overlapping flow logging (only thermal dilution) in 0.5-m sections in 0.1-m steps for detailed identification of flowing fractures. Several overlapping flow logging sequences were carried out with different drawdowns for comparison (0, 1, 2, 4, 8 and finally at 22 m drawdown). In addition, two measurement sequences by sequential logging in 3-m sections were performed for comparison. Finally, a special overlapping logging sequence using both the thermal pulse- and thermal dilution methods for flow measurement was made in the short interval 204–226 m.

The overlapping flow logging at 22-m of drawdown was combined with measurements of the electric conductivity of the water in selected fractures to test the merits of the latter measurements. The measurements of fracture-specific electric conductivity at selected flow anomalies lasted longer than standard flow measurements in order to study the transient behaviour of the former parameter.

The main aims of this report are firstly, to interpret the results of the difference flow logging measurements in the methodology study in the interval 200–400 m and secondly, based on these results, to make implications of the use of difference flow logging in site investigations. Therefore, it was decided to also include selected results from the entire measured borehole interval 200–1,400 m in this study in order to get a complete basis to asses the merits of the Posiva Difference Flow Meter in site investigations.

Chapter 2 presents the measurement principles and the equipment of the Posiva Difference Flow Meter together with calculation of hydraulic parameters. Chapter 3 gives an overview of the flow logging campaigns by the Posiva Flow Meter in KLX02 and the main results. Chapter 4 presents the results of the special methodology study in the interval 200–400 m. Chapter 5 deals with the correlation between flow anomalies and other measured parameters and logs, i.e. Single-Point resistivity, Caliper log and the electrical conductivity of the water. In Chapter 6, a comparison of selected results from Campaign 1 and 2 is made.

Chapter 7 presents the transient measurements of the fracture-specific electrical conductivity of water in fractures while Chapter 8 discusses potential uncertainties of difference flow measurements. Finally, Chapter 9 deals with the design of relevant measurement programs for difference flow logging in site investigations. The conclusions of the methodology study in KLX02 are presented in Chapter 10.

2 Description of the Posiva Flow Log/Difference Flow Meter

2.1 Measurement principles and equipment

Posiva Flow Log consists of a Transverse Flow Meter (TRANS) and a Difference Flow Meter (DIFF). Only the Difference Flow Meter is discussed in this report.

The ordinary borehole flow meters measure flow along a borehole. However, the changes of flow with depth are generally useful, not the flow along the borehole itself. The name "Difference Flow Meter" comes from the fact that this flow meter measures directly differences of flow along the borehole. These differences of flow are flows from the bedrock into the borehole or flows from the borehole into the bedrock.

With the flow guide, the flow into or out from the borehole in the test section is the only flow that passes through the flow sensor. Flow along the borehole outside the test section is directed so that it does not come into contact with the flow sensor. Instead of inflatable packers, rubber disks are used at both ends of the test section for separating the section from the remainder of the borehole. These disks guide the flow to be measured, see Figure 2-1 and Figure 2-2.

There are four rubber disks at the upper end of the section. Six rubber disks are normally used at the lower end of the section. The distance between rubber disks is about 4 cm for the four uppermost rubber disks and about 6 cm for the two lowermost ones. Centralisers are used to keep the tool and rubber disks in the middle of the borehole.

The difference in head over the rubber disks used in the flow guide is small since the tube connecting the section through the flow sensor to the rest of the borehole is open. The rubber disks are designed in such a way that they are always pressed against the borehole wall. Difference flow measurements differ from the conventional double packer tests in that there is no extra hydraulic pressure in the borehole section being measured. This means that there is also minimal pressure change in the section when the tool is moved from one position to another.

2.2 Measurement methods and parameters

The Posiva difference flow meter can be used in several ways. In standard measurements the following parameters can be measured:

- Flow rate by the thermal pulse method.
- Flow rate by the thermal dilution method.
- Temperature of borehole water.

- Electric conductivity of borehole- and fracture-specific water.
- Single point resistance of borehole wall.
- Depth of the probe based on the cable counter and cable marks.

The fresh water head is measured separately if there is saline water in the borehole and the undisturbed hydraulic head and hydraulic conductivity may be evaluated.

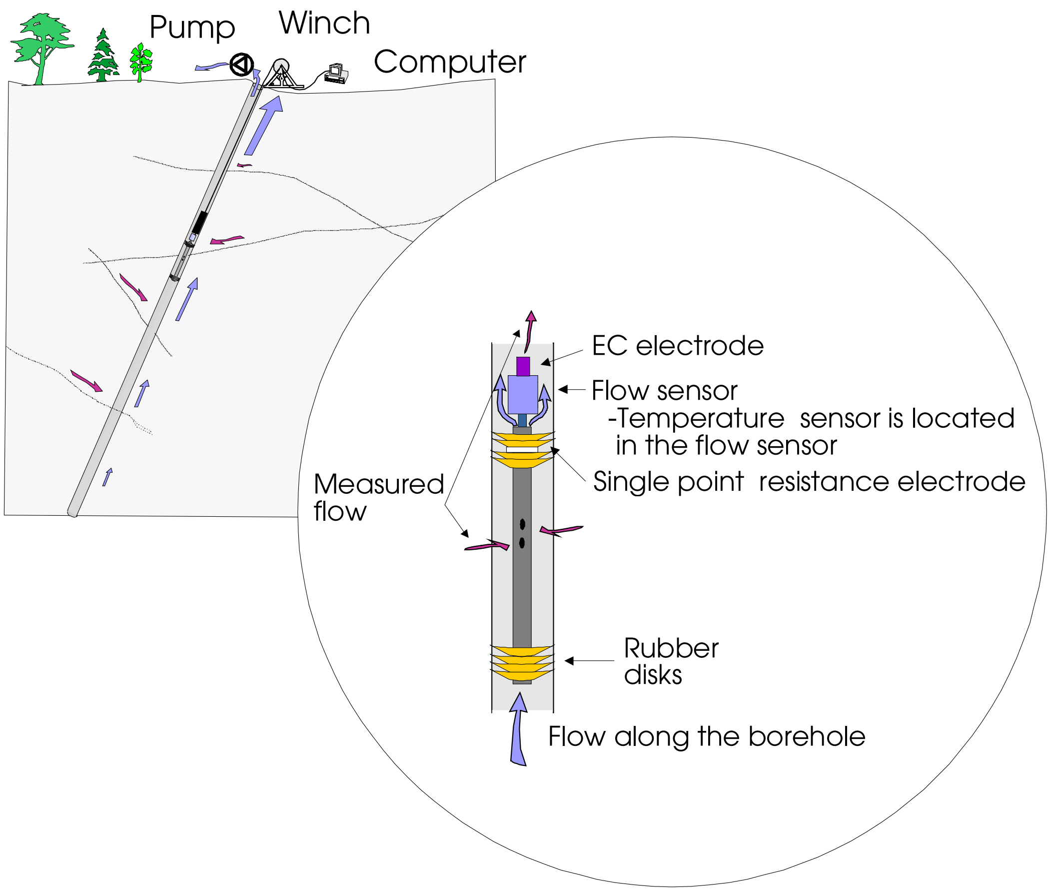

Figure 2-1. *Schematic of the down-hole equipment used in the Posiva difference flow meter.*

2.2.1 Flow logging methods

At present, two different logging methods are most frequently used, i.e. sequential and overlapping flow logging, respectively. In Finland, where the method is developed, the term normal mode and detailed mode, respectively are used for the corresponding flow logging methods. Both types of flow logging can be performed with only one, or two (or more) logging sequences at different drawdowns depending on the purpose of the logging.

Figure 2-2. *The Posiva difference flow meter. A spiral structure is installed within the yellow rubber disks.*

In sequential flow logging, both the thermal pulse- and thermal dilution flow measurement techniques are used resulting in a wide flow measurement range, see below. Sequential flow logging is mainly used for determination of the hydraulic conductivity and undisturbed freshwater head in borehole sections, which require two flow logging sequences at different head conditions in the borehole. Sequential flow logging may also be used for measurements of the natural flow conditions in sections along the hole. In overlapping flow logging, only the thermal dilution method for flow measurements is used to make the measurement faster. Therefore, the depth increments between measurements are usually small in overlapping flow logging which results in a more detailed flow characterisation along the hole. Standard overlapping flow logging is performed with only one logging sequence at pumped conditions.

Previous campaigns with overlapping flow logging, both in Finland and Sweden, have mainly been focussed in locating conductive flowing fractures in short sections, moved stepwise along the hole from only one logging sequence. However, this procedure does not allow estimation of the hydraulic conductivity or the natural head along the hole. As discussed above, the main task of the methodology study was to investigate the possibility of estimating the transmissivity and natural hydraulic head from overlapping flow logging using two (or more) logging sequences at different head conditions in the borehole. The temperature and single point resistance along the hole is also measured during both logging methods.

A single flow measurement in sequential flow logging at one depth interval normally lasts about 12 minutes. This time period includes (i) waiting time for temperature stabilisation, (ii) a flow measurement by the thermal pulse method (measuring range for flow rate is normally 0.1–10 ml/min with this method), (iii) a flow measurement by the thermal dilution method (measuring range for flow rate is 2–5,000 ml/min) and finally, (iv) lifting of the tool to the next depth interval.

In overlapping flow logging, only the thermal dilution method is used for flow measurements. A single flow measurement in overlapping logging at one depth interval normally takes about 30 seconds. The measuring range for flow rate is normally 2–5,000 ml/min. The results are used to determine the exact location of hydraulically conductive fractures and to classify them by flow rate. The section length (the distance between upper and lower rubber disks) and depth increment (the distance between flow measurements) can be varied in both sequential and overlapping logging.

2.2.2 Single-point resistance

The single point resistance measurement (grounding resistance) is another measurement parameter in the Posiva Flow Log. This parameter is always measured during difference flow logging, both sequential and overlapping logging. The electrode of the single point resistance tool is located between the upper rubber disks, see Figures 2-1. This sensitive method is used for exact depth determination of fractures and geological structures.

2.2.3 Fresh water head along the borehole

Density of saline water is higher than density of fresh water. Therefore, the fresh water head in the borehole had to be measured in such cases as in borehole KLX02. In the cases of saline water, the term fresh water head is used instead of hydraulic head, since hydraulic head is not well defined in saline conditions.

Fresh water head in KLX02 was measured with a long tube filled with fresh water. There is a special valve at the lower end of the tube. The valve is opened after it is lowered to the bottom of the borehole. The tube is then permanently open at the both ends. Within a few hours the temperature profile along the tube will be nearly the same as the temperature profile along the borehole. This condition remains even when the tube is lifted. When the tube is lifted the corresponding amount of water is emptied from the lower end of the tube. Therefore the depth position of the water molecules in the tube remains about the same.

The depth of a measurement is the depth of the lower end of the tube. Fresh water head is then the water level in the tube above a reference level. The reference level is usually the initial groundwater level in the borehole. The reference level is chosen in the beginning of the measurements and it is constant though the actual groundwater level in the borehole may vary. The groundwater level in the borehole and the water level in the tube are measured by an electrical water level indicator. The tube must be cut for each water level measurement.

It is important that the temperature profile within the tube is close to the temperature profile in the borehole. It may need more study to define when this condition is met. It could be studied in a fresh-water filled borehole where water levels in the tube and in the boreholes should be the same.

Fresh water head in borehole KLX02 was measured twice without pumping. In both cases the water level in the tube was nearly the same (within 20 cm) as the water level in the borehole at depths less than 1160 m. This fact suggests that the temperature profiles in the tube and in the borehole were close to each other. However, this was not a complete proof of it.

The fresh water head described above does not give absolute pressure values since density variations of fresh water in the tube are not taken into account. Density of fresh water is 1 g/cm3 at 4 °C and smaller when temperature is higher. Compressibility of water increases density of water with depth. Density profile along the tube could be calculated and the absolute pressure at the depth of measurement may then be evaluated.

The calculated undisturbed heads of formations and fractures (described later) are not presented in absolute pressure values since they are derived from the measured fresh water head in the borehole and the measured flow values.

2.2.4 Electric conductivity and temperature of borehole- and fracture specific water

The electric conductivity (EC) of groundwater can optionally be measured alone or during the flow measurements. The EC electrode is attached on the top of the flow sensor, see Figure 2-1. EC- and temperature of the borehole water can be measured using the tool without the flow guide. EC- and temperature measurements of the borehole water in long sections may be non-representative due to insufficient exchange of the borehole water contained in the sections.

The flow guide is used for the measurement of electric conductivity of fracture-specific water. The borehole is pumped so that the flow direction is always from the fractures into the borehole. Both electric conductivity and temperature of flowing water from the fractures are measured.

The simultaneous flow measurement makes it possible to select the fractures for the EC measurement. The tool is moved so that the fracture to be tested will be located within the test section. EC measurements are performed if the flow rate in a certain fracture is larger than a predetermined limit.

The tool is kept on the selected fracture. The measurement is continued at the given depth allowing the fracture-specific water to enter the section. The waiting time for the EC measurement is automatically calculated from the measured flow rate. The aim is to flush the water volume within the test section well enough. The measuring computer is programmed to change the water volume (0.5 l) three times within the 0.5-m long test section. A special spiral structure in the section is used to improve flushing. The spiral is a rubber sealing within the section. It guides the intruding water to move as band flow within the section thus improving flushing.

All the phases of the measurement can be carried out automatically controlled by the logging computer (Rouhiainen and Pöllänen 1998).

2.3 Determination and calibration of flow

Three thermistors are immersed in the flow tube in the flow sensor. The centre thermistor can be used for heating, the other two thermistors are located symmetrically on the both sides of the heating thermistor. These two monitoring thermistors are used to measure the temperature increase caused by the heating thermistor. The heating thermistor can also measure its own temperature, both when heating is on and when it is off.

When thermal pulse method is applied a short thermal pulse is inserted into water with the heating thermistor. The energy of the thermal pulse must be kept low not to create flow because of heating. The heat pulse in water can move by thermal diffusion and by convection. Thermal diffusion is always present, it tends to spread out the thermal pulse to both directions in the tube. If there is no flow in the tube there will be a symmetrical temperature response in the monitoring thermistors and temperature difference between the monitoring thermistors is zero.

If water is moving in the tube heat is moving by convection along with the flowing water and simultaneously spreading out by thermal diffusion. The “downstream” thermistor will see a thermal pulse and the response of the “upstream” thermistor is flat. The transfer time of the thermal pulse is a function of the flow rate.

The heating thermistor is used when flow is measured by thermal dilution method. The thermistor is heated with constant power and its temperature will rise. Flowing water has higher cooling power than stagnant water. The increase of temperature of the heating thermistor is inversely proportional to flow rate. At present, the monitoring thermistors are only used for determination of flow direction when thermal dilution method is used.

The thermal pulse and thermal dilution methods have to be calibrated by known flow rates. The flow rates are measured by weight scale. The points obtained by calibration are plotted on the scale where y-axis is flow rate and x-axis is transfer time (thermal pulse) or increase of temperature (thermal dilution). A calibration function is fitted to these points. In both cases these functions are the form of:

$$Y = a \cdot \exp(-b \cdot X) + c \cdot \exp(-d \cdot X) + e \cdot \exp(-f \cdot X) + .. , \qquad (2\text{-}1)$$

where

X is transfer time (thermal pulse) or increase of temperature (thermal dilution)
Y is flow rate
a, b, c … are chosen for the best fit to the calibration points.

The calibration function of each tool is recorded in a calibration file containing all other calibration results (cable, EC and temperature calibration). The name of the calibration file contains the date of calibration and the identification number of flow meter being calibrated. The interpretation software reads this calibration file until a new calibration file is created.

2.4 Length calibration along borehole

The length of the cable along the borehole is measured by both a cable counter and from depth marks (tapes) on the cable. The depth marks are attached on the cable with 50-m intervals. The marks are detected by an optical sensor at the winch. The logging computer reads the data from the cable counter and optical sensor.

The cable counter is used for the depth determination between the depth marks. If there is a discrepancy between the two methods, it is assumed that the error is in the cable counter and the depth readings from the counter are corrected between the tape marks by linear interpolation. If the discrepancy between the two methods is higher than a predetermined limit the measurement is stopped for checking the tool.

The cable is calibrated (the points of the cable marks checked) once a year on an even road where there are accurate pre-measured distance labels. The cable tension is measured during the calibration because the length of the cable depends on its tension. There is a cable tension meter at the winch. A weight scale is also used at the cable head for the tension measurement. However, the actual cable tension between these end points is not well controlled since there is friction on the road between these points. The tension is chosen simply by pulling the cable from the cable head. It has been noticed experimentally that the best calibration can be achieved when the cable is pulled by the force that corresponds a weight of about 80 kg.

The cable tension varies between boreholes of different inclination, depth to water and the density of the water. Therefore the measured depth is not exact. As a consequence, there is always some depth shift between various borehole-logging methods such as Caliper and borehole TV. The single point resistance tool of the flow meter can be used for depth correlation between the methods mentioned.

If the borehole is marked by depth marks (SKB-standard) they can, in most cases, be detected by single point resistance measurements carried out simultaneously with the flow measurements. Therefore the depth calibration described above can be adjusted to each depth-marked borehole.

2.5 Calculation of hydraulic parameters

If measurements are carried out using two levels of potential in the borehole, then the undisturbed head in each of the sections and their hydraulic conductivity can be calculated. It is assumed that a static flow condition exists.

$$Q_{n1} = K_n \cdot a \cdot (h_0 - h_1) \qquad 2\text{-}2$$

$$Q_{n2} = K_n \cdot a \cdot (h_0 - h_2) \qquad 2\text{-}3$$

where

Q_{n1} and Q_{n2} are the measured flows in a section,
K_n is hydraulic conductivity,
a is a constant depending on the flow geometry,
h_1 and h_2 are the hydraulic heads in the hole
h_0 is the undisturbed (natural) hydraulic head of the measured feature far from the hole

Since, in general, very little is known of the flow geometry, cylindrical flow without skin zones is assumed. Cylindrical flow geometry is also justified because the borehole is at a constant hydraulic head and there are no strong pressure gradients along the borehole, except at the ends of the borehole. For cylindrical flow, constant a is:

$$a = 2 \cdot \pi \cdot L / \ln(R/r_0) \qquad 2\text{-}4$$

where

L is the length of the measured section,
R is the distance to constant potential h_0 and
r_0 is the radius of the hole.

The distance to constant head h_0 is not known and it must be estimated. Here R/r_0 is chosen to be 500. The undisturbed hydraulic head and -conductivity can be deduced from the two measurements:

$$h_0 = (h_1 - b \cdot h_2)/(1-b) \qquad 2\text{-}5$$

$$K_n = (1/a) \cdot (Q_{n1} - Q_{n2}) / (h_2 - h_1) \qquad 2\text{-}6$$

where $b = Q_{n1}/Q_{n2}$

Since the actual flow geometry is not known, calculated hydraulic conductivity values should be taken as indicating orders of magnitude. As the calculated undisturbed hydraulic heads do not depend on geometrical properties but only on the ratio of the flows measured at different hydraulic heads in the borehole they should be less sensitive to unknown fracture geometry (Rouhiainen and Pöllänen 1998).

If the density of the groundwater varies along the borehole, e.g. during pumping, the freshwater head profile along the hole must be measured. From this head profile the actual pressure differences at depth should then be determined and used in Eqns. (2-5) and (2-6) to calculate and the hydraulic conductivity and undisturbed hydraulic head, respectively.

3 Overview of Posiva flow logging in KLX02

3.1 Measurement campaigns

The field operations of the difference flow logging in KLX02 were carried out in two campaigns. The main tasks in Campaign 1 were the sequential flow logging and fresh-water head measurements, both when the borehole was in its natural state (not pumped) and when the borehole was pumped. The section length and the depth increment (step) in the sequential flow logging were both 3 metres. The pumping rate was smaller in the upper part of the borehole (200–400 m) where hydraulic conductivity was assumed to be high.

One of the tasks of the methodology study in Campaign 2 was to test whether overlapping flow logging could be used for determination of transmissivity of individual fractures. The overlapping flow logging utilises only the thermal dilution flow measurement technique. In addition, the thermal dilution method was developed in such a way that it could measure flow direction in addition to flow rate. A special overlapping flow logging sequence using both the thermal dilution and -pulse flow measuring techniques was also performed during the methodology study. Another task in Campaign 2 was the combined electric conductivity of fracture-specific water (EC) measurement and overlapping flow logging between 200 m and 1,400 m.

The measurement programs of the difference flow logging during Campaign 1 and 2 are shown in Table 3-1 and 3-2, respectively.

Table 3-1. Compilation of field works in Campaign 1 of the difference flow logging in KLX02. (After Rouhiainen (2000).

Date	Description
2000-02-04	Installation
2000-02-05 to 2000-02-10	Sequential flow logging 200–1,400 m without pumping
2000-02-11 to 2000-02-12	Fresh water head measurements 200–1,400 m without pumping
2000-02-13 to 2000-02-14	Pumping the borehole at 6.2 m drawdown (about 20 l/min)
2000-02-15	Fresh water head measurements 200–400 m at 6.2 m drawdown
2000-02-16	Sequential flow logging 200–400 m at 6.2 m drawdown
2000-02-17	Preparation for fresh water head measurements at 1,400 m
2000-02-18 to 2000-02-20	Fresh water head transient measurements at 1,400 m at 22 m drawdown
2000-02-21 to 2000-02-22	Fresh water head measurements 400–1,400 m at 22 m drawdown
2000-02-23 to 2000-02-25	Sequential flow logging 400–1,400 m at 22 m drawdown
2000-02-26	Checking results, overlapping logging (L=3 m, step 0.5 m) at 22 m drawdown
2000-02-27	Checking results, sequential flow logging at 22 m drawdown
2000-02-28 to 2000-02-29	Fresh water head measurements 400–1,400 m at 22 m drawdown
2000-03-01	Unpacking

Table 3-2. Compilation of field works in Campaign 2 of the difference flow logging in borehole KLX02. (After Rouhiainen (2000).

Date	Description
2000-05-26	Installation
2000-05-27	Sequential flow logging (L=3 m) 200–400 m without pumping
2000-05-28	Overlapping flow logging (L=3 m, step 0.5 m) 200–400 m without pumping
2000-05-29	Overlapping flow logging (L=0.5 m, step 0.1 m) 200–400 m without pumping
2000-05-30	Overlapping flow logging with thermal pulse (L=0.5 m, step 0.1 m) 205–226 m without pumping
2000-05-31	Beginning of pumping the borehole at 1.0 m drawdown
2000-06-01	Overlapping flow logging (L=0.5 m, step 0.1 m) 200–400 m at 1.0 m drawdown
2000-06-02	Overlapping flow logging (L=0.5 m, step 0.1 m) 200–400 m at 2.0 m drawdown
2000-06-03	Overlapping flow logging (L=0.5 m, step 0.1 m) 200–400 m at 4.0 m drawdown
2000-06-04	Overlapping flow logging with thermal pulse (L=0.5 m, step 0.1 m) 205–226 m at 8.0 m drawdown
2000-06-05	Overlapping flow logging (L=0.5 m, step 0.1 m) 200–400 m at 8.0 m drawdown
2000-06-06	Sequential flow logging (L=3 m) 200–400 m at 8.0 m drawdown
2000-06-07	Overlapping flow logging (L=3 m, step 0.5 m) 200–400 m at 8.0 m drawdown
2000-06-08	Beginning of pumping the borehole at 22 m drawdown
2000-06-09 to 2000-06-10	Pumping the borehole at 22 m drawdown
2000-06-11 to 2000-06-16	Combined EC/Overlapping flow logging 200–1,400 m at 22 m drawdown
2000-06-17	Extra fracture specific EC-measurements
2000-06-18	Extra fracture specific EC-measurements, Unpacking

3.2 General flow characterisation of KLX02

The general flow conditions along borehole KLX02 were interpreted from the difference flow logging during Campaign 1. The measured flows along the hole with and without pumping the hole, respectively are presented in Appendix 3 in Rouhiainen (2000) and the estimated freshwater head conditions along the hole in Appendix 4 in the same reference. The measurements indicated outflow conditions from the borehole to the bedrock along the entire measured interval between 200–1,400 m. It is assumed that inflow occurs at the lower end at the casing at c. 200-m.

In addition, some simple water balance studies were made based on the measured flow along the hole in Campaign 1, see Table 3-3. The table indicates that under natural conditions, the inflow at the casing at c. 200-m is balanced by the same outflow in the borehole interval 200–1,400 m. During pumping with c. 55 l/min a significant inflow (c. 18 l/min) occurs at the casing while the remaining inflow (c. 37 l/min) comes from c. 200 m to the bottom of the hole. Of the latter flow, the major part comes from the interval 200–400 m (c. 95%) whereas only a very minor part (c. 0.1 l/min) is estimated to come from the borehole interval below 1,400 m, based on water balance calculations of the salinity distribution along the hole.

Table 3-3. Measured and estimated inflows and outflows in certain intervals of KLX02 at different drawdown conditions. (s=drawdown).

KLX02	**MEASURED/ESTIMATED INFLOWS TO DIFFERENT BOREHOLE INTERVALS (l/min)**			
Interval (m)	**Measured at natural cond's (Q=0)**	**Measured at Q=20 l/min** (s=6.2 m)	**Measured at Q=55 l/min** (s=20.2 m)	**Estimated at Q=55 l/min** (s=20.2 m)
At casing bottom at c. 200 m	1.2 (inflow)			18.4
200 m-bottom				36.6
200–1,400	–1.2 (outflow)			
200–400		10.5		34.6
400–1,400			1.9	
200–1,400				36.5
Below 1,400				0.1

3.3 Interpretation of flow anomalies

Different sequences of flow logging were performed in the borehole interval 200–400 m in 0.5-m sections and step length 0.1-m as part of the methodology study in KLX02. More exactly, the measurements start at c. 204 m and stop at c. 406 m. Furthermore, overlapping flow logging in 0.5 –m sections was performed in the entire interval 200–1,400 m. All depths are given with "top of casing" as reference level. The quality of the data from the flow logging is regarded as good. The locations of the interpreted flowing fractures in the borehole interval 200–400 m together with the flow rates at different drawdown are presented in Appendix 13 in Rouhiainen (2000), (Appendix 1 in this report). The corresponding results in the remainder of the hole are presented in Appendix 18 in Rouhiainen (2000).

In the plots in Appendix 13 and 18 in Rouhiainen (2000), a long line represents the depth of an interpreted ("certain") flowing fracture whereas a short line indicates that the existence of the fracture is uncertain. The flow rates were measured at several drawdowns. The measurement range for overlapping flow logging is from 2 ml/min (120 ml/h) to 5,000 ml/min (300,000 ml/h). Measured flows below 2 ml/min (120 ml/h) are uncalibrated and qualitative. Furthermore, the measured single point resistance log and the previous caliper log are also presented in Appendix 13 and 18 in Rouhiainen (2000).

The vertical length of a plotted flow anomaly of a single fracture corresponds to the section length in the flow plots. Flow from a fracture is measured as long as the fracture stays within the section. Therefore the minimum length of a plotted flow anomaly is the section length minus the step length used, i.e. in this case 0.4 m. By convention, the flowing fracture is always located at the lower boundary of the anomaly in the plots (Rouhiainen 2000). If the distance between flowing fractures is less than the section length the anomalies will be overlapped, i.e. the flows from several fractures within the section are summed up as long as they stay within the section. Flowing fractures near each other can better be resolved with a short section length.

The minimum length of flow anomalies is an important fact when possible leaks of rubber disks are studied. Shorter plotted anomalies than 0.4 m cannot be real when a step length of 0.5 m is used. For example, the apparent flow anomalies between 219–220 m are probably caused by leaking rubber disks, see Appendix 13 in Rouhiainen (2000). No flowing fractures were interpreted here. The flow data from the overlapping flow logging with 22-m drawdown are affected by a noise, which causes an increased (changing) base-flow level. Possible reasons to this fact are discussed in Section 8.2.

During the overlapping flow logging in the methodology study in the interval 200–400 m in KLX02, only very small effects of rise of saline water in the borehole were noticed from the EC-loggings of borehole water before and after the measurements. Thus, the density was assumed to be constant in this borehole interval. However, at the logging with a drawdown of 22-m the salinity increased in this interval. At larger depths saline water was present in the borehole, c.f. Appendix 19 in Rouhiainen (2000). This item will be discussed in more detail in Section 8-3.

The interpreted flow anomalies in the borehole interval 200–400 m according to Appendix 1 in this report (Appendix 13 in Rouhiainen 2000) together with the depths at which the noise level changed abruptly are listed in Table 3-4. For some of the fractures, no flow was detected at 22-m drawdown, because they were covered by the increased noise of the base-flow level. Small fractures, which are considered as very uncertain, are within brackets in Table 3.4. On the other hand, one additional potential flowing fracture is included at depth c. 385.4 m since the base-flow level changed significantly at this depth, see below.

Table 3-4. Depth, flow rate and transmissivity of interpreted flowing fractures together with depths with major changes of the base-flow level (in bold) in the overlapping flow logging in Campaign 2 in the borehole interval 200–400 m. Flowing fractures within brackets are below the measurement limit and thus uncertain. After Rouhiainen (2000).

Depth (m)	Q (s=22m) (ml/h)	T(0–22m) (m2/s)	Baseflow (ml/h)	Depth (m)	Q (s=22m) (ml/h)	T(0–22m) (m2/s)	Baseflow (ml/h)
212.0	2964	$3.6 \cdot 10^{-8}$		268.0	16905	$2.1 \cdot 10^{-7}$	
213.3	158662	$1.9 \cdot 10^{-6}$		269.0	213	$2.5 \cdot 10^{-9}$	
214.0	16757	$2.0 \cdot 10^{-7}$		269.7	7977	$9.7 \cdot 10^{-8}$	
215.2	5031	$6.1 \cdot 10^{-8}$		271.1	36168	$4.4 \cdot 10^{-7}$	
216.7	302	$3.6 \cdot 10^{-9}$		273.8	715	$8.5 \cdot 10^{-9}$	
220.7	572	$6.8 \cdot 10^{-9}$		(275.0	0	–)	
224.4	12542	$1.5 \cdot 10^{-7}$		276.9	462	$5.5 \cdot 10^{-9}$	
224.9	1823	$2.2 \cdot 10^{-8}$		290.5	796	$9.5 \cdot 10^{-9}$	
226.0	6625	$7.9 \cdot 10^{-8}$		292.6	219	$2.6 \cdot 10^{-9}$	
227.7	30680	$3.7 \cdot 10^{-7}$		295.1	30324	$3.6 \cdot 10^{-7}$	
231.9	778	$9.2 \cdot 10^{-9}$		295.6	4393	$5.2 \cdot 10^{-8}$	
232.4	38	–		298.3	698	$8.3 \cdot 10^{-9}$	
233.9	5337	$6.4 \cdot 10^{-8}$		300.6	801	$9.5 \cdot 10^{-9}$	
234.2	166	$2.0 \cdot 10^{-9}$		(307.9	0	–)	
237.8	359	$4.3 \cdot 10^{-9}$		(310.5	0	–)	
238.0	86	–		(314.7	0	–)	
239.1	604	$7.2 \cdot 10^{-9}$		**317.1**	**452519**	**$5.5 \cdot 10^{-6}$**	**100→300**
241.4	990	$1.2 \cdot 10^{-8}$		(325.4	0	–)	
242.3	121	–		(327.8	0	–)	
243.3	2870	$3.5 \cdot 10^{-8}$		(328.6	0	–)	
243.8	714	$8.5 \cdot 10^{-9}$		(329.2	0	–)	
244.9	733	$8.7 \cdot 10^{-9}$		(332.7	0	–)	
246.7	22150	$2.7 \cdot 10^{-7}$		337.9	9576	$1.2 \cdot 10^{7}$	
248.6	15479	$1.9 \cdot 10^{-7}$		338.9	12983	$1.7 \cdot 10^{-7}$	
249.2	1623	$2.0 \cdot 10^{-8}$		**339.1**	**34185**	**$4.2 \cdot 10^{-7}$**	**300→500**
250.1	578	$6.9 \cdot 10^{-9}$		339.6	7170	$1.0 \cdot 10^{-8}$	
251.3	**458764**	**$5.5 \cdot 10^{-6}$**	**20→100**	(377.2	0	–)	
251.6	111455	$1.4 \cdot 10^{-6}$		(383.5	0	–)	
252.9	41867	$5.0 \cdot 10^{-7}$		**385.4 ***	**c. 15000**	**–**	**500→20**
254.1	1269	$1.6 \cdot 10^{-8}$		389.3	375	$4.5 \cdot 10^{-9}$	

* potential flowing fracture (uncertain), not interpreted by Rouhiainen (2000).

4 Results of special study in the interval 200–400 m

In this chapter the results of the special methodology study in the interval 200–400 m in KLX02 during Campaign 2 are presented and discussed.

4.1 Number of interpreted flow anomalies

Firstly, a compilation of the number of interpreted flowing fractures from the different flow logging sequences in the special methodology study in the interval 200–400 m is shown in Table 4-1. The flowing fractures are determined from the overlapping flow logging. For comparison, also the number of conductive 3-m sections (above the measurement limit), identified from the sequential flow logging is shown. The number of flowing fractures, interpreted from the overlapping flow logging is presented in 10-m long depth intervals along the hole whereas the number of conductive 3-m sections from the normal-mode logging is presented in 30-m (3x10-m) intervals.

Also the total number of fractures in the 10-m depth intervals is presented for comparison with the number of flowing fractures. The former information was retrieved from the SICADA database from the PetroCore core mapping. The total fracture frequency includes both the numbers of natural (coated) fractures in the rock and fractures in interpreted crush zones. The total numbers of fractures in each depth interval, including fractures in crush zones (CZ), are shown in Table 4-1.

The interpretation of the number of flowing fractures for each flow logging sequence in Table 4-1 was carried out independently of the results of the other logging sets in order to obtain as objective and unbiased results as possible from each logging sequence. The interpreted flowing fractures from the overlapping flow logging sequences with L=0.5 m and dL=0.1 m at different drawdowns are presented in Appendix 1 in this report and in Appendix 13 in Rouhiainen (2000).

The interpretations are made from measured flows, plotted on a logarithmic scale. This fact may possibly reduce the resolution of the interpretation somewhat in comparison to a linear flow scale. The interpretations of the flow loggings with a section length of 3-m may be somewhat subjective due to the lower length resolution (longer sections) of these measurements. However, this fact will not change the main conclusions drawn from the comparisons. The special overlapping logging sequence using the thermal pulse method in the interval 204–226 m is not included in Table 4-1.

As will be discussed more in detail below, Table 4-1 shows that the number of flow anomalies decreases significantly at natural conditions (no drawdown, s=0), both for the sequential and overlapping flow logging. Furthermore, the overlapping flow logging in 3 m sections results in fewer anomalies (about half the number) compared to the corresponding measurements (at the same drawdown) with 0.5 m section length. In addition, the latter measurements are, in general, easier to interpret and less subjective.

Finally, the overlapping flow logging in 0.5-m sections shows that the number of interpreted anomalies remains relatively constant for drawdowns of 1 m and higher.

As can be seen from Table 4-1, the highest number of flow anomalies is located in the upper part of the interval 200–400 m whereas the lower part, from c. 340-m, contains rather few anomalies. Table 4-1 shows that only a small portion of the total number of fractures is interpreted as flowing fractures. The total number of fractures in this interval, including fractures in crush zones, is 374. If fractures in crush zones are excluded, the number of fractures in the rock is 279, see Table 4-1.

The maximal number of interpreted flowing fractures in this interval is 59 (from the overlapping flow logging at a drawdown of 8 m). This number corresponds to an average conductive fracture frequency (CFF) of c. 0.3 fractures/m, i.e. 1 conductive fracture every 3.4-m in the rock outside the crush zones. However, Table 4-1 shows that the distribution of conductive fractures is very uneven along the hole. It should also be noted that the number on CFF is strongly related to the lower measurement limit of the actual measurements, see Section 9.2.

Table 4-1. Number of interpreted conductive sections (#Sec) and number of flow anomalies from different flow logging sequences within depth intervals (30 m and 10 m, respectively) of the borehole section 200–400 m in KLX02. Also the total number of fractures in corresponding depth intervals from the core log including fractures in crush zones (CZ), are shown.

Flow log Mode	**Norm.**	**Norm.**		**Det.**	**Det.**	**Det.**	**Det.**	**Det.**	**Det.**	**Det.**	**Det.**
L (m) / dL (m)	**3 / 3**	**3 / 3**		**3/ 0.5**	**3/ 0.5**	**0.5/ 0.1**	**0.5/ 0.1**	**0.5/ 0.1**	**0.5/ 0.1**	**0.5/ 0.1**	**0.5/ 0.1**
Drawdown (m)	**s=0**	**s=8**	**Core log**	**s=0**	**s=8**	**s=0**	**s=1**	**s=2**	**s=4**	**s=8**	**s=22**
Interval (m)	**#Sec**	**#Sec**	**Total/CZ**	**Number of flow anomalies**							
200–210			8	0	0	0	0	0	0	0	0
210–220			26	1	2	4	5	5	5	5	5
220–230	6	9	19	2	3	2	5	5	5	5	5
230–240			25/9	1	3	1	7	7	7	7	7
240–250			31	1	3	4	8	8	8	8	8
250–260	8	9	34/11	2	3	4	5	5	5	5	5
260–270			29/5	1	1	2	3	3	3	3	3
270–280			10	1	3	1	3	3	4	4	3
280–290	3	5	7	0	0	0	0	0	0	0	0
290–300			11	1	3	1	5	5	5	5	5
300–310			7	0	2	0	1	2	2	2	1
310–320	6	9	12	1	2	1	2	2	2	3	1
320–330			11	0	2	0	3	4	4	4	0
330–340			29/10	2	2	4	5	5	5	5	4
340–350	3	6	6	0	0	0	0	0	0	0	0
350–360			7	0	0	0	0	0	0	0	0
360–370			5	0	0	0	0	0	0	0	0
370–380	0	3	3	0	1	0	0	1	1	1	1
380–390			86/60	0	2	0	1	1	2	2	2
390–400	1	2	8	0	0	0	0	0	0	0	0
TOTAL	**27**	**43**	**374/95**	**13**	**32**	**24**	**53**	**56**	**58**	**59**	**49**

4.2 Dependence of section length on flow logging

The dependence of the section length used on the number of flow anomalies interpreted is discussed in conjunction with Table 4-1 above. This is further demonstrated in Figures 4-1 and 4-2. The figures show the number of flow anomalies interpreted from the overlapping flow logging with 3-m and 0.5-m section length, respectively at a drawdown of 0 m and 8 m, respectively. As discussed above, about double the number of anomalies were interpreted from the 0.5-m measurements. This is mainly due to the increased resolution of both section length and step length of the 0.5-m measurements.

As pointed out by Rouhiainen (2000) flowing fractures located close to each other can better be resolved by a shorter section length. On the other hand, loggings with a short section length may be uncertain in borehole intervals of bad condition, e.g. due to fracturing, which may result in untight rubber discs. This may be the case at depth of 385 m as indicated by e.g. the caliper log. At the depth of 385 m, the results from both the loggings in 3-m and 0.5 m may be false since the length of the damaged borehole interval is more than 3 m (Rouhiainen 2000).

The apparent flow anomalies between the depths of 218.6–219.8 m are judged as leaks in the rubber disks because the plotted anomalies are too short. The caliper curve is smooth here and single point resistance does not show any large anomaly. There may be vertical voids along the borehole wall at this depth.

As discussed above, the figures also show the reduced number of anomalies for the logging sequences at zero drawdown compared to the loggings at 8-m drawdown. The dependence on section length on the transmissivity (or specific flow) of the flow anomalies is discussed below.

4.3 Comparison of sequential and overlapping flow logging

4.3.1 Number of conductive 3-m sections and interpreted flow anomalies

Since the sequential flow logging was made in 3-m long sections and the overlapping flow logging results in individual flow anomalies, no direct comparison of the number of flow anomalies from these loggings can be made. The sequential flow logging has a lower flow detection limit. However, depth intervals with zero interpreted flow anomalies, i.e. below the detection limit from the overlapping flow logging, e.g. 350–380 m and 380–400 m, can be compared with the results from the sequential flow logging. Table 4-1 shows that not even the latter measurements could detect any conductive 3-m sections in these intervals at a drawdown=0, despite the lower detection limit of the latter measurements. However, at s=8 m, the sequential flow logging detected a few conductive 3-m sections.

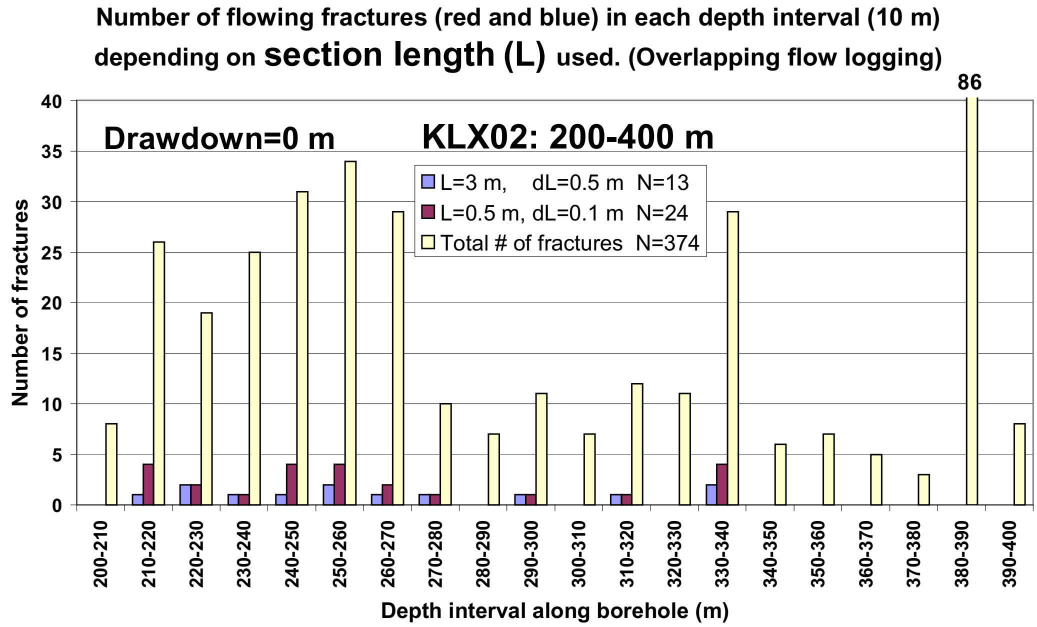

Figure 4-1. *Number of flowing fractures together with total number of fractures in depth intervals (10 m) from overlapping flow logging in 3-m and 0.5-m sections, respectively at natural conditions (s= 0-m) in the interval 200–400 m in KLX02.*

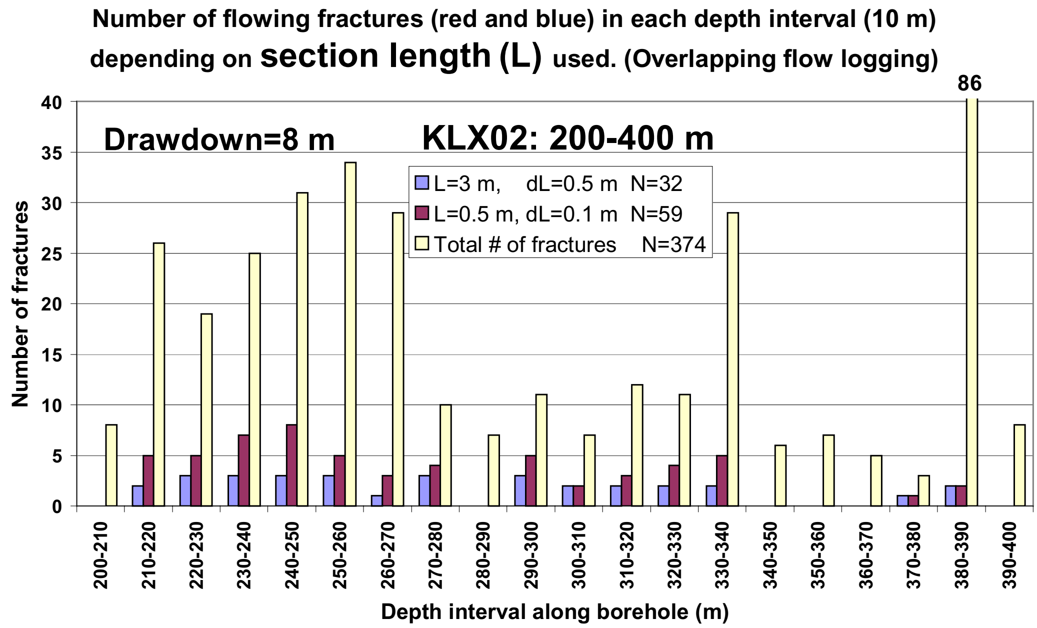

Figure 4-2. *Number of flowing fractures together with total number of fractures in depth intervals (10 m) from overlapping flow logging in 3-m and 0.5-m sections, respectively at a drawdown of 8-m in the interval 200–400 m in KLX02.*

The dependence of the magnitude of drawdown on the results of sequential and overlapping flow logging is illustrated in Figures 4-3 and 4-4, respectively. Figure 4-3 shows the number of conductive 3-m sections in depth intervals from sequential flow logging at a drawdown of 0 and 8 m, respectively. The figure shows that the number of conductive sections increases from 27 to 43 due to the higher drawdown applied. The same information can be seen in Table 4-1. Similarly, Figure 4-4 shows that the number of flowing fractures increases from 13 to 32 in the overlapping flow logging in the same 3-m sections at corresponding drawdown conditions. The dependence of the magnitude of drawdown on the results of the overlapping flow logging with L=0.5 m is discussed in Section 4.5.1.

4.3.2 Comparison of specific flow

Another way to compare sequential and overlapping flow logging is to calculate the specific flow (Q/s) for 3-m sections from sequential flow logging at a certain drawdown (s). These values can then be compared with the cumulative specific flows in 0.5–m sections from the overlapping flow logging, covering the same 3-m sections. Figure 4-5 shows such a comparison at a drawdown of 8-m. The specific flow may in many cases be assumed to be a good estimator for transmissivity, see below.

Figure 4-5 shows a rather good agreement for specific flows larger than about $5 \cdot 10^{-9}$ m^2/s. The cumulative specific flows from the 0.5-m measurements are however somewhat higher than those from the 3-m measurements which may indicate minor leakage. The deviating point at Q/s(3-m) at c. $1 \cdot 10^{-8}$ m^2/s corresponds to the 3-m section at c. 219-m where the borehole is in bad condition as discussed above.

Interestingly, the sequential flow logging in 3-m sections at c. 385 m indicates no measurable flow whereas the cumulative flow from the overlapping logging in 0.5-m sections over the same 3-m section is significant, see Figure 4-5. The cumulative flow corresponds to a specific flow of c. $2 \cdot 10^{-8}$ m^2/s. The results from the overlapping flow logging at 22 m drawdown show even higher flow, corresponding to a specific flow of c. $1 \cdot 10^{-7}$ m^2/s at this depth, see Appendix 13.10 in Rouhiainen (2000). The borehole interval at c. 385-m is highly fractured which may possibly result in untight rubber discs in the flow logging, c.f. Section 4.2.

The figure also gives an indication of the possible measurement limits of specific flow for the two logging methods. If lower flows than 120 ml/h are accepted in the overlapping flow logging, the lower measurement limit of specific flow may be at c. $5 \cdot 10^{-9}$ m^2/s for these measurements. The corresponding lower limit for the sequential flow logging seems to be at c. $2 \cdot 10^{-10}$ m^2/s. The leftmost point corresponds to a flow of c. 6 ml/h, which is the estimated lower measurement limit for flow in sequential flow logging. The upper measurement limit for specific flow seems to be slightly higher than $1 \cdot 10^{-5}$ m^2/s for both logging methods. A more rigorous discussion of the measurement limits of the different methods of difference flow logging is presented in Section 9-2.

The flows between 6–600 ml/h were measured by the thermal pulse method during the sequential flow logging. During the overlapping flow logging, only the thermal dilution method was used. These results are considered as only qualitative below 120 ml/h. This fact explains the deviation of the points below c. $5·10^{-9}$ m^2/s in Figure 4-5. The cumulative flows below this value in the overlapping flow logging are also distorted by the cumulative base-flows (c. 20 ml/h in each 0.5-m section, totally c. 120 ml/h in a 3-m section).

4.4 Overlapping flow logging with thermal pulse

A special overlapping flow logging sequence (L=0.5 m, dL=0.1 m) with also the thermal pulse method included was carried out in the interval 205–226 m, both at a drawdown=0 and 8 m, respectively, see Appendix 11 and 12 in Rouhiainen (2000). The purpose of this logging was to study the effect of the lower detection limit for flow using the thermal pulse method. Normally, this method is only used in sequential flow logging since it is very time-consuming. To speed up the logging, the flow measurement range was in this case reduced to 30–600 ml/h instead of the general range 6–600 ml/h with the thermal pulse method. The results in Appendix 11–12 indicate however that no additional flow anomalies could be detected by the thermal pulse method compared to the thermal dilution method. It should be noted that the base-flow level is not shown in Appendix 11-12 (logarithmic flow scale) since they are zero or undefined.

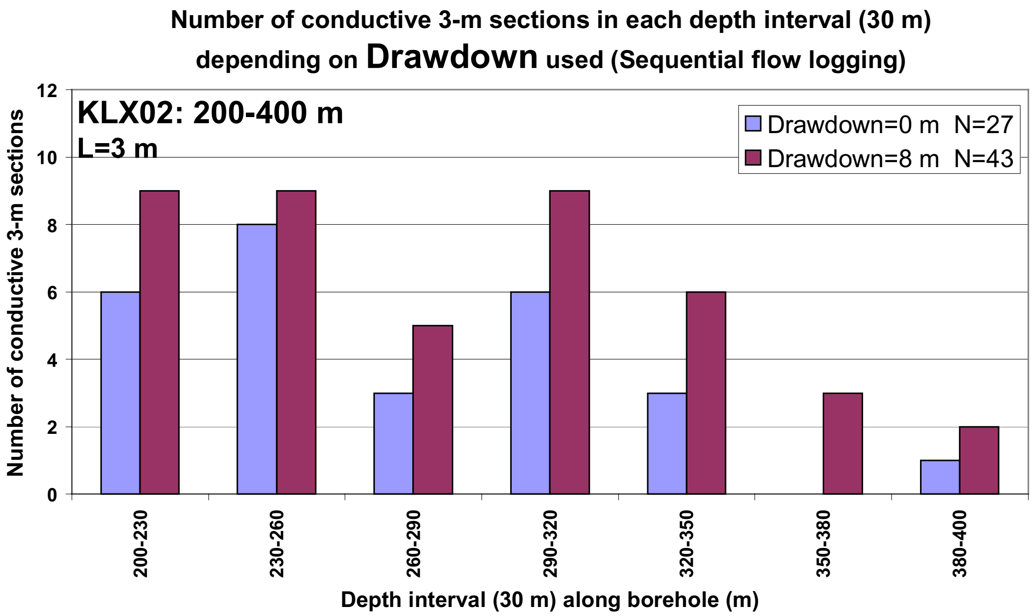

Figure 4-3. *Number of flowing fractures in depth intervals (30 m) at a drawdown of 0 and 8 m, respectively from sequential flow logging in 3-m sections in the interval 200–400 m in KLX02.*

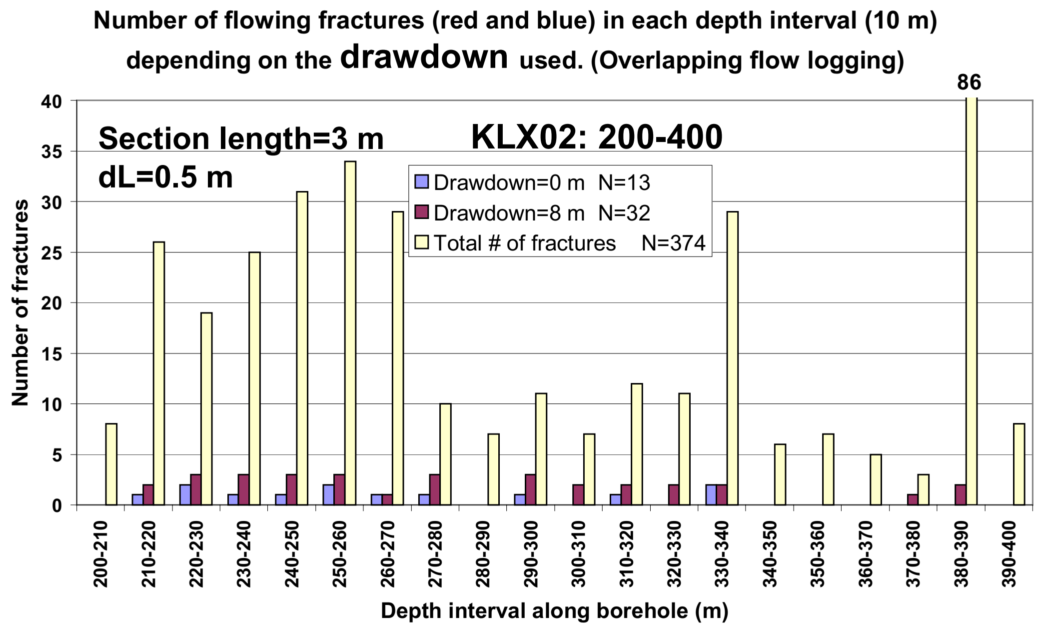

Figure 4-4. Number of flowing fractures together with total number of fractures in depth intervals (10 m) at a drawdown of 0 and 8 m, respectively from overlapping flow logging in 3-m sections in the interval 200–400 m in KLX02.

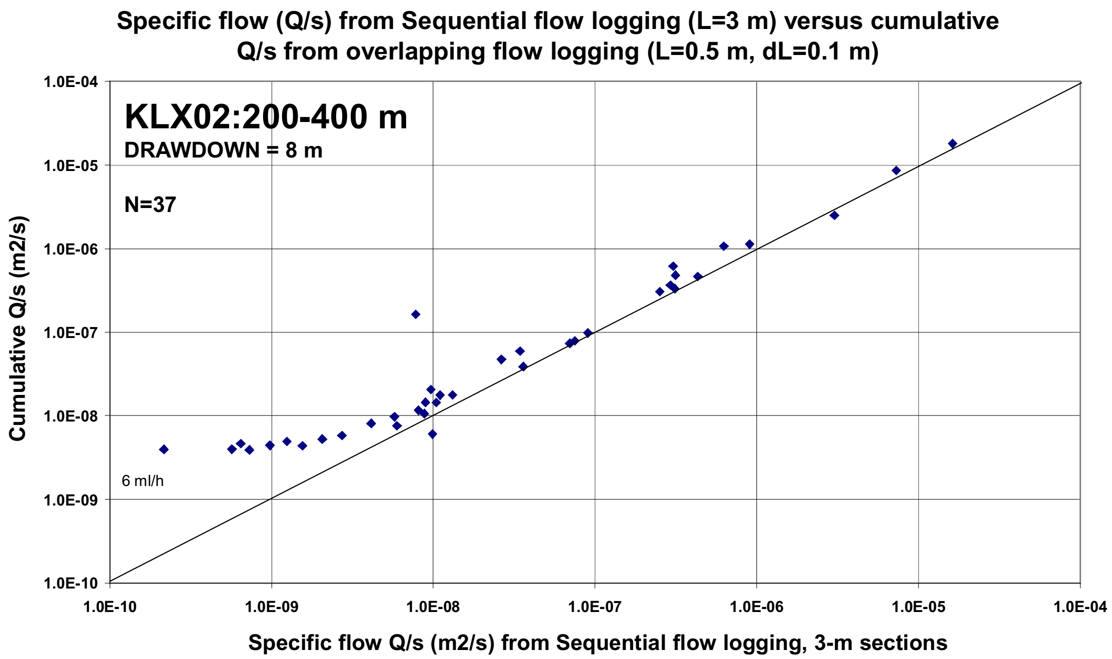

Figure 4-5. Comparison of specific flow (Q/s) from sequential flow logging in 3-m sections with cumulative Q/s of included 0.5-m sections from overlapping flow logging at a drawdown of 8 m.

4.5 Overlapping flow logging at different drawdowns

4.5.1 Interpreted flow anomalies

The interpreted flowing fractures from the overlapping flow logging with 0.5-m section length in the borehole interval 200–400 m, shown in Appendix 1, are listed in Appendix 2 together with the measured flows at different drawdowns. The lower measurement limit for the flow measurements is about 120 ml/h. Lower flow rates are uncalibrated and considered as qualitative. The direction of flow cannot be determined for flows below 120 ml/hr. Relative freshwater head values were only calculated for fractures with flows exceeding 120 ml/h.

Figure 4-6 shows the total number of interpreted flowing fractures at the different drawdowns applied. The number of flowing fractures increases significantly when the drawdown is increased from 0 to 1 m. On the other hand, increasing drawdown between 1–8 m only results in a slight increase of the number of flowing fractures. However, at a drawdown of 22 m, the number of identified flowing fractures decreases. This depends on the increased noise and background flow level at 22-m drawdown, masking some of the flow anomalies. Figure 4-7 shows the number and distribution of interpreted flowing fractures in depth intervals at different drawdowns (0, 8 m and 22 m) applied in the borehole.

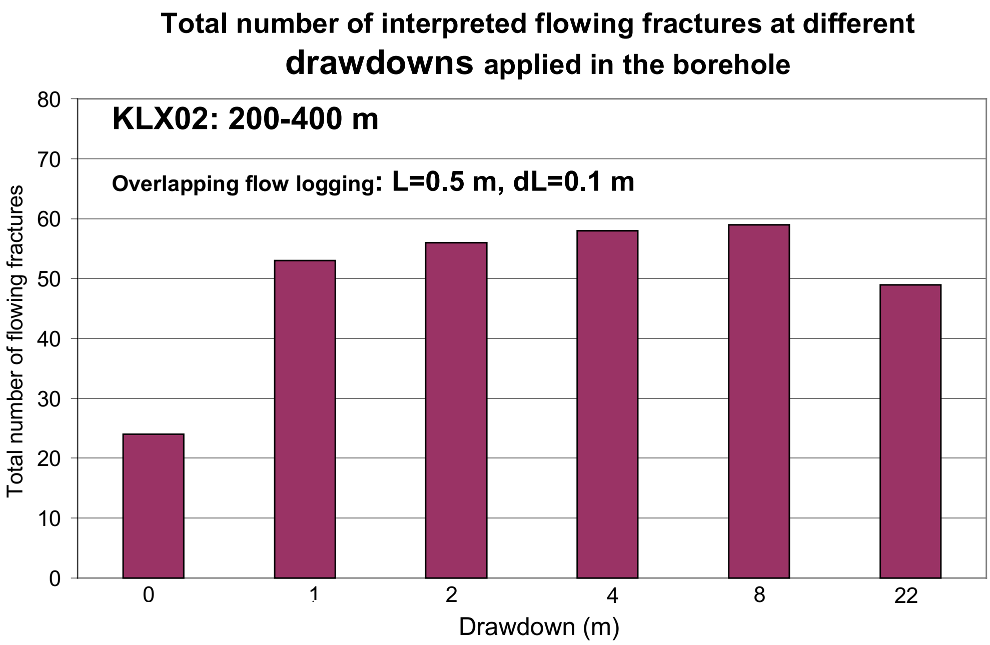

Figure 4-6. Total number of interpreted flowing fractures in the interval 200–400 m in KLX02 from overlapping flow logging in 0.5-m sections at different drawdowns. The total number of fractures in this interval is 374.

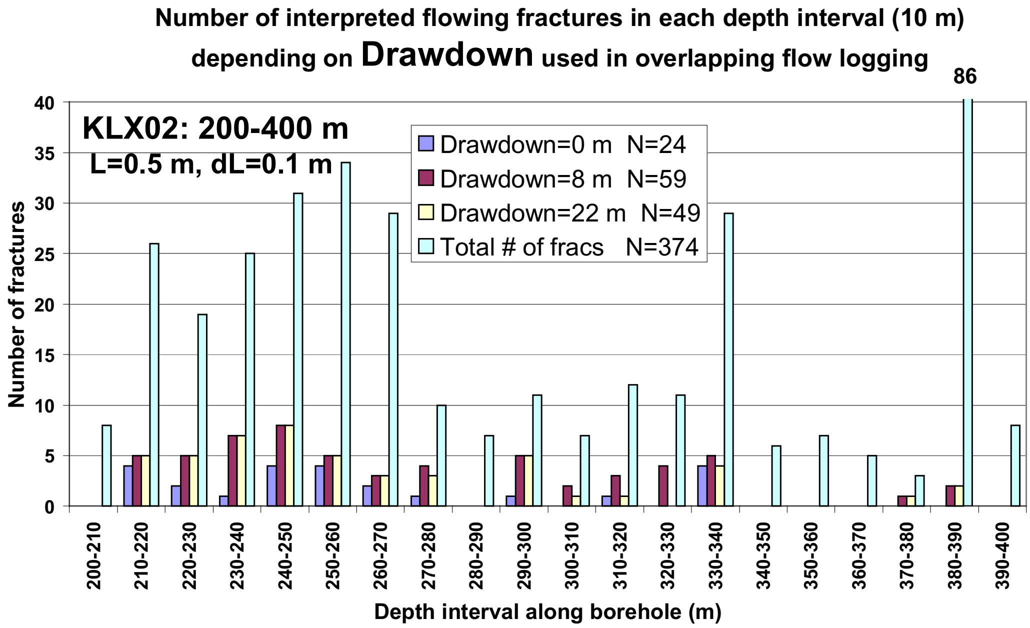

Figure 4-7. *Number of interpreted flowing fractures together with total number of fractures in depth intervals (10 m) of the interval 200–400 m in KLX02 from overlapping flow logging in 0.5-m sections at different drawdown (0, 8 and 22 m, respectively).*

4.5.2 Linearity of measured flow

The measured flows for each flowing fracture at different drawdown were plotted versus the drawdown of the groundwater level (s). The flows were also plotted versus the actual head change (dh), as determined from the average, relative head values (h0) of flowing fractures in Appendix 2. Since previous sequential flow logging has indicated outflow conditions in the interval 200–400 m in KLX02 (Rouhiainen 2000) when the borehole was not pumped, the relative freshwater heads are negative under natural conditions. Similarly, the measured flows at zero drawdown in Appendix 2 are negative.

The flow versus drawdown- (and estimated actual head change-) plots for all interpreted fractures are shown in Appendix 3. All measured flows are included, also flows below 120 ml/h. An example of such plots is shown in Figure 4-8 for the flowing fracture at 213.3 m. The linearity of the measured flows was estimated by linear regression, quantified by the regression coefficient R^2. The determined regression coefficients for all flowing fractures together with their specific flow at a drawdown of 8 m are shown in Figure 4-9.

Figure 4-9 shows that the regression coefficients generally are close to 1 in this case for most of the flowing fractures, indicating good linearity of the measured flows for the actual drawdown values. However, for the most low-conductive fractures the linearity is

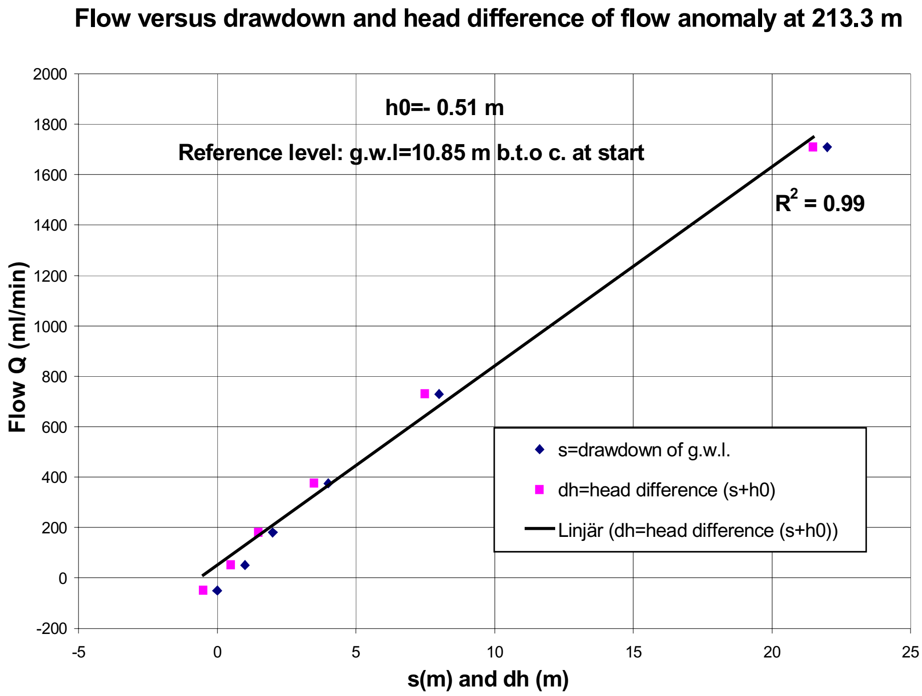

Figure 4-8. *Measured flow versus drawdown of the water level in the borehole (s) and actual head change (dh) of the flowing fracture at 213.3 m from overlapping flow logging in KLX02.*

poor. In fact, several of these fractures are below the measurement limit of flow in overlapping flow logging. In Figure 4-9, the potential flow anomaly at 385 m is included. As discussed above, this anomaly is uncertain due to bad borehole conditions at this depth. A slight parabolic form of the flow versus drawdown curves is generally observed as indicated in Figure 4-8. This phenomenon is common in flow measurements. Possible reasons for non-linear flows are:

- Turbulent flow in fractures.
- Friction losses in the tubing connected to the flow sensor and in the flow sensor itself can be notable with flows larger than 3 l/min, but they have hardly any effects with flows less than 1 l/min.
- These friction losses with high flow rates (> 3 l/min) may also cause leakage through the rubber disks.
- At a drawdown of 22 m, saline water appeared at the upper part of the borehole. Therefore the actual pressure change in the borehole is less than 22 m.
- Possible errors in calibration of the flowmeter could cause unlinearity.

An example of a high-transmissivity fracture with non-linear flow at depth 251.6 m is shown in Figure 4-10. Some anomalies (e.g. at 232.4 m) with measured flows below the measurement limit (120 ml/h) show though a rather good linearity while others (e.g. at 310.5 m) show no correlation at all. In the latter case, flow was detected only at 8-m drawdown (35 ml/h), while at 22-m drawdown it was masked by noise in the base-flow.

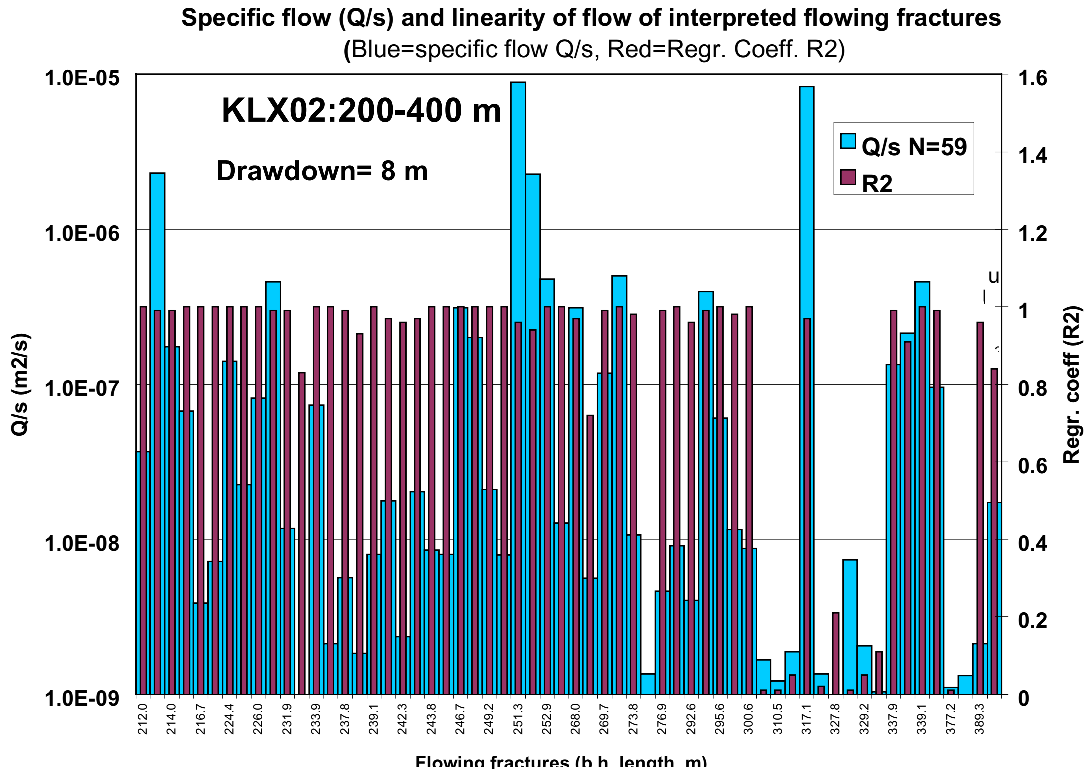

Figure 4-9. *Histogram showing the regression coefficient (R^2) and specific at a drawdown of 8 m for the interpreted flowing fractures flow from overlapping flow logging in the interval 200–400 m in KLX02.*

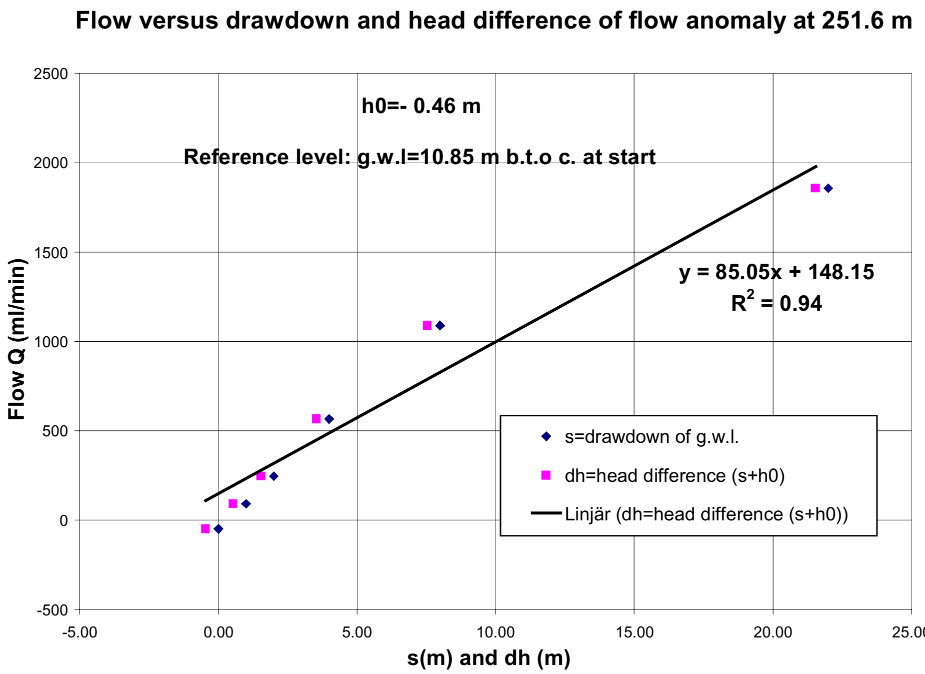

Figure 4-10. *Measured flow versus drawdown of the water level in the borehole (s) and actual head change (dh) of the flowing fracture at 251.6 m from overlapping flow logging in KLX02.*

4.5.3 Specific flow

The specific flow rate was calculated for all interpreted flow anomalies from the over-lapping flow logging with a section length of 0.5-m for all drawdowns applied. The specific flow rate was based both on the drawdown (s) and the actual head change ($dh=s+h_0$), respectively, where h_0 is the calculated undisturbed, relative (fresh-water) head of the flowing fracture. An example, showing the specific flow rates at a drawdown of 1-m is shown in Figure 4-11. The figure shows that the Q/dh-values are generally slightly higher than the Q/s-values. This is due to that the dh-values are slightly lower than the s-values since most of the calculated h0-values are c. –0.5 m in this case (Appendix 2).

Since the relative freshwater head (dh) could only be determined for anomalies with flows greater than 120 ml/h, c.f. Section 4.7, the number of calculated specific flow rate values based on the actual head change (Q/dh) is lower than the Q/s-values. The latter parameter can always be calculated for non-zero flows at a certain drawdown. Thus, for statistical analysis, it may be an advantage of using Q/s, which thus may a more robust estimator (larger number of values) in this case, particularly for low flows near the lower measurement limit. In such analyses, it may be beneficial to have a larger number of Q/s-values with somewhat lower quality than a fewer number of higher-quality Q/dh-data. A comparison between specific flow rate and transmissivity of the flowing fractures is made in Section 4.6.

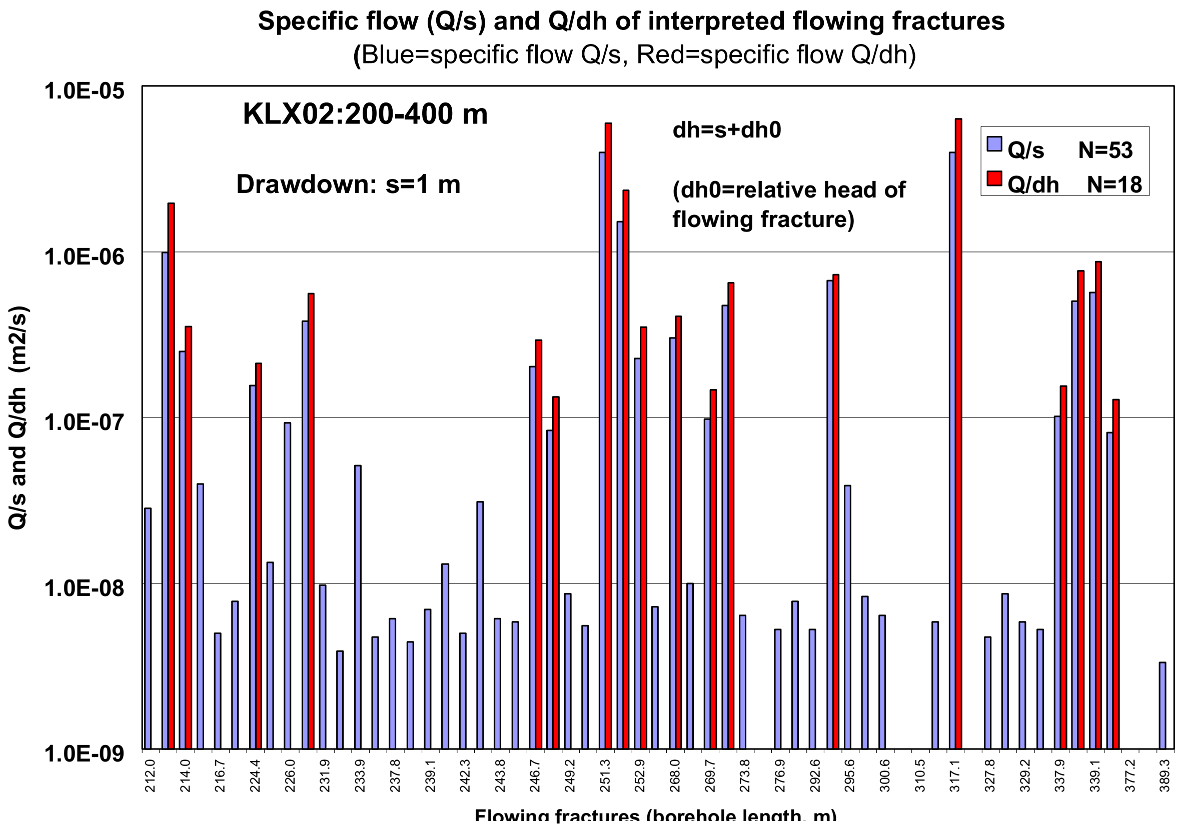

Figure 4-11. Comparison of specific flow Q/s and Q/dh for interpreted flowing fractures in the borehole interval 200–400 m at a drawdown of 1 m from the overlapping flow logging in borehole KLX02.

4.5.4 Consistency of flows

The plots in Appendix 1 showing measured flows for the overlapping flow logging in 0.5-m sections at different drawdowns indicate that the consistency of the measured flows in general is very good for the different drawdowns, both of the flow anomalies and between these. However, the base-flow level (noise level) at zero drawdown (black) is different from the other flow curves (coloured) due to different calibrations of the flow.

Due to the noise at 22-m drawdown, the base-flow level is significantly increased. This fact causes that some of the smaller flow anomalies are masked at this drawdown, resulting in fewer interpreted flow anomalies at this drawdown, c.f. Section 4.5.1. Possible reasons to the increase of the base-flow level, which occurred only at 22-m drawdown, are discussed in section 8.2.

4.6 Transmissivity of flow anomalies

One of the main tasks of the methodology study is to investigate the possibility to estimate the transmissivity of the identified flowing fractures from overlapping flow logging using two measurement sequences at different drawdowns, see Section 2.5. In Rouhiainen (2000, Appendix 14), transmissivity values were calculated from two measurement sequences at different drawdowns, one of the sequences always being at zero drawdown. It is also of interest to calculate the transmissivity based on other drawdown combinations for comparison.

4.6.1 Comparison of transmissivity based on different drawdowns

Transmissivities based on different combinations of two logging sequences with different drawdown were calculated and compared. Firstly, transmissivities based on small drawdowns (0 and 1m) were compared with transmissivities at high drawdowns (8 m and 22 m), see Figure 4-12. In this comparison, the calculations of transmissivity are based on all measured flow values, also flows below 120 ml/h (considered as the lower measurement limit) were included. The agreement between the two sets of transmissivities is rather good, except at the lower end.

If flow values below 120 ml/h are accepted, the figure indicates that the lower measurement limit for transmissivity seems to be c. $5 \cdot 10^{-9}$ m^2/s for overlapping flow logging. If only flows higher than 120 ml/h are accepted, the minimal transmissivity is c. $1 \cdot 10^{-8}$ m^2/s, c.f. Section 9-2. Furthermore, transmissivities based on 2 m and 4 m were compared with those based on 8 and 22-m drawdown, as before, see Figure 4-13. In this case the values at the lower end are more consistent between the two data sets.

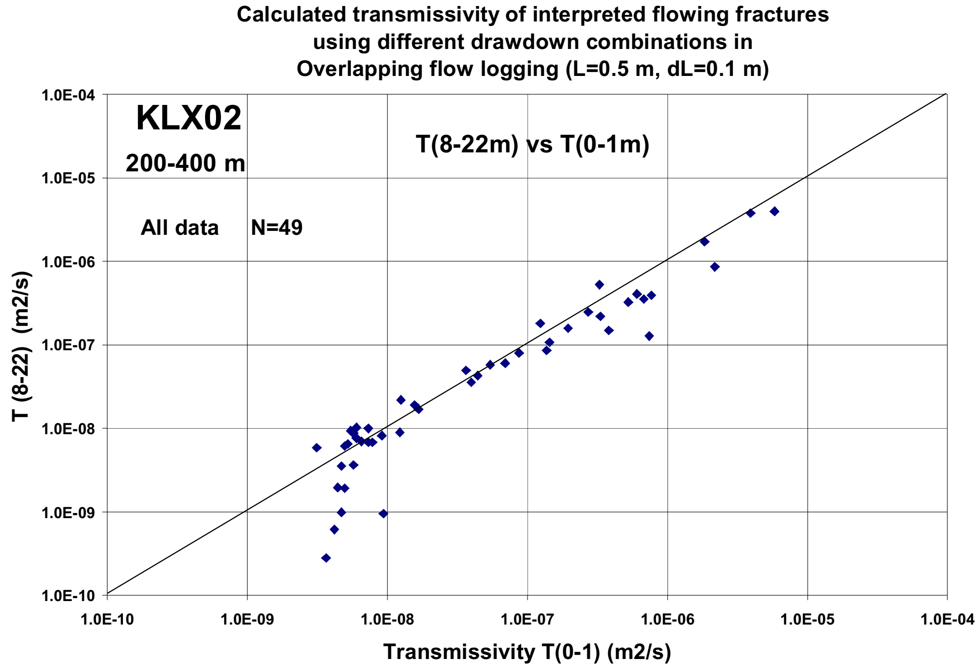

Figure 4-12. *Comparison of calculated transmissivity T(0-1) and T(8-22), based on overlapping flow logging at drawdowns of 0 and 1 m and 8 m and 22 m, respectively in borehole KLX02.*

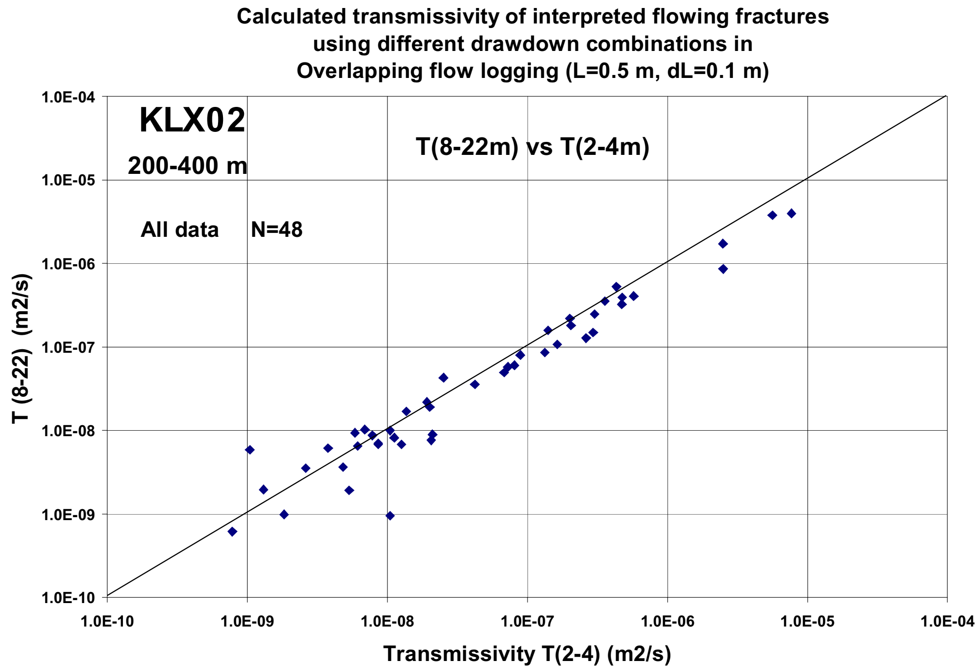

Figure 4-13. *Comparison of calculated transmissivity T(2-4) and T(8-22), based on overlapping flow logging at drawdowns of 2 and 4 m and 8 m and 22 m, respectively in borehole KLX02.*

4.6.2 Comparison between transmissivity and specific flow

A comparison between calculated transmissivity, based on overlapping flow logging at 0- and 8- m drawdown respectively, and the specific flows at 8-m drawdown is shown in Figure 4-14. The highest number of interpreted flow anomalies occurred at 8-m drawdown, c.f. Figure 4-6. The agreement between the transmissivity T(0-8) and the specific flows at 8-m drawdown is very good in this case. This indicates that the transmissivity values are strongly influenced by the measured flows at 8-m drawdown in this case.

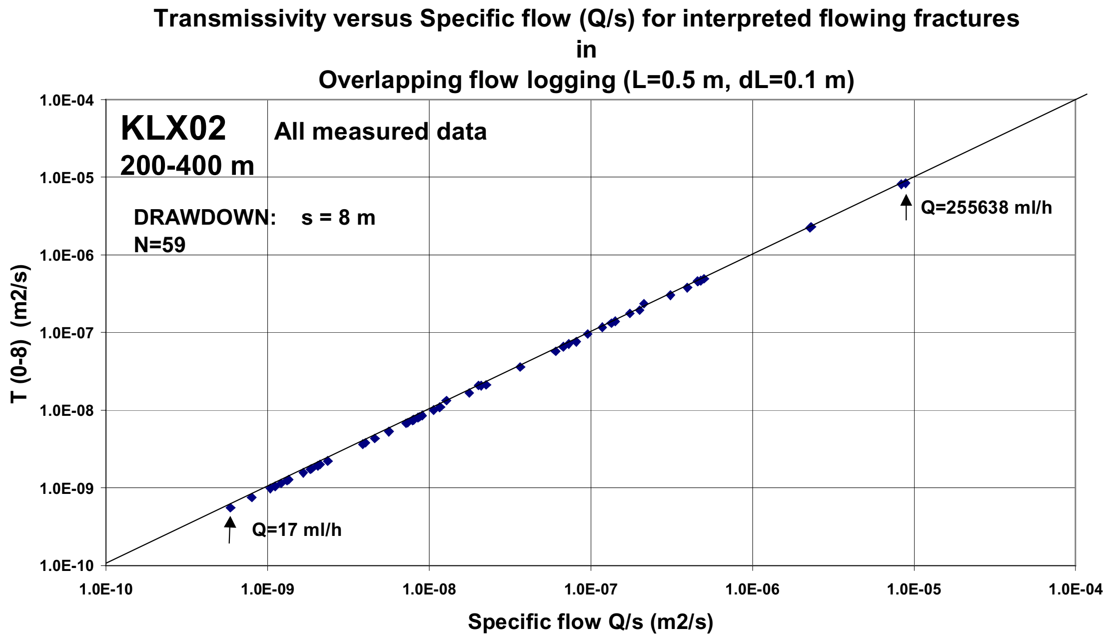

Figure 4-14. *Comparison of calculated transmissivity T(0-8) and specific flow at 8-m drawdown from overlapping flow logging using all interpreted flowing fractures in borehole KLX02.*

Also for overlapping flow logging at other drawdowns, the agreement between transmissivity and specific flow is very good. Thus, it seems that specific flow is a good estimator of transmissivity in this case. However, this may not always be the case, e.g. if large variations of the undisturbed head occur along the hole, c.f. Section 2.5. In KLX02, rather small head variations occur in the interval 200–400 m, c.f. Section 4.7.

All measured flow values (also below the measurement limit) from the overlapping flow logging at 8-m drawdown have been used in the above figures. In Figure 4-14 the lowest specific flow and transmissivity (c. $6{\cdot}10^{-10}$ m^2/s) corresponds to a flow of only 17 ml/h which is much below the postulated lower measurement limit for flow (120 ml/h). Still, the correlation between transmissivity and specific flow is good in this case. The highest calculated transmissivity and specific flow (c. $1{\cdot}10^{-5}$ m^2/s) corresponds to a flow of 255 638 ml/h (4261 ml/min) which is slightly below the postulated, upper measurement limit for flow (5,000 ml/min).

4.6.3 Comparison of specific flow at different drawdowns

The specific flows at different drawdowns of the interpreted flowing fractures from the overlapping flow logging were compared with the transmissivity T(0-22). The specific flow was calculated both based on the drawdown of the water level in the hole and on the estimated actual head change dh, respectively, see above. The comparisons indicated that the two types of specific flow values are more scattered at low drawdowns. This is due to the fact that the undisturbed head of the fractures affects small drawdowns in the hole to a larger extent. At small drawdowns, the specific flow based on the actual head change (Q/dh) is a better estimator of transmissivity, provided that the relative head for the flowing fracture can be estimated. However, already at a drawdown of 1 m, both specific flows and the transmissivity are very similar and stabilise at a relatively constant value at larger drawdowns.

4.7 Natural freshwater head of flow anomalies

Natural fresh-water heads in 3-m sections were estimated from the sequential flow logging in Campaign 1 along the borehole, see Appendix 4 in Rouhiainen (2000). Furthermore, natural fresh-water heads for interpreted flow anomalies were calculated from the overlapping flow logging in Campaign 2 in the borehole interval 200–400 m using different drawdown combinations (pairs), see Appendix 15 in Rouhiainen (2000).

The relative, natural freshwater head of the flow anomalies was calculated from the flow logging according to Eqn. (2.5) using drawdowns used instead of hydraulic heads. This fact means that the natural freshwater head is expressed relative to the groundwater level in the borehole. The natural freshwater head was calculated, only if the flows in both logging sequences of the actual pair exceed the measurement limit of 120 ml/h for the actual fracture. The calculated, relative fresh water heads in the interval 200–400 m were all smaller than 1 m (below the groundwater level in the hole), see Section 4.5.2.

The relative fresh-water head was also calculated from other drawdown combinations from the overlapping flow logging in Campaign 2. Firstly, drawdown combinations with one drawdown always being zero were used, e.g. h_0 (0–1m), h_0 (0–2m) etc. Cross-plots of these combinations indicated that the spread in calculated head values generally increased with increasing drawdown, c.f. Figures 4-15 and 4-16. In the figures, all relative head values calculated when the measured flows from both logging sequences were non-zero, are included. This is considered as justified since zero flows are below the measurement limit. This means that (relative) natural head values were only estimated for 24 of the 59 interpreted flowing fractures in the interval 200–400 m.

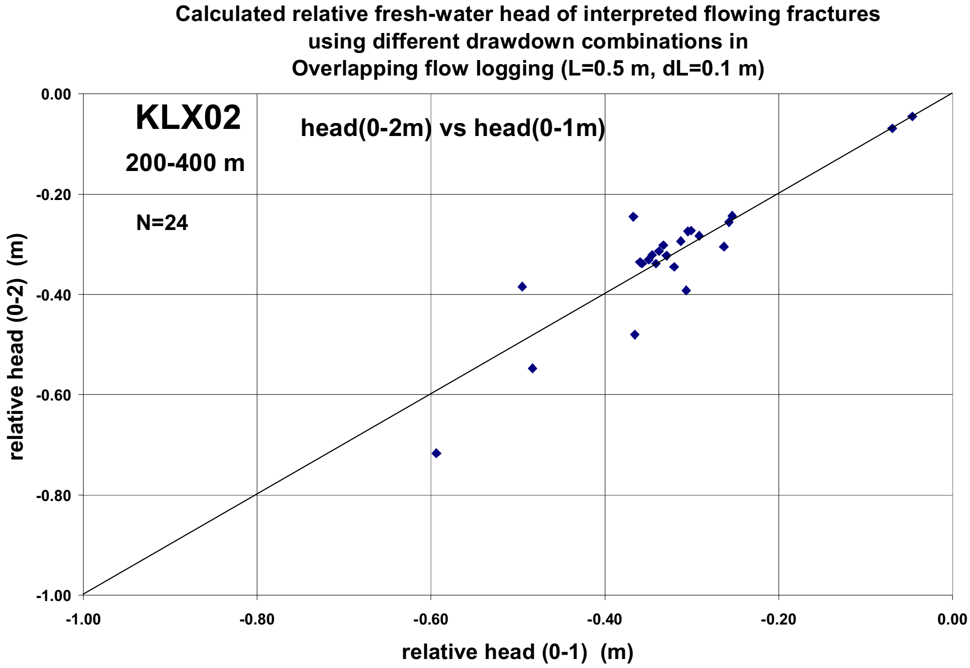

Figure 4-15. *Comparison of calculated relative fresh-water heads for flowing fractures for drawdown combinations of 0-1m and 0-2m, respectively from overlapping flow logging in borehole KLX02.*

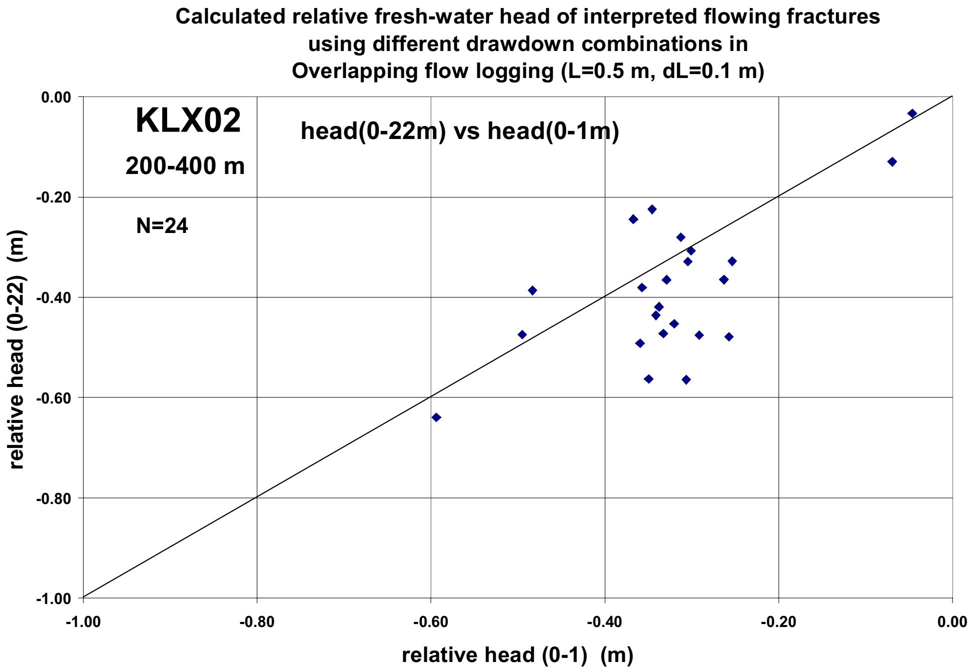

Figure 4-16. *Comparison of calculated relative fresh-water heads for flowing fractures for drawdown combinations of 0-1m and 0-22m, respectively from overlapping flow logging in borehole KLX02.*

Secondly, relative freshwater head values were calculated for combinations with both drawdowns greater than zero, e.g. h_0 (4–8m), h_0 (8–22m) etc. However, the calculated head values for these combinations were unstable and unrealistic. This might indicate that one of the drawdowns always must be zero in order to obtain reasonable estimations of the relative freshwater head of flowing fractures.

Ideally, the two drawdowns selected in each pair should be below and above the actual head value of the flowing fractures, respectively. This means that the calculated head values in such cases are interpolated rather than extrapolated. However, such drawdown conditions are difficult to always meet in practise. In addition, the linearity between measured flow and drawdown for the flowing fractures (Section 4.5.2) may strongly affect the calculated head values. In particular, this fact may be a problem for flows near both the lower as well as the upper measurement limits, respectively.

The calculation of the in-situ fresh water head by interpolation is explained graphically in Fig. 4-17 for the interpreted flowing fracture at 224.4 m. At zero drawdown (no pumping) the measured flow rate for this fracture was –190 ml/h, indicating outflow conditions, c.f. Table 3-3. At the drawdown of 4 m the measured flow rate was 2448 ml/h. The uncertainty intervals (± 10%) of the measured flows are also indicated in the figure.

The drawdown at which the flow rate is 0 ml/h can be interpolated from Fig. 4-17 and is about 0.3 m. This drawdown balances the outflow from the fracture. The in-situ head in the fracture is the same as this drawdown value but with the opposite sign (because drawdown is chosen to be positive downwards). The same interpolation can be carried out at other drawdowns with about the same result if one of the drawdowns is zero.

The situation for the interpolation (or extrapolation) radically changes if both flow rates are measured at larger (non-zero) drawdowns, c.f. Figure 4-18. The drawdown pair chosen is now at 2-m and 4-m drawdown. The extrapolation gives an in-situ fresh water head of the fracture of about 0.8 m, i.e. positive head. The error limits of the flows are also drawn in the figure. The error limits of fresh water head of the fracture range from + 2.3 m to – 0.3 m. This wide variation is obtained with the assumption of ±10 % error of the measured flow rate. The error range had been smaller with the drawdown pair at 1 m and 4 m drawdown but larger with the pair at 4 m and 8 m drawdown.

The following points should be noted when choosing a proper drawdown pair for calculation of the natural (in-situ) freshwater head:

- Extrapolation to a distant point amplifies the errors of flow measurement.
- Extrapolation to a distant point amplifies the errors caused by unlinearity of the system.
- The error of the flow measurements is larger at larger flow rates. The error is assumed to be ±10 % of the flow rate measured in this example (which is the actual error in the flow measurements).
- The undisturbed in-situ head of a fracture can be measured most accurately if it is measured near the balance condition, i.e. one of the chosen drawdown is near the in-situ (natural) head in the fracture.

Generally, one of the drawdowns should be at no pumping or at a small pumping rate (i.e. drawdown) to get a reliable value of the undisturbed head. A drawback of this choice is that there are fewer points where the in-situ head can be calculated since there are less measurable flows at zero drawdown than with large pumping. The accuracy of the undisturbed head- and transmissivity interpretations can be improved when several drawdowns are used. This may not be possible in practice due to economical reasons.

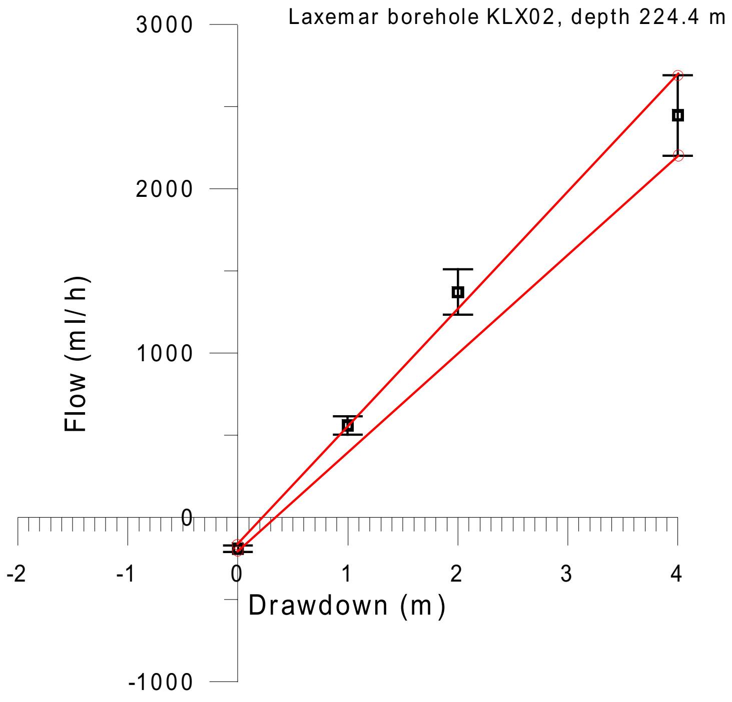

Figure 4-17. *Interpolation of natural fresh-water head for flowing fracture at 224.4 m.*

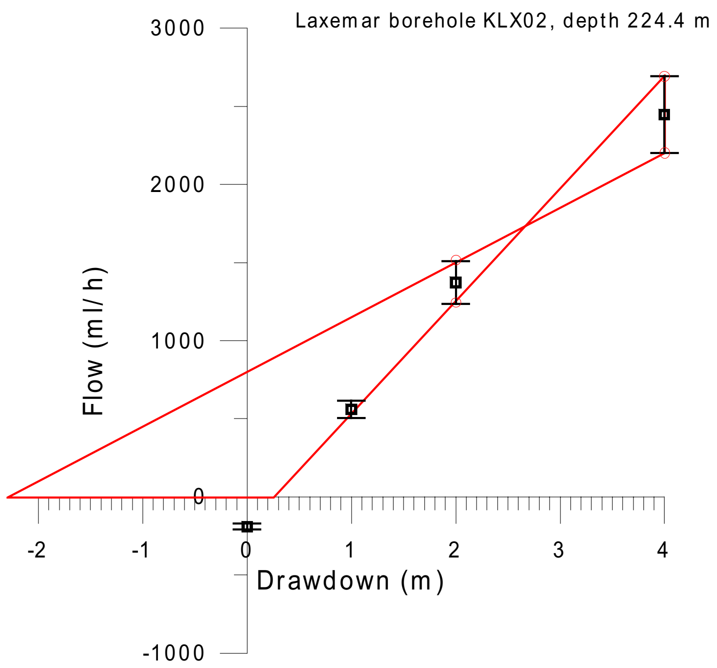

Figure 4-18. *Extrapolation of natural fresh-water head for flowing fracture at 224.4 m.*

As the calculated natural freshwater heads do not depend on geometrical properties but only on the ratio of the flows measured at different heads in the borehole they should be less sensitive to unknown fracture geometry, see Chapter 2.

Finally, the eventual correlation between the calculated head values and the corresponding transmissivities at the same drawdown combination was studied. As shown in Figure 4-19 the correlation between freshwater head and transmissivity for the drawdown combination of 0 and 1 m is weak or insignificant as indicated by the linear regression coefficient R^2. The results were similar for the drawdown combination of 0 and 22 m. The two deviating points with low calculated heads corresponds to the flowing fractures at 251.3 m and 295.1 m, respectively. The former fracture shows non-linearity between flow and drawdown, see Appendix 1, possibly due to that the flow at 22-m drawdown exceeds the upper measurement limit. The latter fracture at 295.1 m shows good linearity.

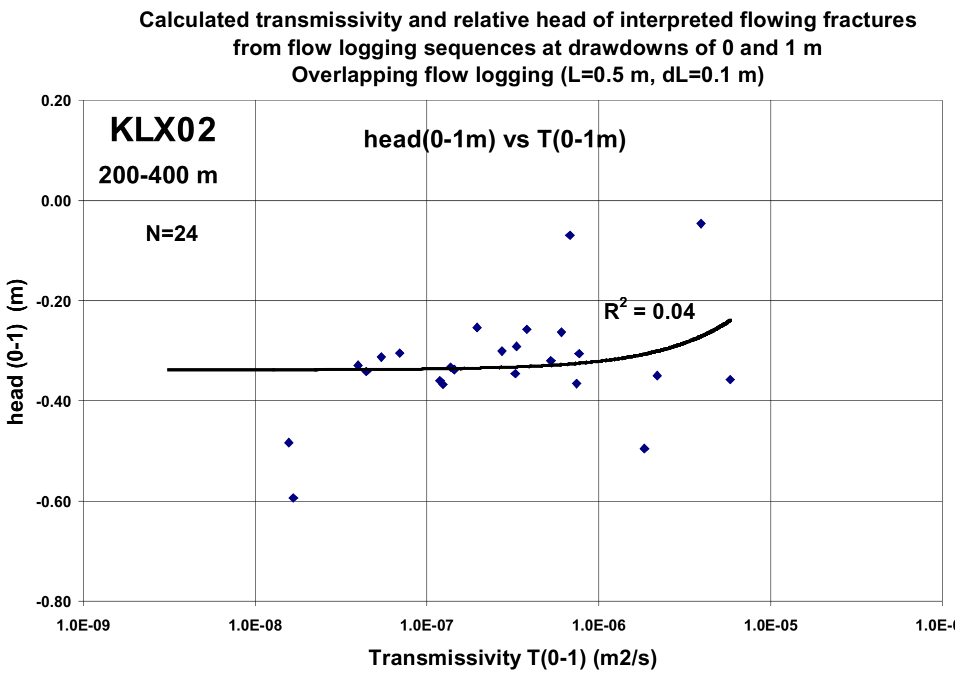

Figure 4-19. *Calculated relative fresh-water heads and transmissivity for flowing fractures for the drawdown combination of 0 and 1m from overlapping flow logging in borehole KLX02.*

The thermal dilution method, used in overlapping flow logging, was in this case developed so both the flow rate and flow direction could be measured. As described above, an outflow from the borehole into fractures was observed during natural conditions (zero drawdown) in the interval 200–400 m of the borehole. The estimated relative freshwater heads of the flowing fractures were in most cases about –0.5 m, i.e. 0.5 m below the stable groundwater level in the borehole in this borehole interval. This implies that the flow should be reversed and directed into the borehole already at a drawdown of 1 m in the hole. This was also the case for all interpreted flowing fractures above the measurement limit (Rouhiainen 2000), see Appendix 2.

5 Correlation of flow anomalies with other measured parameters

Table 5-1 shows the measured values of flow, Single-Point Resistance (SPR), Caliper and Electrical conductivity (EC) for the interpreted flow anomalies from the overlapping flow logging in the interval 200–400 m in KLX02. Appendix 1 shows that the base level for SPR in this interval is at about 1E+4 (ohm). Table 5-1 indicates significantly lower values at most of the flow anomalies, which suggest that SPR is a good correlation parameter with flow rate.

The caliper log shows only slightly increased values at the interpreted flow anomalies. On the other hand, the caliper log is useful to identify borehole sections in bad condition. In such intervals, e.g. crush zones, there is a risk of leakage at the rubber discs, which may result in uncertain flows, see Section 8.2. The measured electrical conductivity of the water at the flow anomalies is generally much lower in comparison to that of the borehole water, indicating relatively fresh water in the fractures in this borehole interval. Below the anomaly at c. 317-m, the EC increases. The measurements of fracture specific EC along the hole are discussed in Chapter 7.

Table 5-1. Correlation of flows, Single-Point Resistance, Caliper and Electrical conductivity for the interpreted flow anomalies from the overlapping flow logging in the interval 200–400 m in KLX02.

Flow anomaly (m)	Flow (ml/h) at s=22 m	Single-point Resistivity (ohm)	Caliper (mm)	El. cond. (S/m)
212.0	2964	2287	75.750	0.05798
213.3	158662	1399	75.570	0.04842
214.0	16757	198	81.607	0.04695
215.2	5031	2397	75.490	0.06490
216.7	302	3319	75.490	–
220.7	572	4032	75.750	–
224.4	12542	3025	75.917	0.05341
224.9	1823	2542	75.750	–
226.0	6625	4433	75.917	0.06625
227.7	30680	1089	75.833	0.04717
231.9	778	5763	76.000	–
232.4	38	2358	75.966	–
233.9	5337	3568	76.000	0.06373
234.2	166	5737	76.000	–
237.8	359	4897	76.100	–
238.0	86	6941	76.100	–
239.1	604	6270	76.130	–
Table 5-1 cont.				

241.4	990	5916	76.130	–
242.3	121	7545	76.130	–
243.3	2870	5771	76.200	0.07160
243.8	714	2700	76.130	0.06856
244.9	733	5878	76.140	–
246.7	22150	3509	76.130	0.05138
248.6	15479	2846	76.200	0.05398
249.2	1623	3056	76.130	0.07829
250.1	578	6005	76.160	–
251.3	458764	711	76.643	0.06808
251.6	111455	513	78.700	0.06845
252.9	41867	3604	76.166	0.05425
254.1	1269	3793	76.200	–
268.0	16905	1197	76.200	0.05694
269.0	213	1725	76.390	–
269.7	7977	1563	76.270	0.05882
271.1	36168	845	76.300	0.07655
273.8	715	4810	76.423	–
276.9	462	3677	76.233	–
290.5	796	485	76.200	–
292.6	219	3560	76.293	–
295.1	30324	3323	76.293	0.07346
295.6	4393	1360	76.267	0.08208
298.3	698	2082	76.267	–
300.6	801	4931	76.230	–
317.1	452519	499	76.200	0.189
337.9	9576	528	76.230	0.210
338.9	12983	1812	76.270	0.220
339.1	34185	437	76.170	0.238
339.6	7170	844	76.270	0.229
389.3	375	290	77.290	–

6 Comparisons between Campaign 1 and 2

6.1 Flows in sequential flow logging in 3-m sections

Results of the sequential flow logging from Campaign 1 and 2 are presented on the same plot, see Appendices 7 and 8 in Rouhiainen (2000). Single point resistance curves of the both measurements are also presented. There is a depth shift of about 20-cm between these two measurements. The depth shift in the overlapping flow logging results of Campaign 1 and Campaign 2 during pumping varied between 10 and 20 cm.

The flow rates of both measurements without pumping are compared in a single plot, see Figure 6-1. The deviation between the two measurements is large in two points marked with a circle. A similar plot of flow rates with pumping is presented in Figure 6-2. The points with large discrepancy are marked with a circle. The depths of the marked points are also written on the Figures 6-1 and 6-2. There was a large deviation at the depth of 336.42 m which is not shown in Figure 6-2 because of the logarithmic scale (the other flow rate was zero).

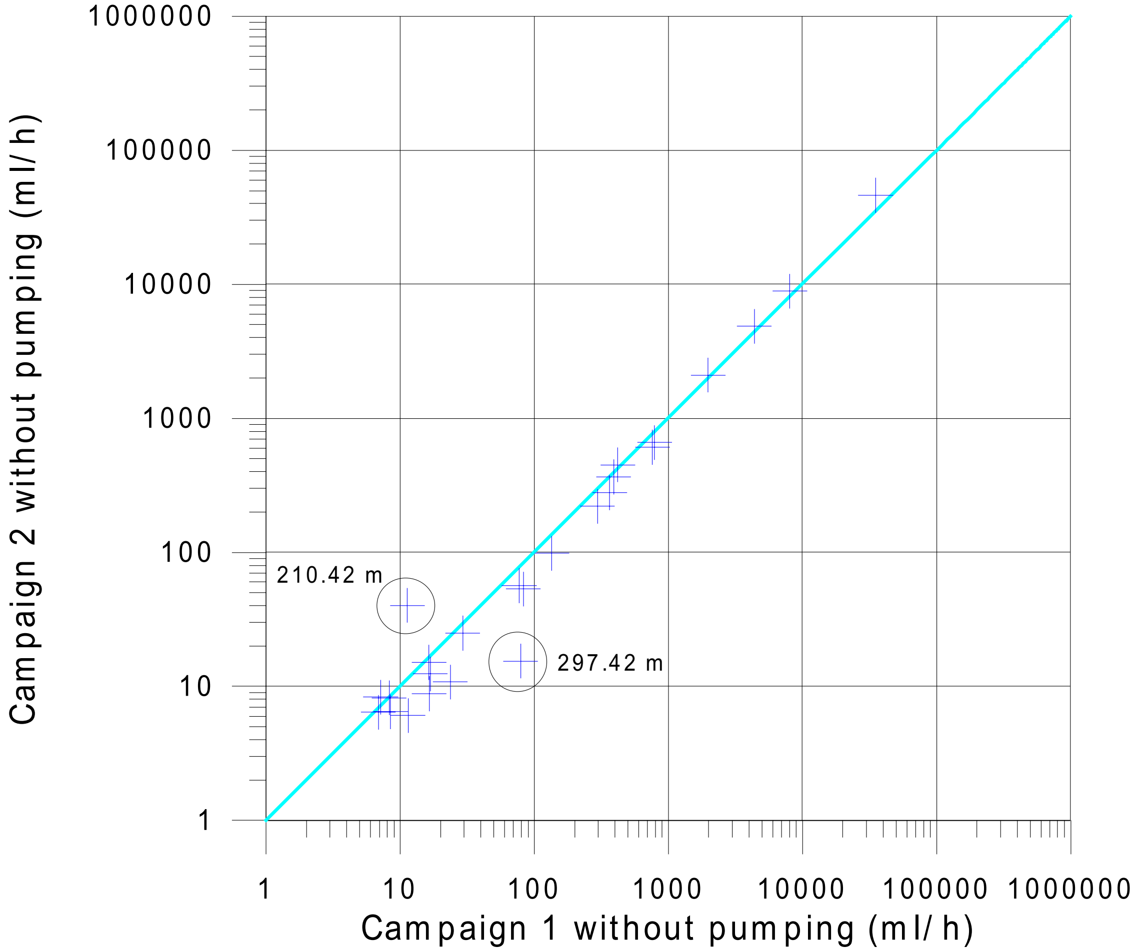

Figure 6-1. *Flow rates during sequential flow logging in Campaign1 and 2 without pumping.*

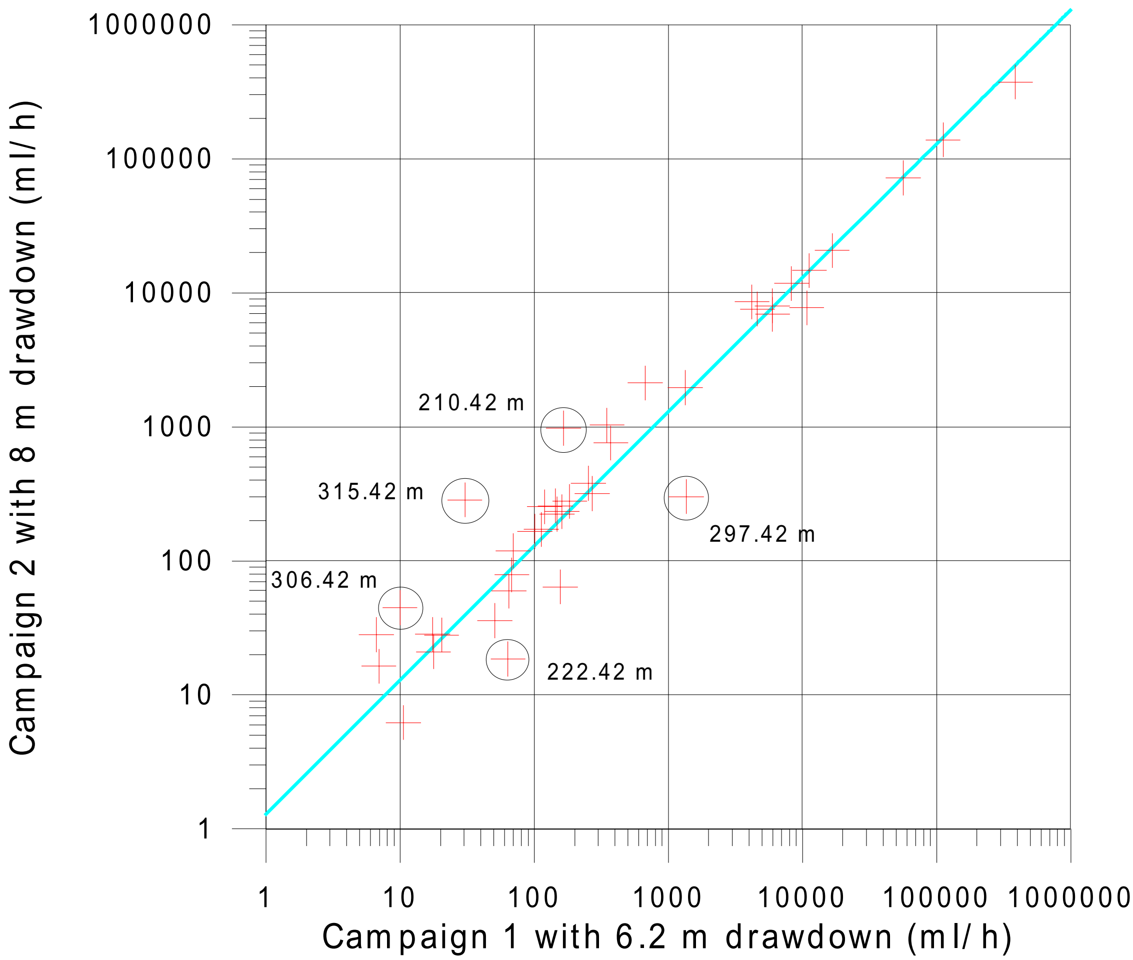

Figure 6-2. *Flow rates during sequential flow logging in Campaign1 and 2 with pumping.*

The drawdown of Campaign 2 was larger than that of Campaign 1. Therefore the flow rates of Campaign 2 should be larger by the factor of 8/6.2= 1.29 if the other conditions remain the same. The lines of equal theoretical flow rates are drawn in Figures 6-1 and 6-2.

One possible reason to the discrepancy is the depth shift between the measurements. This may be critical if there are flowing fractures at the ends of the section. The depths of Figures 6-1 and 6-2 are gathered to Table 6-1.

It was found that in all these cases there is a fracture near the section end, see Appendix 9 and 10 in Rouhiainen (2000). When there is a fracture near the lower end the flow rate in Campaign 2 was larger than in Campaign 1. Conversely, when there is a fracture near the upper end the flow rate in Campaign 1 was larger than in Campaign 2.

The probable explanation to the discrepancy of these depths is the depth shift. The cable was longer during Campaign 2 than Campaign 1. When a fracture was near the lower end it was within the section during Campaign 2 but not during Campaign 1. The opposite happened when the fracture was near the upper end of the section.

Table 6-1. Points of largest discrepancy between measured flow rates in sequential flow logging in Campaign 1 and 2 including the depth of a leaky fracture near the end of the section.

Depth (m)	Phase	Fracture depth (m) at the upper end of section from Appendix 13 in Rouhiainen (2000).	Fracture depth (m) at the lower end of section from Appendix 13 in Rouhiainen (2000).	Larger flow in Campaign 2 than Campaign 1
210.42	No pumping		212.0	Yes
297.42	No pumping	295.6		No
210.42	Pumping		212.0	Yes
222.42	Pumping	220.7		No
297.42	Pumping	295.6		No
306.42	Pumping		307.9	Yes
315.42	Pumping		317.1	Yes
336.42	Pumping		337.9	Yes

6.2 Length scale of measurements

The depth shift between the measurements can be studied on the basis of single point resistance anomalies. The results of a comparison are presented in Figure 6-3. The depth shifts of the various measurements are drawn relative to the sequential flow logging results of Campaign 1, without pumping, see Appendix 4. The maximum depth shift of the corresponding sequential flow logging with pumping was 0.15 cm. This depth shift is critical since it is assumed that the same sections are measured in both measurements.

The depth shifts of the overlapping flow logging in Campaign1 and Campaign 2 relative to the sequential flow logging of Campaign 1 were also studied. The maximum depth shift of the overlapping flow logging in Campaign 2 was 0.6 m. The depth shift seems to increase with time. The cable was longer during the later measurements. The cable was about three months old in February 2000 and borehole KLX02 was the longest ever measured with it. The cable was apparently stretched out during the measurements.

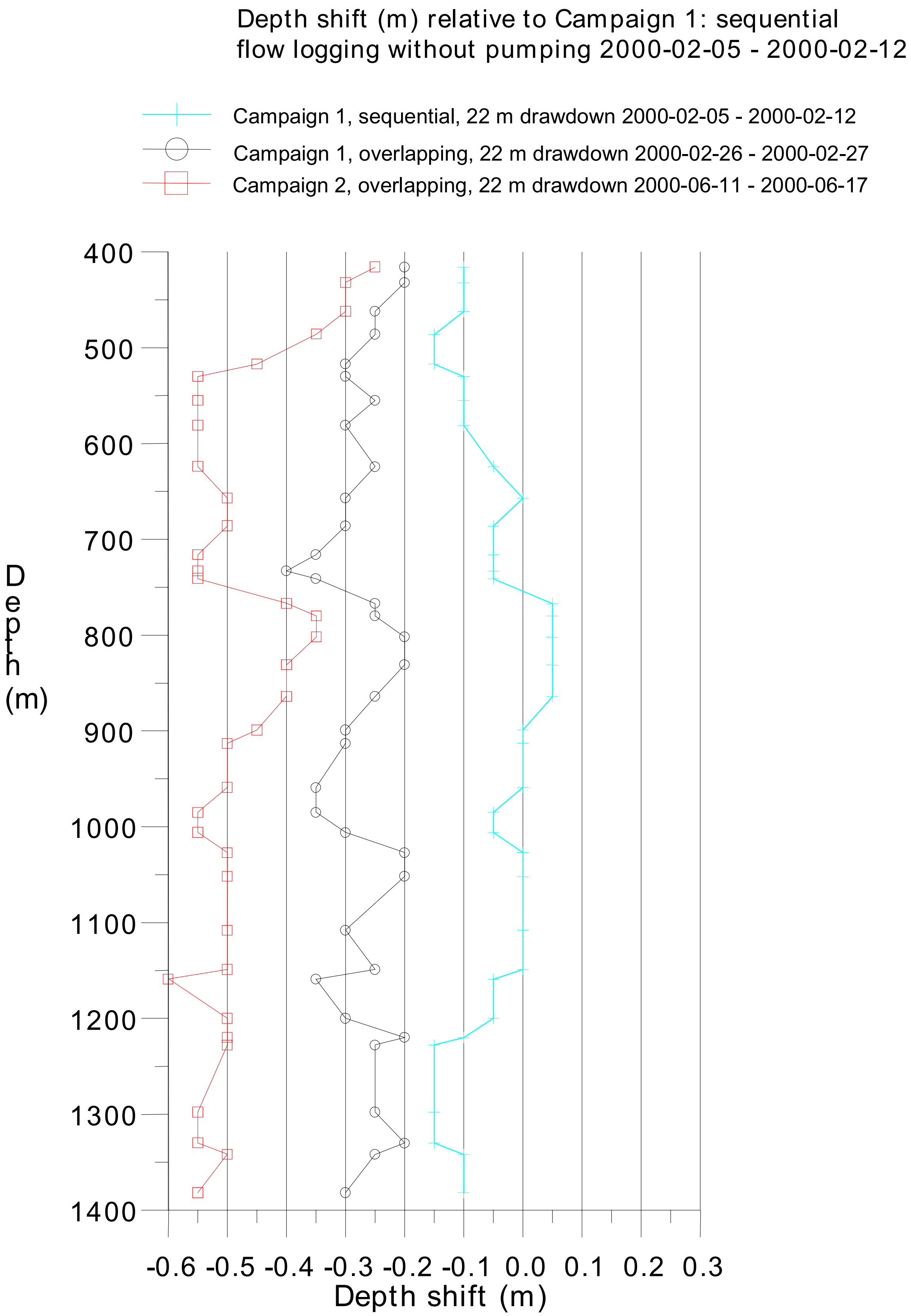

Figure 6-3. *Depth shift between different flow logging measurements in Campaign 1 and 2.*

6.3 Single-point resistance

Single point resistance is measured during the flow measurements in difference flow logging. The single point resistance curves to be compared were chosen from the overlapping flow logging in Campaign 1 and Campaign 2 when the borehole was pumped at 22 m drawdown, black and red curves, see Appendix 5. In February 2000, overlapping flow logging was performed between the depths of 363 m and 1,400 m with 3-m section length and 0.5 m depth increment. In June 2000, overlapping flow logging was made in the borehole between the depths of 200 m and 1,400 m with 0.5-m section length and 0.1 m depth increment.

The single point resistance is measured while the tool is moving. The speed of the overlapping flow logging was faster in Campaign 1 than in Campaign 2. Therefore there are less data points in the resistance curve in Campaign 1 than Campaign 2. The point interval in Campaign 1 was about two centimetres. In Campaign 2 it was less than one centimetre but all points within one centimetre were summed up to a single average value for each centimetre. This is one reason for the more noisy results of Campaign 1.

The base level of resistance (resistance at an intact part of the bedrock) between the depths of 363 m and 386 m was lower in Campaign1, especially between 365.6 m and 368.4 m, compared to Campaign 2. It is evident that something was stuck between the upper rubber disks and borehole wall in Campaign1, opening a way for electrical current to flow along the borehole. There is a clearly widened part in the borehole at the depth of 386 m. The object (or objects) had probably escaped there when the tool was moving downwards in Campaign 1.

The base level is about the same in both overlapping flow logging sequences above about 1,100 m (except the mentioned part). Below the depth of 1,100 m, there is lower resistance in Campaign 2 than in Campaign 1. The electrical conductivity (EC) of the borehole water was lower in Campaign 1 than Campaign 2 and there is a step to higher EC at the depth of 1,100 m. It is not fully clear whether this fact explains the difference in the base level of the single point resistance at the most saline part of the borehole. Another possible explanation could be material between the upper rubber disks and borehole wall in Campaign 2.

There is occasionally constant periods of disturbance of the base level in the resistance curves during both campaigns, for example between the depths of 1,240 m and 1,320 m. A similar disturbance can also be seen in the resistance curve during the overlapping flow logging at 22 m drawdown (Campaign 1) but not during the sequential flow logging without pumping (Campaign 1). This disturbance may be of instrumental origin rather than something in the borehole wall or bedrock.

The anomalies of the single point resistance are very similar in both overlapping flow logging sequences. There are only a few exceptions of this, one is at the depth of 467.5 m where two peaks in Campaign 1 were not visible in Campaign 2.

The resistance curves during the sequential and overlapping flow logging in Campaign 1 at 22 m drawdown (thin blue and black curves) follow each other closely if the depth shift between the curves would be corrected, see Appendix 4.

6.4 Electric conductivity of borehole fluid

The electrical conductivity of borehole water was measured several times during Campaign 1 and Campaign 2. In February 2000, sequential flow logging was performed between the depths of 200 m and 1,400 m without pumping. Flow, electric conductivity and temperature was measured in 3 m depth increments, see Appendix 3 and 4–5 in Rouhiainen (2000), respectively. In Campaign 2, corresponding EC-measurements were performed in the borehole interval 0–400 m. The electrical conductivity profile along the hole during sequential flow logging without pumping in Campaign 1 and 2 is shown in Figure 6-4. The borehole contained fresh water down to 1,160 m where the sharp boundary of saline water was met.

The upper part of the borehole was measured again without pumping in May 2000. The electric conductivity of the borehole water was anomalous in the casing tube between the depths of 30 m and 200-m. The electrical conductivity was nearly the same in May as in February between the depths of 200 m and 400 m.

The electric conductivity of the borehole water was also measured during overlapping flow logging at pumped conditions during Campaign 1 and Campaign 2, see figure 6-5. The borehole was measured in Campaign 1 at 22-m drawdown between the depths of 400 m and 1,400 m, using 0.5-m depth increments and 3 m section length and in Campaign 2 using 0.1-m depth increments and 0.5 m section length. In addition, in Campaign 2 the tool was stopped at conductive fractures for fracture-specific EC- measurements.

The pumping rate above 400 m was different in Campaign 1 than in Campaign 2 and the EC-results are not as well comparable there.

The electric conductivity of borehole water below 400 m was lower in Campaign 1 than Campaign 2. The electric conductivity was lower in Campaign 1 also at flowing fractures although the measured electric conductivity had hardly stabilised to a fracture-specific value that is apparently even lower than the measured one. This suggests that the borehole water and also the fracture-specific water had changed to more saline water with more pumping in Campaign 2.

The EC-electrode was calibrated before Campaign 1, between the two campaigns and after Campaign 2. The calibration function was kept unchanged on the basis of these calibrations. Therefore a change in calibration of the EC electrode is not a likely explanation to the difference of borehole EC values between Campaign 1 and Campaign 2.

The measuring geometry is well adapted to fracture-specific EC measurements but not well adapted to borehole EC-measurements. The tool may carry water from previous depths. This may cause noise-like behaviour in the EC-curve. This fact is more pronounced in the measurements of Campaign 1 than Campaign 2 because the section length (water volume within the section) was larger in Campaign 1. However, this fact does not explain the systematic difference explained above.

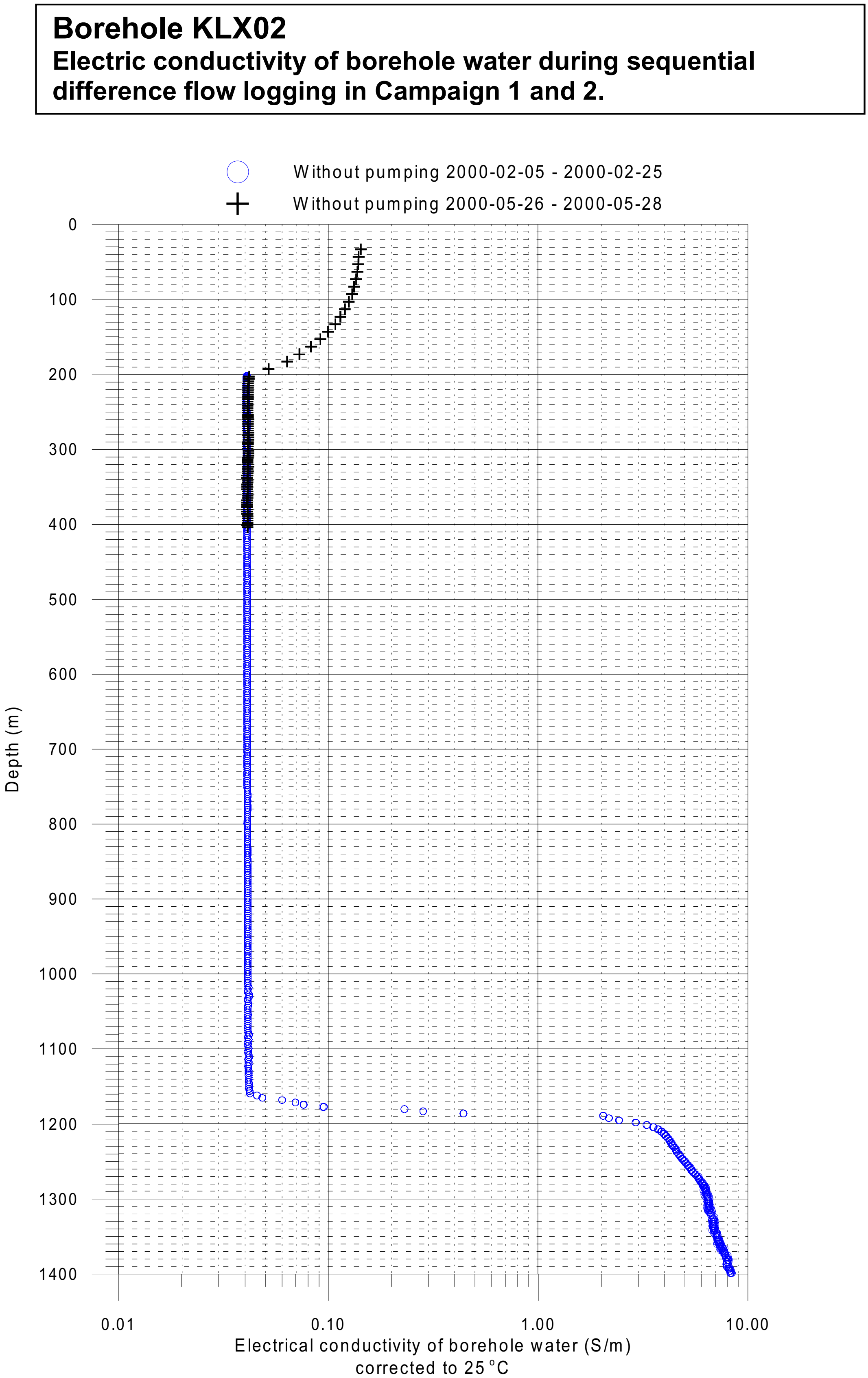

Figure 6-4. Electric conductivity of borehole water from sequential flow logging without pumping in Campaign 1 and 2.

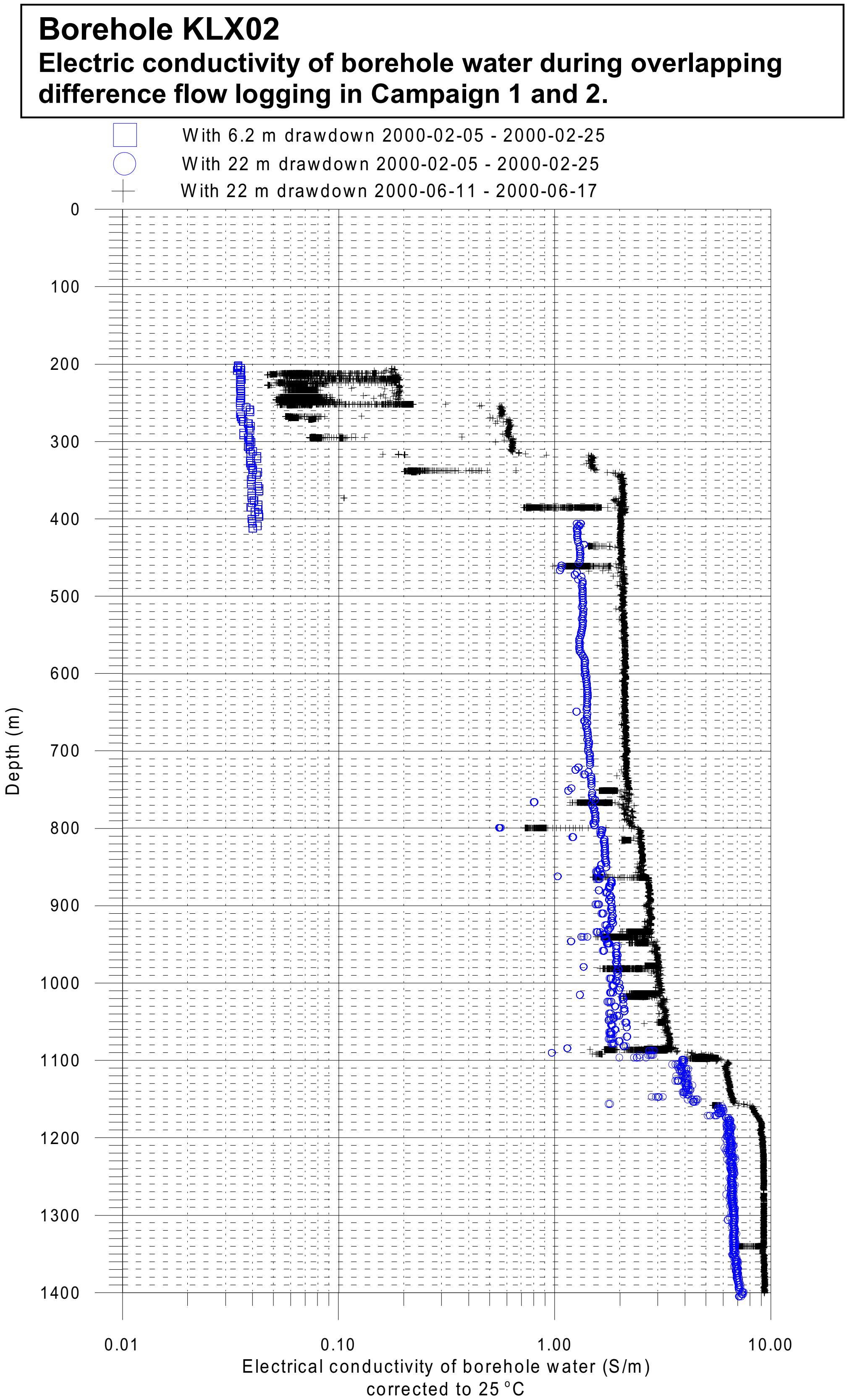

Figure 6-5. *Electric conductivity of borehole water from overlapping flow logging during pumping in Campaign 1 and 2.*

7 Fracture-specific electrical conductivity

The last values of the fracture-specific EC measurements are listed in Table 7-1. They are presented in the order they were measured. The first column is the depth of EC-measurement (upper rubber disks) and the next column is the depth of the fracture from which the measured water was sampled. The flow rate during the mentioned fracture is also given as well as the duration of the fracture-specific EC measurements. Both measured EC values and temperature-corrected EC values are presented. The EC values were corrected to 25 °C. No averaging because of noise has been applied. The reliability of the results may depend on the origin of water being measured, on the stability of EC with time and possibly, on the degree of noise in the EC results.

The origin of the measured water can be evaluated on the basis of the anomalies of flow, caliper (borehole diameter) and single point resistance. "1" denotes that the measured water was probably fracture specific water and "0" denotes that there is a risk that borehole water could have been mixed into the targeted fracture-specific water.

If the rubber disks, upper or lower ones, were on a widened part of the borehole the result was judged as "0". Caliper- and single point resistance anomalies were used in the judging. There is a depth shift between caliper- and single point resistance anomalies. In most cases this depth shift can be determined by comparing these two curves and the exact depth of the widened part of the borehole in relation to the rubber disks can be evaluated.

The shape of the flow anomalies in the plots was also used in reliability analysis since it is indicative of possible leaks at the rubber disks. A square, 0.5-m long anomaly indicates a good position for reliable measurement. Rounded flow anomalies and short spikes indicate a risk of leak.

The stability of EC of each transient EC-series was qualitatively analysed (Rouhiainen, 2000, Appendices 21 and 23), column "Transient stabilised". "1" denotes well stabilised and "0" denotes not stabilised EC values. The length of the measuring period was generally short, less than one hour. Therefore, possible long-term changes discussed in the previous Chapter cannot be seen in these transients. The stability of the transient series evaluated here is a measure of how well the water volume within the section was flushed rather than how representative water from fractures was measured. The stability of very noisy results can be questioned, however, they were judged as stable results if the average value seemed to be stable.

Noise in EC results was also evaluated. No noise in EC is more reliable and was denoted by "1". If noise was approximately three times higher than normal it was marked with "0" indicating noisy result. There is very high variation in degree of noise among these results classified with "0". The EC value itself was not used in the reliability evaluation although a fracture-specific EC value close to the EC value of borehole water may be a sign of a leak.

The following statistics can be calculated from Table 7-1:

- 69 depths for fracture-specific EC were measured.
- 41 of these (59%) were considered to be reliable when the origin of water was evaluated on the basis of the flow, caliper and single point resistance anomalies.
- Transient was stable in 58 cases of all 69 measured (84%).
- Transient was stable in 40 cases of those 41 ones where the origin of water was evaluated to be reliable (98%).
- The EC results were noiseless in 32 cases of all 69 measured (46%)
- The EC results were noiseless in 16 cases of those 41 ones where the origin of water was evaluated to be reliable (39%). If gas in gas form is the reason for the noise 61% of fracture-specific samples contained gas bubbles.

The target fractures were chosen automatically and a part of depths was not favourable for fracture-specific measurement. Evaluation of reliable depths is partially subjective and there is a need for more quantitative criteria for reliability. It is clear that with larger section length it would be possible to obtain larger percentage of reliable fracture-specific measurements. The expense of this is elongated measuring time because it needs more time until the larger section volume is flushed well enough.

The transient was stable in most of the measurements, 84% of all and 98% of the reliable ones. In other words only 2 % of the reliable ones but 36 % of the unreliable ones were unstable. Therefore a leak at the rubber disks seems to be the most important reason for instability. The used flushing duration for water volume (three times of the section volume 0.5 l) was long enough for the cases of good tool position.

A probable reason of the random-like noise is gas. Since gas is electrical insulator it possibly tends to decrease the measured EC value. Larger gas bubbles moving through the EC electrode can cause level changes and instability with time.

The fracture-specific EC values are plotted as a function of depth, see Figure 7-1. Only those points of Table 7-1 were plotted which were considered reliable (Fracture specific water =”1”). There seems to be correlation between flow rate and the measured EC value. For example, the fractures at the depth of 1,092.1 m have lower EC than the fractures above and below it, see Table 7-1. The flow rate of the fracture at the depth of 1,092.1 m is much higher than the flow rate of the other fractures

Table 7-1. Fracture-specific EC results in borehole KLX02. For explanation, see text.

EC Measuring Depth (m)	**Fracture Depth (m)**	**Flow (ml/h)**	EC measuring time (min)	Tempe-rature °C	EC (S/m)	Temp. corrected EC (S/m)	Fracture specific water	Transient stabilised	No noise
385.30			12	13.19	0.921	1.210	0	0	1
435.43	435.6	10656	12	13.89	1.119	1.445	1	1	1
461.00	461.30	2682	36	14.29	0.921	1.178	1	1	0
751.29	751.5	2230	42	18.83	1.446	1.658	1	1	0
766.46	766.8	2600	38	19.06	1.294	1.476	1	1	0
799.62	800.0	15187	12	19.51	0.811	0.916	0	0	1
815.62			22	19.88	2.013	2.253	0	0	1
863.12	863.5	5080	20	20.59	1.447	1.593	1	1	0
863.52			22	20.69	2.455	2.698	0	1	1

Table 7-1 cont.

933.52	934.0	1500	59	21.78	2.318	2.486	0	1	0
940.42	940.6	2200	41	21.89	1.689	1.806	1	0	0
948.12			21	22.04	2.539	2.707	0	0	1
977.72	978.2	1000	10	22.49	2.815	2.971	0	0	1
981.42	981.7	2900	31	22.57	1.905	2.008	1	1	0
1013.72	1013.9	1890	47	23.09	2.367	2.466	1	1	0
1017.72	1017.9	2250	40	23.17	2.517	2.619	1	1	0
1050.72	1051.0	1500	59	23.66	2.966	3.053	1	1	0
1085.12			38	24.09	2.810	2.866	0	1	0
1085.52			36	24.10	2.828	2.884	0	1	0
1085.92	1086.2	8000	13	24.09	1.707	1.741	0	1	0
1086.32			17	24.10	2.477	2.525	0	1	0
1086.72			42	24.12	3.040	3.099	0	1	0
1091.82	1092.1	25000	12	24.15	1.627	1.658	1	1	1
1096.02	1096.4	2000	44	24.27	4.814	4.892	1	1	0
1096.82			53	24.30	5.465	5.549	0	1	0
1097.42	1097.7	2700	34	24.28	4.809	4.885	1	1	0
1158.02	1158.2	9500	12	25.26	5.524	5.496	1	1	0
1340.22			12	28.36	9.778	9.128	0	0	1
1340.62			47	28.40	9.972	9.303	0	1	1
211.72	212.0	2964	34	10.75	0.041	0.058	1	1	0
213.12	213.3	158662	12	10.42	0.034	0.048	1	1	1
213.52			12	10.44	0.033	0.047	0	1	1
213.92	214.0	16757	12	10.89	0.132	0.184	0	1	1
214.82	215.2	5031	22	10.74	0.046	0.065	1	1	0
224.02	224.4	12542	10	10.78	0.038	0.053	1	1	0
225.62	226.0	6625	16	10.79	0.047	0.066	1	1	0
227.32	227.7	30680	12	10.66	0.034	0.047	1	1	1
233.52	233.9	5337	19	10.84	0.046	0.064	1	1	0
242.92	243.3	2870	45	10.91	0.051	0.072	1	1	0
243.32	243.8	714	35	10.88	0.049	0.069	1	1	0
246.32	246.7	22150	12	10.79	0.037	0.051	1	1	1
247.72			27	10.88	0.048	0.067	0	1	0
248.12	248.6	15479	12	10.82	0.039	0.054	1	1	0
248.52			12	10.84	0.061	0.085	0	0	1
248.92	249.2	1623	22	10.84	0.056	0.078	0	1	0
251.02	251.3	458764	12	10.76	0.049	0.068	0	1	1
251.42	251.6	111455	12	10.88	0.049	0.068	0	1	1
251.82			38	11.48	0.157	0.215	0	1	0
252.62	252.9	41867	12	11.07	0.039	0.054	1	1	1
253.02			12	11.14	0.042	0.058	0	1	1
267.62	268.0	16905	12	11.45	0.041	0.057	1	1	1
269.52	269.7	7977	13	11.56	0.043	0.059	1	1	1
270.72	271.1	36168	12	11.38	0.056	0.077	1	1	1
271.12			29	11.52	0.054	0.075	0	0	0
294.72	295.1	30324	12	11.68	0.054	0.073	1	1	1
295.12			12	11.68	0.060	0.082	0	0	0
295.52	295.6	4393	23	11.79	0.075	0.102	1	1	1
316.72	317.1	452519	12	11.90	0.139	0.189	1	1	1
317.12			12	11.91	0.149	0.202	0	1	1
337.62	337.9	9576	11	12.38	0.157	0.210	1	1	1
338.62	338.9	12983	12	12.30	0.163	0.220	1	1	1
339.02	339.1	34185	12	12.27	0.177	0.238	1	1	1
339.42	339.6	7170	16	12.42	0.170	0.228	1	1	1
385.32			12	13.21	1.256	1.649	0	0	1
724.6	724.6	900	104	18.45	1.941	2.245	1	1	0
732.32	732.6	300	342	18.58	2.001	2.307	1	1	0
772.3	772.3	380	275	19.21	2.019	2.294	1	1	0
796.32	796.7	400	247	19.56	2.061	2.323	1	1	0
812.42	812.7	1000	102	19.83	1.938	2.171	1	1	0

Similar case is between the depths of 700 m and 850 m, see Figure 7-1. The blue points were measured as last points in the Campaign 2. They are all fractures with low flow rate. The measured EC value was higher in these points than in the fractures nearby measured earlier.

The observations above seem to suggest that water is more saline in fractures of smaller transmissivity. The borehole has been open a long time and fresh water flowed into the fractures between the depths 200-m and 1,400-m. The amount of fresh water flow into the fractures depends on transmissivity and freshwater head of the fractures. Therefore, the surface water apparently not equally affected them.

Later on, fracture-specific EC-measurements of the Loviisa, Olkiluoto and Laxemar sites were re-evaluated. Often measurements of very low-flow fractures have fracture-specific EC close to borehole- (background-) EC. It seems to be the case too often, these results are apparently questionable. The limit is approximately 2 l/h, below this value the fracture-specific EC are probably not reliable. This has to be taken into account when using the data.

The probable reason is mixing of fracture- and borehole waters near the EC electrode (but not a leak at the rubber disks). The electrode has to be open to allow flow. The drawback is possible mixing with borehole water of much higher flow rate. The reason can be tested and the construction possibly improved.

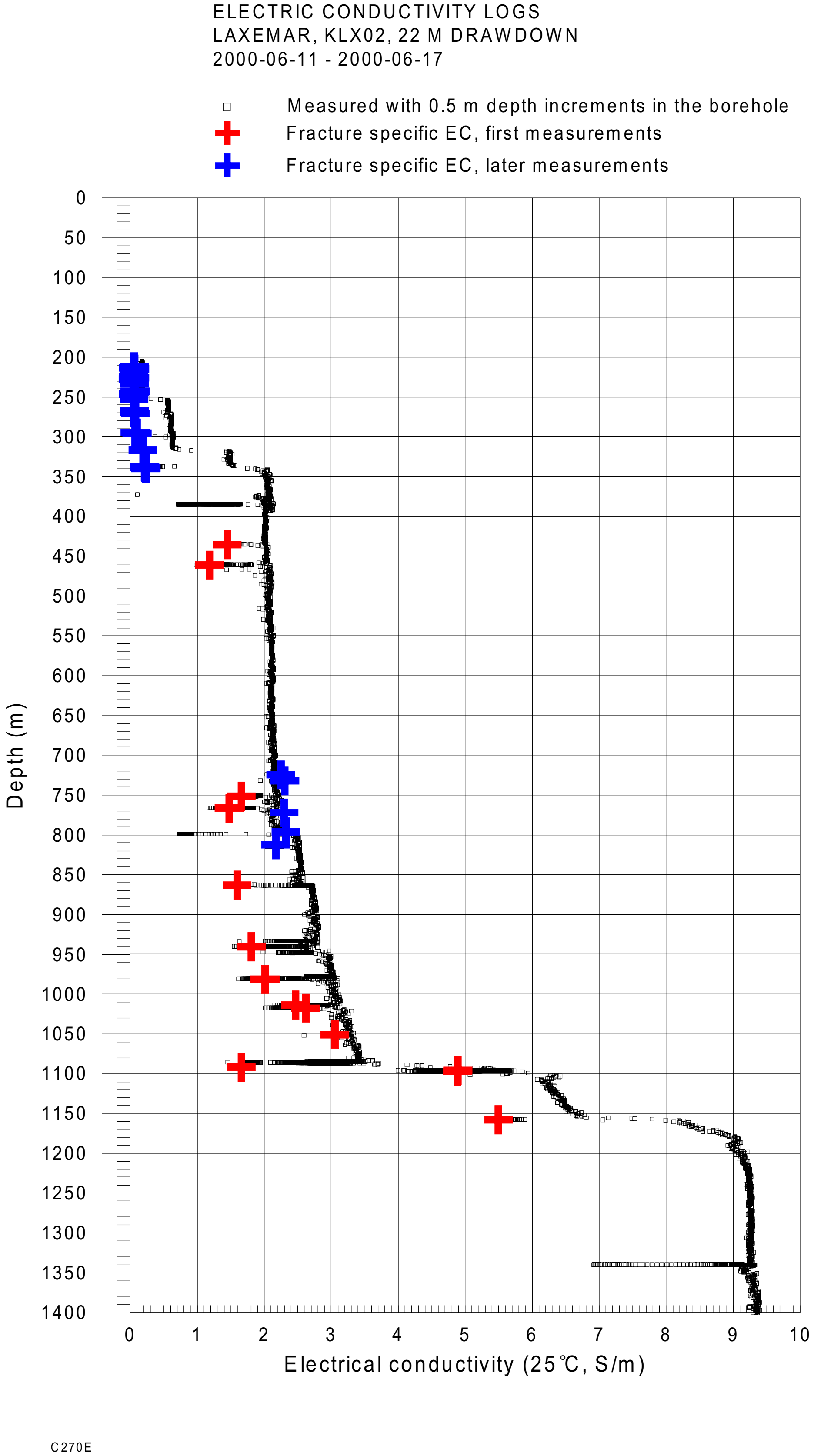

Figure 7-1. *Fracture-specific EC results, only those points are plotted which were judged as reliable in Table 7-1 (Points for which fracture-specific water ="1").*

8 Potential uncertainties of difference flow logging

8.1 Untight rubber discs

In order to identify as many flowing fractures along the borehole as possible, a rather short section length is generally selected in the overlapping-flow logging. However, as discussed in Section 4.2, measurements with a short section length can be misleading where the borehole wall is in "bad" condition (e.g. due to cavities) longer than the section length, see e.g. the depths of 219 m and 385 m in Appendix 1. No flowing fractures are interpreted at these depths in Appendix 1. However, the interpretation may be uncertain due to long cavities along the hole (c.f. the caliper log) which may cause leakage. According to the core mapping results in Stanfors et al. (1997, p. 81), the rock is tectonized at 219 m with increased fracture frequency. At c. 385 m, a crush zone associated with a greenstone vein is present with a significant increase of fracture frequency. Several other crush zones are interpreted along the hole. This problem is discussed in more detail in the next section.

Sometimes there are leaks when the rubber disks, upper or lower, are at the widened position in the borehole. When the widened part is between the upper and lower rubber disks, the flow can be correctly measured. This kind of case is at the depth of 732. 6 m. The leaks can be seen as peaks of flow anomaly (Appendix 18 in Rouhiainen 2000). The bedrock is very fractured and the borehole is partially widened between 800–960 m. However, the flow anomalies look mostly good except at the depths of 816, 865, 934 and 948 m.

Possible flow anomalies in which leaks may have occurred may be identified in the linear plots between flow and drawdown in Appendix 2. Moreover, Figure 4-5 indicates that the cumulative specific flows from 0.5-m sections were slightly higher than the flows from the corresponding 3-m sections, which may possibly indicate small leakages. In particular, at c. 219 m, where the rock is tectonized, the former values were significantly higher.

8.2 Noise in the base-flow level

As discussed above, "noise" in the base-flow level was observed in the overlapping flow logging at 22-m drawdown, especially during the combined flow rate/EC measurements at certain flow anomalies, see Appendix 18 in Rouhiainen (2000).

As can be seen in Table 3-4, most depths at which the base-flow level changed abruptly, corresponds to interpreted flowing fractures with high inflow rates and transmissivity. In addition, large single point resistance anomalies occur at these depths, see Chapter 5. In fact, most of these depths at which the base-flow level changed distinctly are interpreted as crush zones with distinct increase of the fracture frequency in the geological interpretation of KLX02 (Stanfors et al., 1997).

In Table 8-1, depths at which major changes of the base-flow level occurred during the combined overlapping flow- and EC-logging at 22-m drawdown, are listed. In addition, the corresponding depths of interpreted flowing fractures from the overlapping flow logging according to Appendix 13 and 18 in Rouhiainen (2000) together with their approximate flow rates and geological interpretation according to Stanfors et al., 1997, is shown in the table.

Table 8-1. Depths at which major changes of the base-flow level (Q_{min}) occurred together with the corresponding depths of interpreted flowing fractures, their flows and geological interpretation.

Depth at major change of Q_{min} (m)	Change in Q_{min} (ml/h)	Flow anomaly (m)	Flow (ml/h)	Geological character
c. 252	20→100	251.3	$4.6 \cdot 10^5$	Crush zone
"	"	251.6	$1.1 \cdot 10^5$	"
c. 318	100→300	317.1	$4.5 \cdot 10^5$	Fracture fill of iron
c. 340	300→500	339.1	$3.4 \cdot 10^4$	Crush zone
c. 386	500→20	(385.4)	$1.5 \cdot 10^4$	Crush zone (60 fr/m)
c. 437	20→80	436.1	$1.0 \cdot 10^4$	Crush zone
c. 462	30→800	461.3	$3 \cdot 10^3$	Oxidised rock
c. 467	700→500	467.3	$1.5 \cdot 10^3$	Crush zone
c. 752	100→500	751.5	$2 \cdot 10^3$	Crush zone
c. 767	300→600	766.8	$3 \cdot 10^3$	(Crush zone at c. 760 m)
c. 801	150→50	800.0	$1.5 \cdot 10^4$	Crush zone, oxidised
c. 813	50→200	812.7	$1 \cdot 10^3$	Crush zone
c. 817	200→80	(816.2)	$4 \cdot 10^3$	Crush zone
c. 864	300→30	863.5	$5 \cdot 10^3$	Crush zone
c. 913	100→200	912.6	$9 \cdot 10^2$	Altered rock, Crush zone at 908 m
c. 935	300→600	934.0	$4 \cdot 10^3$	Crush zone
c. 950	600→200	(949)	$5 \cdot 10^3$	Crush zone
c. 979	100→40	978.2	$9 \cdot 10^3$	Crush zone
c. 982	40→800	981.7	$4 \cdot 10^3$	Crush zone
c. 1014	300→700	1013.9	$2 \cdot 10^3$	Crush zone at 1016 m
c. 1087	500→1000	1086.2	$1 \cdot 10^4$	Crush zone, rock contact
c. 1342	300→40	(1341)	$3 \cdot 10^4$	Parallel fracture (BIPS)

N.B. Values within brackets may be uncertain and possibly affected by leakage.

As indicated in Table 8-1, the changes in the base-flow level generally occurred just below the interpreted flow anomalies. The flow loggings were made downward through the hole. In the borehole intervals between the flow anomalies, the base-flow level changed gradually to certain depths at which it then stayed almost constant for long borehole intervals. At most of the flow anomalies, the base-flow level increased, but at certain depths, e.g. c. 385 m and c. 1342 m, the flow rate decreased across the anomalies. Table 8-1 shows that the depths of major changes of the base-flow level in most cases correspond to interpreted crush zones. In these zones the base-flow rates generally increased, particularly between c. 200–320 m. Small increases of the base-flow rate occur at lower depths.

At some depths (within brackets), relatively big changes of the base-flow rate occur but no flow anomalies are interpreted at these depths in Rouhiainen (2000). The flow rates at these depths, shown in Table 8-1, may be uncertain. Furthermore, relatively large increases of the borehole diameter are measured at these depths from the caliper log. Thus, the reliability of flow logging in short sections in these intervals may be questioned due to the risk of leakage at the rubber discs, particularly if the actual flow in the zones is high. At c. 385 m, open, potentially conductive fractures are interpreted from borehole TV-(BIPS) images (Carlsten et al. 2001). On the other hand, there is no certain information from other sources of the actual flow rate at these depths. The overlapping flow logging with 3-m section length did not either show clear flow at these depths. Also these measurements are uncertain if the borehole is widened longer than 3 m. This was the case at c. 385-m.

Another problem with the noise, i.e. changes in the base-flow rate, is that certain minor flow anomalies may be masked by an increased base-flow to c. 1,000 ml/h at some borehole intervals. Since there is a good correlation between inflow zones and changes of the background level of flow, the changes must probably depend on the character (chemical/physical composition, gas content etc.) of the in-flowing water from the fractures. The changes also depend on the magnitude of inflow since the noise only appears during the logging at 22-m drawdown. The noise probably also depends on the duration of the flow measurements at each fracture, which was longer for the 22-m logging due to the EC-fracture measurements.

One possible reason for the noise at 22 m drawdown is gas in the water from some fractures (Rouhiainen, 2000). All the measurements were carried out downward. At 22-m drawdown, more gas might enter into the test section because of the higher pumping rate and because the tool was stopped on some fractures for the fracture specific EC measurements. The gas could possibly escape from the section when the upper rubber disks arrived to the widened part of the borehole at the large caliper anomalies.

At all depths mentioned above (within brackets in Table 8-1), and at most depths, the base-flow levels increased. There are also depths where the base-flow levels decreased. A common thing at the latter depths is the increase of the borehole diameter. This seems to support the assumption of gas as a noise source in these cases. Gas bubbles could possibly escape from the flow guide at depths where the borehole was widened and the rubber disks were not tight.

Similar noise behaviour was seen earlier at the Olkiluoto site in Finland. There, the combined overlapping flow logging/EC measurements were carried out from the bottom upward. Increased noise level was obtained above some fractures where fracture specific EC was measured (Rouhiainen 2000).

There are some observations that are against the assumption of gas as a noise source. The noise level of flow does not always increase at those fractures where there is noise in EC results. There are also a few such cases where the noise level of flow increases even if there is very little noise in the EC results. Nevertheless, the reason for the increased noise in flow seems to be a property of the water that comes in from some fractures and is flushed away where the borehole is clearly widened. The reason for this kind of noise is not completely clear. The feature causing noise in EC and noise in flow may not necessarily be the same (Rouhiainen 2000).

A known source of noise is muddy water. This has been found mostly in such boreholes, which have low transmissivity at depth. They are therefore difficult to clean from the drilling mud. In such cases the noise level may be high at depth, even without pumping.

Another potential source of noise may be the significantly different chemical and physical properties of waters in flowing fractures and in the borehole at the same depth, e.g. density and viscosity. The effects of these differences on the flow measurements should be investigated further.

The results from the difference flow logging can only to some extent be compared with previous flow logging (UCM) and hydraulic tests. The previous UCM-logging was relatively unstable and showed a big data scatter (c. 5 l/min) in the flow measurements, which may mask smaller flow anomalies. However, at c. 385 m the mean flow increases (c. 5 l/min) but decreases above this depth, possibly depending on the enlargement of the hole at this depth, c.f. caliper log. Hydraulic tests have only been performed in long sections in KLX02, but the resolution is insufficient to compare with the results from the flow logging. Thus, to resolve the uncertainties of the flow logging in some of the interpreted crush zones, hydraulic tests, e.g. injection tests, should be made in relatively short sections, or alternatively, another type of flow logging.

8.3 Changes in fluid density along the hole

In surface boreholes, difference flow measurements can be performed during natural conditions without pumping and when the borehole is pumped at a constant drawdown. The hydraulic head along the borehole is then assumed to be constant since the hydraulic conductivity of the borehole is very high compared to the conductivity of the bedrock. Constant hydraulic head along the borehole implies that the water density in the hole is constant (both under natural conditions and during pumping) and that there are no losses due to friction.

If the water density is not constant, as in KLX02, the hydraulic head at the measuring depth needs to be determined. Since the density of saline water is higher than density of fresh water, the fresh water head should be measured in such cases. In cases of saline water, the term fresh water head is used instead of hydraulic head, since hydraulic head is not well defined in saline conditions (Rouhiainen 2000).

In Campaign 2, the electric conductivity of the borehole water was measured during different drawdown conditions. In the interval 200–400, only minor increases of the electric conductivity occurred at drawdowns ranging from 0 to 8 m, see Appendix 16 in Rouhiainen (2000). At 22-m drawdown, EC started at c. 0.2 S/m at 205 m, increasing to c. 0.6 S/m below the flowing fractures at c. 251 m and to c. 1.5 S/m below the flowing fracture at c. 317 m. Then EC slightly increased to c. 2 S/m at 400

m. At 1,400 m, EC of the borehole water was c. 10 S/m, see Appendix 18 in Rouhiainen (2000).

8.3.1 Measurements of fresh water head profiles

During Campaign 1, the fresh water head profile along the borehole was measured, both without and with pumping the borehole, respectively. The head measurements were made by filling a tube, inserted in the borehole, with tap water. The bottom of the tube was lowered to 1,406 m. The valve at the lower end of the tube was then opened and the water level in the tube was measured at different depths in this way, e.g. every 100 m, and compared with the groundwater level in the hole. For example, the relative fresh water head at 1,400 m was c. 7 m without pumping, i.e. the water level in the tube was 7 m higher than the groundwater level in the borehole due to saline water at depth, see Appendix 1 in Rouhiainen (2000). Fresh water head measurements in the interval 400–1,400 m was also made after pumping with c. 55 l/min.

8.3.2 Calculations of fresh water head profiles

An attempt was made to calculate the relative fresh water head along the hole after pumping with c. 55 l/min and compare with the measured one. The hydrostatic pressure P_s along the hole may be calculated from the measured electrical conductivity in 3-m sections in Campaign 1 as follows:

$$P_s = \Sigma(\rho_{wi} \cdot g \cdot L_i) \qquad (8\text{-}1)$$

ρ_{wi} = water density (kg/m^3) in section i
g = acceleration of gravity (g=9.81 m/s^2)
L_i = length of borehole section i (m)

The water density was based on an empirical relationship between electric conductivity at Äspö:

$$\rho_w = 0.9972 + 4.6 \cdot 10^{-6} \cdot EC \text{ at } 25°C \qquad (EC \text{ in mS/m}) \qquad (8\text{-}2)$$

The water density was then corrected according to the measured temperature in the 3-m sections (ρ_{wi}). The hydrostatic pressure profile along the hole was then calculated at pumping with c. 55 l/min ($P_{s,\ pump}$). To compare this profile with the measured one, the hydrostatic pressure was converted to fresh water head ($H_{f,pump}$) according to the following relationship:

$$H_{f,\ pump} = P_{s,\ pump} / \rho_f \cdot g \qquad (8\text{-}3)$$

$H_{f,\ pump}$ = freshwater head (m) at pumping
ρ_f = density of fresh water (kg/m^3), temperature corrected

Furthermore, the head difference between the actual freshwater head profile ($H_{f,\ pump}$) at a certain depth and an equivalent freshwater column from the groundwater level in the hole to the actual depth ($H_{f,\ eqv}$), was calculated as:

$$dH_f = H_{f,\ pump} - H_{f,\ eqv} \qquad (8\text{-}4)$$

The calculated relative fresh-water head (dH_f) was plotted versus depth together with the measured relative fresh water head in Figure 8-1. At the upper part of the borehole, the relative freshwater head profile corresponds to the drawdown of the groundwater level in the hole. The agreement between the calculated and measured head is rather good down to c. 1100 m but deviates then at depth. At 1400 m, the deviation is c. 6 m. The deviation may depend on non-representative conversion formula between density and electric conductivity, errors in measured EC or calculation errors. However, the calculations show that it may be possible to estimate the relative freshwater head profile along the hole if no head measurements are carried out, provided that proper EC-measurements are available.

Fresh water head calculations from the borehole EC measurement may be useful because it is faster than fresh water head measurement with fresh water tube. The possibly non-representative conversion formula between density and electric conductivity (Eqn. 8-2) could be improved by calibration in borehole, i.e. the constants in Eqn. (8-2) can be adjusted if both borehole EC and fresh water head measurement with fresh water tube have been carried out in the same borehole. In this way the amount of measurements with fresh water tube could be decreased.

One problem in fresh water head calculation from the borehole EC measurement is muddy water. Solid particles may increase density of water. This cannot bee seen by EC measurements and it is therefore a source of error in muddy boreholes.

Another alternative is to measure the hydrostatic pressure at each measuring section. This requires a pressure transducer with a high resolution and accuracy attached to the measuring probe, e.g. quartz crystal gauge.

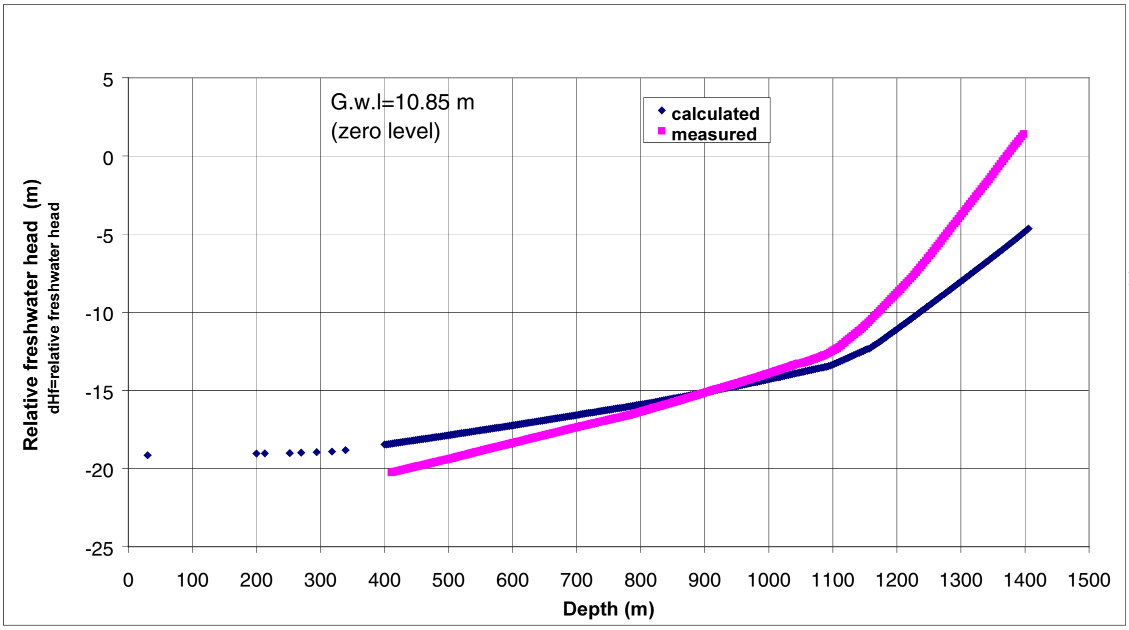

Figure 8-1. *Comparison of measured and calculated relative fresh-water head along borehole KLX02 at stop of pumping with Q=55 l/min in Campaign 1.*

8.4 Potential errors in calculated transmissivity

The transmissivity of flowing fractures may be calculated by Eqn. (2-6). It is based on the differences of flow in a borehole section at two different drawdowns. The error in the flow measurements is ±10 %. Thus, the maximum error in the difference between two flows is ±30 %, which affects the calculated transmissivity to a varying extent depending on the ratio of the measured flows.

In Eqn. (2-6) the factor $\ln(R/r_0)$ is included, in which R is the radius of influence and r_0 is the borehole radius. It is generally assumed that this factor is constant which means that the radius of influence is constant in all sections along the hole. In this case R/r_0 is assumed to be 500 and thus $\ln(R/r_0)=6.2$. Since the borehole radius is 0.038 m, the radius of influence is 19 m. If R is assumed to vary between 1–100 m, the factor $\ln(R/r_0)$ varies between 3.3 and 7.9. With these assumptions the transmissivity could vary from – 47 % to + 27 % due to this factor. If R is assumed to vary between 10–100 m, the corresponding potential error in transmissivity is c. ± 20% in this case.

Furthermore, since Eqn. (2-6) is based on radial flow, a linear relationship between flow and drawdown is assumed. This is not always the case as discussed in Section 4.5.2, together with potential sources of non-linear flow. However, the effect of this factor on the transmissivity calculations is difficult to quantify and may also depend on the source to non-linear flow. However, all methods based on radial flow (without head losses) suffer from this limitation.

The transmissivity calculation also depends on the difference in hydraulic head (drawdown) applied in the borehole. For non-saline conditions, the error in drawdown values may be negligible (within a few percent) but for saline conditions the errors may be substantial towards the bottom of the hole, c.f. Section 8.3. This is well demonstrated during the freshwater head measurements along the hole with pumping in Campaign 1.

Near the surface, the freshwater head difference in the borehole was c. 20 m during pumping but at c. 1400-m depth the head difference decreased to c. 5.5 m, c.f. Appendix 1 in Rouhiainen (2000). If the freshwater head profile is measured along the hole the actual head difference along the hole should be used in Eqn. (2-6). However, if no head measurements were carried out and a constant head difference of c. 20-m was used along the hole, an error in transmissivity at c. 1400-m depth of a factor of c. 3.6 had been the case. This example demonstrated the importance of performing head measurements along the hole.

As discussed in Section 8.1, another potential source of error in transmissivity is of conceptual nature and depends on the actual borehole conditions. For example, in fractured intervals, the borehole walls may be in bad condition due to caving etc. which may cause leakage at the rubber discs, possibly resulting in incorrect flow measurements. This kind of error depends on the actual situation and cannot be quantified in a general sense.

Finally, as discussed in Section 8.2, noise in the base-flow level may affect the flow measurements and decrease the resolution of the flow measurements. This fact may affect the transmissivity calculations in low-conductive sections due to masking of anomalies with small flows if the base-flow level is increased.

9 Design of measurement programs

9.1 Duration of flow logging sequences

The total duration spent in one flow measurement consists of the time of the flow measurement itself and the time while the tool is staying at the target position and finally, the time of moving the tool to the next depth. In sequential flow logging, both the thermal pulse- and thermal dilution method are used as discussed in Section 2.2.1. In overlapping flow logging, only the thermal dilution method is used which makes the measurements faster but less sensitive to small flows.

The statistics in Table 9-1 are derived from the methodology test in Campaign 2. For comparison, one overlapping flow logging sequence from Campaign 1 is also included. In Campaign 2 there were some problems with data communication before the reason to it was found. It delayed some of the Campaign 2 measurements. These delays were not taken into account in Table 9-1, nor preparations, installations etc.

The speed of sequential flow logging with 3-m depth increments (step length) is about 11 m/hour. The speed of overlapping flow logging with 0.5-m depth increments is about 20 m/hour. The speed of the corresponding measurements in Campaign 1 was much faster, 67 m/hour. The duration of the flow measurement itself (when the tool was staying at the depth of measurement) was the same in these two cases, about 15 seconds. The large difference of the total speed is because the tool was moved faster in Campaign 1 and because EC-fracture was not measured in Campaign 1. It is not fully

Table 9-1. Compilation of the actual duration and speed of one flow logging sequence in one direction in sequential- and overlapping flow logging, respectively during Campaign 2 and -1 in KLX02.

Mode	Depth intervals (m)	Number of flow measurem.	Average duration of one logging sequence (min)	Speed of measurement (m/hour)
Campaign 2				
Sequential flow logging, L=3 m, dL=3 m, without pumping	210–411	68	15.79	11.4
Sequential flow logging, L=3 m, dL=3 m, at 8 m drawdown	210–414	69	15.89	11.3
Overlapping flow logging, L=3 m, dL=0.5 m, without pumping	210–412	405	1.70	17.6
Overlapping flow logging, L=3 m, dL=0.5 m, at 8 m drawdown	207–440	475	1.33	22.6
Overlapping flow logging, L=0.5 m, dL=0.1 m, without pumping	210–413	2021	0.48	12.5
Overlapping flow logging, L=0.5 m, dL=0.1 m, at 8 m drawdown	212–418	2061	0.53	11.3
Campaign 1				
Overlapping flow logging, L=3 m dL=0.5 m, at 22 m drawdown	370–1413	2087	0.45	66.7

known how much this fast movement disturbed the flow conditions. The fast movement of the tool may cause pressure transients. The overlapping flow logging in Campaign 1 was used for the first time for fast checking of the sequential flow logging results.

The speed of the overlapping flow logging with 0.1-m depth increments is about 12 m/hour. The corresponding flow logging in Campaign 2 was carried out more carefully in the way the method is normally used.

9.2 Measurement limits

9.2.1 Lower limit

Based on the results of the methodology study, the lower measurement limits in Table 9-2 may be proposed for sequential- and overlapping difference flow logging, respectively. However, the measurement limits are somewhat subjective and may depend on the actual test conditions in the borehole. As described above, a sequential flow logging consists of combined thermal pulse- and thermal dilution flow measurements. Thus, the measurement range in sequential logging is wider than in overlapping logging. The lower measurement limit in sequential logging is governed by the flow limit of the thermal pulse method. On the other hand, the lower measurement limit in overlapping logging is governed by the thermal dilution method.

The lower measurement limit for the specific flow in Table 9-2 is assumed to be slightly lower than that for transmissivity since the former is only an estimator and directly based on individual, measured flows (which may be below the measurement limit). The transmissivity is generally regarded as a more rigorous parameter, based on pairs of measured flow values with certain measurement limits. Thus, a higher uncertainty may in many cases be accepted for specific flow as an estimator of transmissivity. However, specific flow cannot be calculated for zero drawdown. The lower measurement limit for transmissivity is also dependent of the magnitude of the drawdown applied.

Table 9-2. Estimated lower measurement limits for measured flow rate and calculated specific flow and transmissivity for sequential and overlapping difference flow logging, respectively.

Flow logging method	Flow rate (ml/h)	Specific flow rate (m^2/s)	Transmissivity (m^2/s)
Sequential	6	c. $1 \cdot 10^{-10}$	c. $2 \cdot 10^{-10}$
Overlapping	120 *	c. $2 \cdot 10^{-9}$	$1 \cdot 10^{-8}$ ($5 \cdot 10^{-9}$)*

* lower limit for flow measurements will be improved in the future.

The lower measurement limits in Table 9-2 correspond to ideal test conditions, e.g. a stable and low base-flow level, constant salinity conditions along the hole and a drawdown of a few meters. The results of this study indicate that the minimum measurable flow rate could be lower than 120 ml/h in overlapping flow logging. Preliminary studies with the thermal dilution method show that there are good prospects to decrease the lower limit by changing the software of the thermal dilution method. The lower measurement limit for transmissivity in Table 9-2 is however based on a minimal flow of 120 ml/h.

9.2.2 Upper limit

Based on the results of the methodology study, the upper measurement limits in Table 9-3 may be proposed for difference flow logging. The upper measurement limit is governed by the maximal flow rate of the thermal dilution method, used in overlapping logging, since this method is used in both sequential and overlapping flow logging.

As for the lower limit, the upper measurement limit for the calculated transmissivities is dependent of the magnitude of drawdown applied. The upper limit for specific flow is regarded as slightly higher than that for transmissivity since also flow values above the rigorous upper measurement limit may also be included in the estimation of specific flow.

Table 9-3. Estimated upper measurement limits for measured flow rate (thermal dilution method) and calculated specific flow and transmissivity in difference flow logging.

Flow logging method	Flow rate (ml/h)	Specific flow rate (m^2/s)	Transmissivity (m^2/s)
Overlapping	300 000	c. $2 \cdot 10^{-5}$	$1 \cdot 10^{-5}$

9.3 Possible measurement programmes

Firstly, possible single flow logging methods (with only one logging sequence), both sequential and overlapping flow logging methods, are proposed. Secondly, possible measurement programmes including both single flow logging methods (with one or several logging sequences) and combined logging (with both sequential and overlapping flow logging), are proposed for different testing purposes. The programmes are general and should only be used as guidelines by the design of relevant difference flow logging programmes. Other combinations of flow logging methods and logging sequences may be selected.

9.3.1 Single flow logging methods

In Table 9-4 below, a number of possible single flow logging methods and logging sequences are proposed. The proposed flow logging sequences include relevant section length (L), drawdown (s) and step length (dl). Furthermore, additional parameters measured during flow logging and the main information obtained from each sequence are listed together with the estimated measurement limits based on the results of this study. Finally, the estimated test times (including pumping) for each logging sequence, excluding preparations and installation, are estimated. The estimates of test time are based on a c. 1000-m deep borehole with a diameter of 56 or 76 mm diameter with hydraulic conditions similar to KLX02.

The basic idea with Table 9-4 is to present individual flow logging methods (toolbox) which may either be performed alone or in combinations of two or more methods and sequences, see Table 9-5. If only one logging sequence is performed, no calculations of transmissivity or relative fresh water head can be made but only the specific flow (except for zero drawdown).

9.3.2 Combined flow logging programmes

In Table 9-5 below, a number of single method- and combined programmes (A-H) are proposed for difference flow logging for different purposes together with the main information obtained and the estimated total testing time (but exclusive preparations and installation). The programmes range from very simple, single flow logging sequences to complete flow logging programmes for hydraulic characterisation of the borehole. The purposes, listed in the table, are only examples of investigations that could be performed by the different programmes.

The last programme in Table 9-5 (programme H) is an optional programme, in which sequential flow logging (using both the thermal pulse- and thermal dilution method) and overlapping flow logging is made during the same logging sequence. The sequential flow logging is carried out with a section length of e.g. 2–10 m and the overlapping flow logging (only thermal dilution method) is performed with a step length of e.g. L/5. The benefit with this programme is faster measurements in some cases, compared to separate sequential and overlapping flow logging sequences, respectively. It may be an alternative if both the sequential and overlapping flow logging sequences are chosen with a large section length (L=2–10 m).

Table 9-4. Possible single flow logging methods (only one logging sequence) together with main information obtained, test time and measurement limits.

Single Flow logging method	L (m)	dL (m)	Other measurements	Drawdown (m)	Main Information obtained	Test time/ 1000 m (days)***	Measurement limits (m^2/s)
Sequential	2 – 20 *	=L	S.P.Res., (EC-bh, temp-bh)**. (Standard, no extra time)	s=0	Natural flows in b.h. sections (L) (inflow/outflow)	**7** (L=2 m) **3** (L=20 m)	$(Q)_{min}$ = 0.1 ml/min $(Q)_{max}$ = 5000 ml/min
Sequential	2 – 20 *	=L	Same as above	s>0	Q/s of borehole sections (L)	**7** (L=2 m) **3** (L=20 m)	$(Q/s)_{min} = 1\ 10^{-10}$ $(Q/s)_{max} = 2 \cdot 10^{-5}$
Fresh-water head profile			2xPressure- and EC-bh- logging (before and after pumping)	s=0 and s>0	Freshwater head- and EC-bh-profile along borehole	**7** (depth interval=20 m)	
Overlapping	0.5 – 5*	0.1–0.5	Standard	s=0	Position of flow anomalies Depth resolution = dL (m) Natural flows in borehole (in/outflow)	**5** (dL=0.1 m) **3** (dL=0.5 m)	$(Q)_{min}$ = 2 ml/min $(Q)_{max}$ = 5000 ml/min (flow direction)
Overlapping ****	0.5 – 5*	0.1–0.5	Standard	s>0	Position and Q/s of flow anomalies Depth resolution = dL (m)	**5** (dL=0.1 m) **3** (dL=0.5 m)	$(Q/s)_{min} = 2 \cdot 10^{-9}$ $(Q/s)_{max} = 2 \cdot 10^{-5}$
Same as above +EC-frac	0.5 – 5*	0.1–0.5	Standard +EC–frac	s>0	Same as above +EC–frac in selected fractures	**7–9** (dL=0.1 m) **5–7** (dL=0.5 m)	Same as above

* the choice of section length should be co-ordinated with other borehole testing, e.g. injection tests

** EC-bh and temp-bh are not appropriate in long sections due to insufficient exchange of the water in the section

*** total test time including pumping but exclusive installation etc.

**** overlapping flow logging in short sections may be restricted to conductive intervals identified by previous flow logging

Table 9-5. Possible combined difference flow logging programmes (A–H) together with main information obtained, test time and examples of specific purposes of the different programmes.

Combined Programmes	Flow logging sequences (a–b)	L (m)	dL (m)	Drawdown (m)	Main Information obtained	Total test time (days)***	Example of purposes of measurem. programme
A	1) Sequential	2 – 20 *	=L	s=0	Natural flows in b.h. sections (L) (inflow/outflow)	**3** (L=20) — **7** (L=2)	Water balance studies in borehole
B	1) Sequential	2 – 20 *	=L	s>0	Q/s of borehole sections (L)	Same as above	Q/s-logging in sections, low measurement limit
C	1) Overlapping	2–5	0.5	s>0	Position and Q/s of flow anomalies Depth resolution = 0.5 (m)	**3**	Hydrochemical sampling, standard depth resolution
D	1) Overlapping 2) d:o ****	2 – 5 0.5–1	0.5 0.1	$s_1>0$ $=s_1$	As above but with detailed depth resolution (0.1 m) of interpreted flow anomalies	**8**	Hydrochemical sampling, detailed depth resolution
E	1) Sequential 2) Sequential	2 – 20 * same as in 1	=L =L	$s_1=0$ $s_2>0$	Natural flows in b.h.-sections (inflow/outflow) with low measurement limit. Transmissivity and head of borehole sections	**6** (L=20) – **14** (L=2)	Water balance studies in borehole. Compliment to injection testing with low measurement limit
F	1) Overlapping 2) Overlapping	0.5–5 same as in 1	0.1–0.5 0.1–0.5	$s_1\geq0$ $s_2>0$	Natural flow (if s=0) or actual flows (s>0) in anomalies, high measurement limit. Position, Transmissivity and head of flow anomalies. Depth resolution 0.1 (m)	**6** (dL=0.5) – **10** (dL=0.1)	Prel. estimation of CFF. Compliment to injection testing with higher measurement limit

Table 9-5 cont.

G	1). Sequential 2). Sequential 3) Fresh-water head logging 4) Overlapping 5) Overlapping ****	2 – 20 * same as in 1) 0.5–1 same as in 4)	=L =L 0.1 0.1	$s_1≥0$ $s_2>0$ s=0 and s>0 $s_4≥0$ $s_5>0$	If s=0: natural flow in borehole sections (L). Transmissivity and head of borehole sections Freshwater head and EC-bh-profiles** along borehole at pumped and non-pumped cond´s. Position, Transmissivity and head of interpreted flow anomalies. Depth resolution 0.1 m	2x Sequential logging: **6** (L=20 m)–**14** (L=2 m) 2x Fresh-w.h.-logging: **7** (depth interval =20 m) 2x Overlapping logging: **10** **Total: 23–31**	Complete difference flow logging, both sequential and overlapping incl. fresh-water head measurements Prel. estimation of CFF.
Option	EC-frac measurem. during overlapping flow logging	0.5–1	0.1	s>0	Fracture-specific EC of water at selected fractures	**2–4** (depending on the number of fractures)	Hydrochemical characterisation of water in fractures
H	Simultaneous (both sequential and overlapping)	2–10, e.g. 5	=L in sequential = 0.5–1 m in overlapping	s=0 and/or s>0	Natural flows (if s=0) (inflow/outflow) and actual flow (if s>0) in b.h. sections Position and Q/s of interpreted flow anomalies Depth resolution = 0.5 (m)	**5** (sequential:L=5 m, overlapping:dL=0.5m)	Fast logging with both sequential and overlapping logging in the same run

* the choice of section length should be co-ordinated with other borehole testing, e.g. injection tests

** EC-bh and temp-bh are not appropriate in long sections due to insufficient exchange of the water in the section

*** total test time including pumping but exclusive installation etc.

**** overlapping flow logging in short sections may be restricted to conductive intervals identified by previous flow logging

9.3.3 Design of measurement parameters

The detailed design of a selected measurement program again depends on the specific purpose of the measurements and time and cost available. Design parameters, which could be altered, include e.g. number and magnitude of drawdown sequences applied, length of measurement section, step length (in overlapping logging). Furthermore, decisions of additional parameters to be measured, e.g. fracture-specific EC, must be taken. Based on the results of the methodology study, some guidelines by the design of these parameters are discussed below in particular for overlapping logging.

Section length (L) and step length (dL)

This item is studied in Section 4.2 and 4.3. It was shown that about double the number of flow anomalies could be detected from overlapping flow logging in 0.5-m sections with dL=0.1 m compared to the corresponding logging in 3-m sections with dL=0.5 m. This is valid both for zero drawdowns and higher drawdowns. This is mainly due to the increased resolution in the depth scale (both section length and step length, the latter being most important).

Furthermore, in the overlapping flow logging in 3-m sections it was more difficult to identify the flow anomalies. This may depend on the fact that more than one flow anomaly are likely to be present within the measurement section when longer sections are used. For the overlapping flow logging with 0.5 m section length, only a few cases more than one flow anomaly was present within the test section, e.g. the flow anomalies at 251.3 m and 251.6 m, c.f. Table 3-2 and Appendix 2.

On the other hand, flow logging with a short section length may be uncertain in borehole intervals of bad condition, e.g. due to fracturing and caving, which may result in un-tight rubber discs. Several intervals in bad condition are present in KLX02. The results of the flow loggings in these intervals are uncertain. However, a comparison of the calculated specific flow from measurements in 3-m sections with the cumulative specific flows for 0.5-m sections in corresponding 3-m sections, showed rather good agreement in the interval 200–400 m. The latter values were, in general, only slightly higher, possibly indicating minor leakage. In borehole intervals of bad condition, a combination of long and short measurement sections would be beneficial.

Based on the results of the methodology study, a section length of 0.5 m (or possibly 1 m) is suggested for overlapping in site investigations provided that the measured borehole interval is in good condition. Alternatively, an exploratory flow logging with longer section length, e.g. 3-m or 5-m, could be made first. Then, a more detailed flow logging can be performed, either along the entire borehole (interval) or only in conductive intervals, as identified from the previous logging. Sequential flow logging is generally performed in longer sections, e.g. 5 m or 20 m.

The effect of the magnitude of the step length was not explicitly investigated in the methodology study. However, experience from previous difference flow logging in Finland indicates that a ratio of L/dL of 5–10 is optimal. The step length dL determines the depth resolution. Fractures that are closer to each other than dL cannot be separated from each other. In conclusion, the total logging time in overlapping flow logging depends almost entirely on the size of the chosen step length.

Number of drawdown sequences

A minimum of two flow logging sequences is required for calculation of the transmissivity and in-situ head of the interpreted flow anomalies. The methodology study has shown that additional sequences (more than 2) with higher drawdowns may not always significantly increase the amount of information from the flow logging. For example, overlapping flow logging sequences at different combinations of drawdown gave similar results regarding calculated transmissivity, see Section 4.6.

However, as discussed in Section 4.7, one of the logging sequences should be at zero (or small) drawdown to get reliable estimates on the undisturbed head of the flow anomalies. A drawback with such a small drawdown is that the in-situ head can only be calculated for a less number of flow anomalies since there are fewer anomalies with measurable flows in this case. The accuracy of the in-situ head and transmissivity determinations can be improved if several flow logging sequences at different drawdowns are performed. However, this may not always be possible in practise due to economical and time constraints.

The methodology study has also shown that the specific flow rate (Q/s) may a good estimator of transmissivity if a relatively high drawdown is applied, see Section 4.6.2. However, this is only valid for relatively small variations of the in-situ head distribution along the hole, as in the interval 200–400 m in KLX02. In such cases, only one drawdown sequence may be sufficient. The in-situ head can not be determined in this case.

Magnitude of drawdown

The overlapping flow logging with different drawdown in the interval 200–400 m showed that the number of interpreted flow anomalies decreased significantly (about half) for flow logging with zero drawdown compared to those from other drawdown. For higher drawdown the number of interpreted anomalies was similar. No specific flow can be estimated with zero drawdown. However, an advantage with zero drawdown is that the natural flows and flow direction (in- or outflow) can be estimated under natural conditions. This may be of interest in water balance studies along the hole and in regional groundwater studies.

Another advantage is, that only the flow logging sequences with zero drawdown gave consistent and stable estimates of the in-situ (natural) fresh-water head in the interval 200–400 m, see Section 4.7. Other drawdown combinations (with two non-zero draw-downs) failed to provide reliable values of undisturbed head in this case. However, in boreholes with large natural head variations along the hole, the result may be different. As discussed in Section 4.7, the selected drawdowns should, ideally, be below and above, respectively, the natural fresh water head in a particular section.

Higher drawdowns are generally needed to reverse the flow direction in naturally out-flowing fractures toward the borehole during pumping. Another reason for selecting a relatively high drawdown is in boreholes with saline water at the bottom. During pumping, the saline water rises in the borehole, resulting in a decreased pressure differential towards the borehole at depth. The same happened in KLX02 during pumping in Campaign 1 and at 22-m drawdown in Campaign 2, see Section 8.3. In such cases, a sufficiently high drawdown (at the surface) must be selected to maintain a pressure gradient directed into the hole, also at higher depths. Otherwise, no inflow can occur from deep fractures, regardless of their transmissivity.

On the other hand, the drawdown should not be too high, particularly if the measurements are made at rather shallow depths. In such cases, a relatively small drawdown may be sufficient for avoiding problems of up-coning of saline water. The methodology study has also clearly shown that a high drawdown may result in a substantial noise on the flow logging, i.e. changes of the base-flow level during logging, see Section 8.2. The noise may mask potential flow anomalies along the hole and distort the results of the flow logging. One way to get rid of the noise might possibly be to lift and sink the flow probe as was tried in KLX02 during some of the fracture-specific EC-measurements.

A too large drawdown may also increase turbulence, which may explain the observed non-linearity at some depths. Turbulent measurement can hardly represent well natural conditions. The measurement limit may be exceeded with high pumping.

Fracture-specific EC

The experience of determining the fracture-specific EC during the methodology study is discussed in Chapter 7. This parameter may be important, e.g. in hydro-chemical assessments and in design and interpretation of hydro-chemical sampling programmes in boreholes. However, the determination of fracture-specific EC may be time-consuming. In addition, this procedure (extra pumping) may lead to an increase the noise level of the base-flow in the borehole, see Section 8.2.

On the other hand, when the method is compared with groundwater sampling, it is fast because the tool can be positioned on a flowing fracture accurately and the section length can be small. The technique needs to be developed for small flow rates.

EC and temperature in the borehole

These measurements are made simultaneously with the flow logging, see Chapter 2. In short sections these measurements are in general representative for the actual borehole depth. However, in long sections, the measurements may be highly uncertain and non-representative for the actual borehole depth due to the large volume of water contained in the flow guide. In such cases, separate lodgings of EC and temperature along the hole can be performed relatively quickly without the flow guides (rubber discs) or without the lower rubber disc.

Single Point Resistance

This parameter is measured as standard in difference flow logging, see Chapter 2. It has proved to be a very important correlation parameter by the determination of the exact position of flow anomalies in overlapping flow logging, c.f. Chapter 5 and 6.

9.3.4 Recommended programmes for site investigations

From the hydrogeological characterisation programme, two types of boreholes may be distinguished, i.e. boreholes in which the chemical characterisation is given highest priority and other boreholes, respectively. In the former boreholes, a rather quick hydrogeological characterisation is generally sufficient with the specific purpose to identify flowing fractures for subsequent groundwater sampling. After the water sampling a more complete hydrogeological characterisation can be carried out. In the other boreholes a complete characterisation can be performed continuously at an early stage.

Hydrochemistry-prioritised boreholes

Recommended programmes for groundwater sampling could be programmes C and D in Table 9.5. Overlapping flow logging with pumping (c. 5 m drawdown in a non-saline borehole, c.10 m drawdown in a saline borehole) with L= 5 m and dL=0.5 m would be carried out first (Programme C). This would take about 3 days in a 1000-m borehole. This measurement would produce information of conductive fractures with 0.5-m depth resolution.

If more accurate measurement is needed the measurements could be continued with overlapping flow logging with the same drawdown but with L=0.5 m and dL=0.1 m (Programme D). This would take 5 more days if the entire borehole is measured but less if only conductive parts are measured. This measurement would produce information of conductive fractures with 0.1-m depth resolution and may be useful if the depth calibration of both flow measurement and groundwater sampling is accurate. The results can also be used for hydrogeological characterisation, as estimating transmissivity of fractures and their orientation together with borehole TV.

The measurement of fracture-specific EC may be useful in planning groundwater sampling, especially in the cases where there are several alternatives for depths of groundwater sampling. This measurement can be done at the same time as the previous overlapping flow logging (L=0.5 m, dL=0.1 m). Its duration strongly depends on flow rates from the target fractures.

Non-hydrochemistry-prioritised boreholes

A recommended programme for hydrogeological characterisation of non-hydrochemistry-prioritised boreholes could be programme G in Table 9.5. The measurement sequence would be started with sequential flow logging (L=5 m, dL=5 m) without pumping and continued with overlapping flow logging (L=5 m, dL=0.5 m) without pumping. These two measurements would take about 6 days together.

Freshwater head and EC-borehole measurements without pumping would be carried out next. They would be repeated a few days after starting the pump. This would take about 7 days together.

The measurement sequence would continue with sequential flow logging (L=5 m, dL=5 m) at pumping and overlapping flow logging (L=5 m, dL=0.5 m) at pumping. These two measurements would take about 6 days together.

The work could be completed with overlapping flow logging (L=0.5 m, dL=0.1 m) at pumping and fracture-specific EC measurements. This phase would take about 8 days.

The measurements could be speeded up if the sequential and overlapping flow logging (L=5 m) are carried out simultaneously, see Table 9-5 (programme H).

This set of measurements would provide fresh water head in the borehole with and without pumping, EC in the borehole with and without pumping, transmissivity and undisturbed (natural) head of the measured sections, transmissivity estimates of individual fractures and fracture-specific EC of the most conductive fractures.

9.4 Future developments

9.4.1 Improvement of flow measurements in overlapping logging

It seems possible to increase the sensitivity of the thermal dilution method without increasing the time of measurement. This would increase the importance of the overlapping flow logging compared to the conventional sequential flow logging. However, the measurement of flow direction of small flows (< 2ml/min) will take as long time as before, since thermal response of the monitoring thermistors is needed for the determination of direction. The development work is going on and it is planned to be completed by the end of the year 2001.

9.4.2 Pressure transducer

Pressure measurements would be faster if they could be carried out during the flow measurements. It would be able to measure absolute pressure instead of fresh water head. Investigation of a proper transducer and of electronics it needs is under way.

9.4.3 Length recording

Elastic, non-linear tension of the logging cable is a potential problem. The Single-Point Resistance log seems to be useful for length correlation. However, the length recording must most likely be improved if correlation with other logging results will be carried out. For example, use of reference points along the borehole in combination with simultaneous caliper type logging and single point resistance logging together with the flow logging must be carried out to achieve a correct and efficient length recording.

10 Conclusions and recommendations

One of the main objectives of the method test was to study whether it is possible to obtain the transmissivity and undisturbed head of individual fractures using overlapping flow logging. This seems to be possible as described in this report.

The conclusion above increases importance of flow measurements in overlapping flow logging relative to the more conventional sequential flow logging. Overlapping logging provides more fracture-specific information to be used together with other methods such as borehole TV. A drawback with overlapping flow logging at present is that it is not as sensitive to small flow rates as sequential flow logging.

The measurements carried out revealed limitations of this type flow measurements. Borehole intervals with increased diameter, e.g. cavities, and fractures along the borehole can cause erroneous results. Therefore it is recommended to double-check measurements with a long section length. This would assure that the widened parts of the borehole would be entirely within the test section and the flow from such locations could be properly measured. This double-checking could be carried out with larger depth increments (0.5–1 m) and therefore fast. In addition, caliper-, single point resistance – and BIPS measurements may also be useful when assessing the reliability of the results.

It is also recommended to perform hydraulic tests, e.g. injection tests, in such, highly fractured borehole intervals to check the results of the flow logging and to get more information on the nature of fracturing. Such tests may also serve the purpose to compare the calculated transmissivity distribution along the hole from different methods.

Experience from measurements in Finland indicates however that injection tests seem to produce over-estimated values of transmissivity in similar environments due to intensive fracturing and local flow routes near the borehole. It is possible that relatively short-duration double-packer injection tests may measure properties of the rock only in the immediate vicinity of borehole. In addition, there is a possibility of injected water from the narrow test section to return to the borehole (i.e. a short-circuit by-pass), which would result in higher calculated T values for the double-packer injection tests compared to long-term pumping- and flow-meter tests.

The methodology study has shown that it is possible to determine the transmissivity of interpreted conductive fractures by different combinations (pairs) of data from overlapping difference flow logging at different drawdowns applied in the hole. Good consistency of calculated transmissivities from different drawdown combinations was generally obtained. In addition, in KLX02, the specific flow rate (Q/s) at each logging sequence was found to be a good estimator of transmissivity. However, this may not be the case in boreholes where large head variations occur along the hole.

This study has also shown that the undisturbed (natural) freshwater head of conductive fractures and borehole sections also may be calculated from difference flow logging by different drawdown combinations (pairs). However, it was found that one of the drawdowns should be zero (or small) to get reliable head values in this case. This may not be the case in boreholes with large natural head variations along the hole.

Muddy water increases the noise level of the flow measurements. Increased noise may cover the smallest flows to be measured. This can make especially sequential flow logging almost useless because no small flow rates can be measured. Therefore it is important to improve methods to clean up the borehole from drilling debris and gauge material from fractures. Drilling debris and gauge material may also harm other methods such as borehole-TV.

Another possible source of noise is gas in the groundwater. This was observed when the pumping rate was large and the tool stayed a long time at some fractures. Gas can convert from gas solution in water to gas bubbles when the pressure is released. This happens when the borehole is pumped with a large drawdown. One way to get rid of gas within the flow guide is to move the tool up and down in the borehole. This helps in extracting gas bubbles from the flow guide. This simple method has worked in practice but it may not be very convenient to apply it frequently.

In addition, possible effects of significantly different chemical and physical properties of waters, e.g. density and viscosity, in fractures and in the borehole on the flow measurements should be investigated further. This may be another source of noise in the flow measurements.

Fresh water head measurements along the borehole are needed for a correct calculation of transmissivity and undisturbed head of fractures. Freshwater head profiles must be measured in boreholes with saline water where density changes can be notable. In KLX02, the relative freshwater head was measured with a fresh-water filled tube. These measurements are slow and must be done separately from the flow logging, at least if the flow measurements are carried out automatically. A pressure transducer within the flow sensor would certainly improve and speed up the head measurements.

Another means to evaluate the fresh-water head conditions in borehole is from calculations of the density distribution of the water along the hole by using the measured electric conductivity of the borehole water. However, a main source of error in these calculations is muddy water that can considerably change the relationship between electric conductivity and density.

The length recording along the hole should be improved by using reference points at different borehole lengths in combination with simultaneous use of caliper-type logging and single point resistance logging to detect the reference points and assist in the length correction of the logging.

11 References

Carlsten, S., Stråhle, A. and Ludvigson, J-E, 2001. Conductive fracture mapping – A study on the correlation between borehole TV- and radar images and difference flow logging results in borehole KLX02.
SKB R-01-48, Svensk Kärnbränslehantering AB

Rouhiainen, P. and Pöllänen, J., 1998. Difference flow measurements in Äänekoski, boreholes KR4, KR12 and KR13. Posiva Oy, 116 p., Working report 98-31e.

Rouhiainen, P., 2000. Difference flow measurements in borehole KLX02 at Laxemar. Äspö Hard Rock Laboratory.
SKB IPR-01-06, Svensk Kärnbränslehantering AB

Stanfors R., Erlström M. and Markström I., 1997. ÄSPÖ HRL – Geoscientific evaluation 1997/1. Overview of site characterization 1986–1995.
SKB TR-97-02, Svensk Kärnbränslehantering AB

Öhberg A. and Rouhiainen P., 2000. Posiva groundwater flow measuring techniques. Report Posiva 2000-12.

Appendix

Note: The terms “Normal mode”, and “Detailed mode” (“Detailed flow logging”) in Appendices 1.1–1:10 and 5:1–5:3 refer to sequential and overlapping flow logging, according to section 2.2.1.

Laxemar, borehole KLX02
Detailed flow logging with thermal dilution,0.5 m section length, 0.1 m step

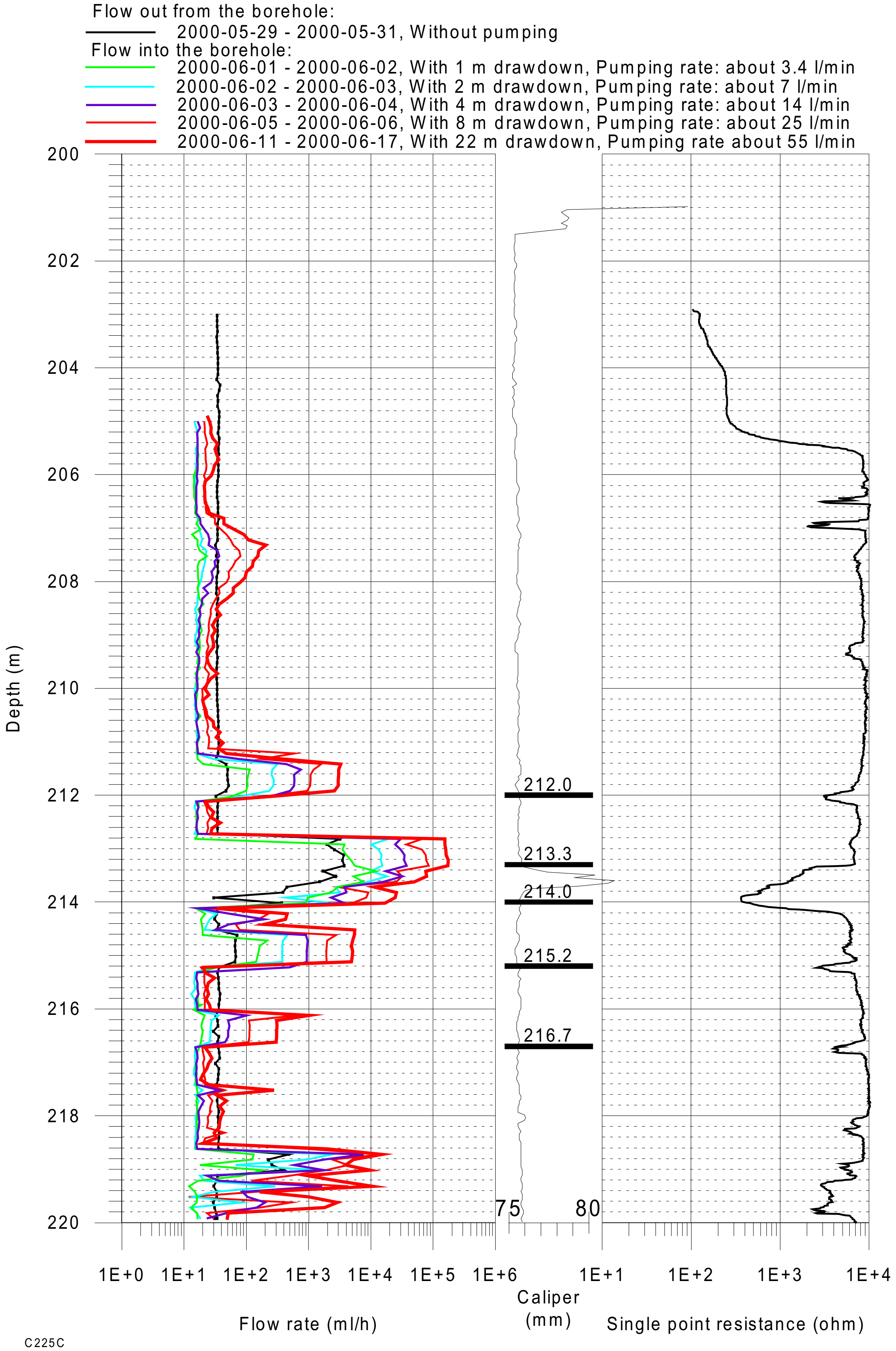

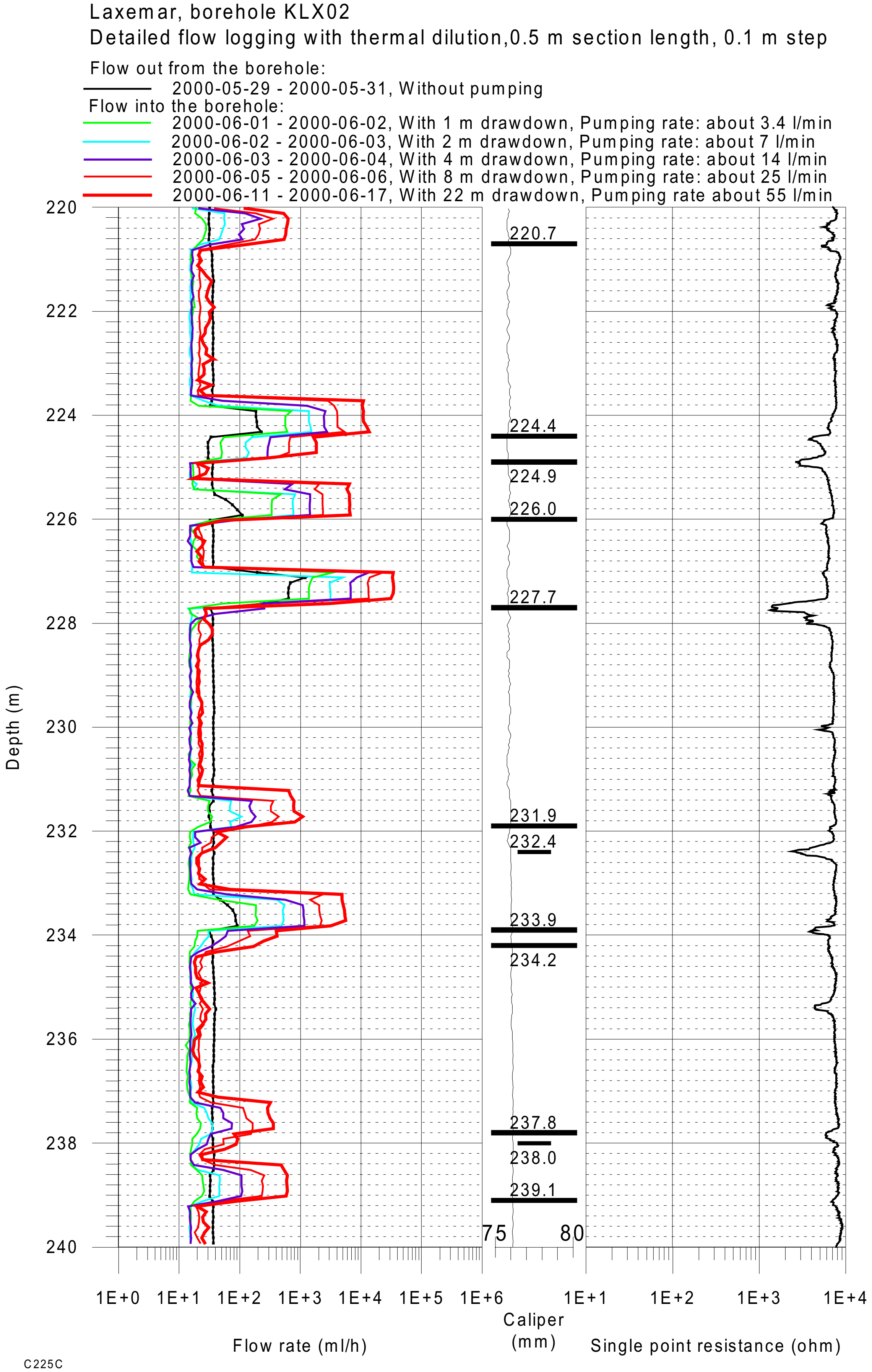

Laxemar, borehole KLX02
Detailed flow logging with thermal dilution,0.5 m section length, 0.1 m step
Flow out from the borehole:
2000-05-29 - 2000-05-31, Without pumping
Flow into the borehole:
2000-06-01 - 2000-06-02, With 1 m drawdown, Pumping rate: about 3.4 l/min
2000-06-02 - 2000-06-03, With 2 m drawdown, Pumping rate: about 7 l/min
2000-06-03 - 2000-06-04, With 4 m drawdown, Pumping rate: about 14 l/min
2000-06-05 - 2000-06-06, With 8 m drawdown, Pumping rate: about 25 l/min
2000-06-11 - 2000-06-17, With 22 m drawdown, Pumping rate about 55 l/min
Depth (m)
220
222
224
226
228
230
232
234
236
238
240
220.7
224.4
224.9
226.0
227.7
231.9
232.4
233.9
234.2
237.8
238.0
239.1
75
80
1E+0
1E+1
1E+2
1E+3
1E+4
1E+5
1E+6
Flow rate (ml/h)
Caliper (mm)
1E+1
1E+2
1E+3
1E+4
Single point resistance (ohm)
C225C

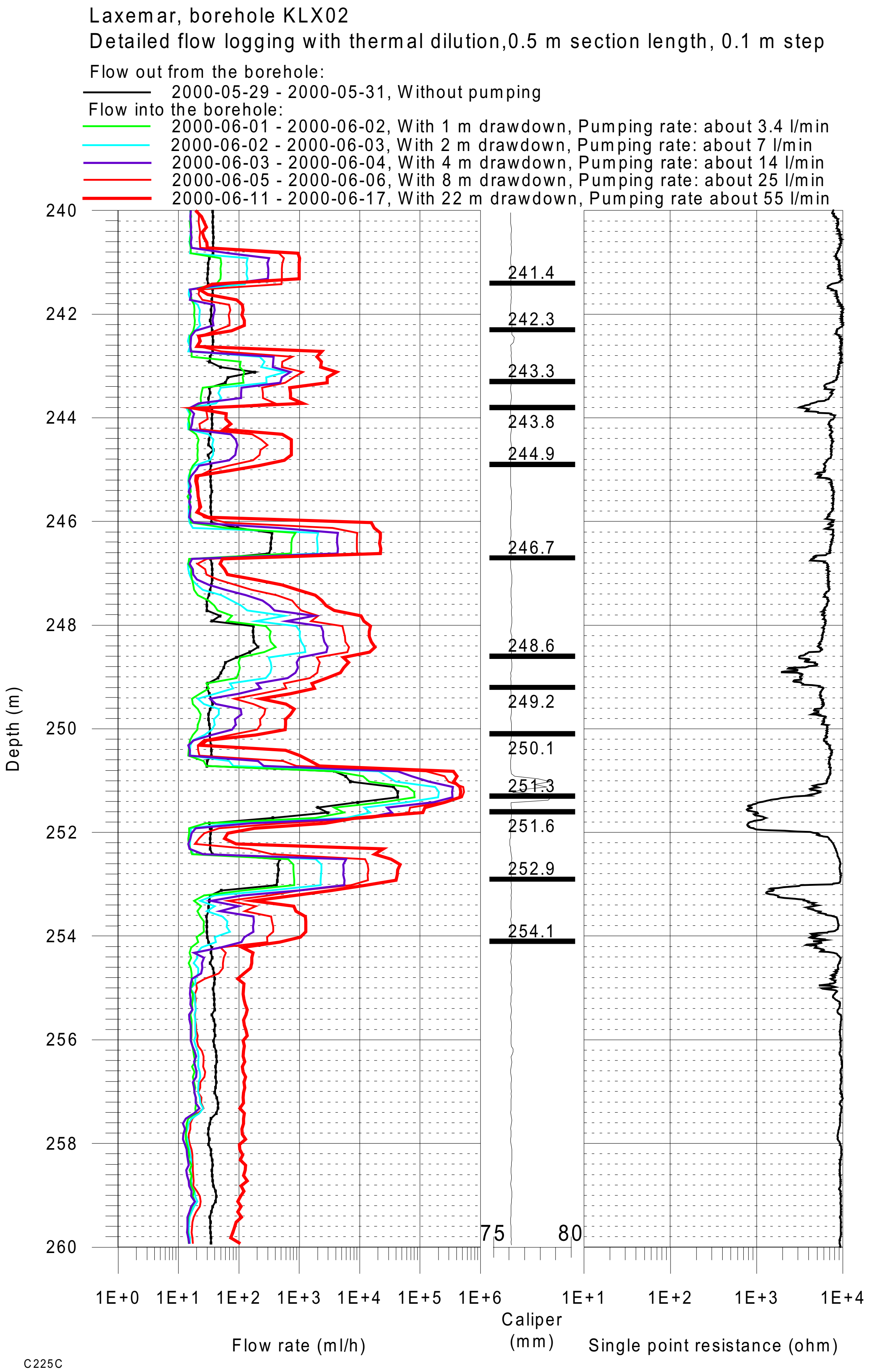

Laxemar, borehole KLX02
Detailed flow logging with thermal dilution,0.5 m section length, 0.1 m step
Flow out from the borehole:
2000-05-29 - 2000-05-31, Without pumping
Flow into the borehole:
2000-06-01 - 2000-06-02, With 1 m drawdown, Pumping rate: about 3.4 l/min
2000-06-02 - 2000-06-03, With 2 m drawdown, Pumping rate: about 7 l/min
2000-06-03 - 2000-06-04, With 4 m drawdown, Pumping rate: about 14 l/min
2000-06-05 - 2000-06-06, With 8 m drawdown, Pumping rate: about 25 l/min
2000-06-11 - 2000-06-17, With 22 m drawdown, Pumping rate about 55 l/min
Depth (m)
240
242
244
246
248
250
252
254
256
258
260
241.4
242.3
243.3
243.8
244.9
246.7
248.6
249.2
250.1
251.3
251.6
252.9
254.1
75
80
1E+0
1E+1
1E+2
1E+3
1E+4
1E+5
1E+6
Flow rate (ml/h)
Caliper (mm)
1E+1
1E+2
1E+3
1E+4
Single point resistance (ohm)
C225C

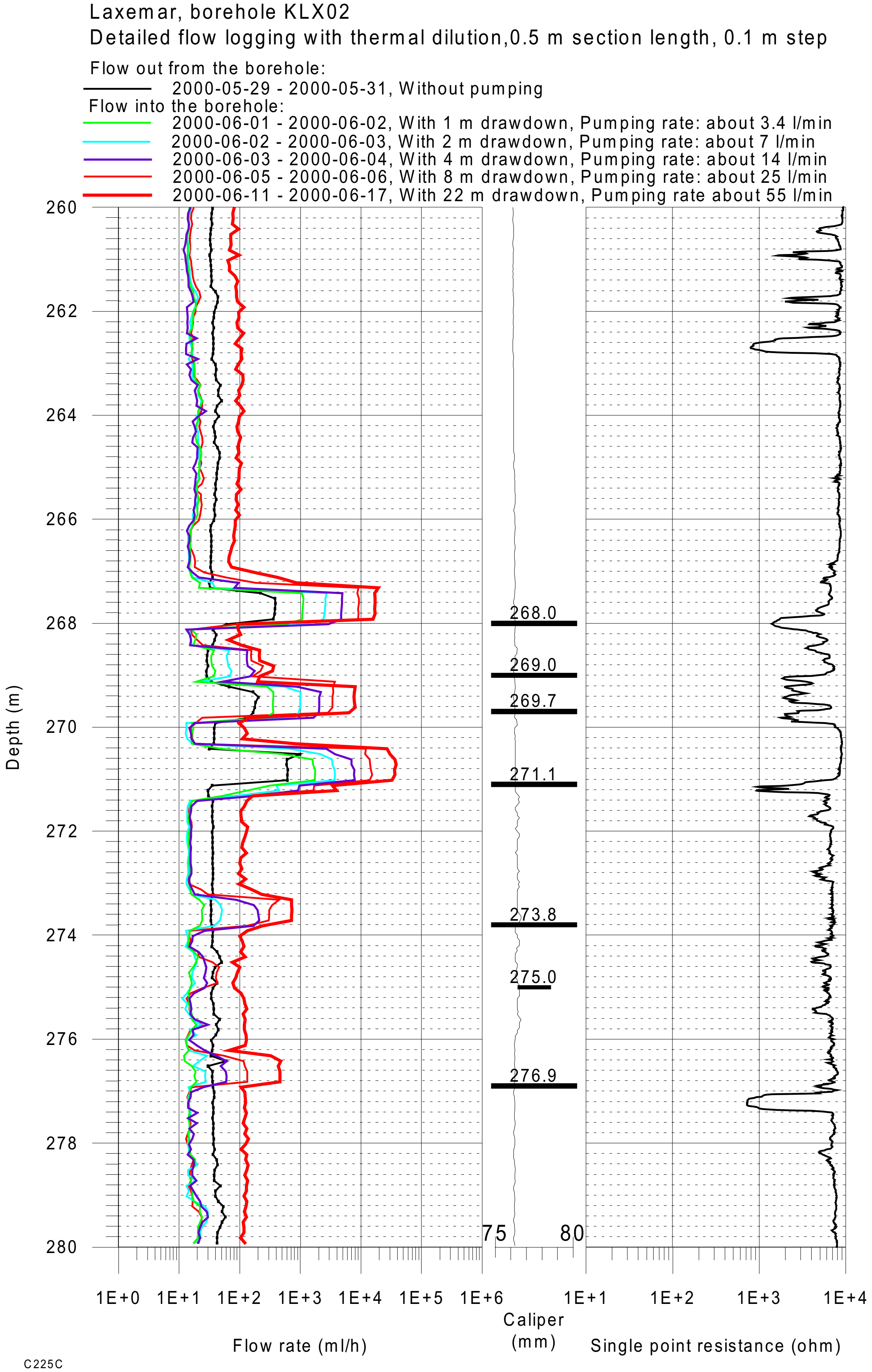

Laxemar, borehole KLX02
Detailed flow logging with thermal dilution,0.5 m section length, 0.1 m step
Flow out from the borehole:
2000-05-29 - 2000-05-31, Without pumping
Flow into the borehole:
2000-06-01 - 2000-06-02, With 1 m drawdown, Pumping rate: about 3.4 l/min
2000-06-02 - 2000-06-03, With 2 m drawdown, Pumping rate: about 7 l/min
2000-06-03 - 2000-06-04, With 4 m drawdown, Pumping rate: about 14 l/min
2000-06-05 - 2000-06-06, With 8 m drawdown, Pumping rate: about 25 l/min
2000-06-11 - 2000-06-17, With 22 m drawdown, Pumping rate about 55 l/min
Depth (m)
260
262
264
266
268
270
272
274
276
278
280
268.0
269.0
269.7
271.1
273.8
275.0
276.9
75
80
1E+0
1E+1
1E+2
1E+3
1E+4
1E+5
1E+6
Flow rate (ml/h)
Caliper (mm)
1E+1
1E+2
1E+3
1E+4
Single point resistance (ohm)
C225C

Laxemar, borehole KLX02
Detailed flow logging with thermal dilution,0.5 m section length, 0.1 m step

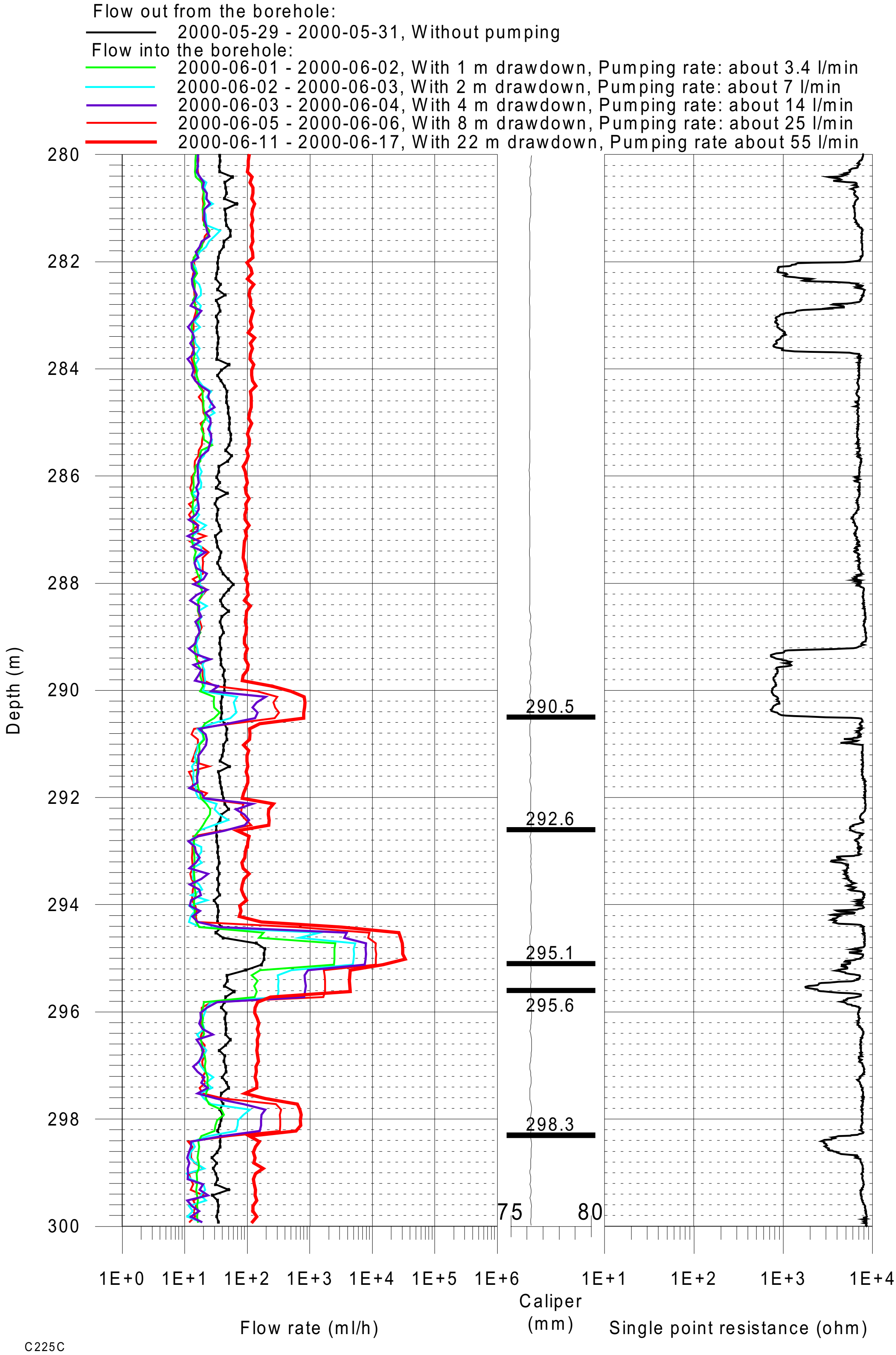

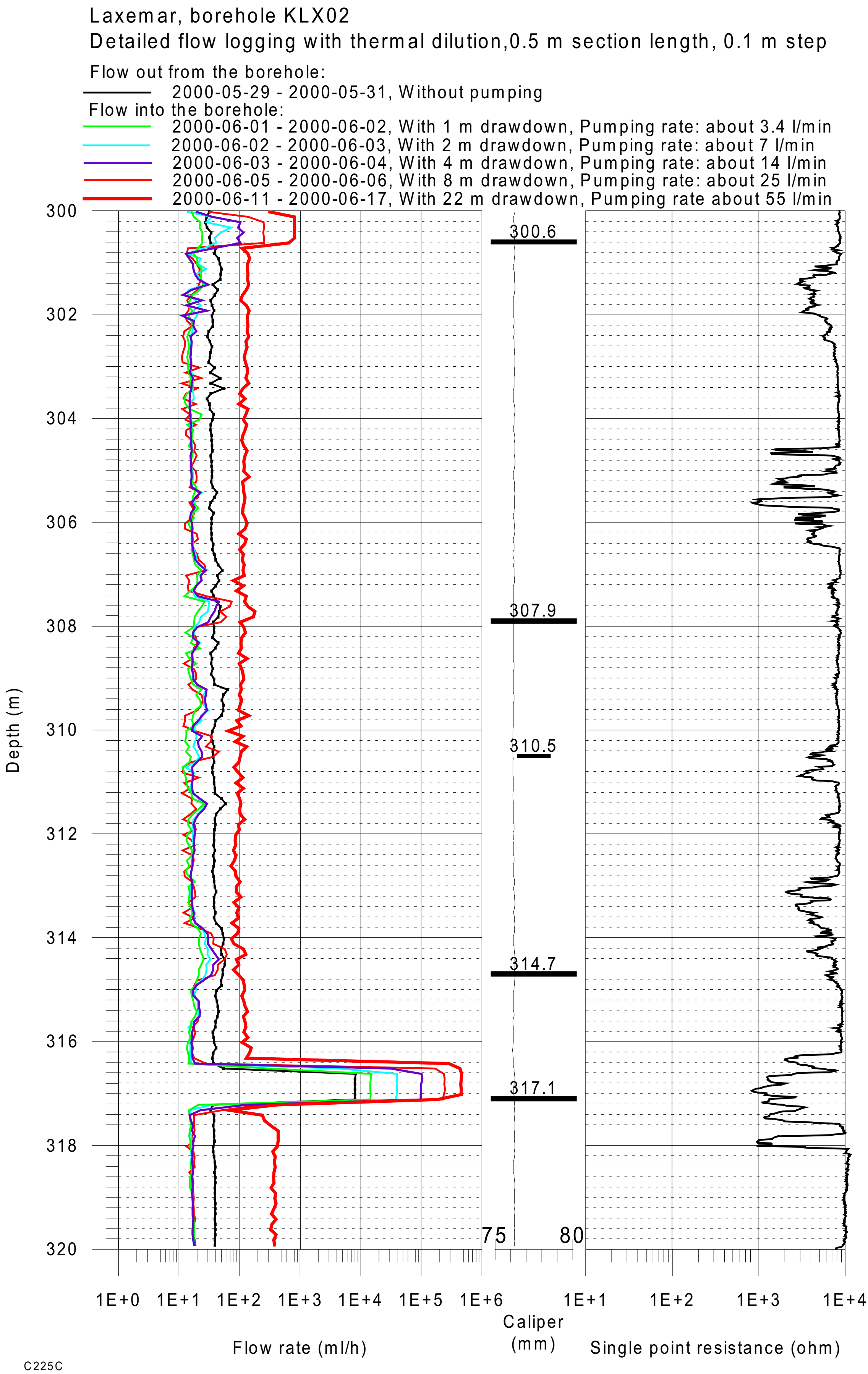

Laxemar, borehole KLX02
Detailed flow logging with thermal dilution,0.5 m section length, 0.1 m step
Flow out from the borehole:
2000-05-29 - 2000-05-31, Without pumping
Flow into the borehole:
2000-06-01 - 2000-06-02, With 1 m drawdown, Pumping rate: about 3.4 l/min
2000-06-02 - 2000-06-03, With 2 m drawdown, Pumping rate: about 7 l/min
2000-06-03 - 2000-06-04, With 4 m drawdown, Pumping rate: about 14 l/min
2000-06-05 - 2000-06-06, With 8 m drawdown, Pumping rate: about 25 l/min
2000-06-11 - 2000-06-17, With 22 m drawdown, Pumping rate about 55 l/min
Depth (m)
300
302
304
306
308
310
312
314
316
318
320
300.6
307.9
310.5
314.7
317.1
75
80
1E+0
1E+1
1E+2
1E+3
1E+4
1E+5
1E+6
Flow rate (ml/h)
Caliper (mm)
1E+1
1E+2
1E+3
1E+4
Single point resistance (ohm)
C225C

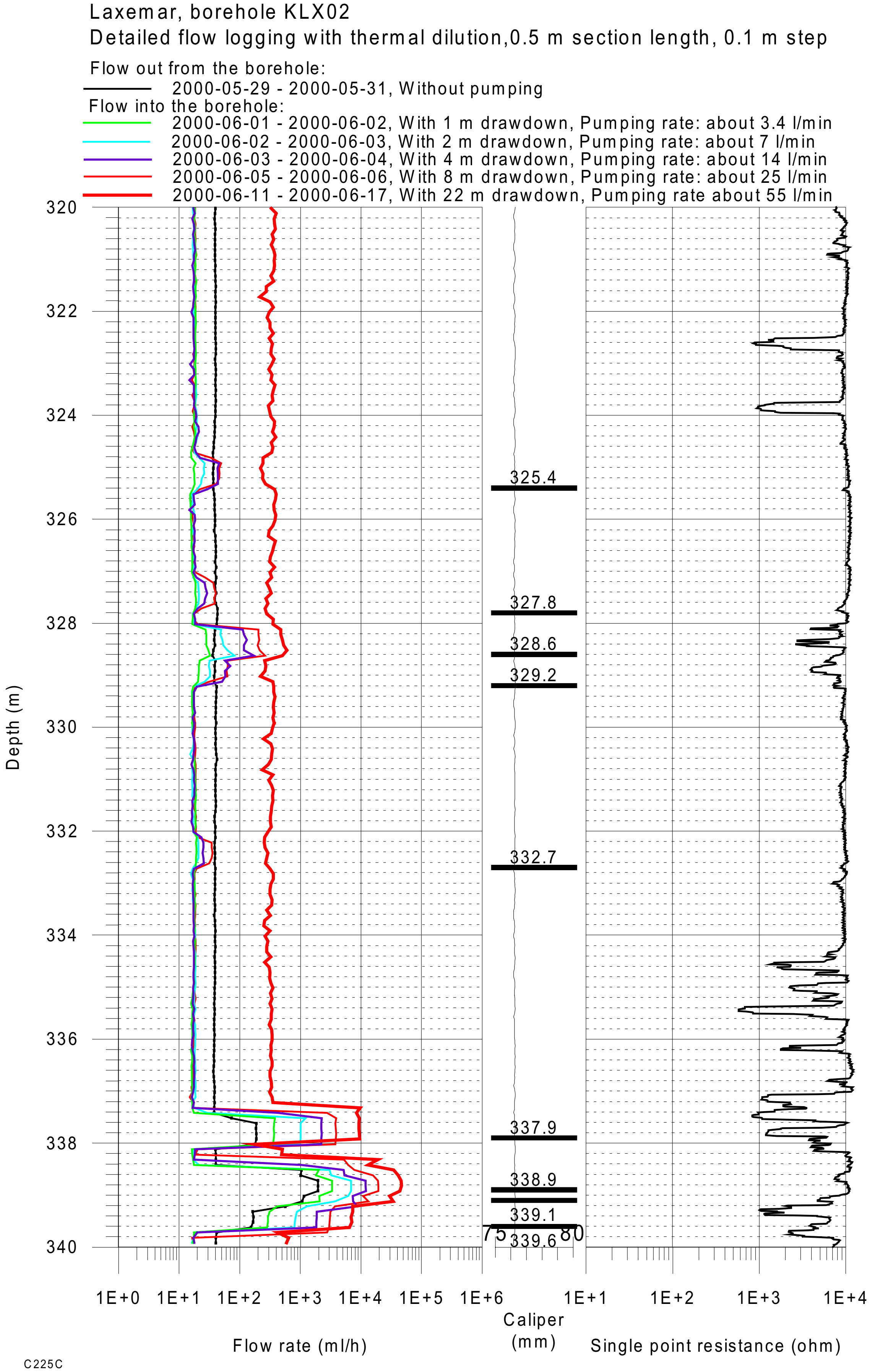

Laxemar, borehole KLX02
Detailed flow logging with thermal dilution,0.5 m section length, 0.1 m step
Flow out from the borehole:
2000-05-29 - 2000-05-31, Without pumping
Flow into the borehole:
2000-06-01 - 2000-06-02, With 1 m drawdown, Pumping rate: about 3.4 l/min
2000-06-02 - 2000-06-03, With 2 m drawdown, Pumping rate: about 7 l/min
2000-06-03 - 2000-06-04, With 4 m drawdown, Pumping rate: about 14 l/min
2000-06-05 - 2000-06-06, With 8 m drawdown, Pumping rate: about 25 l/min
2000-06-11 - 2000-06-17, With 22 m drawdown, Pumping rate about 55 l/min
Depth (m)
320
322
324
326
328
330
332
334
336
338
340
325.4
327.8
328.6
329.2
332.7
337.9
338.9
339.1
339.6
75
80
1E+0
1E+1
1E+2
1E+3
1E+4
1E+5
1E+6
Flow rate (ml/h)
Caliper (mm)
1E+1
1E+2
1E+3
1E+4
Single point resistance (ohm)
C225C

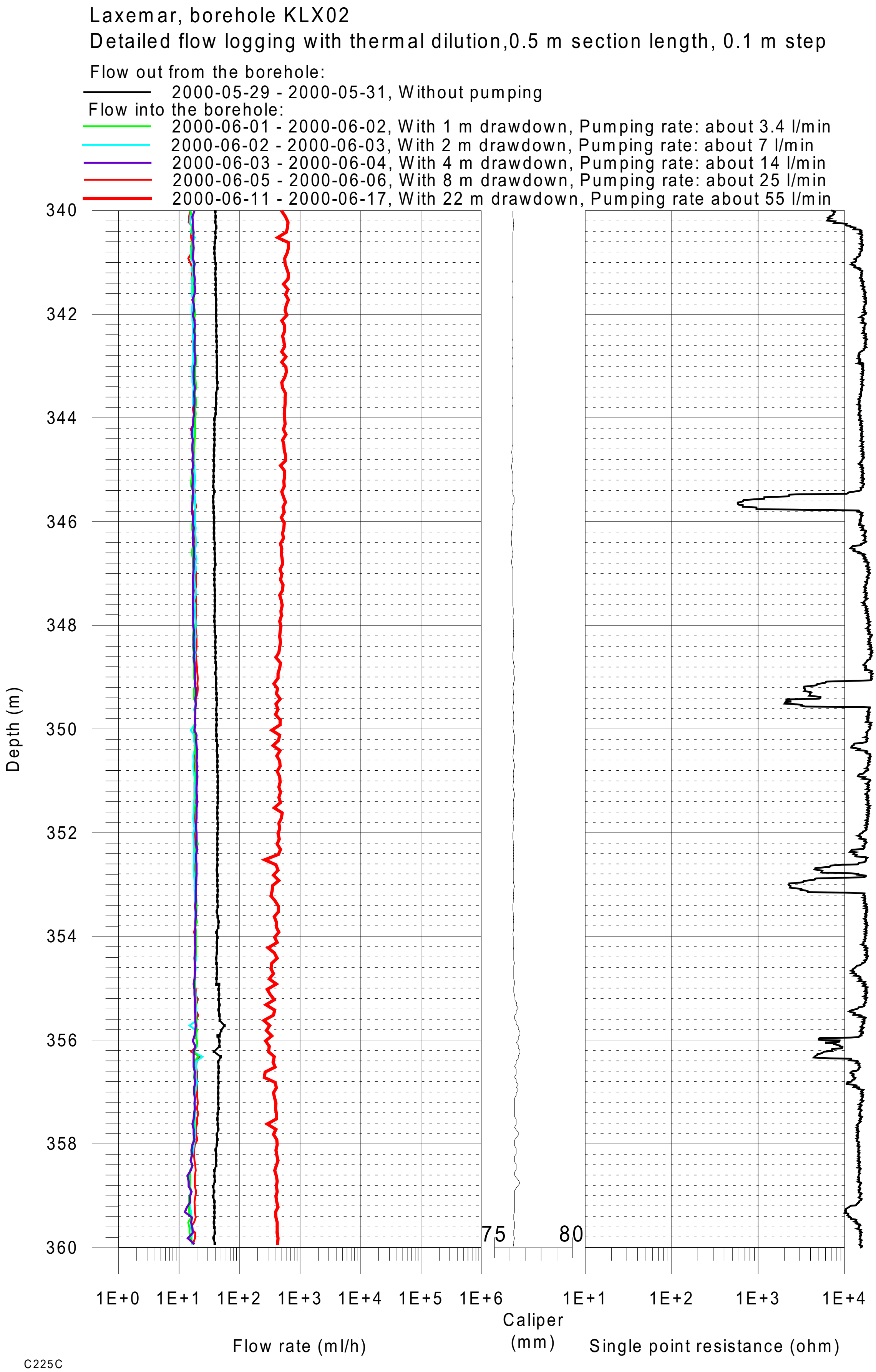
Laxemar, borehole KLX02
Detailed flow logging with thermal dilution,0.5 m section length, 0.1 m step
Flow out from the borehole:
2000-05-29 - 2000-05-31, Without pumping
Flow into the borehole:
2000-06-01 - 2000-06-02, With 1 m drawdown, Pumping rate: about 3.4 l/min
2000-06-02 - 2000-06-03, With 2 m drawdown, Pumping rate: about 7 l/min
2000-06-03 - 2000-06-04, With 4 m drawdown, Pumping rate: about 14 l/min
2000-06-05 - 2000-06-06, With 8 m drawdown, Pumping rate: about 25 l/min
2000-06-11 - 2000-06-17, With 22 m drawdown, Pumping rate about 55 l/min
Depth (m)
340
342
344
346
348
350
352
354
356
358
360
75
80
1E+0
1E+1
1E+2
1E+3
1E+4
1E+5
1E+6
Flow rate (ml/h)
Caliper
(mm)
1E+1
1E+2
1E+3
1E+4
Single point resistance (ohm)
C225C

Laxemar, borehole KLX02

Detailed flow logging with thermal dilution,0.5 m section length, 0.1 m step

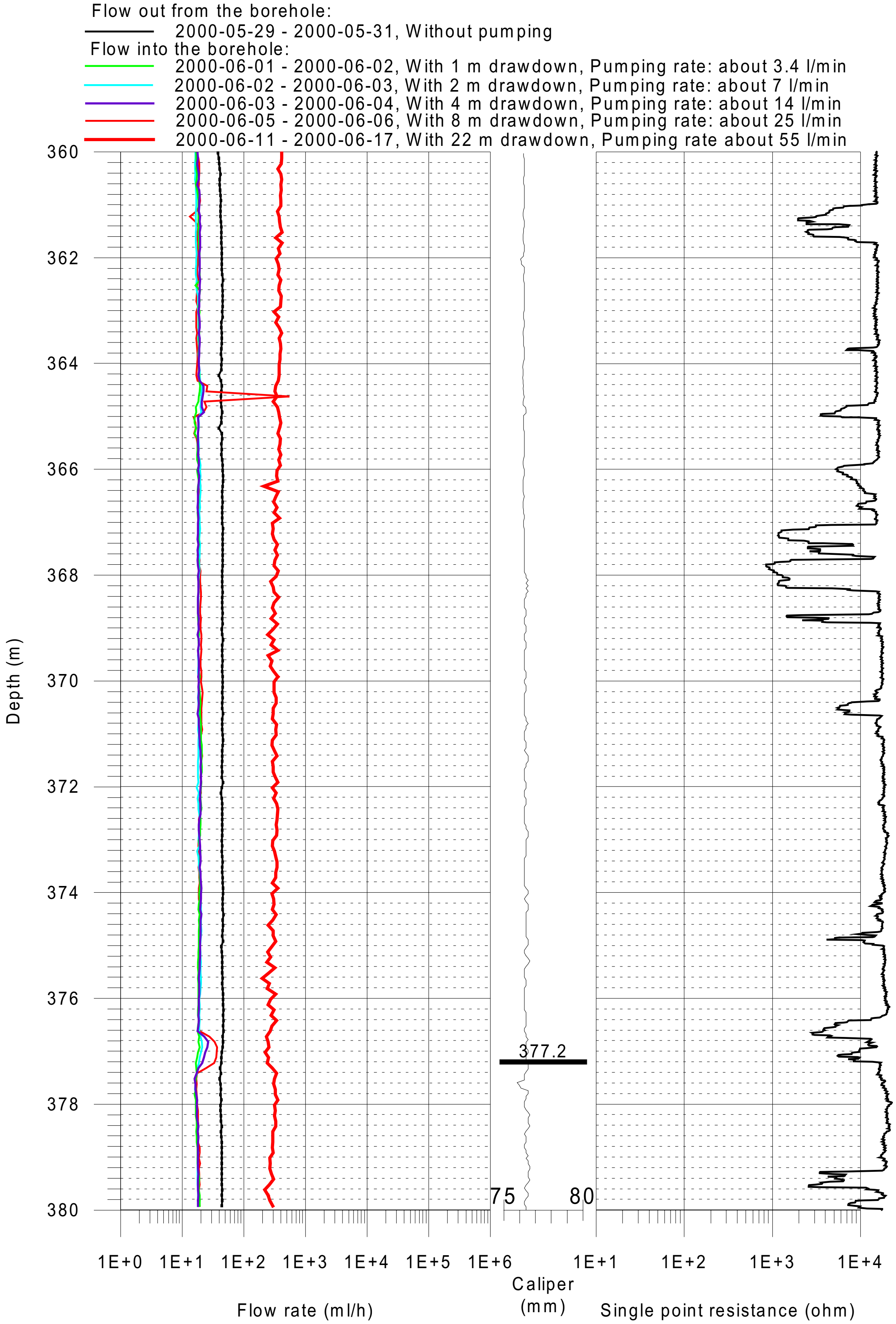

C225C

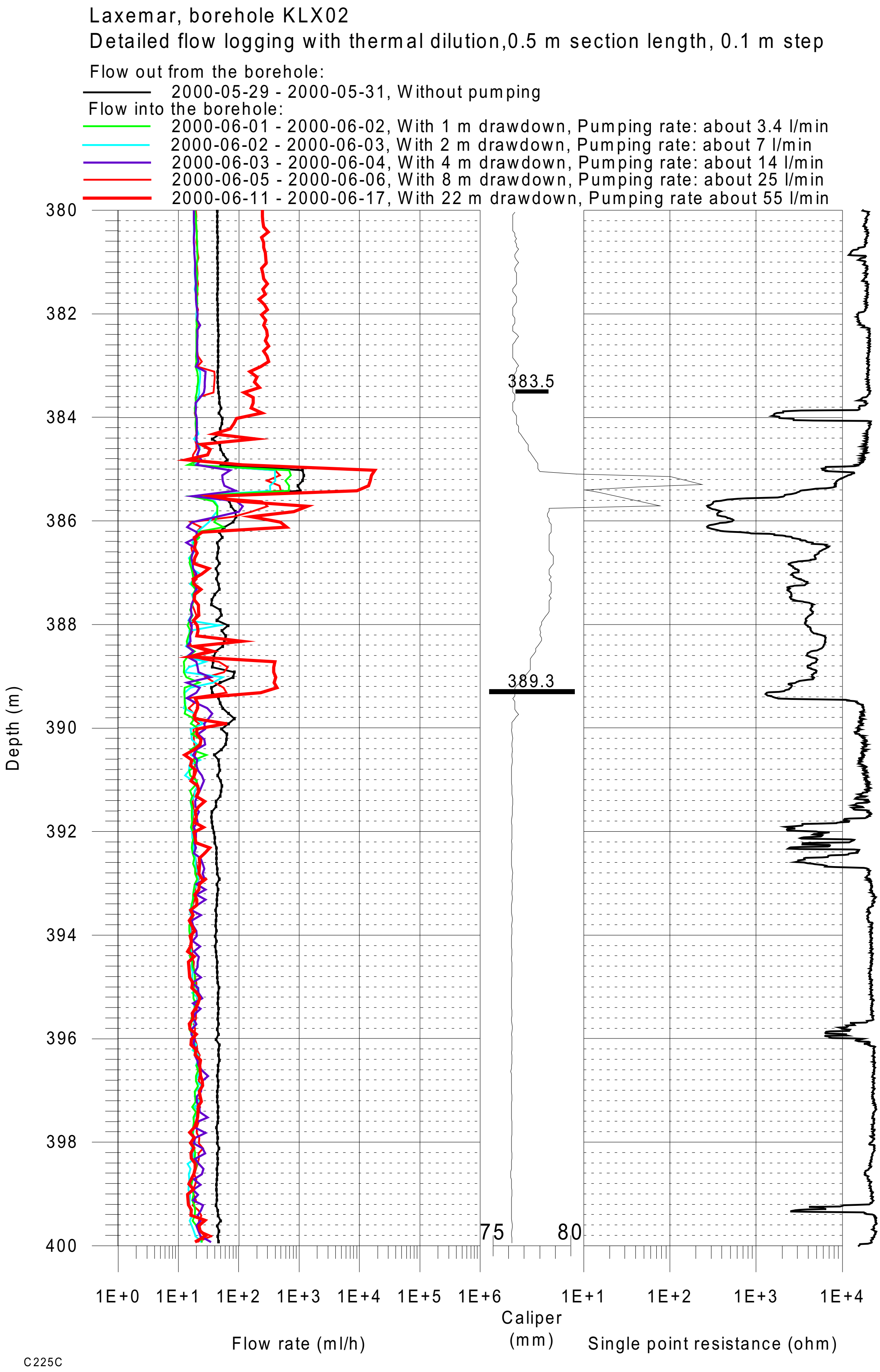
Laxemar, borehole KLX02
Detailed flow logging with thermal dilution,0.5 m section length, 0.1 m step
Flow out from the borehole:
2000-05-29 - 2000-05-31, Without pumping
Flow into the borehole:
2000-06-01 - 2000-06-02, With 1 m drawdown, Pumping rate: about 3.4 l/min
2000-06-02 - 2000-06-03, With 2 m drawdown, Pumping rate: about 7 l/min
2000-06-03 - 2000-06-04, With 4 m drawdown, Pumping rate: about 14 l/min
2000-06-05 - 2000-06-06, With 8 m drawdown, Pumping rate: about 25 l/min
2000-06-11 - 2000-06-17, With 22 m drawdown, Pumping rate about 55 l/min
Depth (m)
380
382
384
386
388
390
392
394
396
398
400
383.5
389.3
75
80
1E+0
1E+1
1E+2
1E+3
1E+4
1E+5
1E+6
Flow rate (ml/h)
Caliper
(mm)
1E+1
1E+2
1E+3
1E+4
Single point resistance (ohm)
C225C

Table A2-1. Measured flows at different drawdown (D) of interpreted flow anomalies (R^2=linear regression coefficient, h0=mean of calculated relative head)

Depth (m)	Flow(0D) (ml/h)	Flow(1D) (ml/h)	Flow(2D) (ml/h)	Flow(4D) (ml/h)	Flow(8D) (ml/h)	Flow(22D) (ml/h)	R2	h0-mean (m)
212	-50	102	260	583	1056	2964	1	
213.3	-3500	3568	14700	33784	66576	158662	0.99	-0.51
214	-370	900	2243	3783	5029	16757	0.99	-0.44
215.2	-65	143	377	933	1942	5031	1	
216.7	0	18	24	44	112	302	1	
220.7	0	28	50	116	207	572	1	
224.4	-190	560	1372	2448	4071	12542	1	-0.32
224.9	0	48	141	288	650	1823	1	
226	0	334	761	1443	2340	6625	1	
227.7	-645	1370	3096	6715	13251	30680	0.99	-0.38
231.9	0	35	68	154	338	778	0.99	
232.4	0	14	17	15	23	38	0.83	
233.9	-81	185	510	1128	2107	5337	1	
234.2	0	17	22	32	61	166	1	
237.8	0	22	35	72	163	359	0.99	
238	0	16	21	27	53	86	0.93	
239.1	0	25	44	110	230	604	1	
241.4	0	47	139	300	510	990	0.97	
242.3	0	18	22	36	68	121	0.96	
243.3	-58	112	285	478	583	2870	0.97	
243.8	0	22	49	109	246	714	1	
244.9	0	21	41	86	230	733	1	
246.7	-314	730	1990	4311	8981	22150	1	-0.31
248.6	-174	300	1246	2814	5783	15479	1	-0.25
249.2	-29	31	77	231	604	1623	1	
250.1	0	20	37	84	228	578	1	
251.3	-696	14345	30142	73118	255638	458764	0.96	-0.34
251.6	-2926	5449	14786	33950	65399	111455	0.94	-0.46
252.9	-432	818	2254	5562	13764	41867	1	-0.31
254.1	-38	26	68	173	368	1269	1	
268	-376	1086	2562	4826	8956	16905	0.97	-0.35
269	0	36	67	147	162	213	0.72	
269.7	-175	351	985	2005	3394	7977	0.99	-0.39
271.1	-610	1710	3391	7800	14473	36168	1	-0.33
273.8	0	23	45	203	307	715	0.98	
275	0	0	0	25	39	0	0	
276.9	0	19	27	56	133	462	0.99	
290.5	0	28	52	132	261	796	1	
292.6	0	19	29	70	116	219	0.96	
295.1	-180	2420	5030	7776	11395	30324	0.99	-0.11
295.6	0	140	315	837	1747	4393	1	
298.3	0	30	68	165	334	698	0.98	
300.6	0	23	38	91	252	801	1	
307.9	0	0	21	30	48	0	0.01	
310.5	0	0	0	0	35	0	0.01	
314.7	0	21	27	39	54	0	0.05	
317.1	-7961	14326	39117	97922	240506	452519	0.97	-0.38
325.4	0	0	22	42	39	0	0.02	
327.8	0	17	17	17	17	0	0.21	

328.6	0	31	62	116	212	0	0.01	
329.2	0	21	31	54	59	0	0.05	
332.7	0	19	19	25	30	0	0.11	
337.9	-186	365	1000	2251	3856	9576	0.99	-0.37
338.9	-1040	1804	3290	5301	6157	12983	0.91	-0.90
339.1	-900	2040	3692	7334	13174	34185	1	-0.55
339.6	-164	292	813	1812	2759	7170	0.99	-0.40
377.2	0	0	18	21	32	0	0.01	
383.5	0	0	0	27	38	0	0	
385.4?	1043	669	330	89	496	8524	0.84	
389.3	0	12	12	20	61	375	0.96	

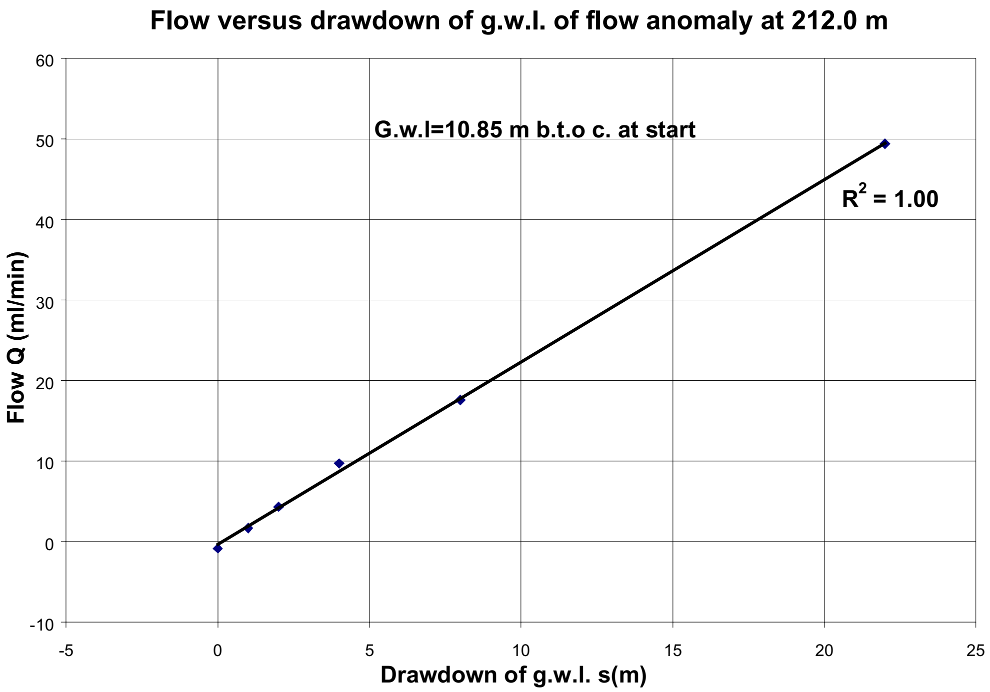
Flow versus drawdown of g.w.l. of flow anomaly at 212.0 m
G.w.l=10.85 m b.t.o c. at start
R2 = 1.00
Flow Q (ml/min)
Drawdown of g.w.l. s(m)
60
50
40
30
20
10
0
-10
-5
0
5
10
15
20
25

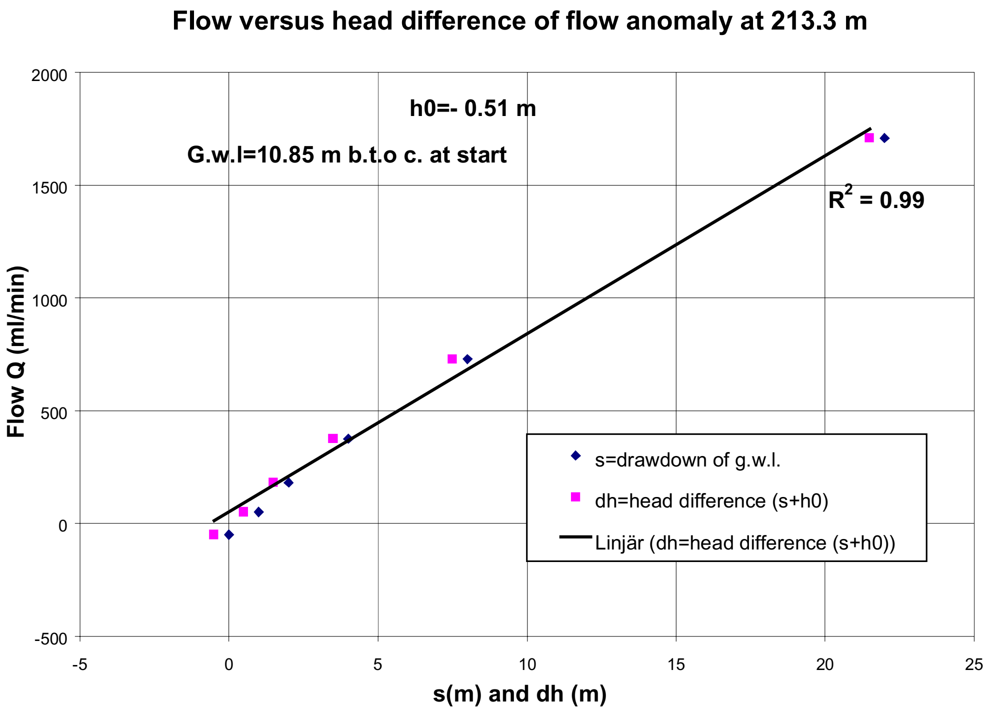
Flow versus head difference of flow anomaly at 213.3 m
h0=- 0.51 m
G.w.l=10.85 m b.t.o c. at start
R2 = 0.99
Flow Q (ml/min)
s(m) and dh (m)
s=drawdown of g.w.l.
dh=head difference (s+h0)
Linjär (dh=head difference (s+h0))
2000
1500
1000
500
0
-500
-5
0
5
10
15
20
25

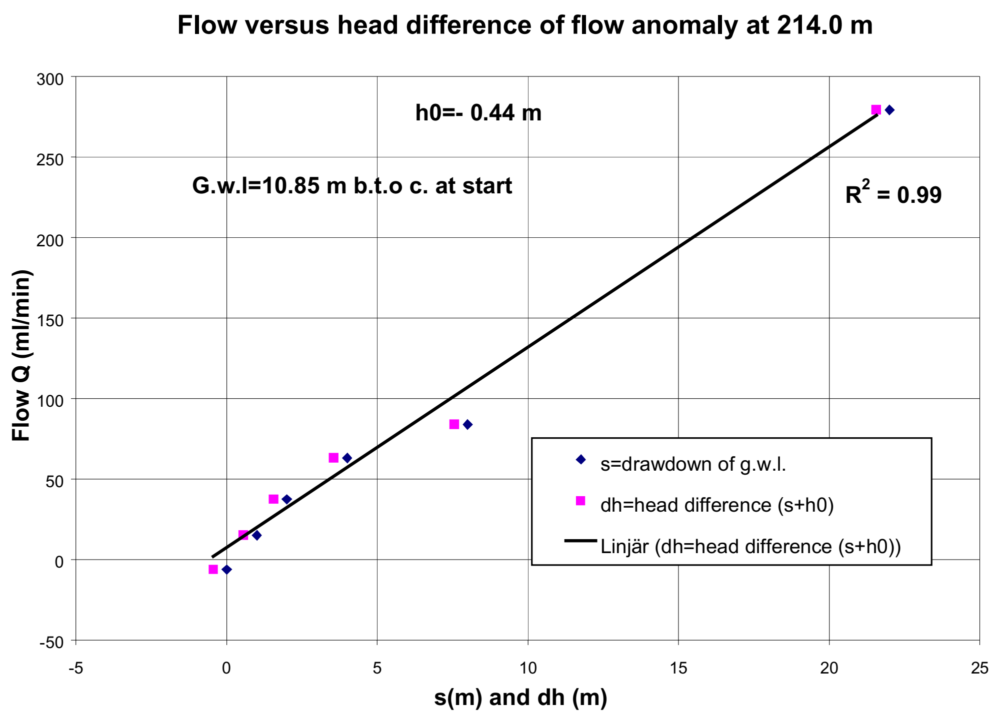
Flow versus head difference of flow anomaly at 214.0 m
h0=- 0.44 m
G.w.l=10.85 m b.t.o c. at start
R2 = 0.99
s=drawdown of g.w.l.
dh=head difference (s+h0)
Linjär (dh=head difference (s+h0))
Flow Q (ml/min)
s(m) and dh (m)
300
250
200
150
100
50
0
-50
-5
0
5
10
15
20
25

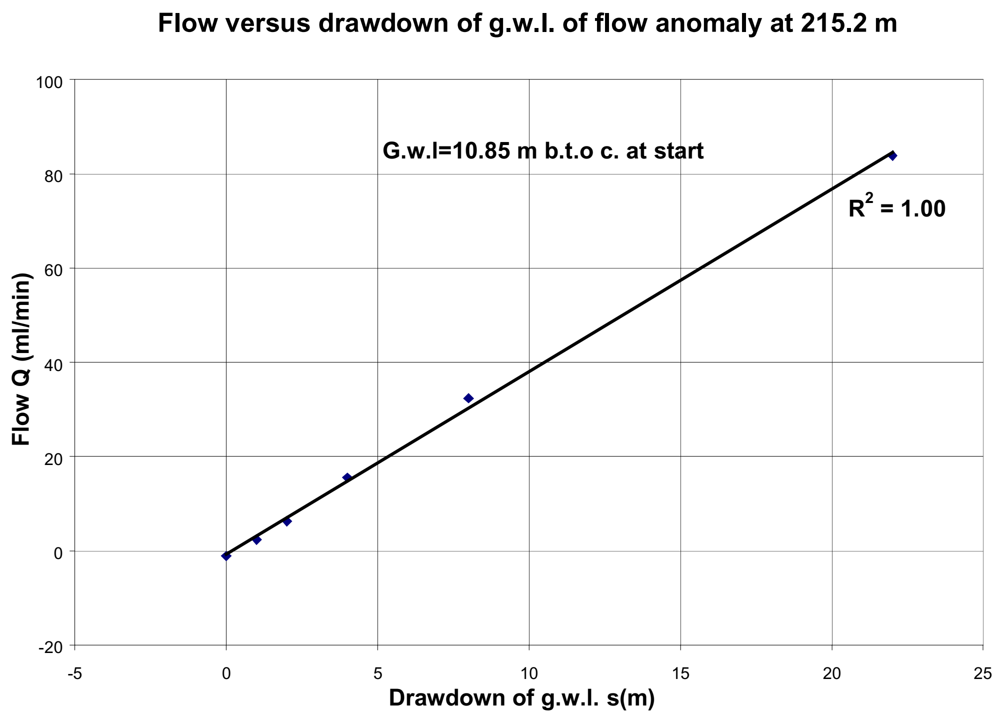
Flow versus drawdown of g.w.l. of flow anomaly at 215.2 m
G.w.l=10.85 m b.t.o c. at start
R2 = 1.00
Flow Q (ml/min)
Drawdown of g.w.l. s(m)
100
80
60
40
20
0
-20
-5
0
5
10
15
20
25

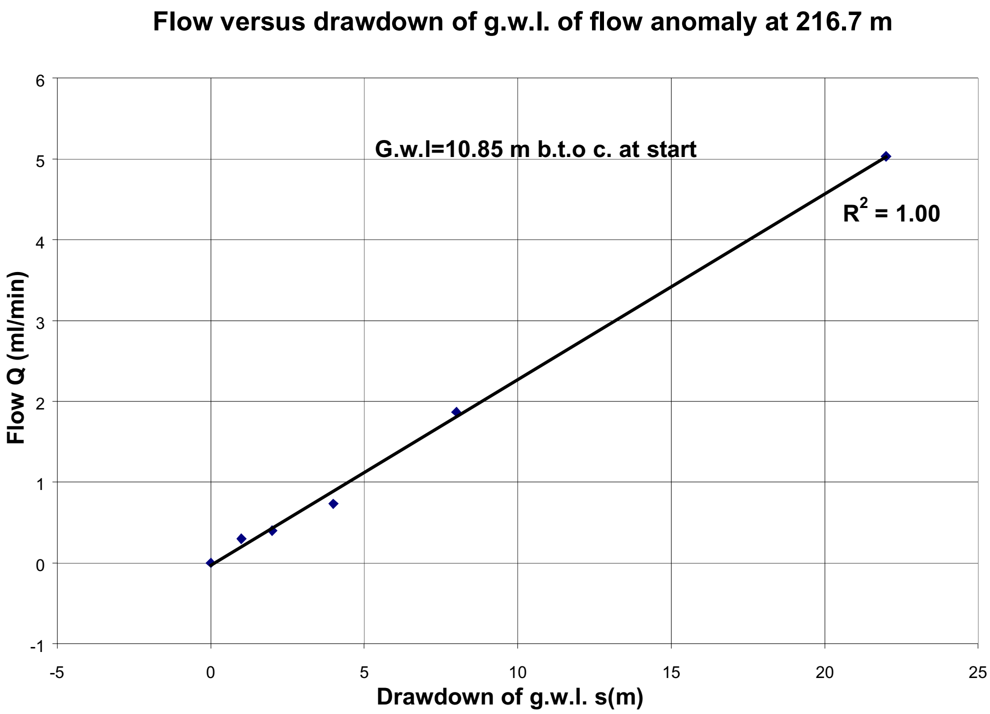
Flow versus drawdown of g.w.l. of flow anomaly at 216.7 m
G.w.l=10.85 m b.t.o c. at start
R2 = 1.00
Flow Q (ml/min)
Drawdown of g.w.l. s(m)
6
5
4
3
2
1
0
-1
-5
0
5
10
15
20
25

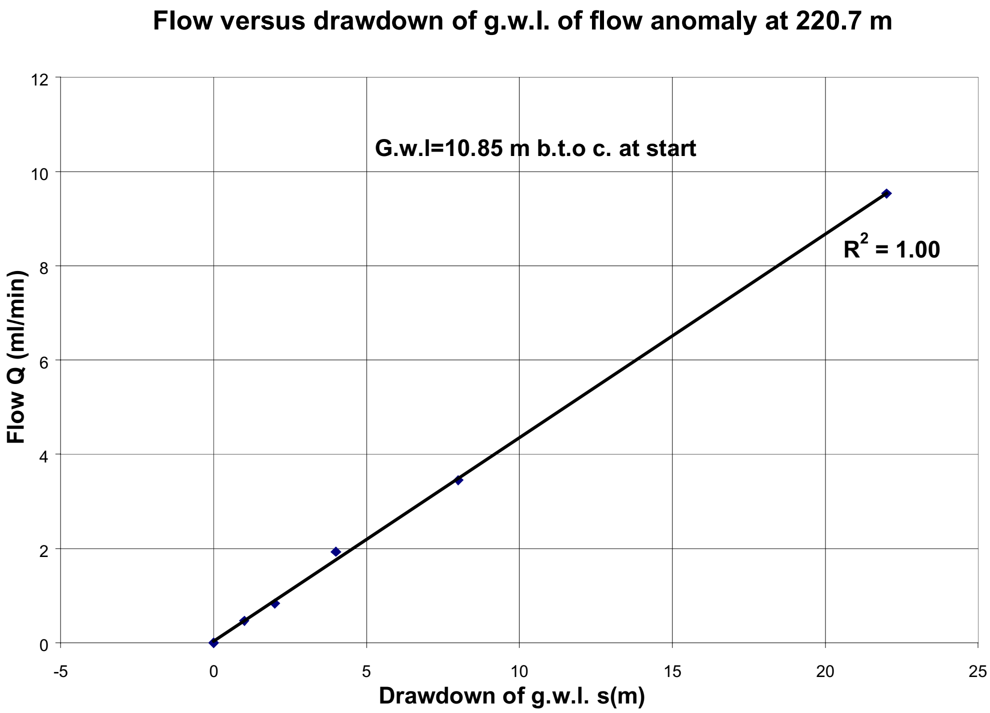
Flow versus drawdown of g.w.l. of flow anomaly at 220.7 m
G.w.l=10.85 m b.t.o c. at start
R2 = 1.00
Flow Q (ml/min)
Drawdown of g.w.l. s(m)
12
10
8
6
4
2
0
-5
0
5
10
15
20
25

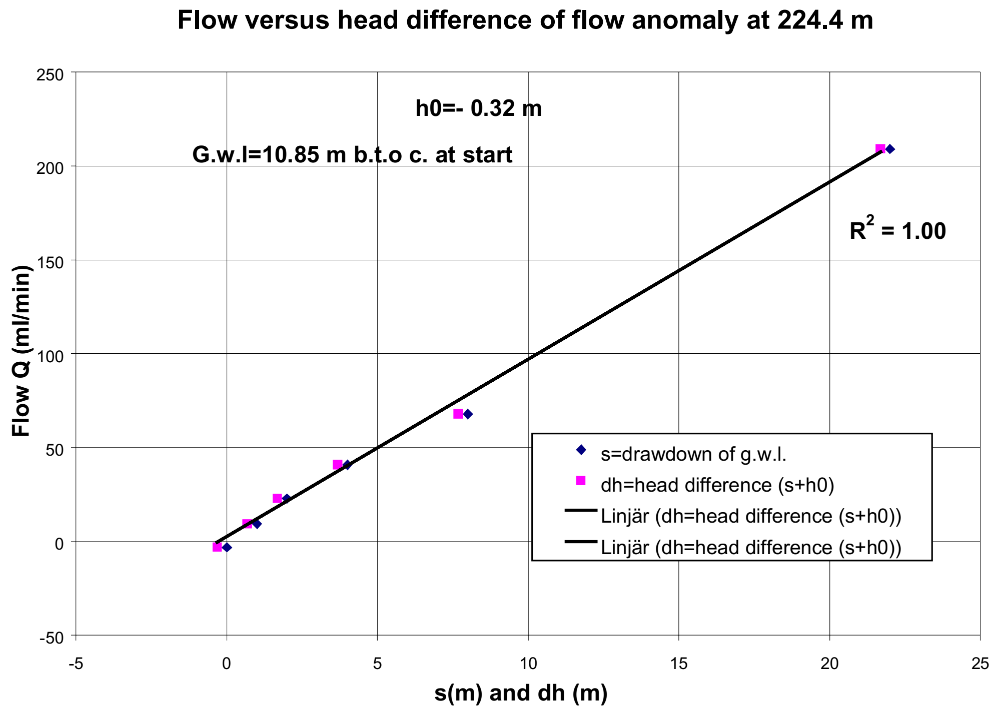
Flow versus head difference of flow anomaly at 224.4 m
h0=- 0.32 m
G.w.l=10.85 m b.t.o c. at start
R^2 = 1.00
Flow Q (ml/min)
s(m) and dh (m)
s=drawdown of g.w.l.
dh=head difference (s+h0)
Linjär (dh=head difference (s+h0))
Linjär (dh=head difference (s+h0))
250
200
150
100
50
0
-50
-5
0
5
10
15
20
25

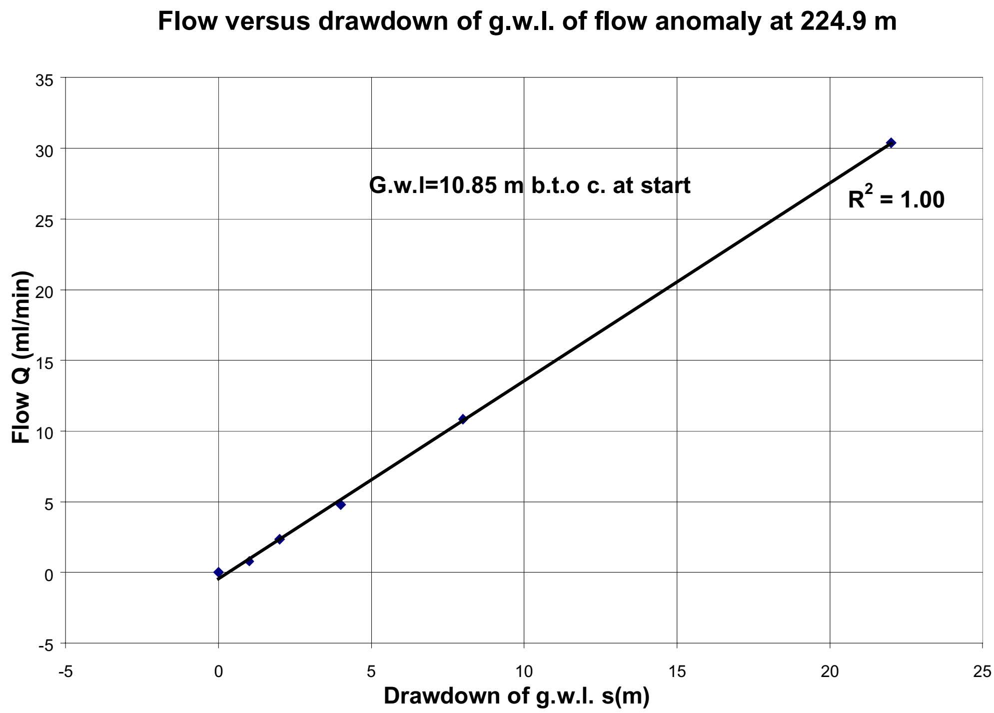
Flow versus drawdown of g.w.l. of flow anomaly at 224.9 m
G.w.l=10.85 m b.t.o c. at start
R^2 = 1.00
Flow Q (ml/min)
Drawdown of g.w.l. s(m)
35
30
25
20
15
10
5
0
-5
-5
0
5
10
15
20
25

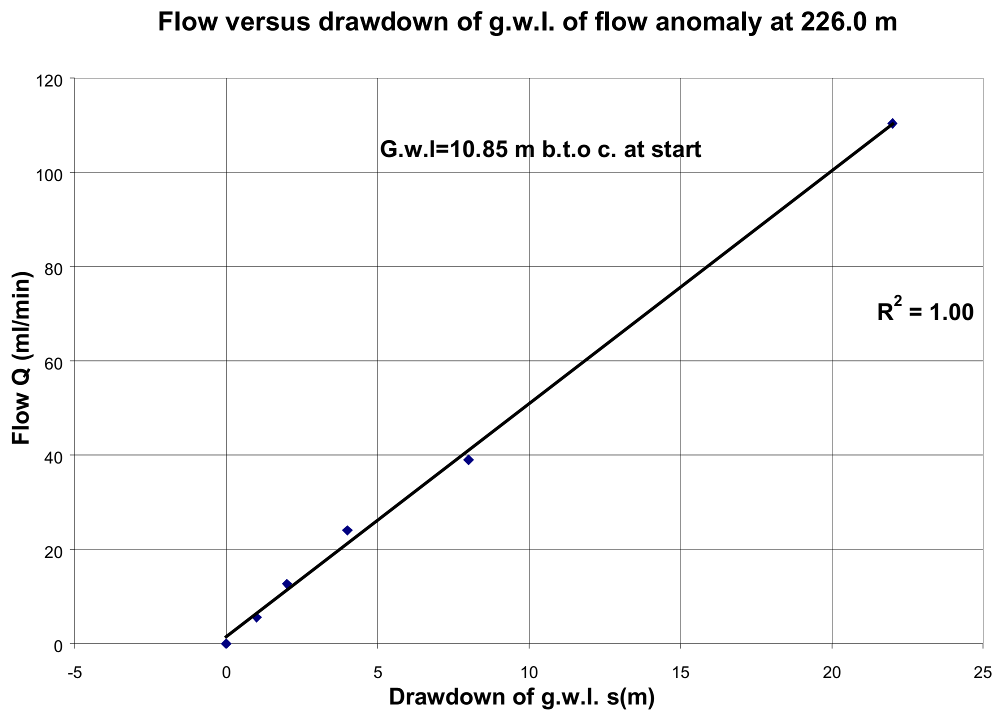

Flow versus drawdown of g.w.l. of flow anomaly at 226.0 m
G.w.l=10.85 m b.t.o c. at start
R^2 = 1.00
Flow Q (ml/min)
Drawdown of g.w.l. s(m)

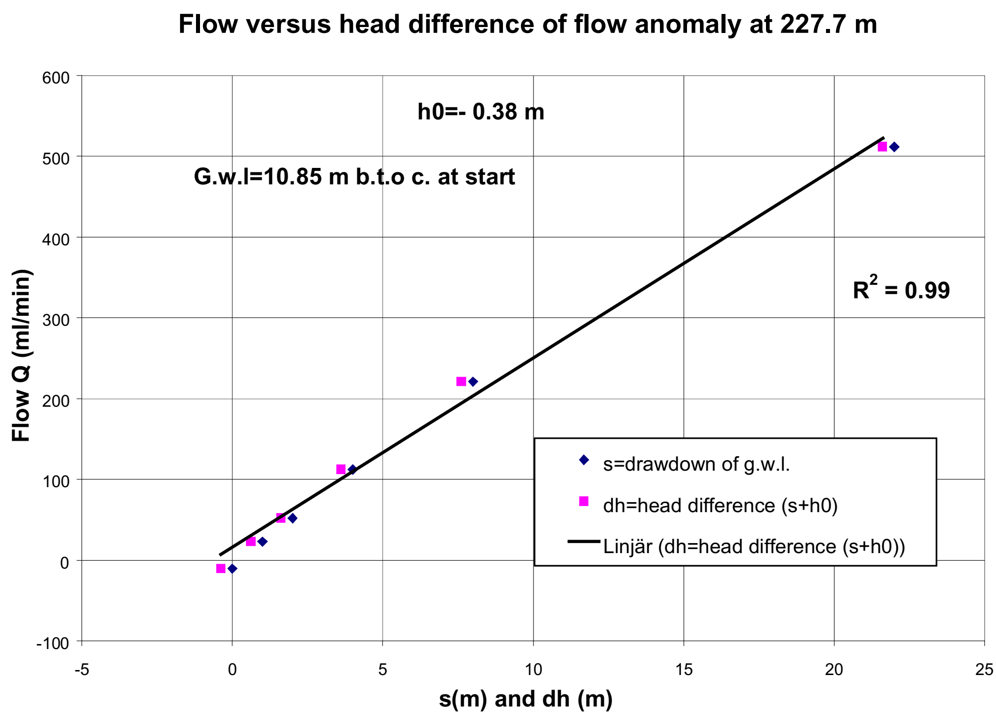

Flow versus head difference of flow anomaly at 227.7 m
h0=- 0.38 m
G.w.l=10.85 m b.t.o c. at start
R^2 = 0.99
s=drawdown of g.w.l.
dh=head difference (s+h0)
Linjär (dh=head difference (s+h0))
Flow Q (ml/min)
s(m) and dh (m)

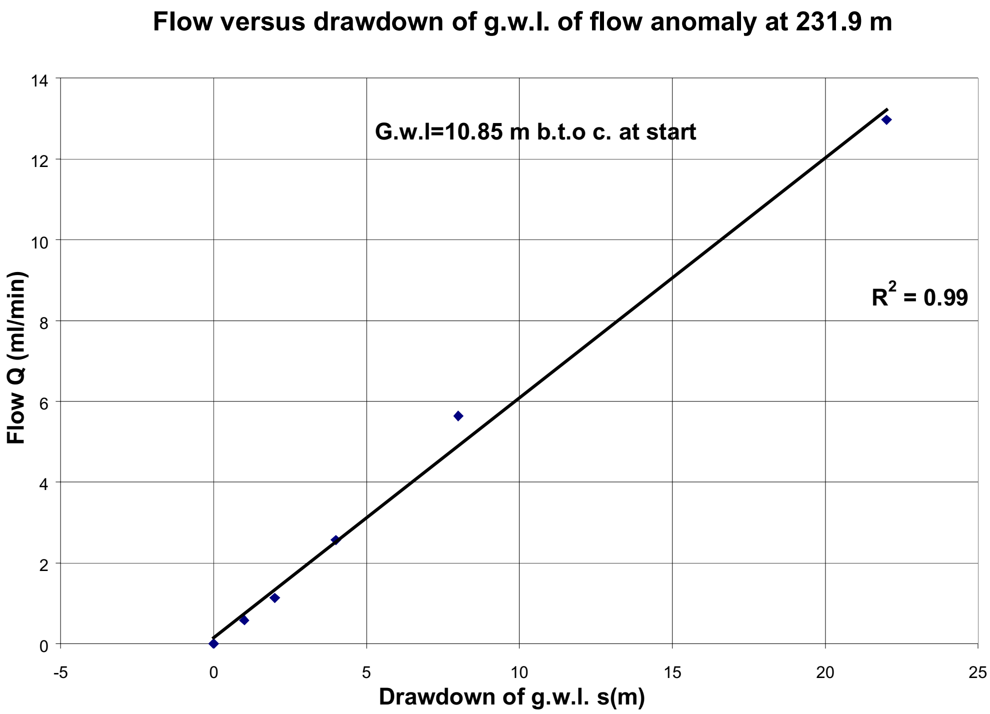
Flow versus drawdown of g.w.l. of flow anomaly at 231.9 m
G.w.l=10.85 m b.t.o c. at start
R^2 = 0.99
Flow Q (ml/min)
Drawdown of g.w.l. s(m)
14
12
10
8
6
4
2
0
-5
0
5
10
15
20
25

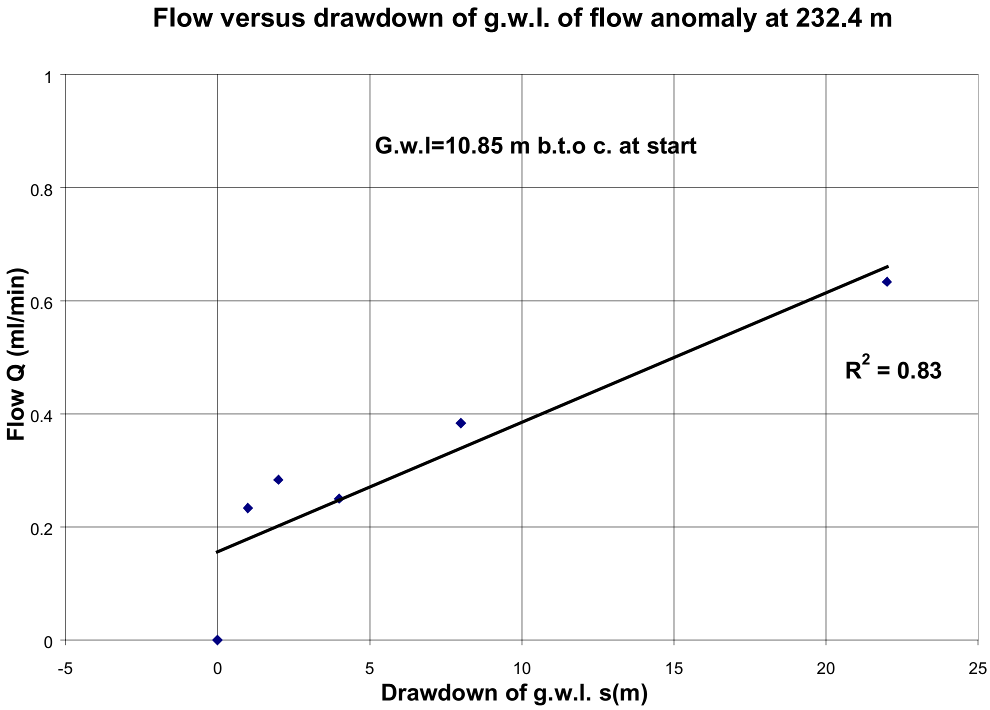
Flow versus drawdown of g.w.l. of flow anomaly at 232.4 m
G.w.l=10.85 m b.t.o c. at start
R^2 = 0.83
Flow Q (ml/min)
Drawdown of g.w.l. s(m)
1
0.8
0.6
0.4
0.2
0
-5
0
5
10
15
20
25

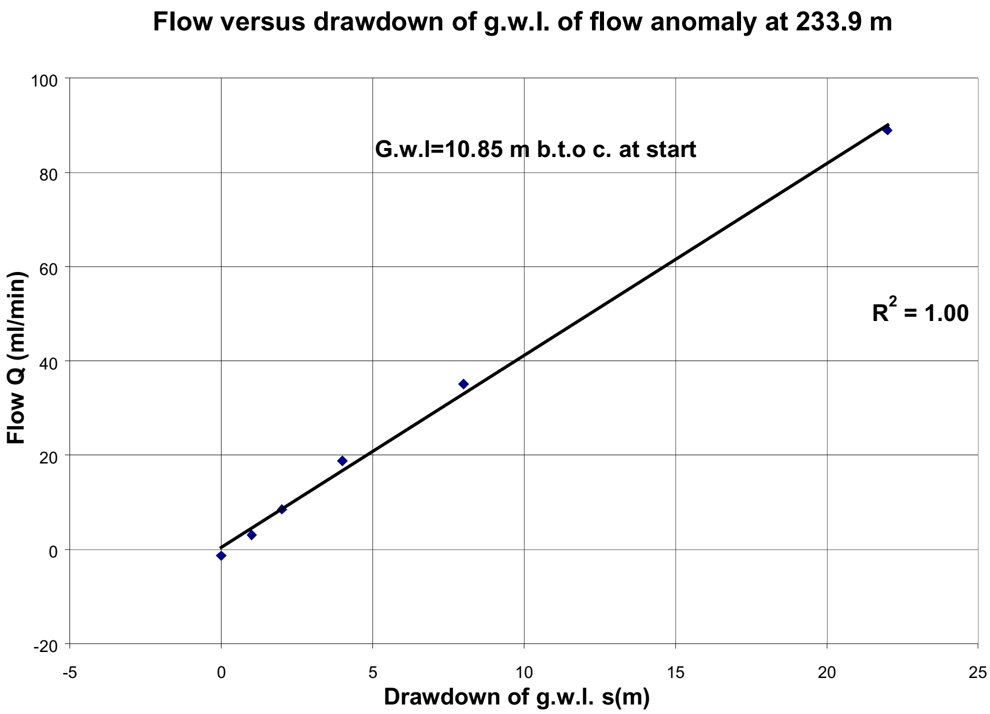

Flow versus drawdown of g.w.l. of flow anomaly at 233.9 m
G.w.l=10.85 m b.t.o c. at start
R^2 = 1.00
Flow Q (ml/min)
100
80
60
40
20
0
-20
-5
0
5
10
15
20
25
Drawdown of g.w.l. s(m)

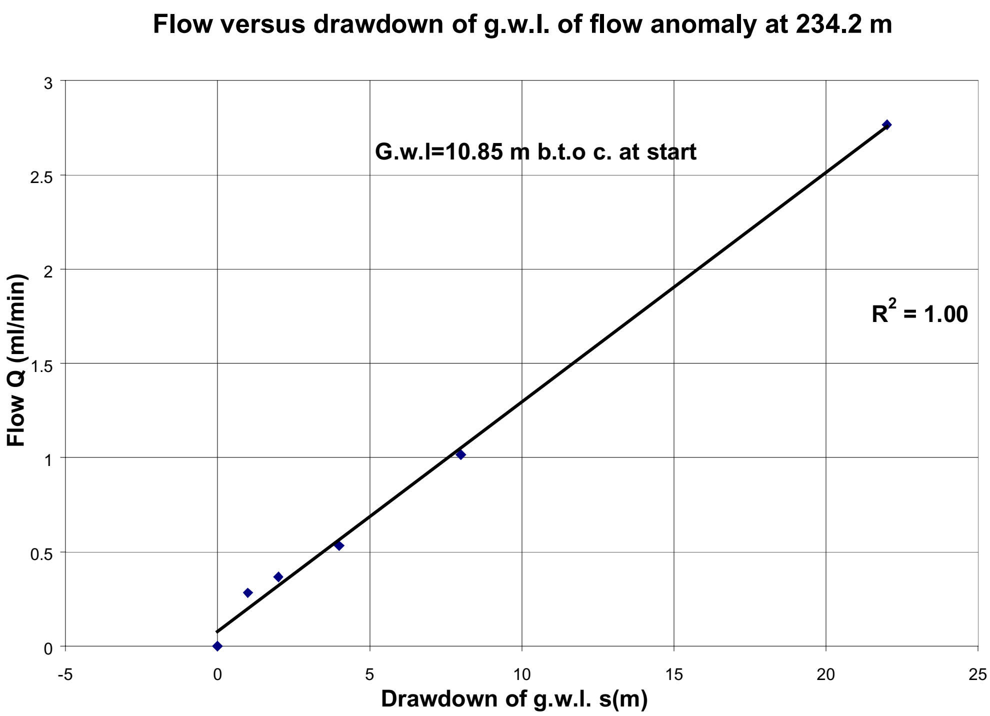

Flow versus drawdown of g.w.l. of flow anomaly at 234.2 m
G.w.l=10.85 m b.t.o c. at start
R^2 = 1.00
Flow Q (ml/min)
3
2.5
2
1.5
1
0.5
0
-5
0
5
10
15
20
25
Drawdown of g.w.l. s(m)

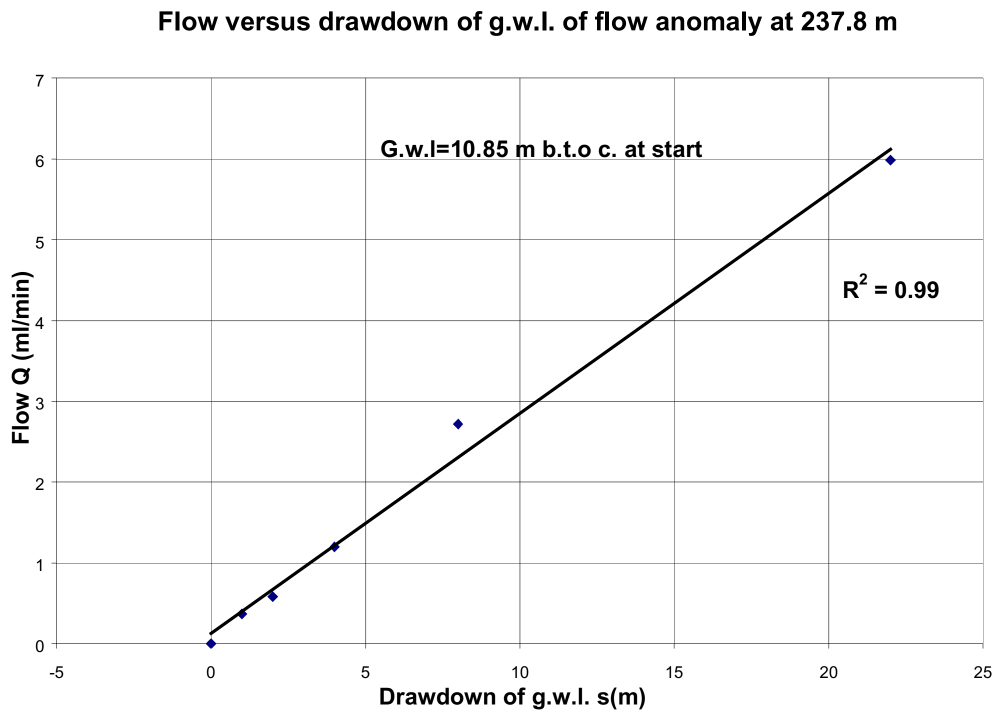
Flow versus drawdown of g.w.l. of flow anomaly at 237.8 m
G.w.l=10.85 m b.t.o c. at start
R2 = 0.99
Flow Q (ml/min)
Drawdown of g.w.l. s(m)
0
1
2
3
4
5
6
7
-5
0
5
10
15
20
25

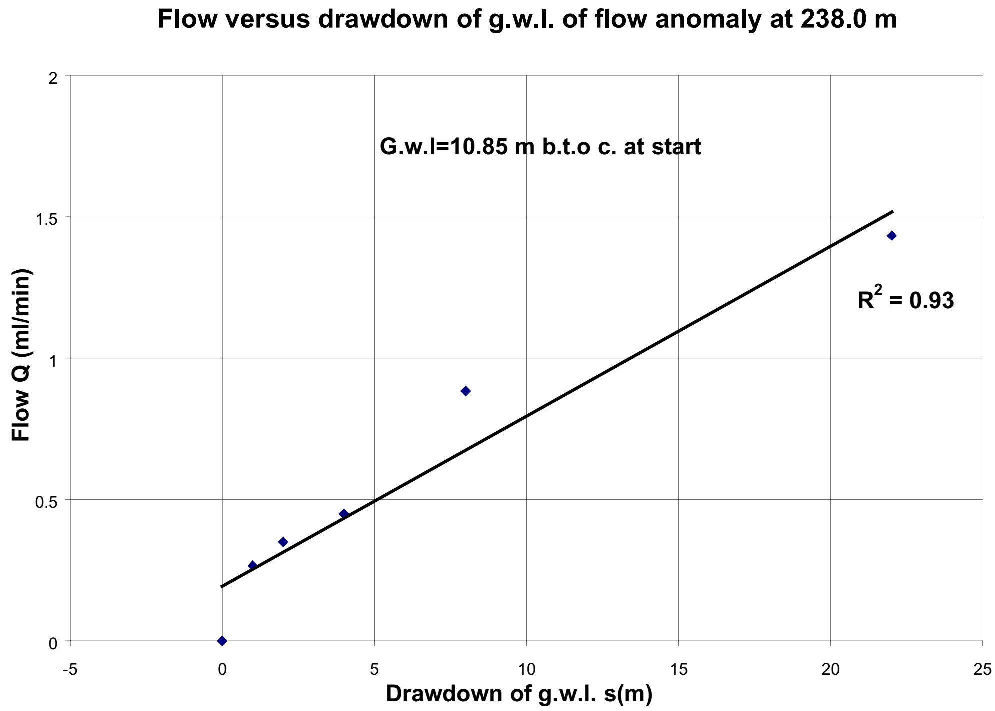
Flow versus drawdown of g.w.l. of flow anomaly at 238.0 m
G.w.l=10.85 m b.t.o c. at start
R2 = 0.93
Flow Q (ml/min)
Drawdown of g.w.l. s(m)
0
0.5
1
1.5
2
-5
0
5
10
15
20
25

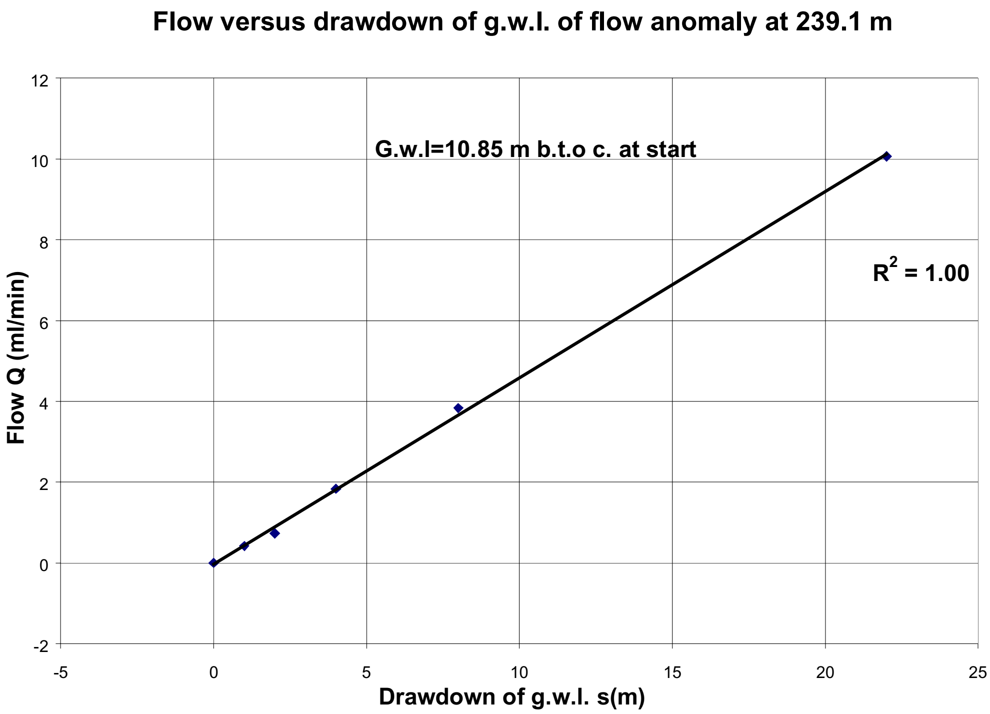

Flow versus drawdown of g.w.l. of flow anomaly at 239.1 m
G.w.l=10.85 m b.t.o c. at start
R2 = 1.00
Flow Q (ml/min)
Drawdown of g.w.l. s(m)
12
10
8
6
4
2
0
-2
-5
0
5
10
15
20
25

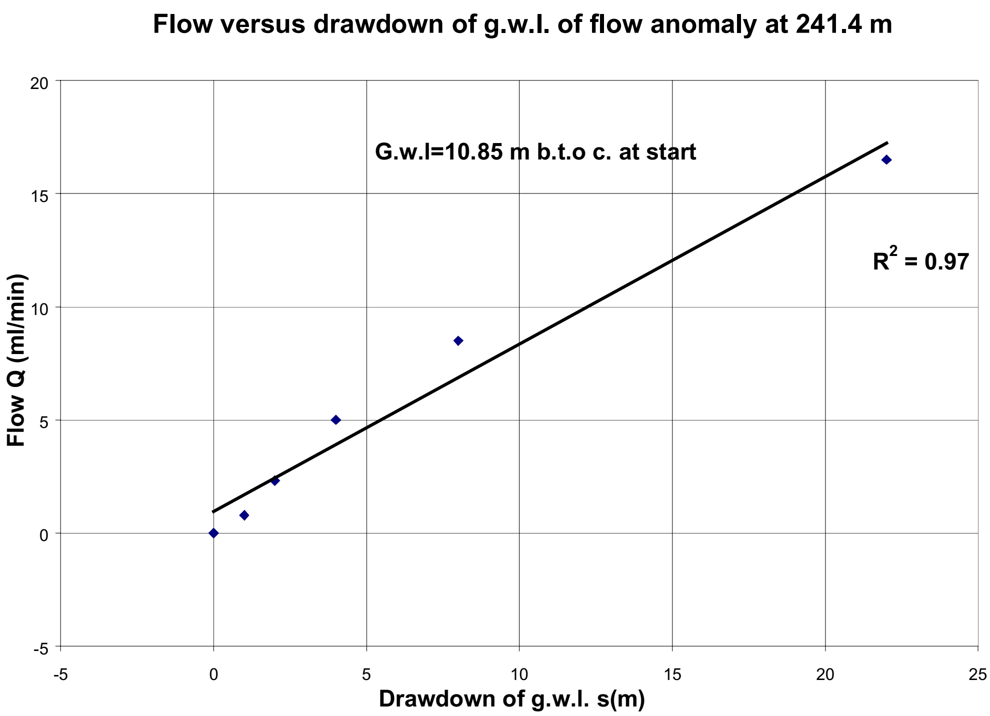

Flow versus drawdown of g.w.l. of flow anomaly at 241.4 m
G.w.l=10.85 m b.t.o c. at start
R2 = 0.97
Flow Q (ml/min)
Drawdown of g.w.l. s(m)
20
15
10
5
0
-5
-5
0
5
10
15
20
25

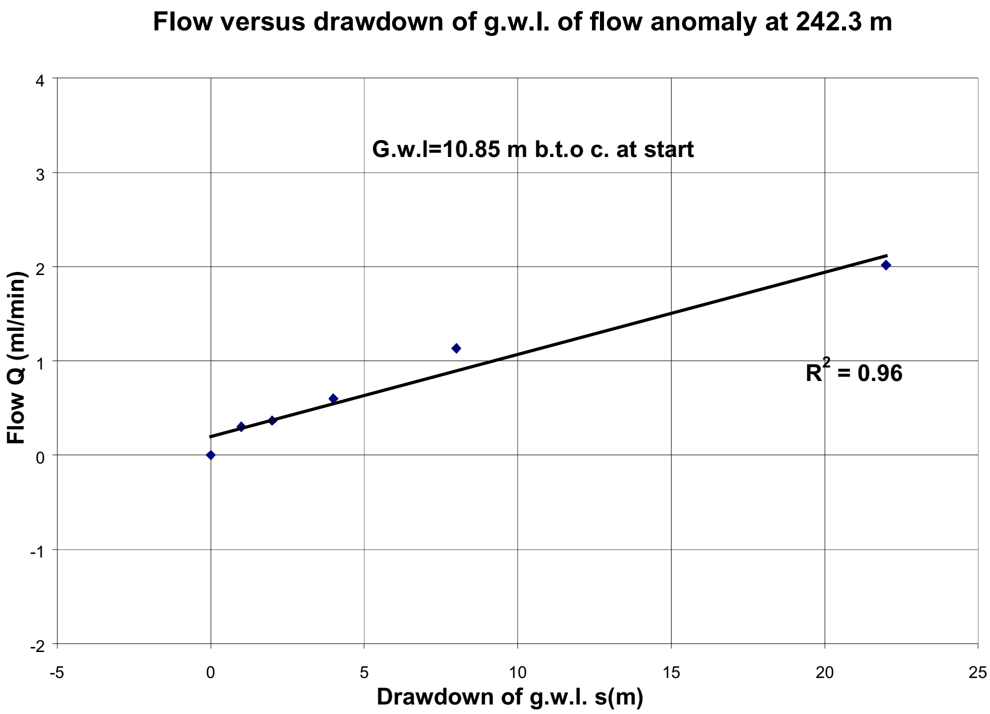

Flow versus drawdown of g.w.l. of flow anomaly at 242.3 m
G.w.l=10.85 m b.t.o c. at start
R² = 0.96
Flow Q (ml/min)
Drawdown of g.w.l. s(m)
4
3
2
1
0
-1
-2
-5
0
5
10
15
20
25

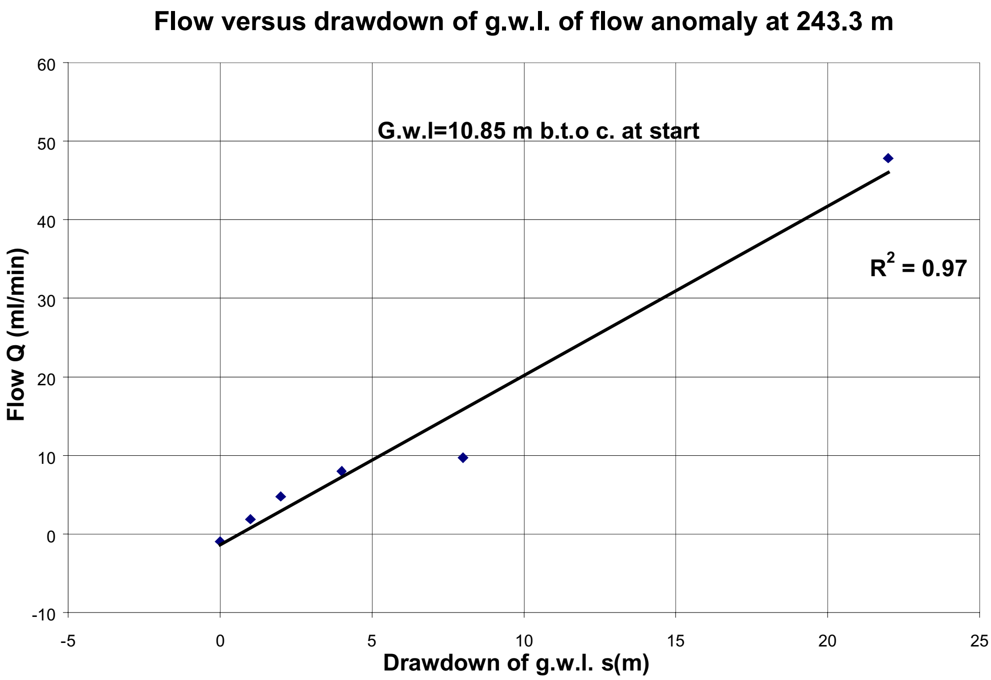

Flow versus drawdown of g.w.l. of flow anomaly at 243.3 m
G.w.l=10.85 m b.t.o c. at start
R² = 0.97
Flow Q (ml/min)
Drawdown of g.w.l. s(m)
60
50
40
30
20
10
0
-10
-5
0
5
10
15
20
25

Flow versus drawdown of g.w.l. of flow anomaly at 243.8 m

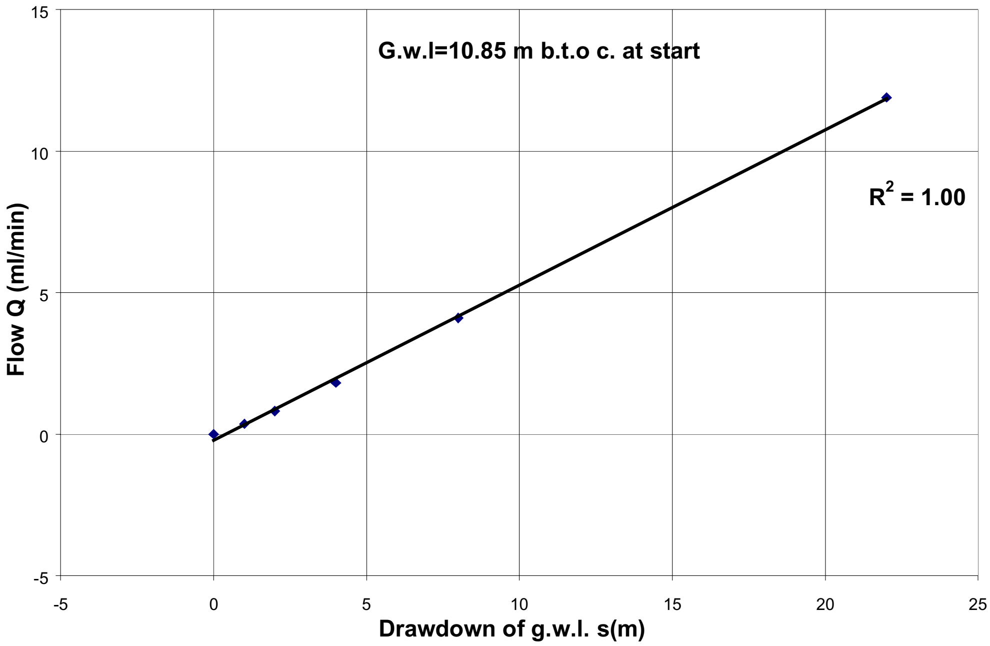

Flow versus drawdown of g.w.l. of flow anomaly at 244.9 m

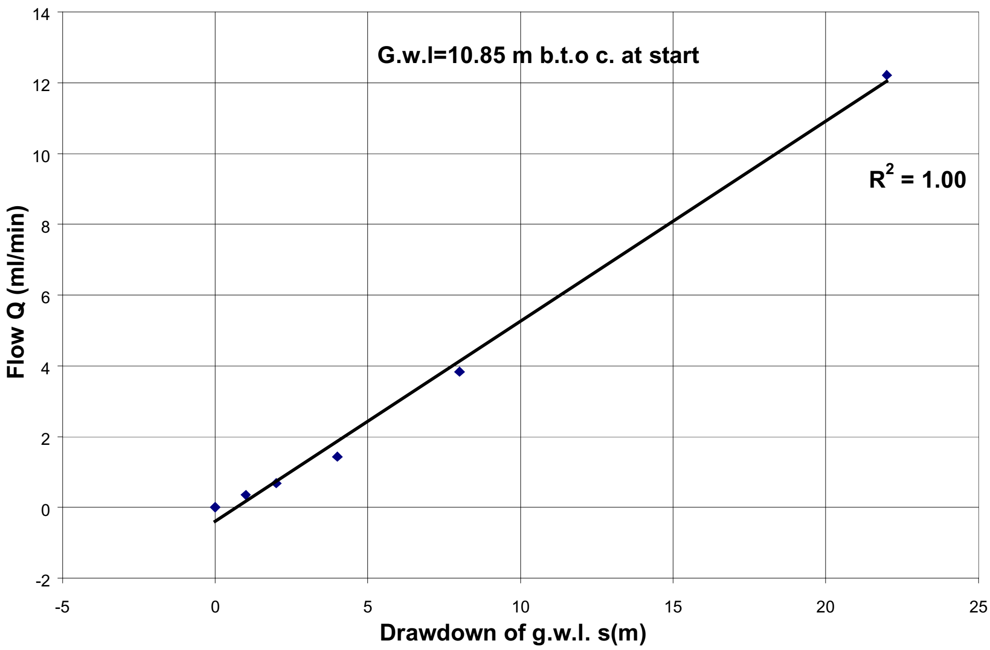

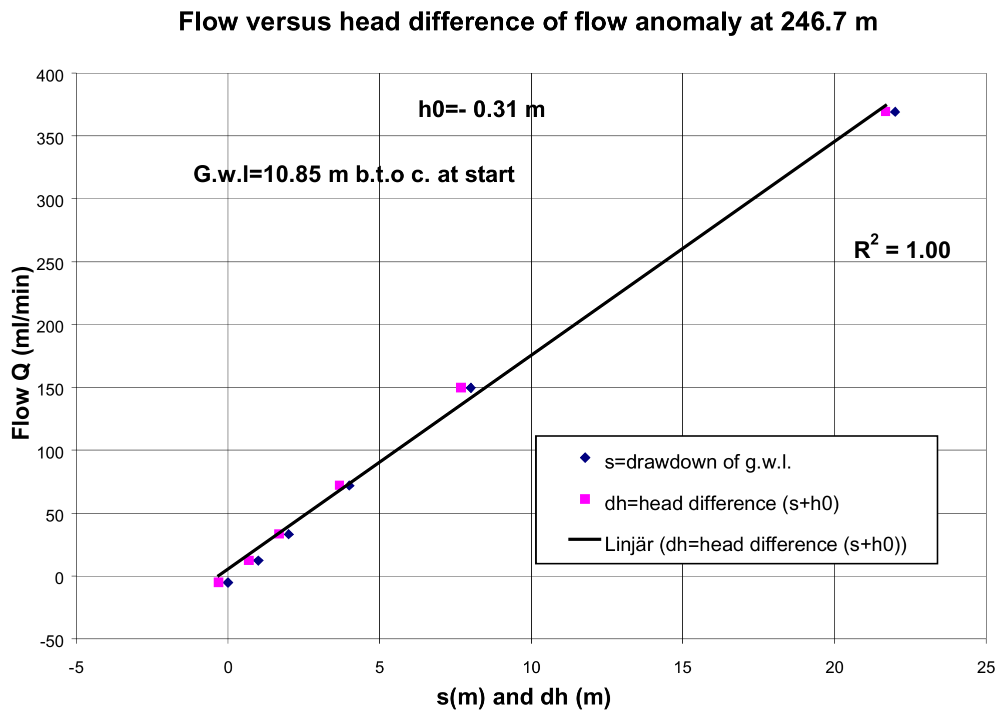

Flow versus head difference of flow anomaly at 246.7 m
h0=- 0.31 m
G.w.l=10.85 m b.t.o c. at start
R2 = 1.00
Flow Q (ml/min)
s(m) and dh (m)
s=drawdown of g.w.l.
dh=head difference (s+h0)
Linjär (dh=head difference (s+h0))
400
350
300
250
200
150
100
50
0
-50
-5
0
5
10
15
20
25

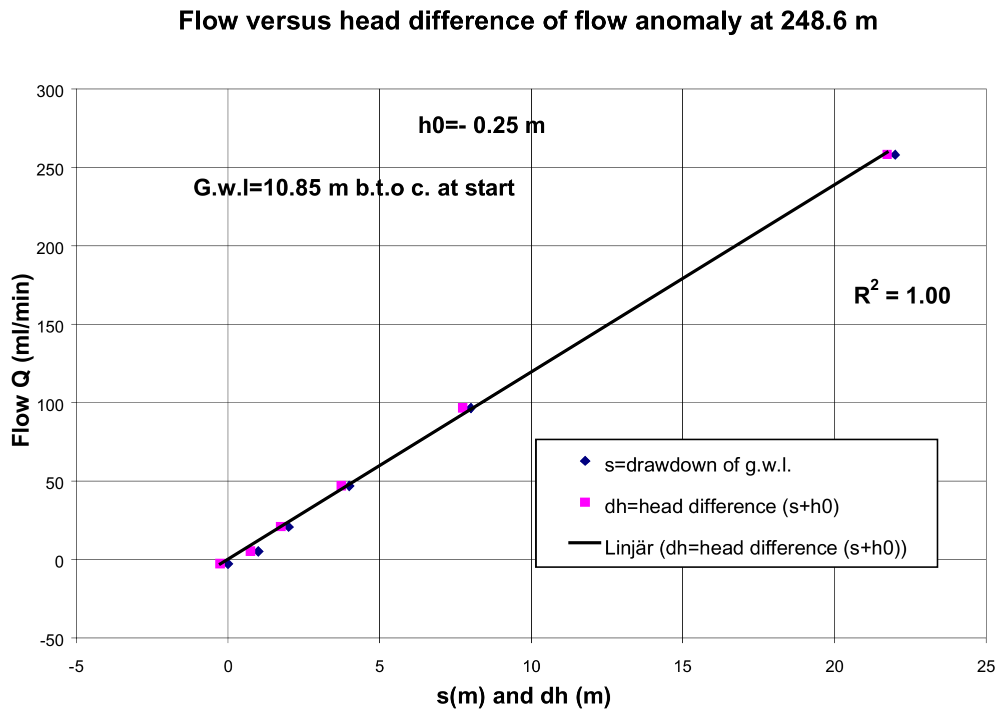

Flow versus head difference of flow anomaly at 248.6 m
h0=- 0.25 m
G.w.l=10.85 m b.t.o c. at start
R2 = 1.00
Flow Q (ml/min)
s(m) and dh (m)
s=drawdown of g.w.l.
dh=head difference (s+h0)
Linjär (dh=head difference (s+h0))
300
250
200
150
100
50
0
-50
-5
0
5
10
15
20
25

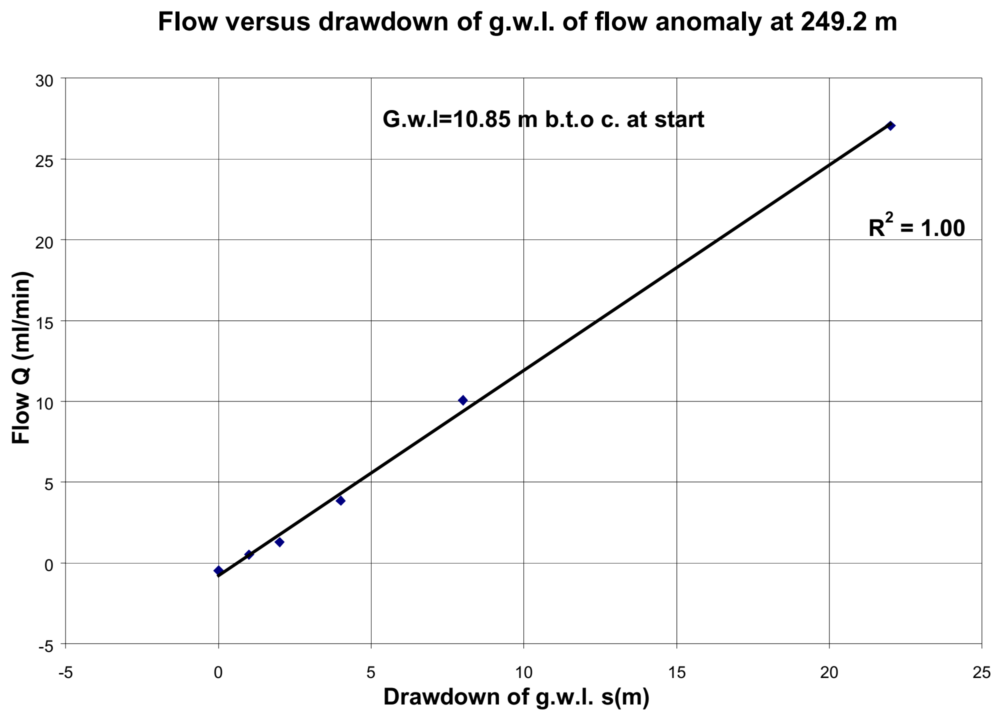

Flow versus drawdown of g.w.l. of flow anomaly at 249.2 m
G.w.l=10.85 m b.t.o c. at start
R^2 = 1.00
Flow Q (ml/min)
Drawdown of g.w.l. s(m)
30
25
20
15
10
5
0
-5
-5
0
5
10
15
20
25

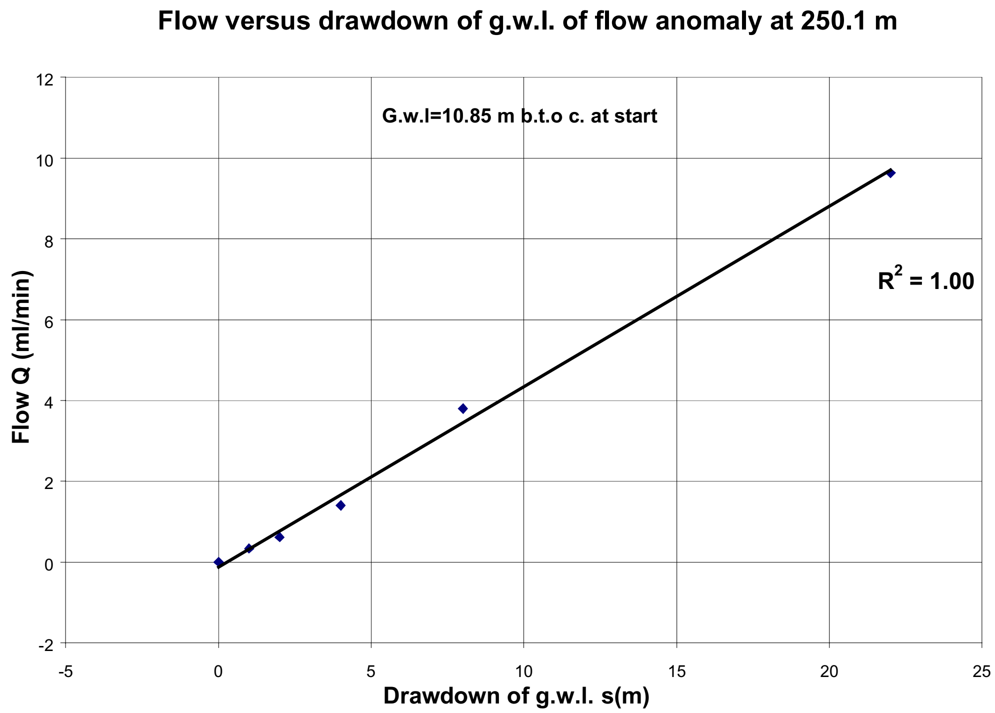

Flow versus drawdown of g.w.l. of flow anomaly at 250.1 m
G.w.l=10.85 m b.t.o c. at start
R^2 = 1.00
Flow Q (ml/min)
Drawdown of g.w.l. s(m)
12
10
8
6
4
2
0
-2
-5
0
5
10
15
20
25

Flow versus head difference of flow anomaly at 251.3 m

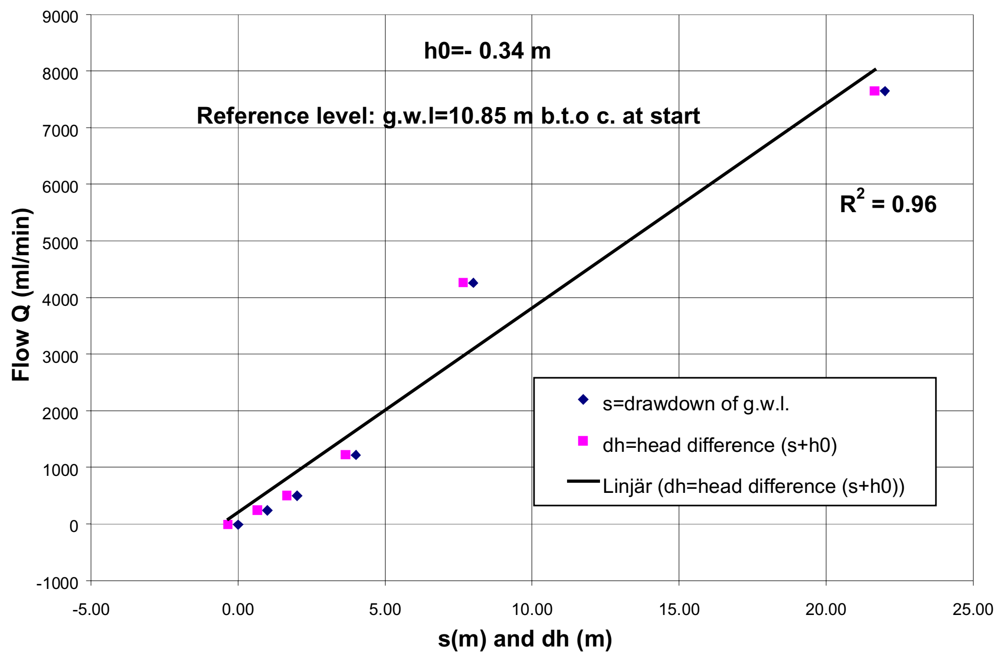

Flow versus head difference of flow anomaly at 251.6 m

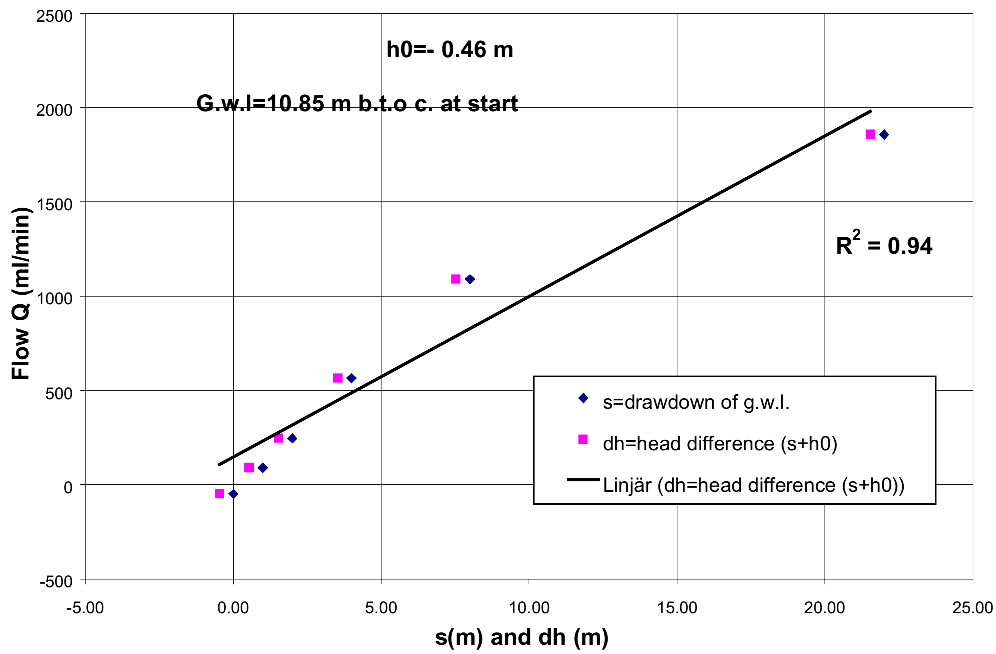

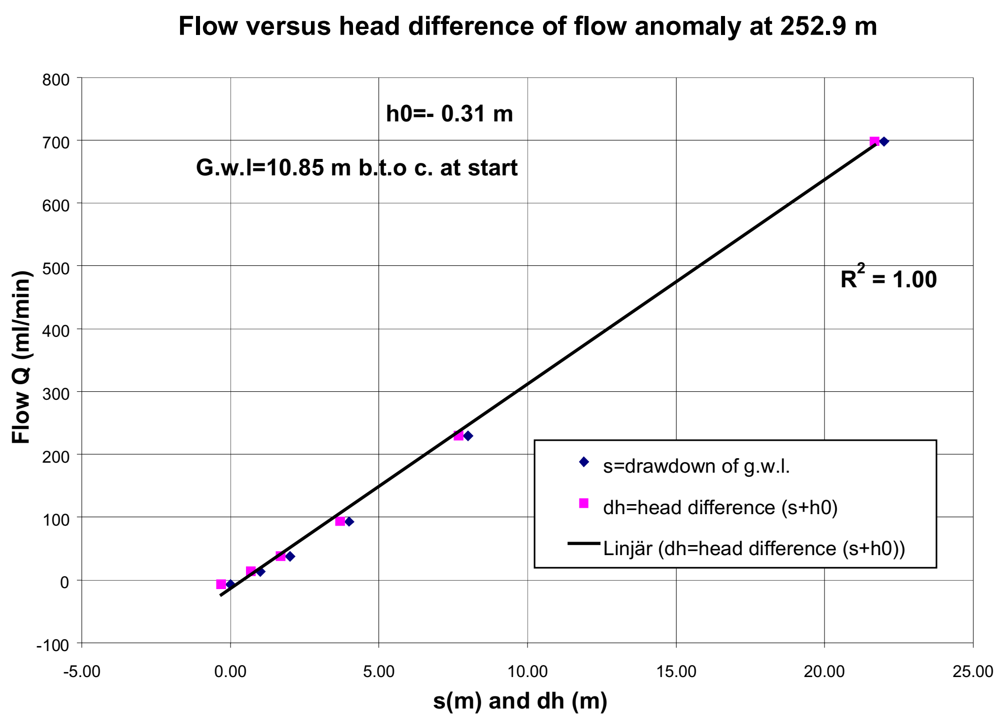
Flow versus head difference of flow anomaly at 252.9 m
h0=- 0.31 m
G.w.l=10.85 m b.t.o c. at start
R^2 = 1.00
s=drawdown of g.w.l.
dh=head difference (s+h0)
Linjär (dh=head difference (s+h0))
Flow Q (ml/min)
s(m) and dh (m)
800
700
600
500
400
300
200
100
0
-100
-5.00
0.00
5.00
10.00
15.00
20.00
25.00

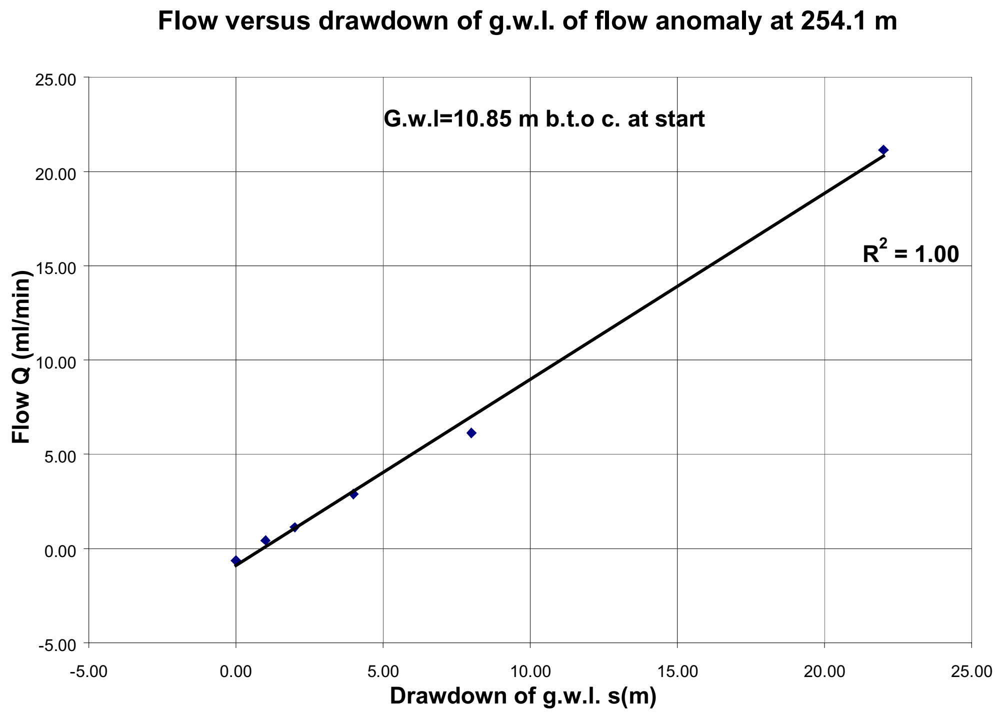
Flow versus drawdown of g.w.l. of flow anomaly at 254.1 m
G.w.l=10.85 m b.t.o c. at start
R^2 = 1.00
Flow Q (ml/min)
Drawdown of g.w.l. s(m)
25.00
20.00
15.00
10.00
5.00
0.00
-5.00
-5.00
0.00
5.00
10.00
15.00
20.00
25.00

Flow versus head difference of flow anomaly at 268.0 m

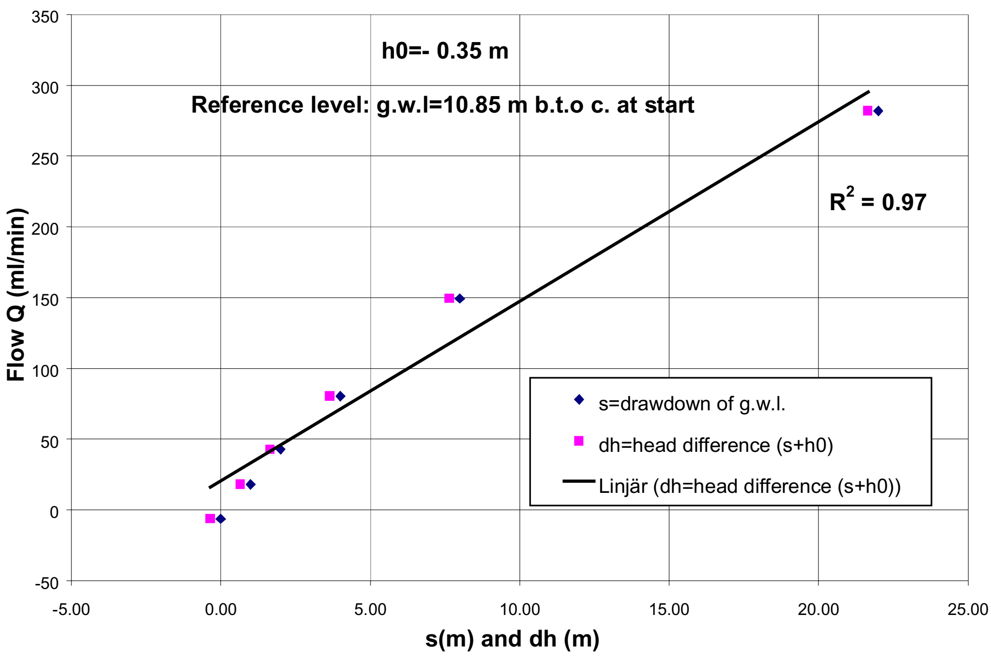

Flow versus drawdown of g.w.l. of flow anomaly at 269.0 m

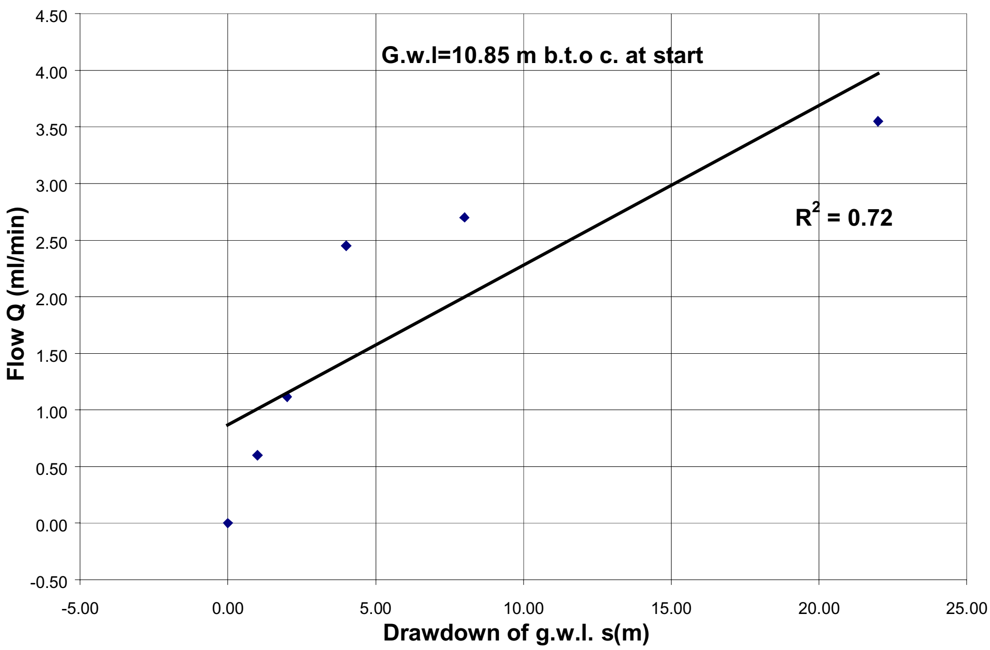

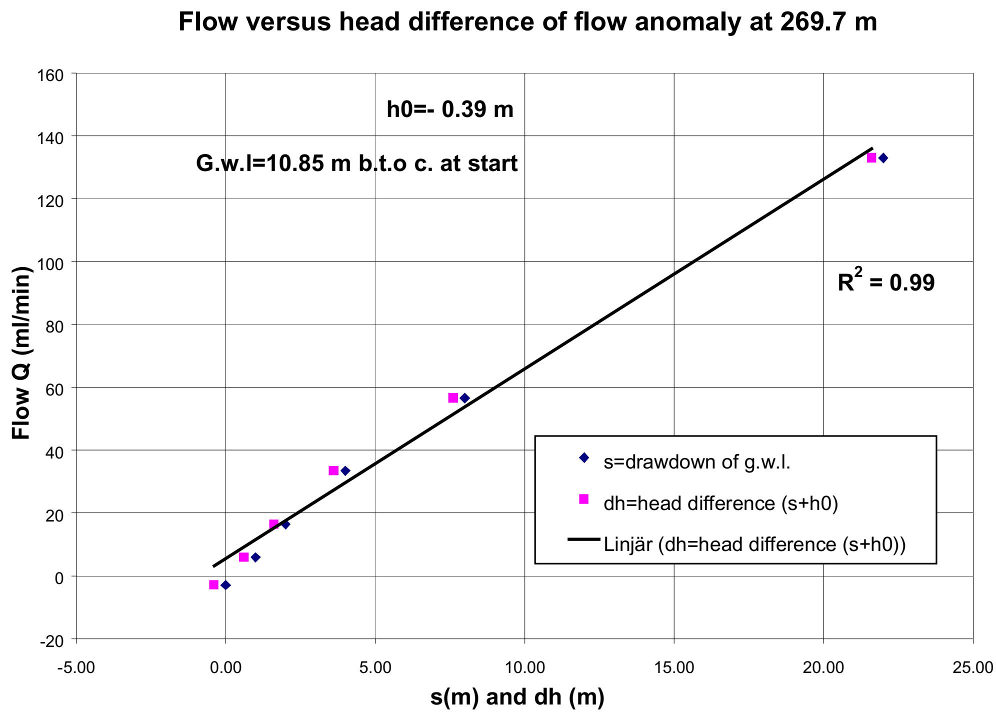
Flow versus head difference of flow anomaly at 269.7 m
h0=- 0.39 m
G.w.l=10.85 m b.t.o c. at start
R2 = 0.99
s=drawdown of g.w.l.
dh=head difference (s+h0)
Linjär (dh=head difference (s+h0))
Flow Q (ml/min)
s(m) and dh (m)
160
140
120
100
80
60
40
20
0
-20
-5.00
0.00
5.00
10.00
15.00
20.00
25.00

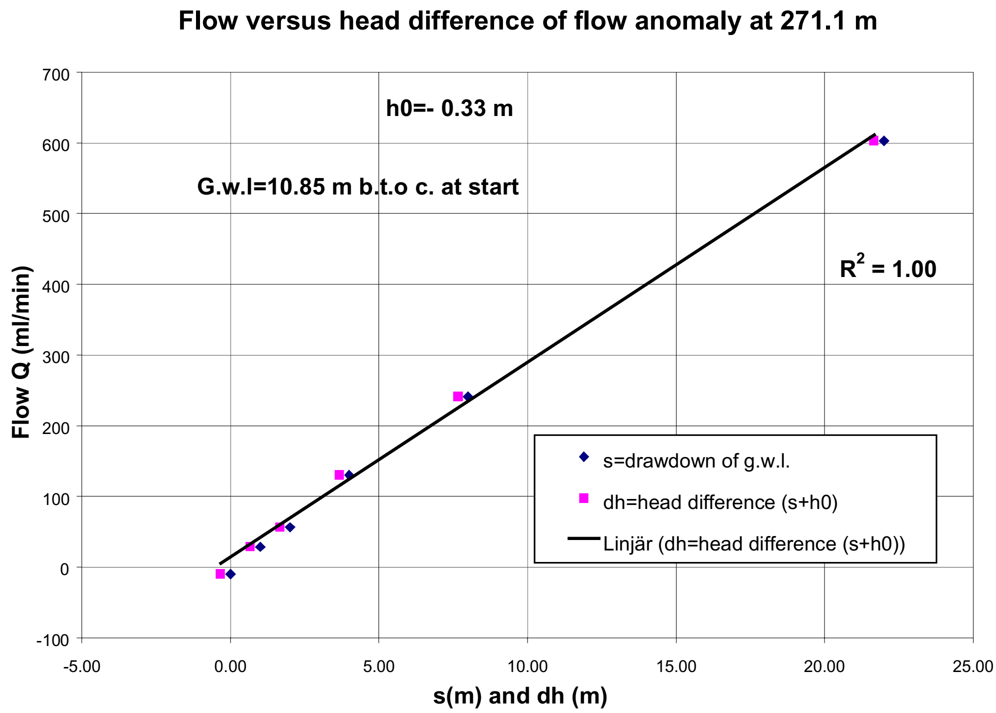
Flow versus head difference of flow anomaly at 271.1 m
h0=- 0.33 m
G.w.l=10.85 m b.t.o c. at start
R2 = 1.00
s=drawdown of g.w.l.
dh=head difference (s+h0)
Linjär (dh=head difference (s+h0))
Flow Q (ml/min)
s(m) and dh (m)
700
600
500
400
300
200
100
0
-100
-5.00
0.00
5.00
10.00
15.00
20.00
25.00

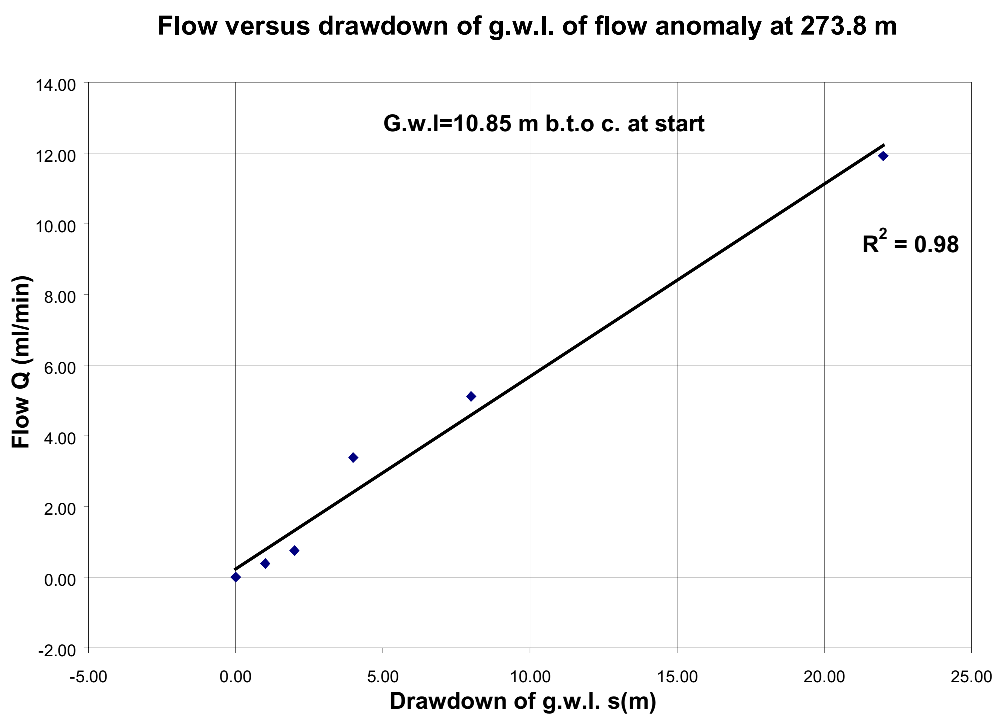
Flow versus drawdown of g.w.l. of flow anomaly at 273.8 m
G.w.l=10.85 m b.t.o c. at start
R^2 = 0.98
Flow Q (ml/min)
14.00
12.00
10.00
8.00
6.00
4.00
2.00
0.00
-2.00
-5.00
0.00
5.00
10.00
15.00
20.00
25.00
Drawdown of g.w.l. s(m)

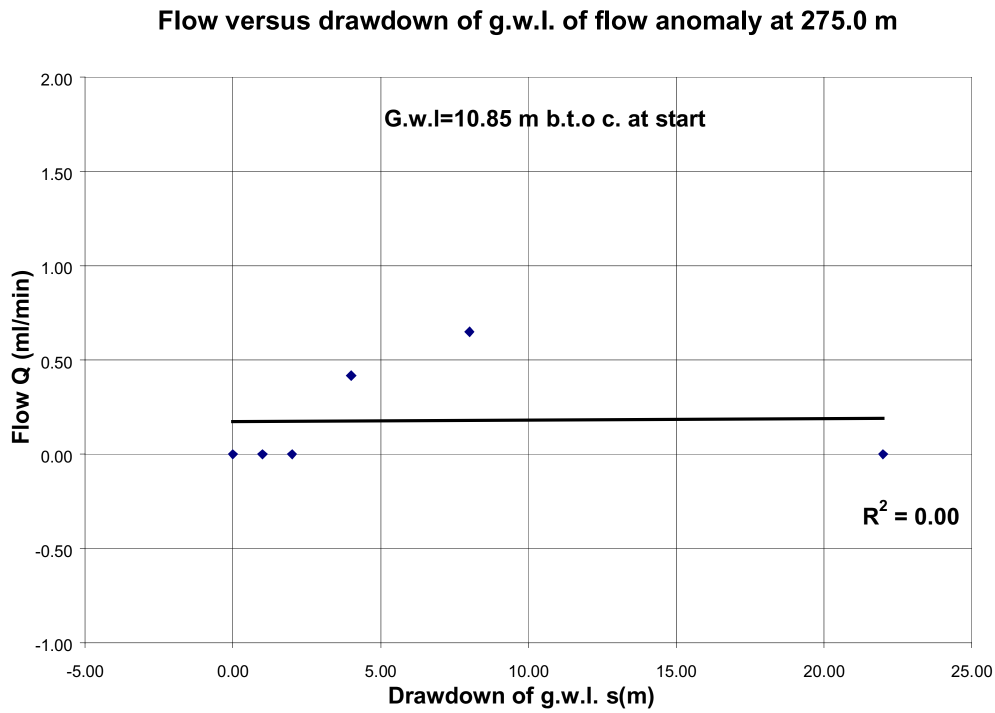
Flow versus drawdown of g.w.l. of flow anomaly at 275.0 m
G.w.l=10.85 m b.t.o c. at start
R^2 = 0.00
Flow Q (ml/min)
2.00
1.50
1.00
0.50
0.00
-0.50
-1.00
-5.00
0.00
5.00
10.00
15.00
20.00
25.00
Drawdown of g.w.l. s(m)

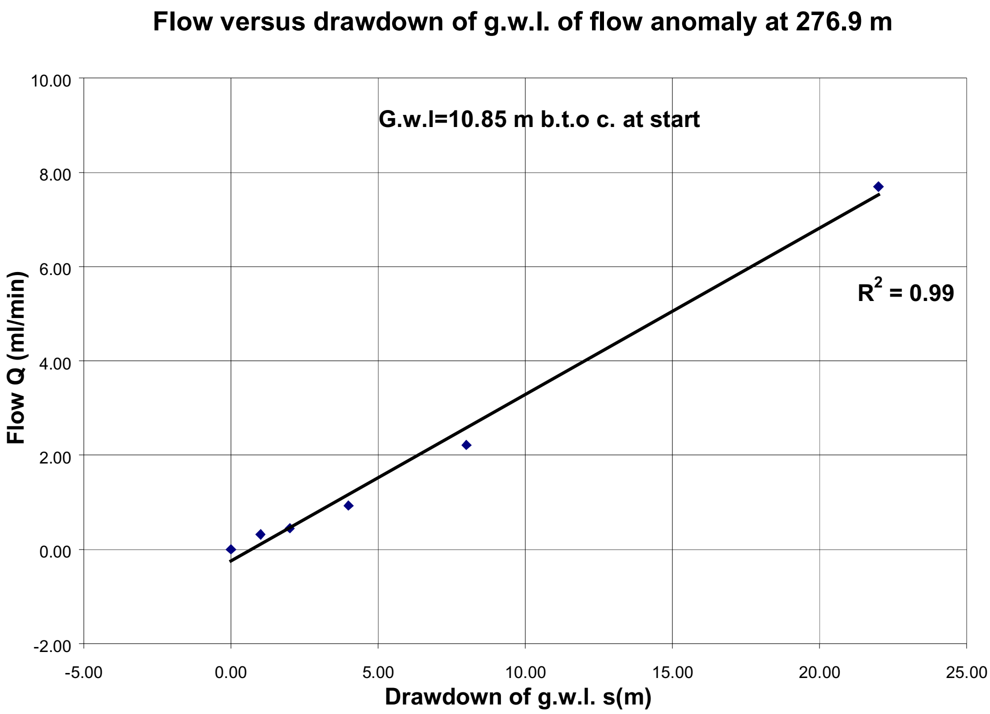
Flow versus drawdown of g.w.l. of flow anomaly at 276.9 m
G.w.l=10.85 m b.t.o c. at start
R^2 = 0.99
Flow Q (ml/min)
Drawdown of g.w.l. s(m)
10.00
8.00
6.00
4.00
2.00
0.00
-2.00
-5.00
0.00
5.00
10.00
15.00
20.00
25.00

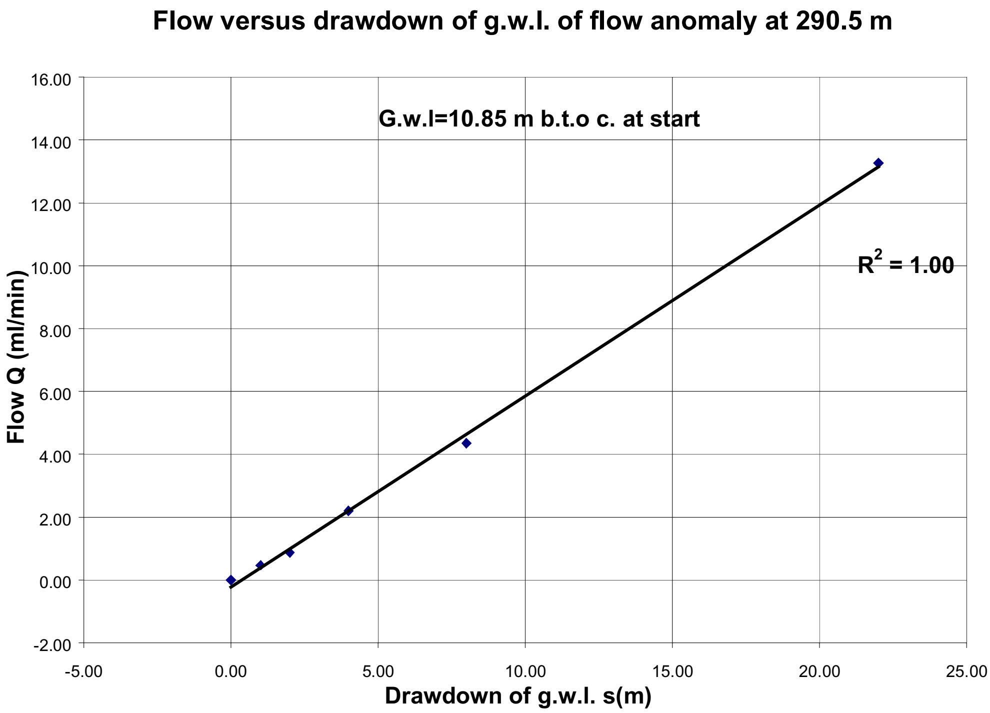
Flow versus drawdown of g.w.l. of flow anomaly at 290.5 m
G.w.l=10.85 m b.t.o c. at start
R^2 = 1.00
Flow Q (ml/min)
Drawdown of g.w.l. s(m)
16.00
14.00
12.00
10.00
8.00
6.00
4.00
2.00
0.00
-2.00
-5.00
0.00
5.00
10.00
15.00
20.00
25.00

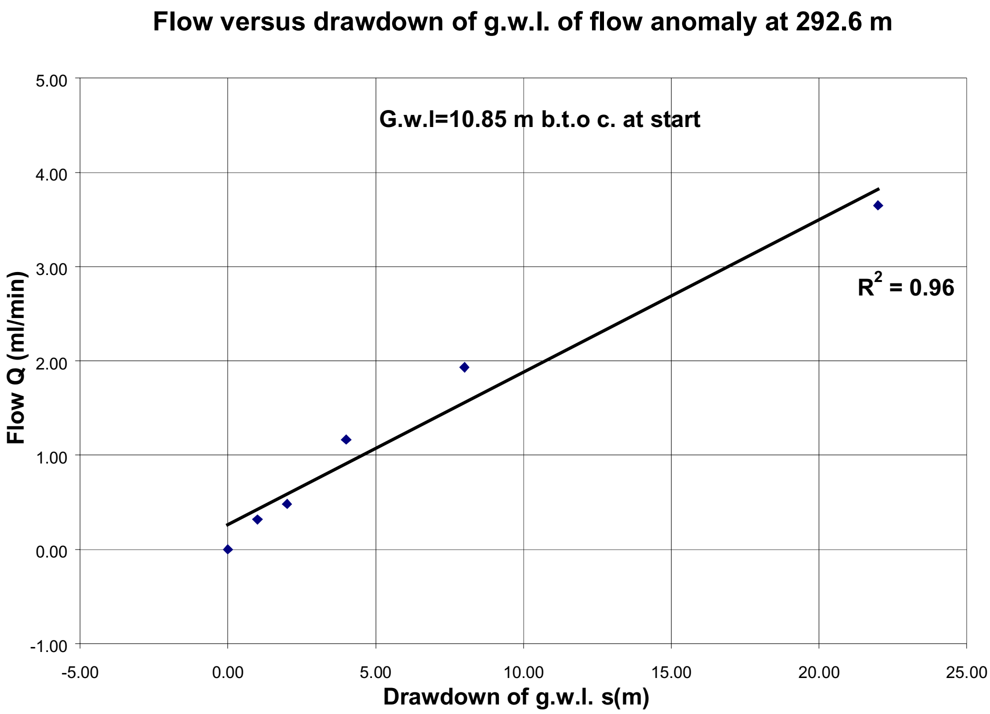
Flow versus drawdown of g.w.l. of flow anomaly at 292.6 m
G.w.l=10.85 m b.t.o c. at start
R^2 = 0.96
Flow Q (ml/min)
Drawdown of g.w.l. s(m)
5.00
4.00
3.00
2.00
1.00
0.00
-1.00
-5.00
0.00
5.00
10.00
15.00
20.00
25.00

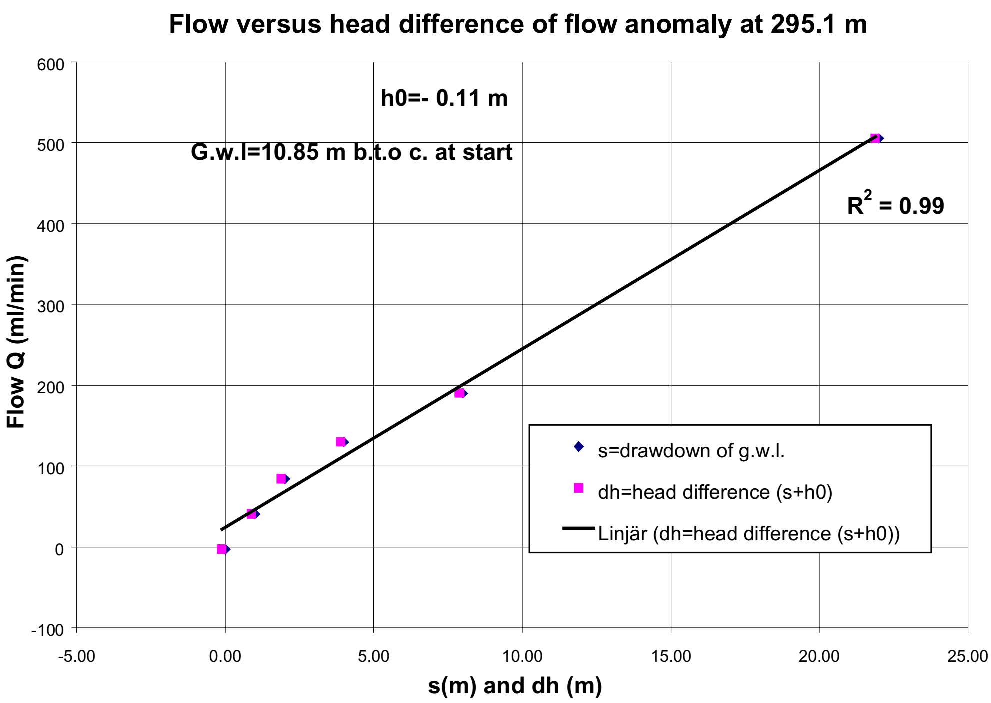
Flow versus head difference of flow anomaly at 295.1 m
h0=- 0.11 m
G.w.l=10.85 m b.t.o c. at start
R^2 = 0.99
s=drawdown of g.w.l.
dh=head difference (s+h0)
Linjär (dh=head difference (s+h0))
Flow Q (ml/min)
s(m) and dh (m)
600
500
400
300
200
100
0
-100
-5.00
0.00
5.00
10.00
15.00
20.00
25.00

Flow versus drawdown of g.w.l. of flow anomaly at 295.6 m

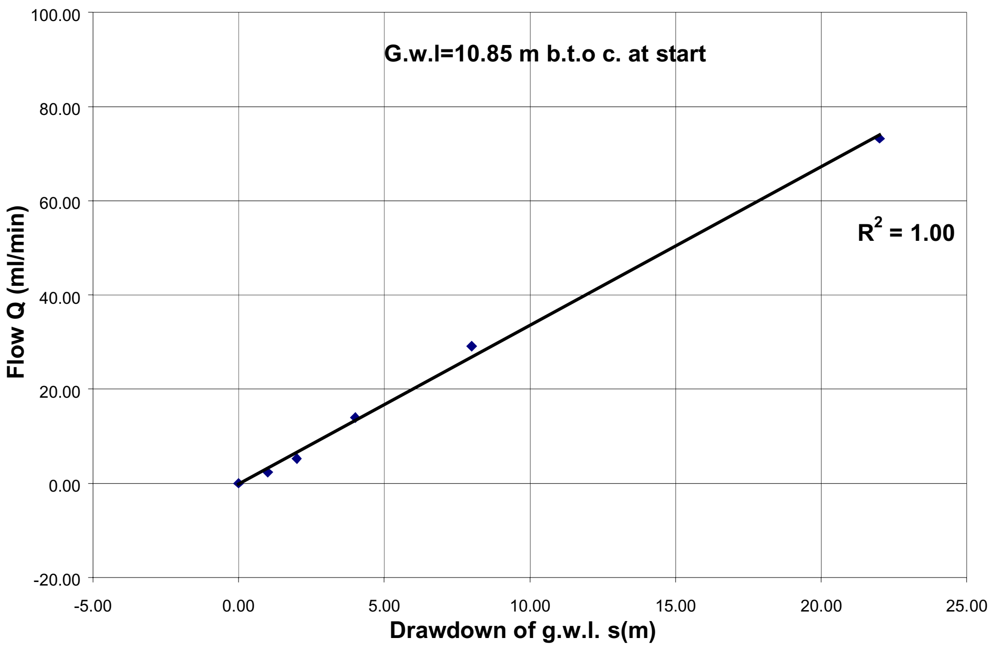

Flow versus drawdown of g.w.l. of flow anomaly at 298.3 m

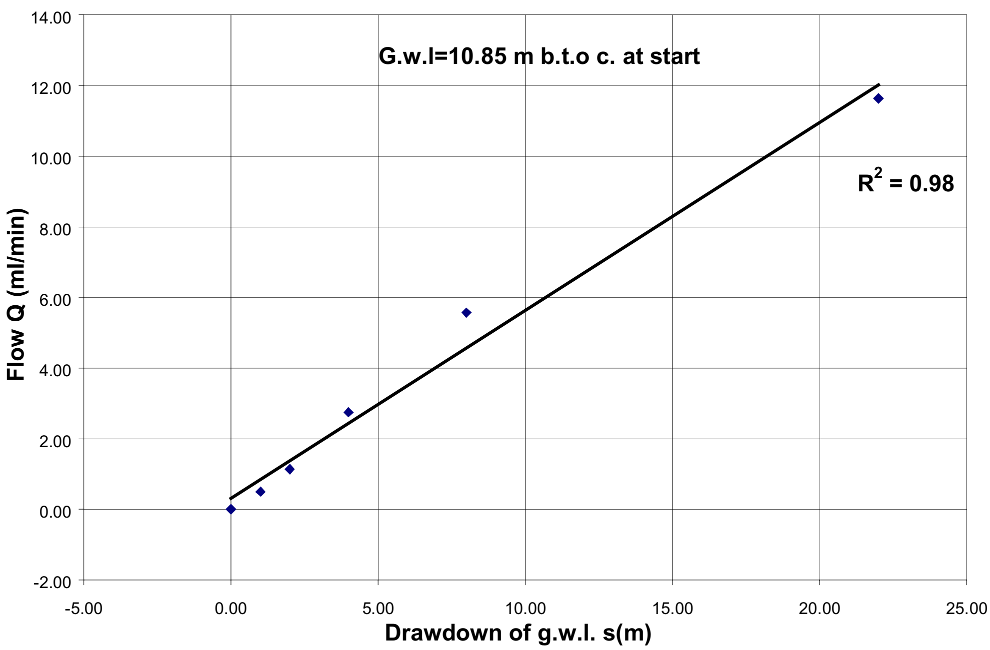

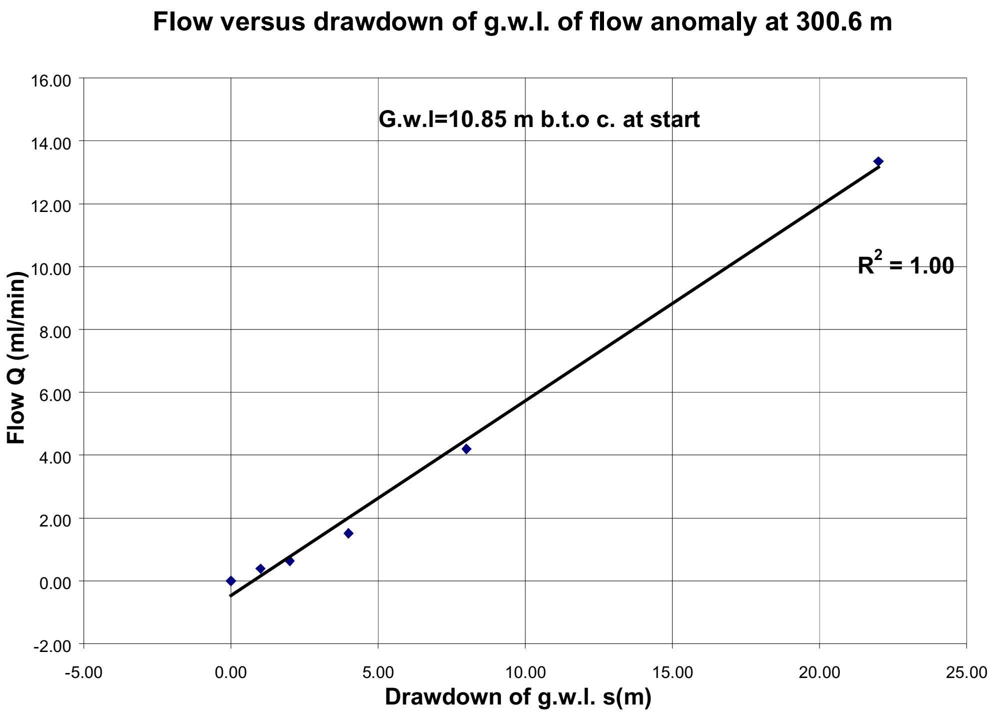

Flow versus drawdown of g.w.l. of flow anomaly at 300.6 m
G.w.l=10.85 m b.t.o c. at start
$R^2 = 1.00$
Flow Q (ml/min)
Drawdown of g.w.l. s(m)
16.00
14.00
12.00
10.00
8.00
6.00
4.00
2.00
0.00
-2.00
-5.00
0.00
5.00
10.00
15.00
20.00
25.00

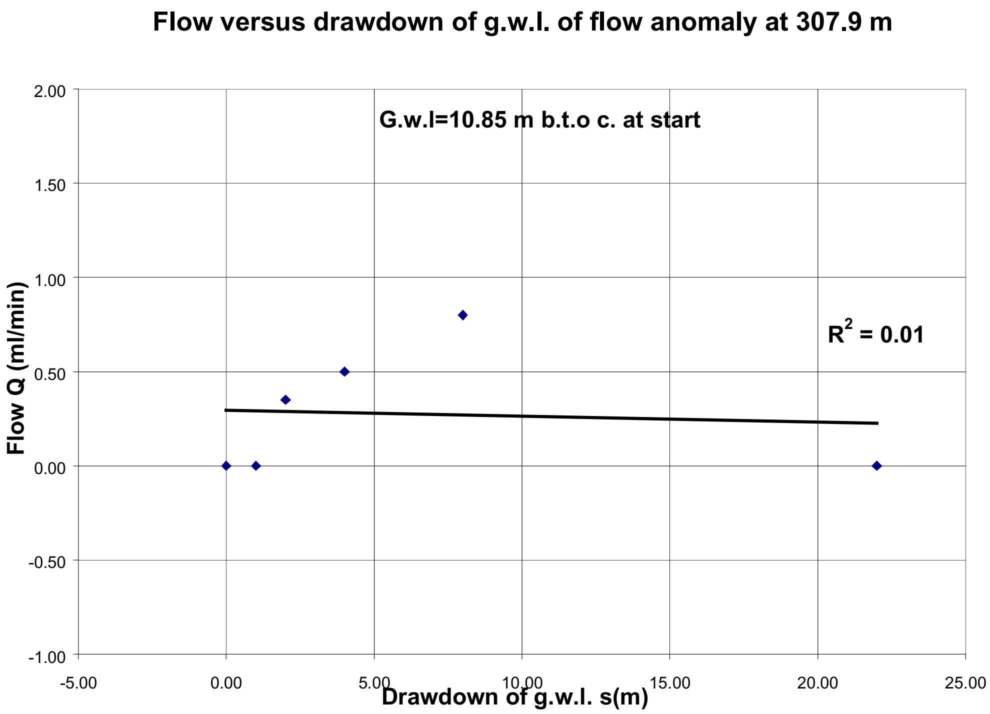

Flow versus drawdown of g.w.l. of flow anomaly at 307.9 m
G.w.l=10.85 m b.t.o c. at start
$R^2 = 0.01$
Flow Q (ml/min)
Drawdown of g.w.l. s(m)
2.00
1.50
1.00
0.50
0.00
-0.50
-1.00
-5.00
0.00
5.00
10.00
15.00
20.00
25.00

Flow versus drawdown of g.w.l. of flow anomaly at 310.5 m

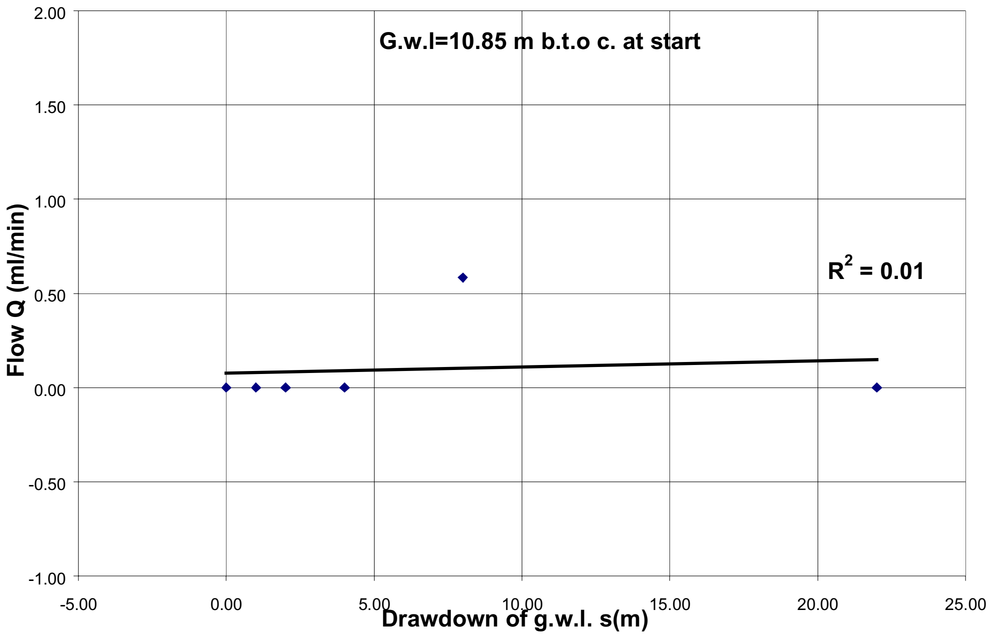

Flow versus drawdown of g.w.l. of flow anomaly at 314.7 m

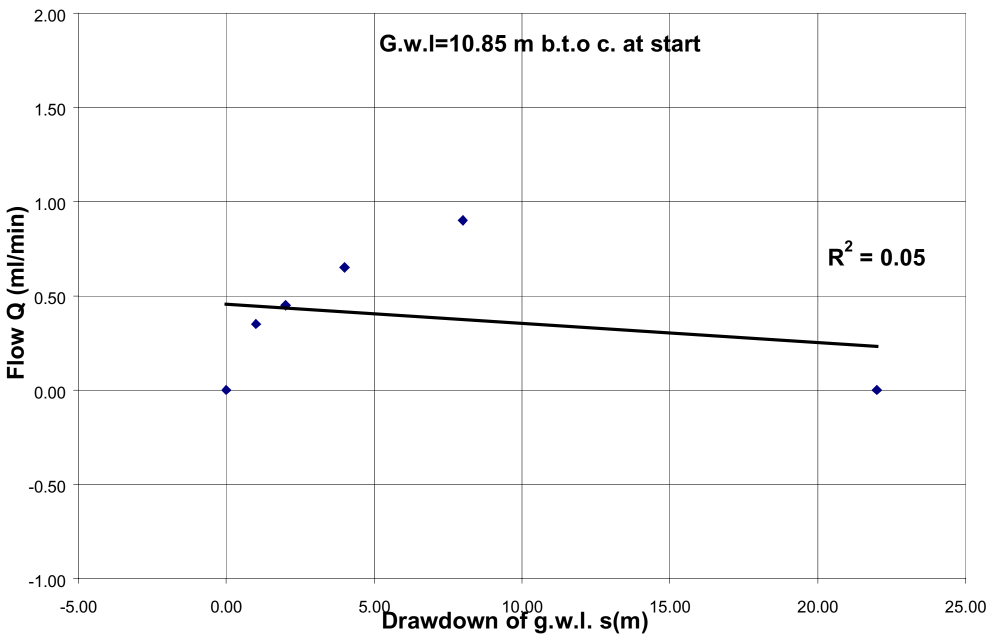

Flow versus head difference of flow anomaly at 317.1 m

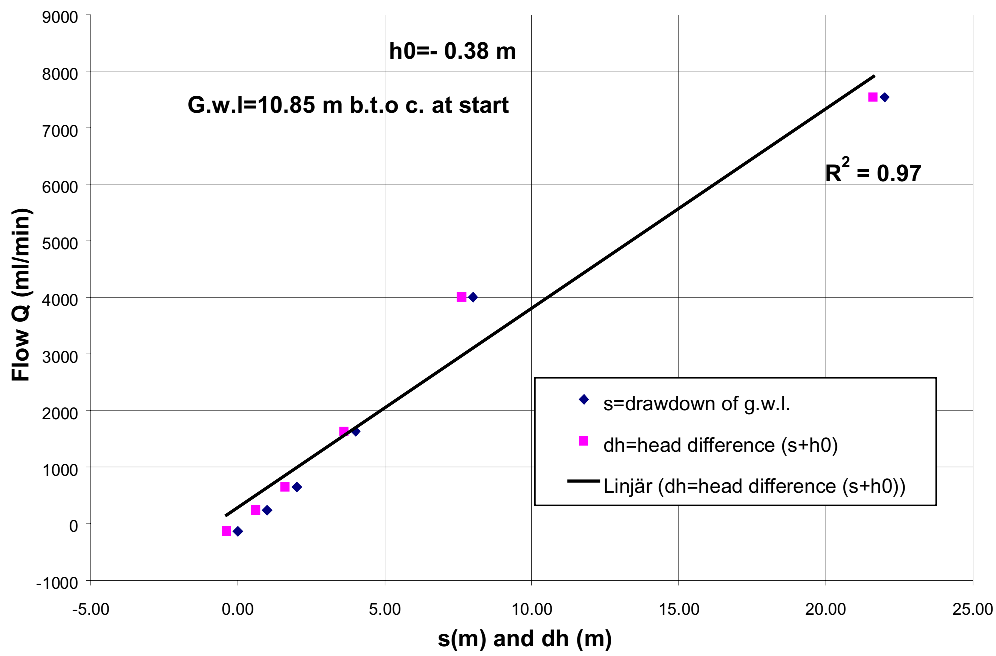

Flow versus drawdown of g.w.l. of flow anomaly at 325.4 m

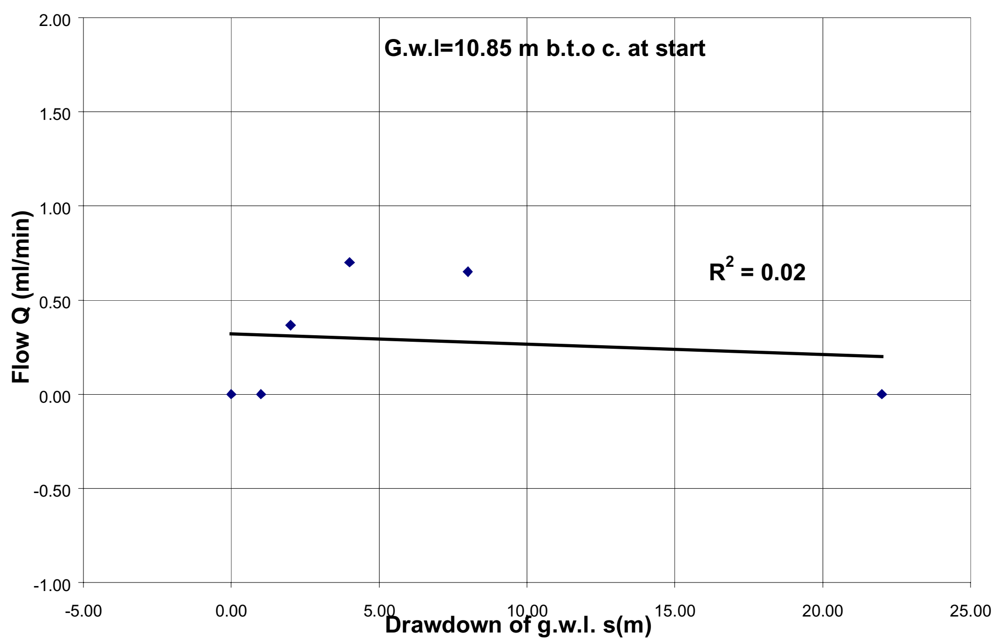

Flow versus drawdown of g.w.l. of flow anomaly at 327.8 m

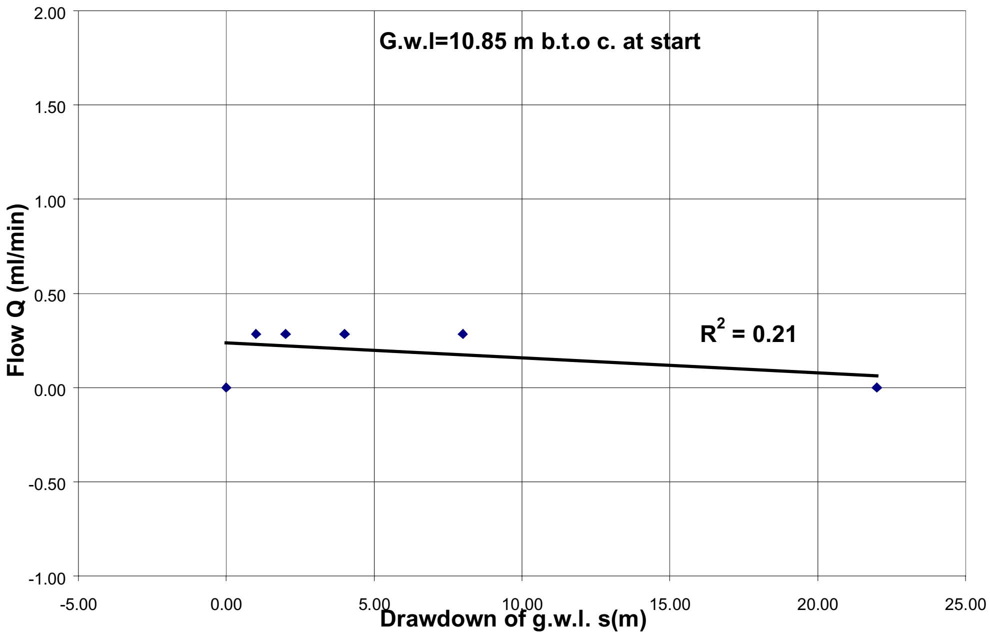

Flow versus drawdown of g.w.l. of flow anomaly at 328.6 m

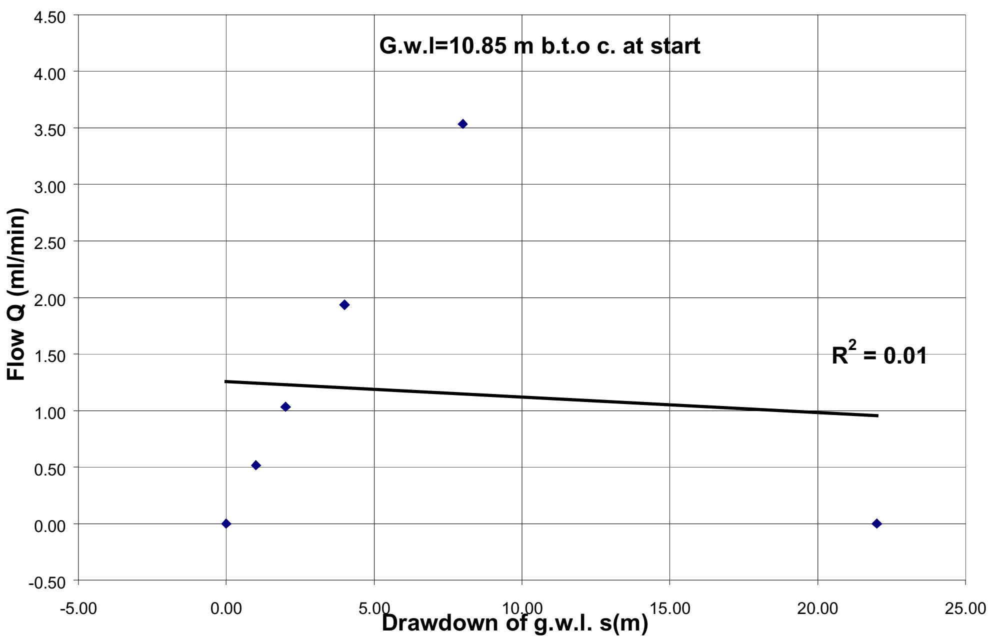

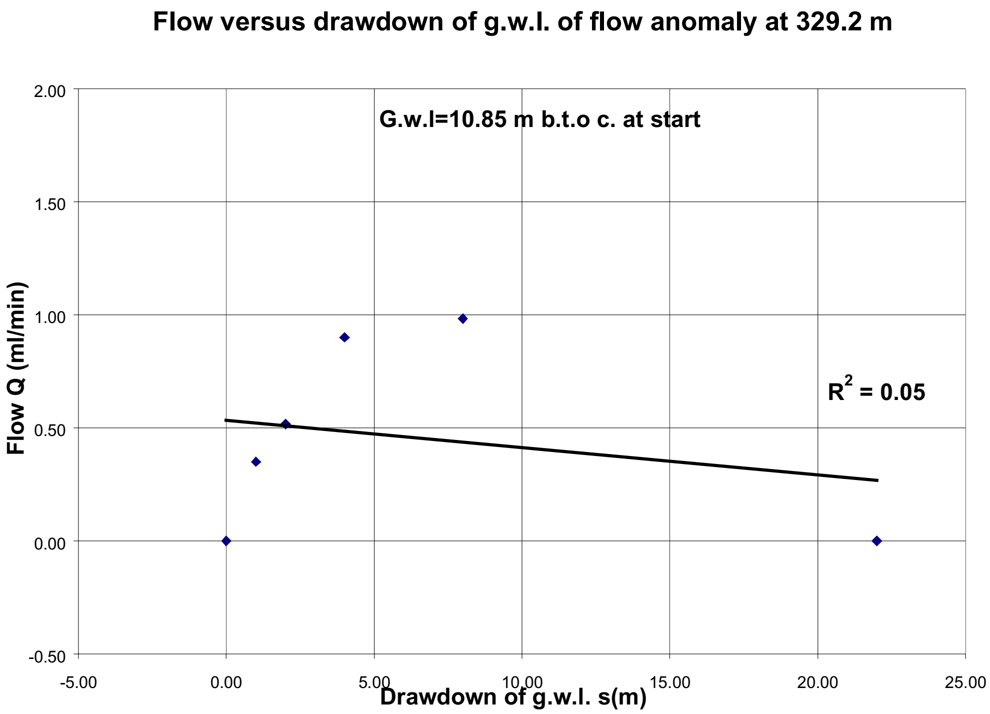
Flow versus drawdown of g.w.l. of flow anomaly at 329.2 m
G.w.l=10.85 m b.t.o c. at start
R^2 = 0.05
Flow Q (ml/min)
2.00
1.50
1.00
0.50
0.00
-0.50
-5.00
0.00
5.00
10.00
15.00
20.00
25.00
Drawdown of g.w.l. s(m)

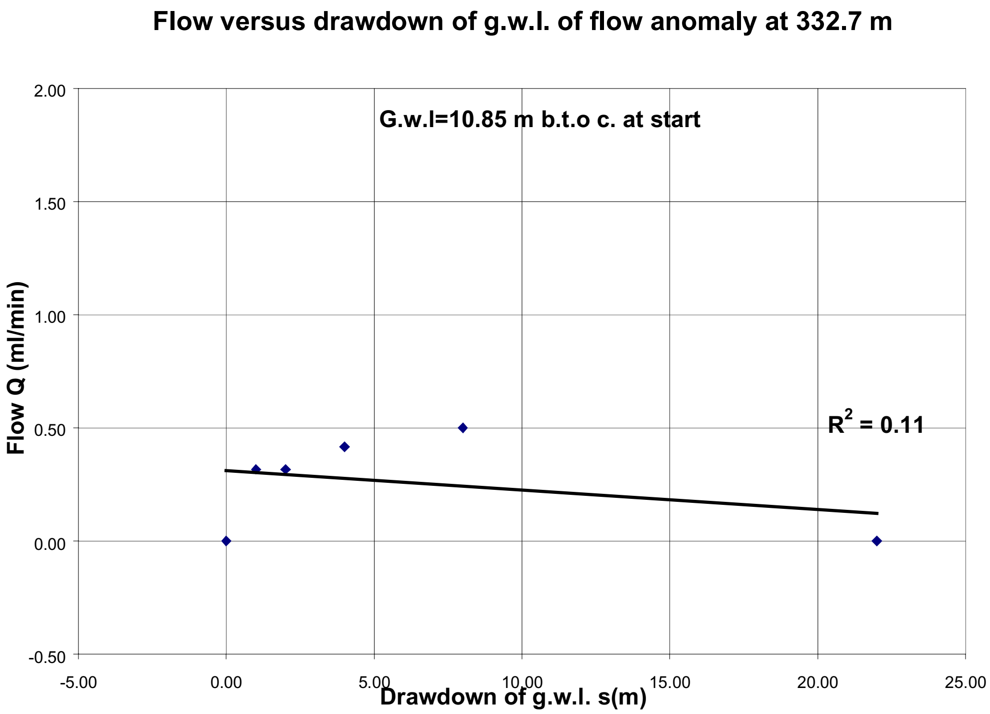
Flow versus drawdown of g.w.l. of flow anomaly at 332.7 m
G.w.l=10.85 m b.t.o c. at start
R^2 = 0.11
Flow Q (ml/min)
2.00
1.50
1.00
0.50
0.00
-0.50
-5.00
0.00
5.00
10.00
15.00
20.00
25.00
Drawdown of g.w.l. s(m)

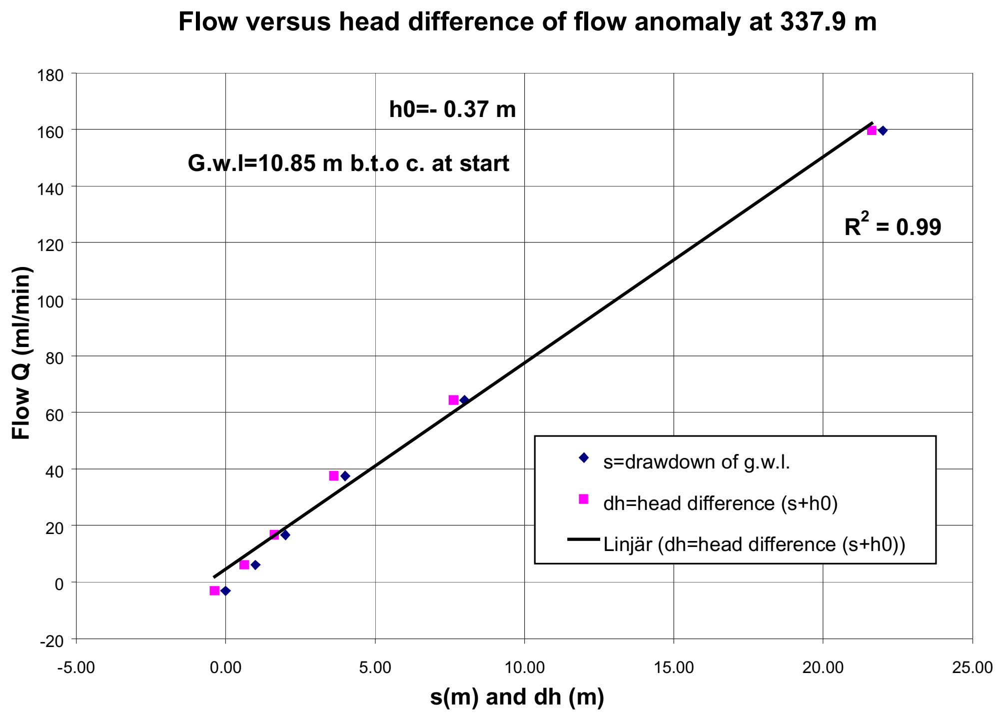
Flow versus head difference of flow anomaly at 337.9 m
h0=- 0.37 m
G.w.l=10.85 m b.t.o c. at start
R^2 = 0.99
Flow Q (ml/min)
s(m) and dh (m)
s=drawdown of g.w.l.
dh=head difference (s+h0)
Linjär (dh=head difference (s+h0))

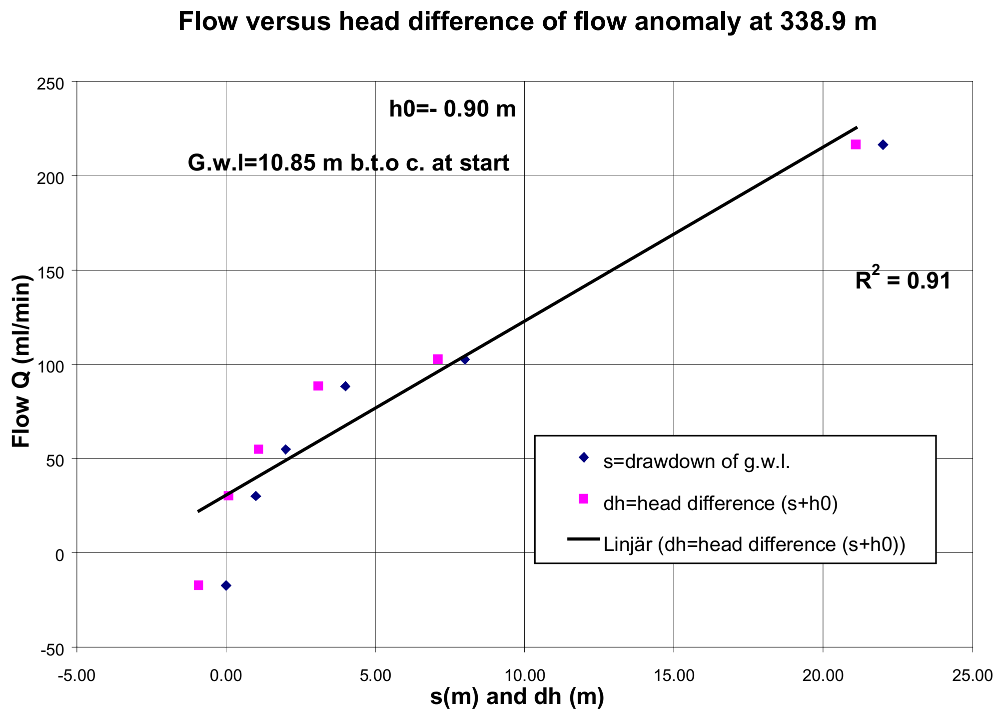
Flow versus head difference of flow anomaly at 338.9 m
h0=- 0.90 m
G.w.l=10.85 m b.t.o c. at start
R^2 = 0.91
Flow Q (ml/min)
s(m) and dh (m)
s=drawdown of g.w.l.
dh=head difference (s+h0)
Linjär (dh=head difference (s+h0))

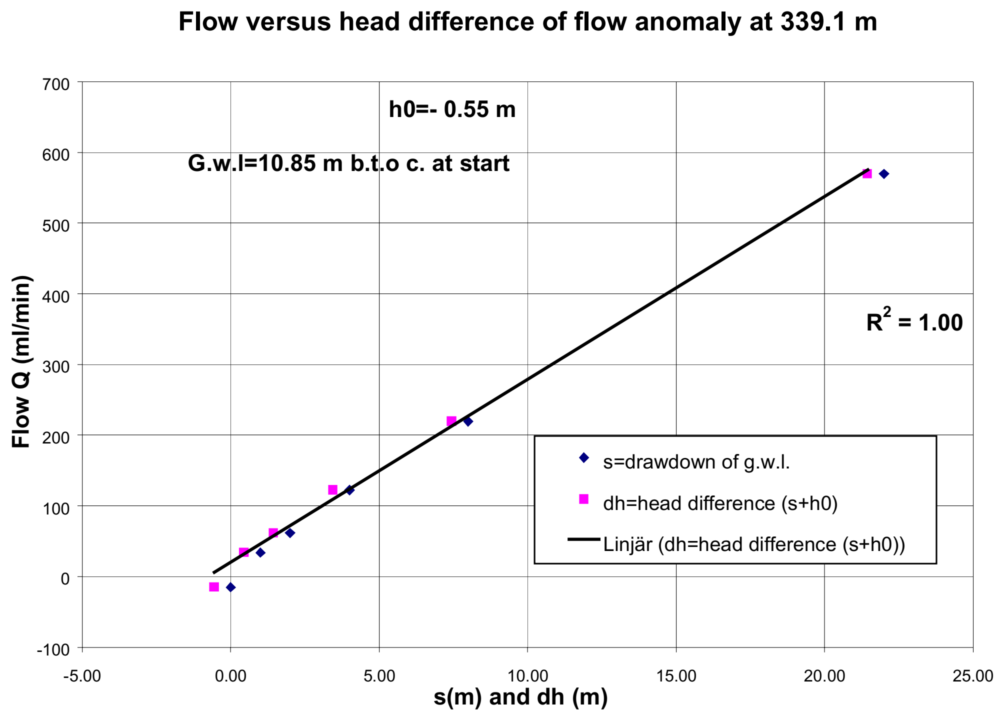
Flow versus head difference of flow anomaly at 339.1 m
h0=- 0.55 m
G.w.l=10.85 m b.t.o c. at start
R2 = 1.00
s=drawdown of g.w.l.
dh=head difference (s+h0)
Linjär (dh=head difference (s+h0))
Flow Q (ml/min)
s(m) and dh (m)
700
600
500
400
300
200
100
0
-100
-5.00
0.00
5.00
10.00
15.00
20.00
25.00

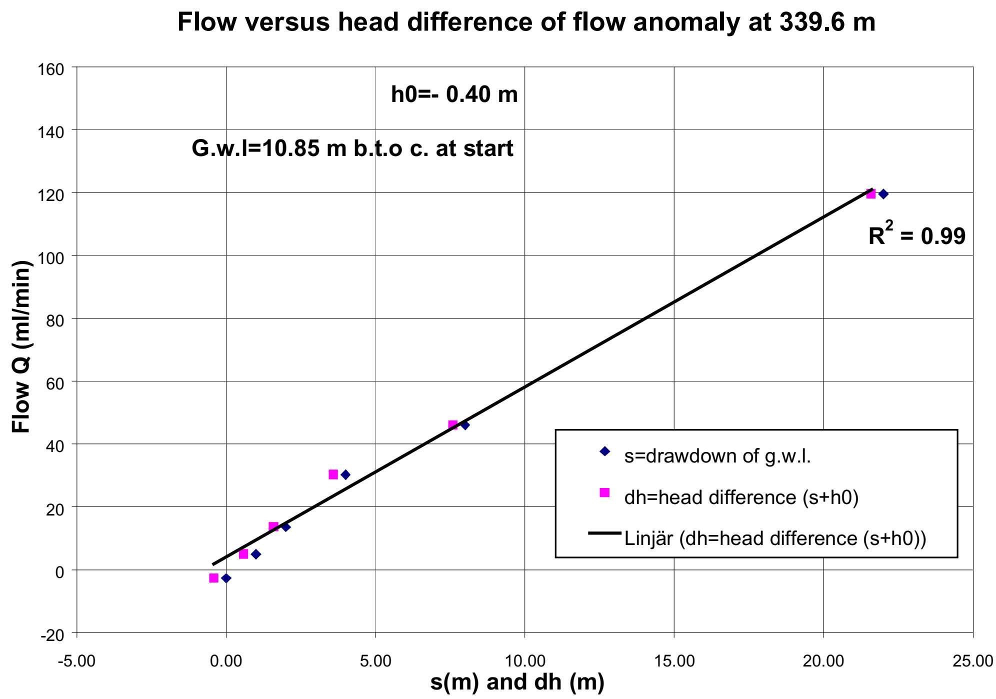
Flow versus head difference of flow anomaly at 339.6 m
h0=- 0.40 m
G.w.l=10.85 m b.t.o c. at start
R2 = 0.99
s=drawdown of g.w.l.
dh=head difference (s+h0)
Linjär (dh=head difference (s+h0))
Flow Q (ml/min)
s(m) and dh (m)
160
140
120
100
80
60
40
20
0
-20
-5.00
0.00
5.00
10.00
15.00
20.00
25.00

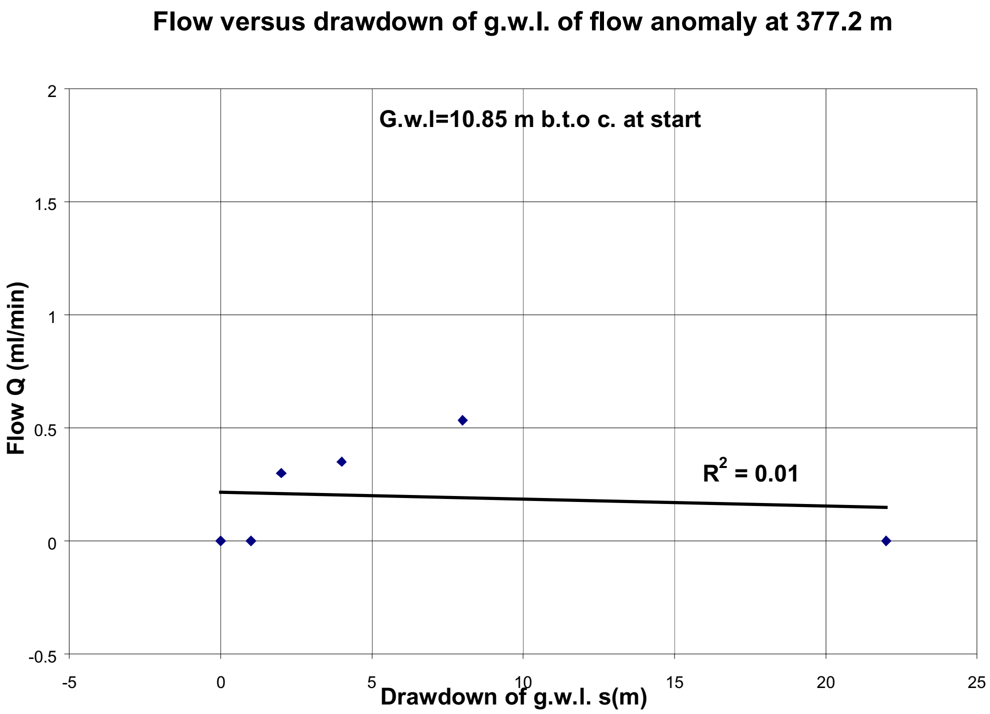

Flow versus drawdown of g.w.l. of flow anomaly at 377.2 m
G.w.l=10.85 m b.t.o c. at start
R² = 0.01
Flow Q (ml/min)
Drawdown of g.w.l. s(m)
2
1.5
1
0.5
0
-0.5
-5
0
5
10
15
20
25

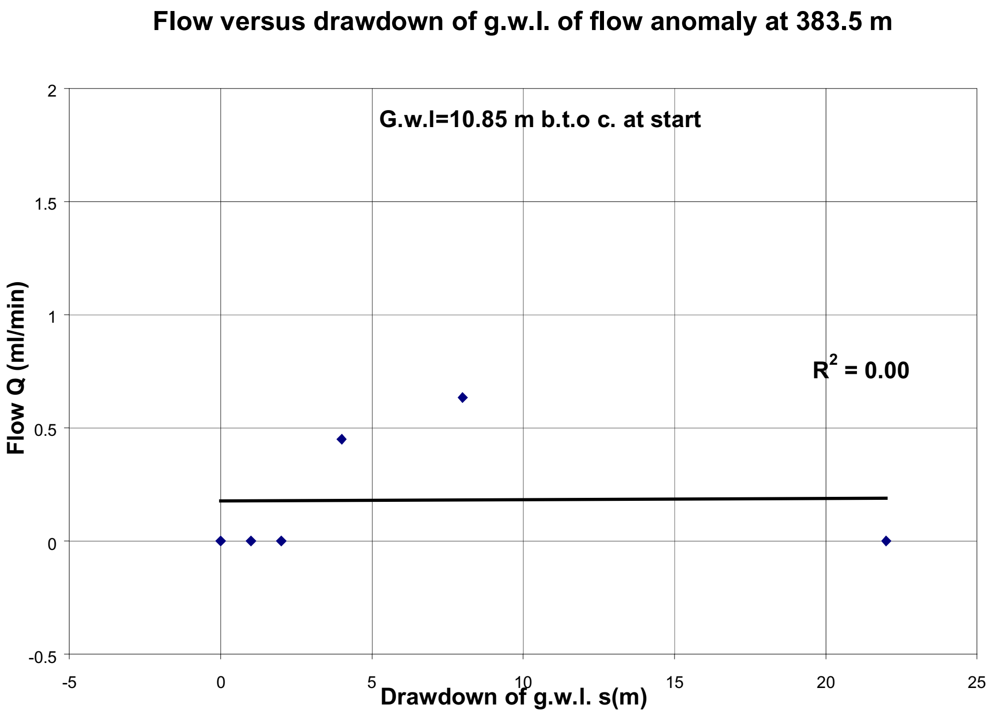

Flow versus drawdown of g.w.l. of flow anomaly at 383.5 m
G.w.l=10.85 m b.t.o c. at start
R² = 0.00
Flow Q (ml/min)
Drawdown of g.w.l. s(m)
2
1.5
1
0.5
0
-0.5
-5
0
5
10
15
20
25

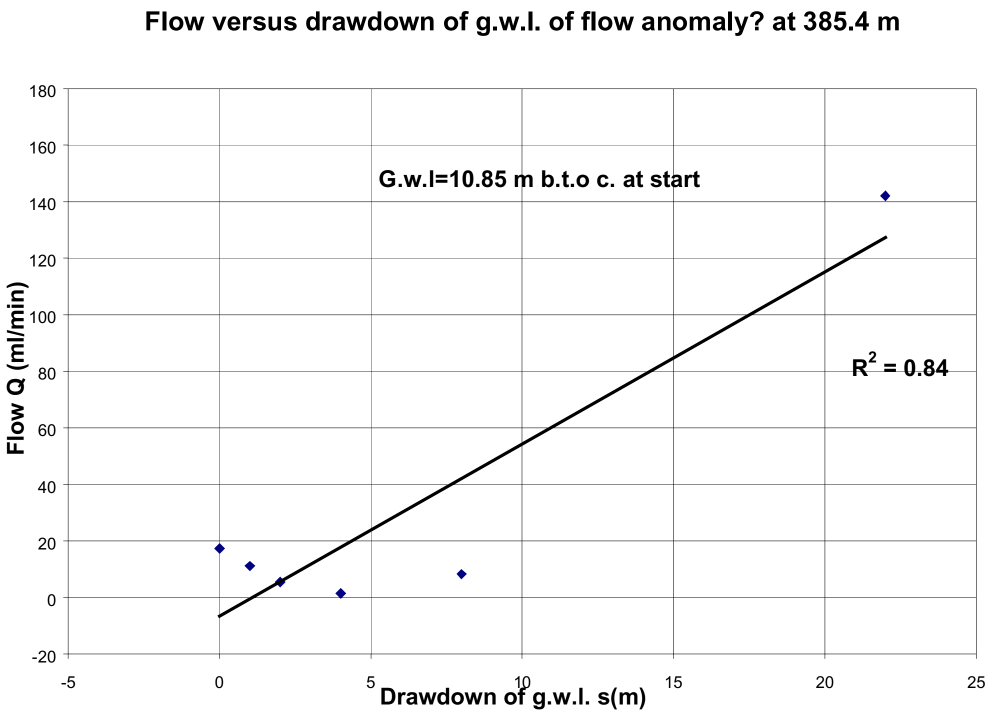
Flow versus drawdown of g.w.l. of flow anomaly? at 385.4 m
G.w.l=10.85 m b.t.o c. at start
R2 = 0.84
Flow Q (ml/min)
Drawdown of g.w.l. s(m)
180
160
140
120
100
80
60
40
20
0
-20
-5
0
5
10
15
20
25

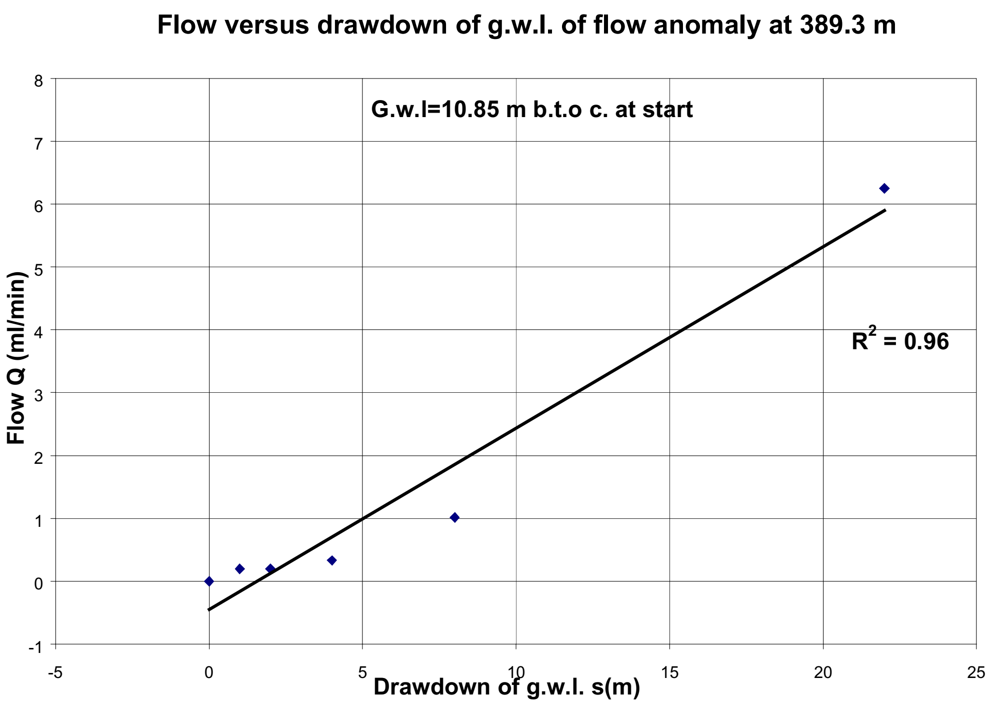
Flow versus drawdown of g.w.l. of flow anomaly at 389.3 m
G.w.l=10.85 m b.t.o c. at start
R2 = 0.96
Flow Q (ml/min)
Drawdown of g.w.l. s(m)
8
7
6
5
4
3
2
1
0
-1
-5
0
5
10
15
20
25

Laxemar, borehole KLX02
Single point resistance during detailed flow logging

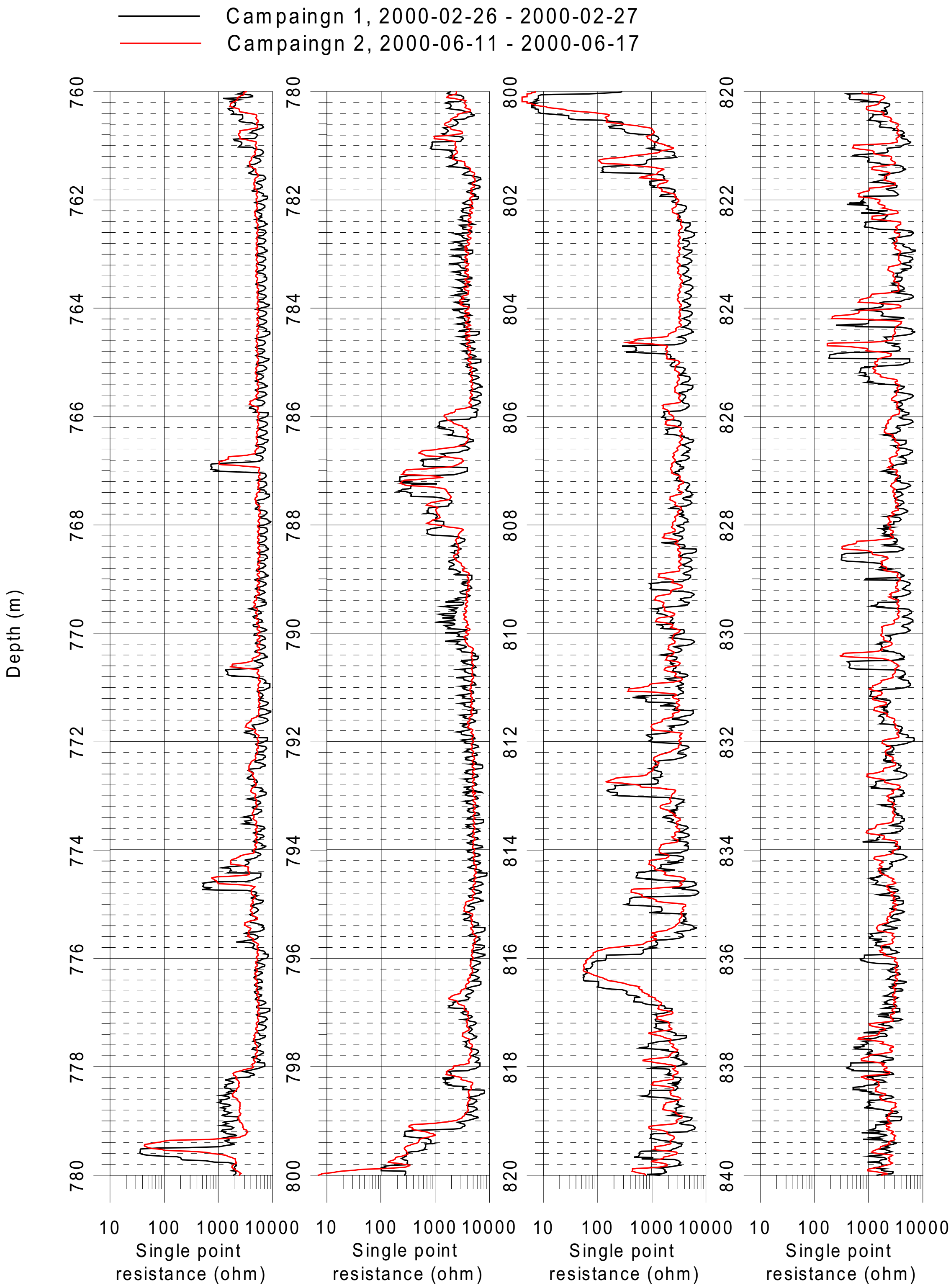

Laxemar, borehole KLX02
Single point resistance during detailed flow logging

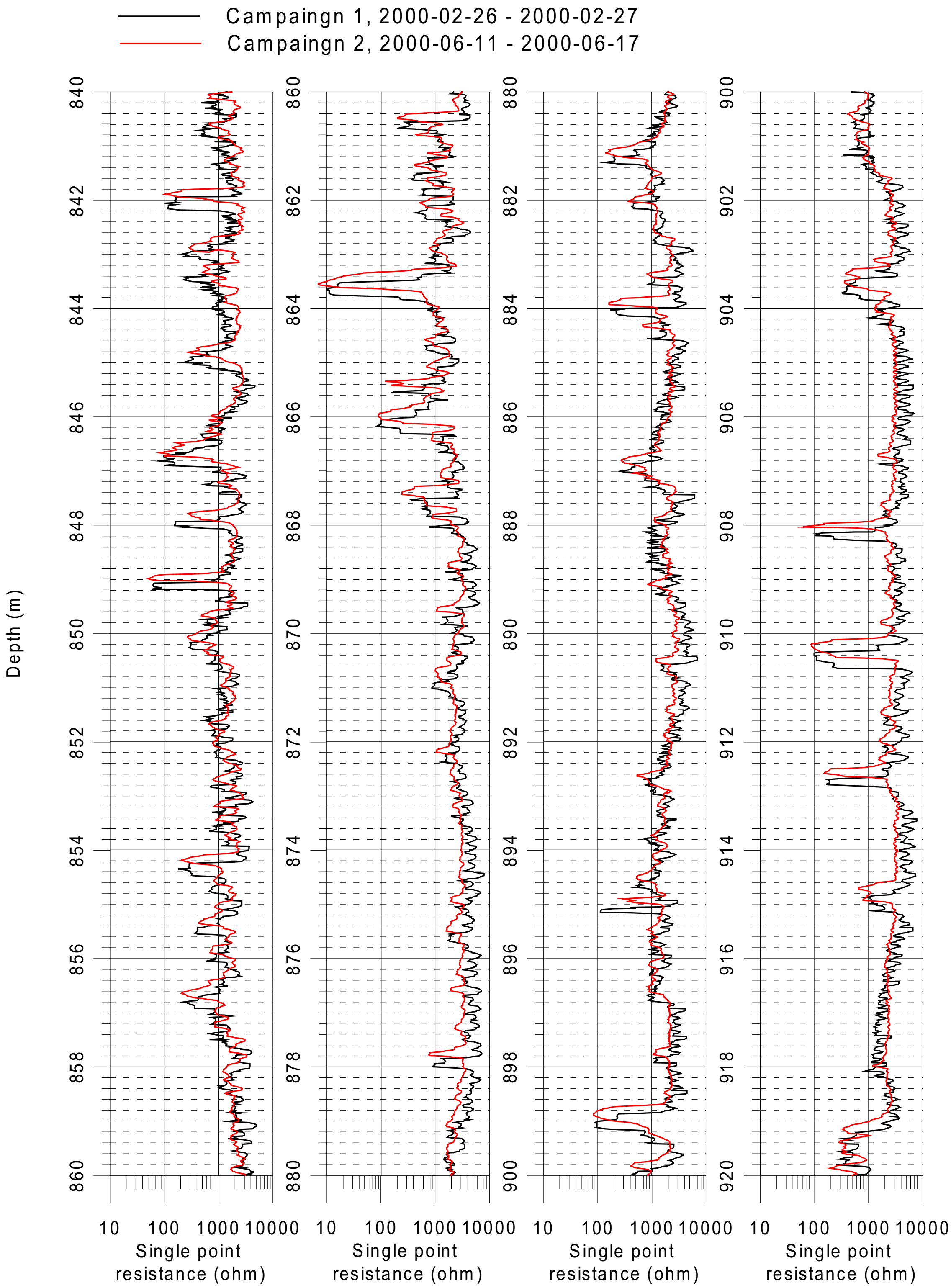

Laxemar, borehole KLX02
Single point resistance during detailed flow logging

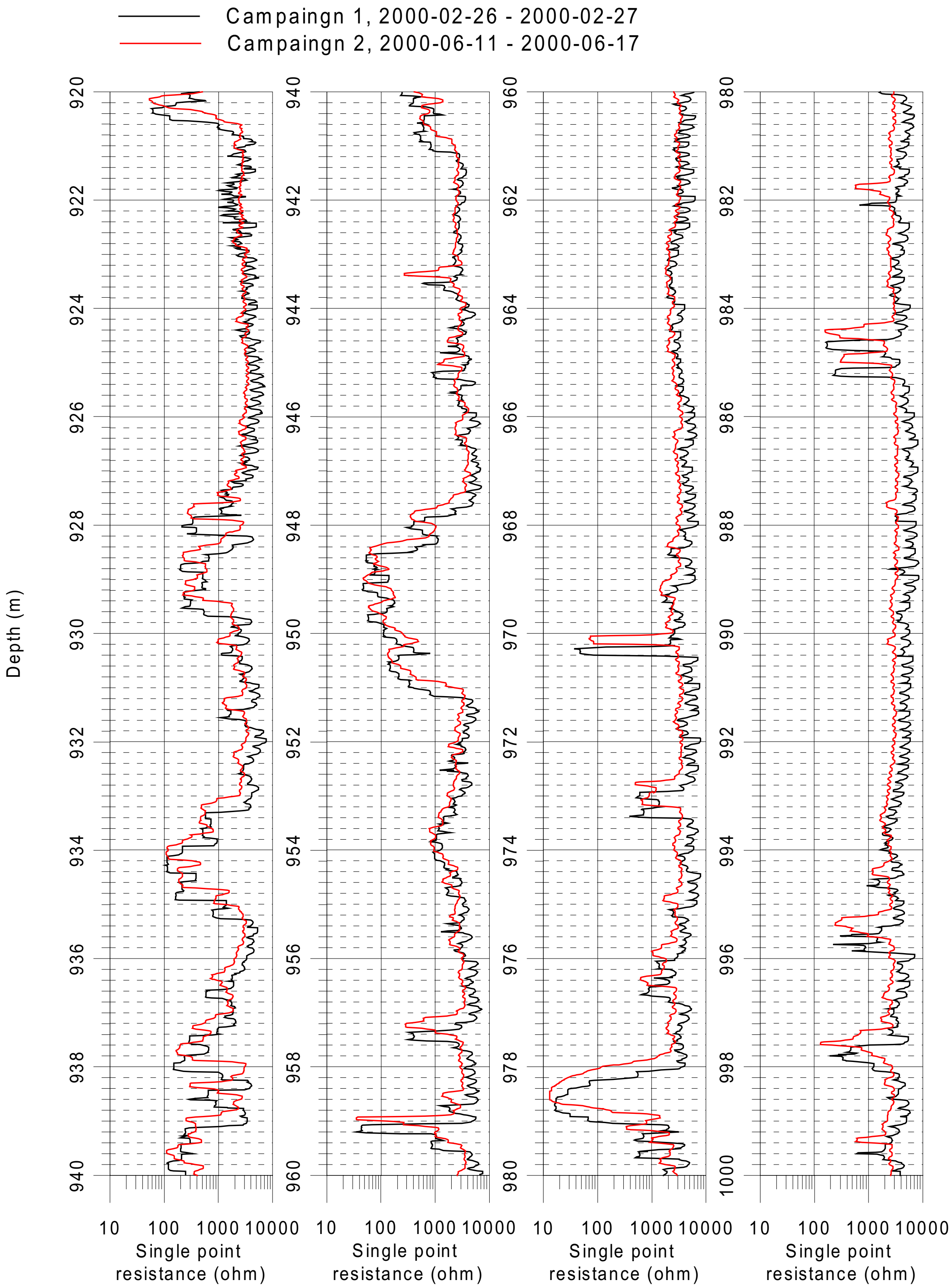

Laxemar, borehole KLX02
Single point resistance during detailed flow logging

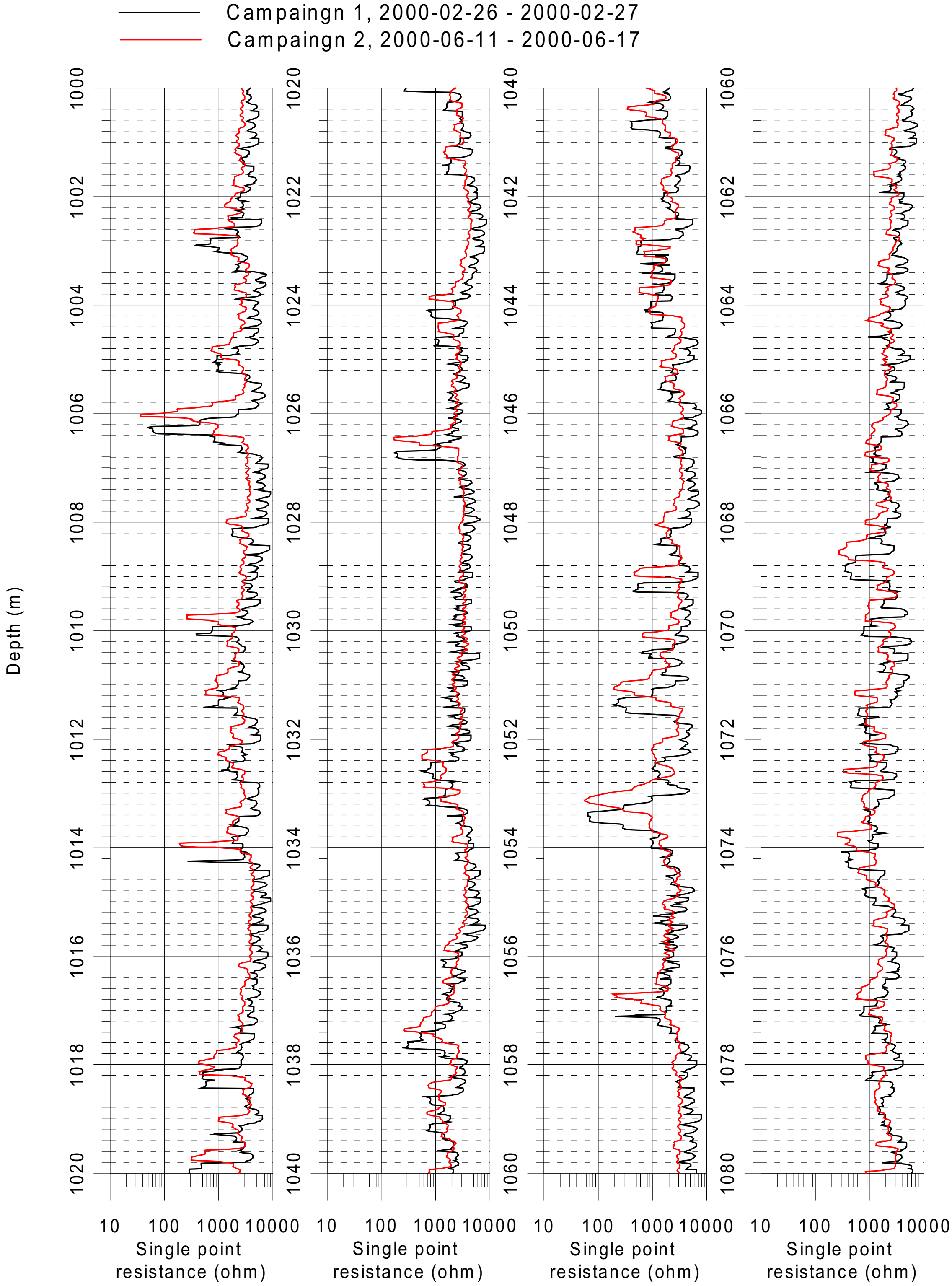

Laxemar, borehole KLX02
Single point resistance during detailed flow logging

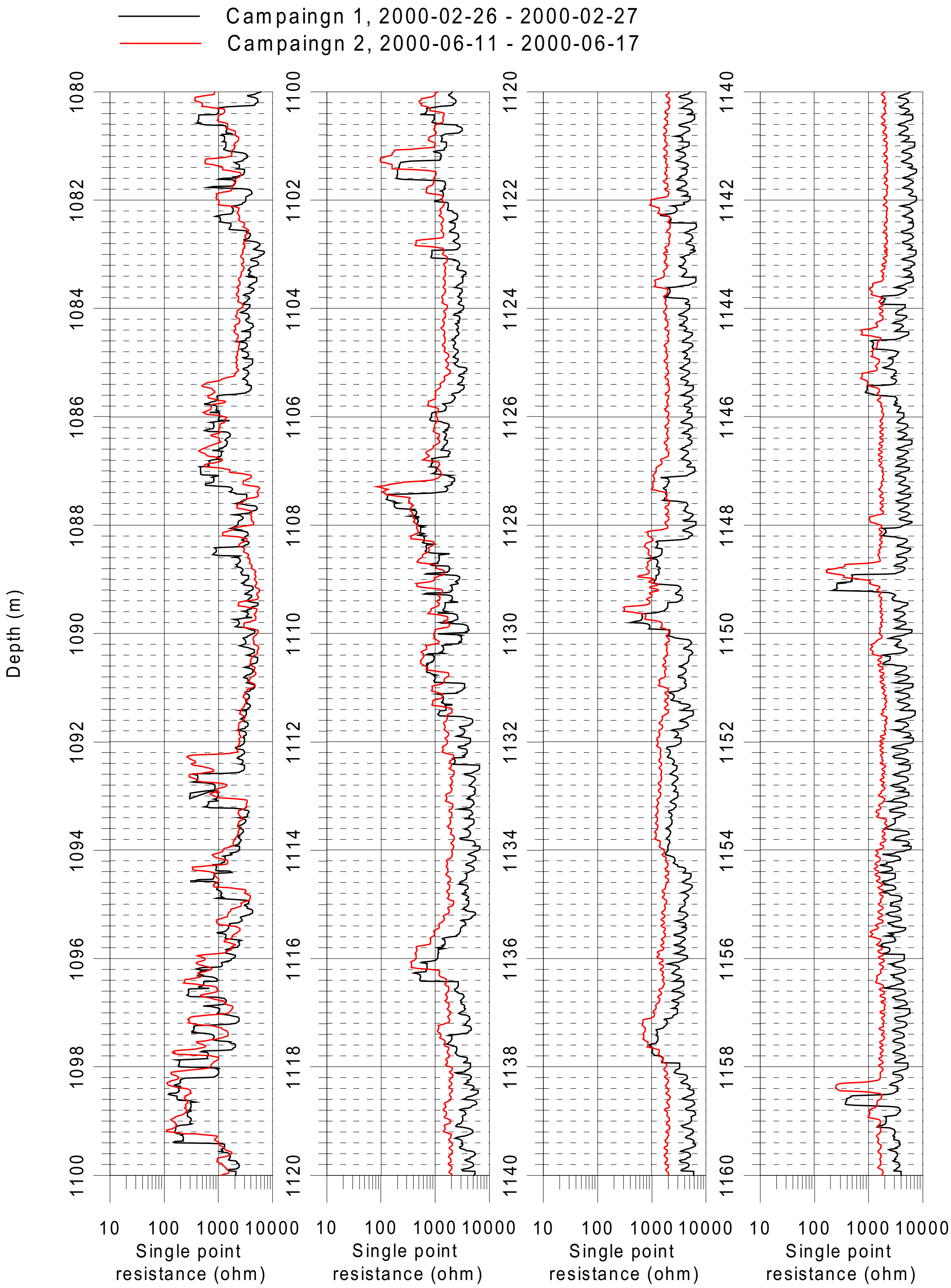

Laxemar, borehole KLX02
Single point resistance during detailed flow logging

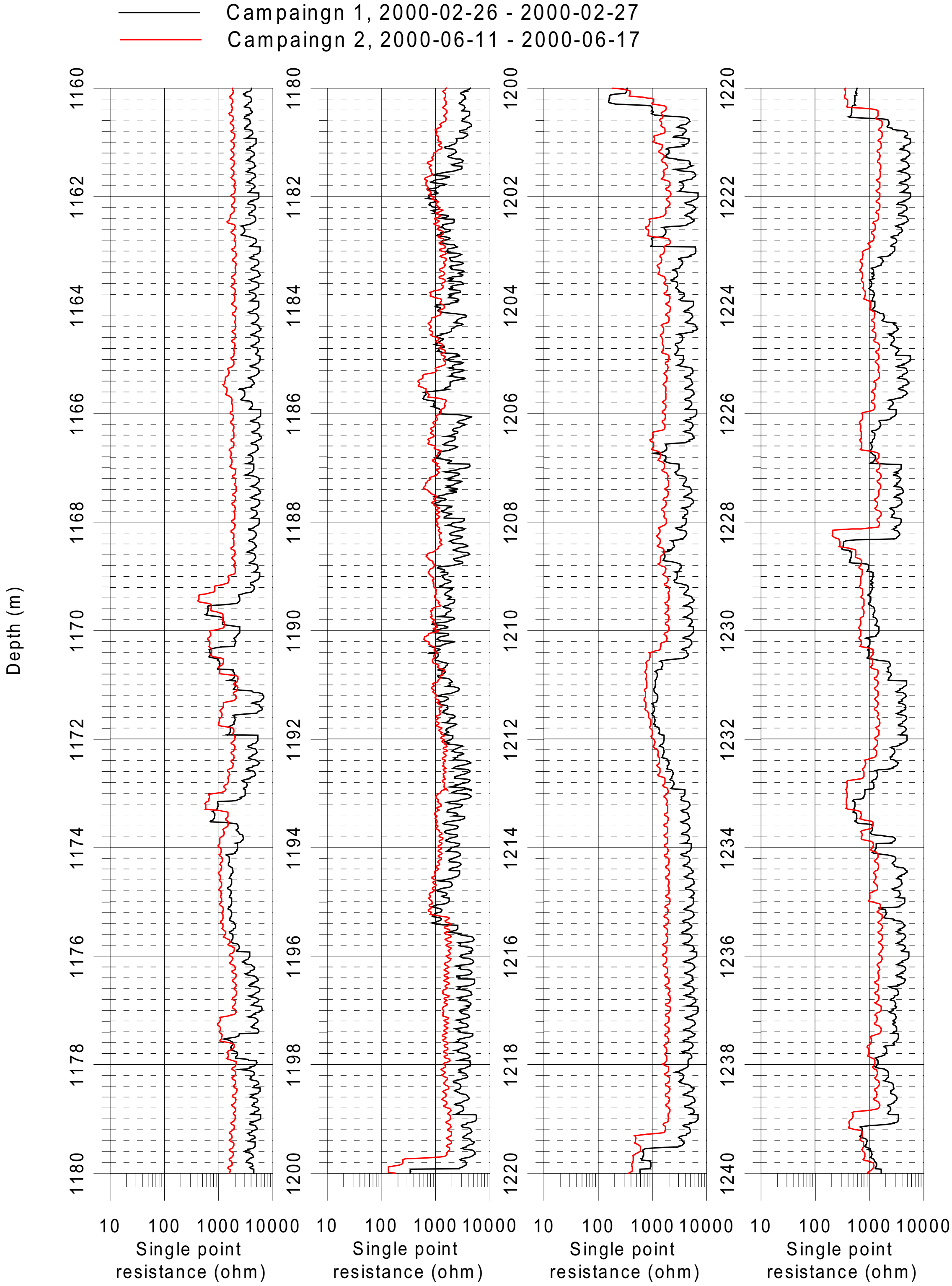

Laxemar, borehole KLX02
Single point resistance during detailed flow logging

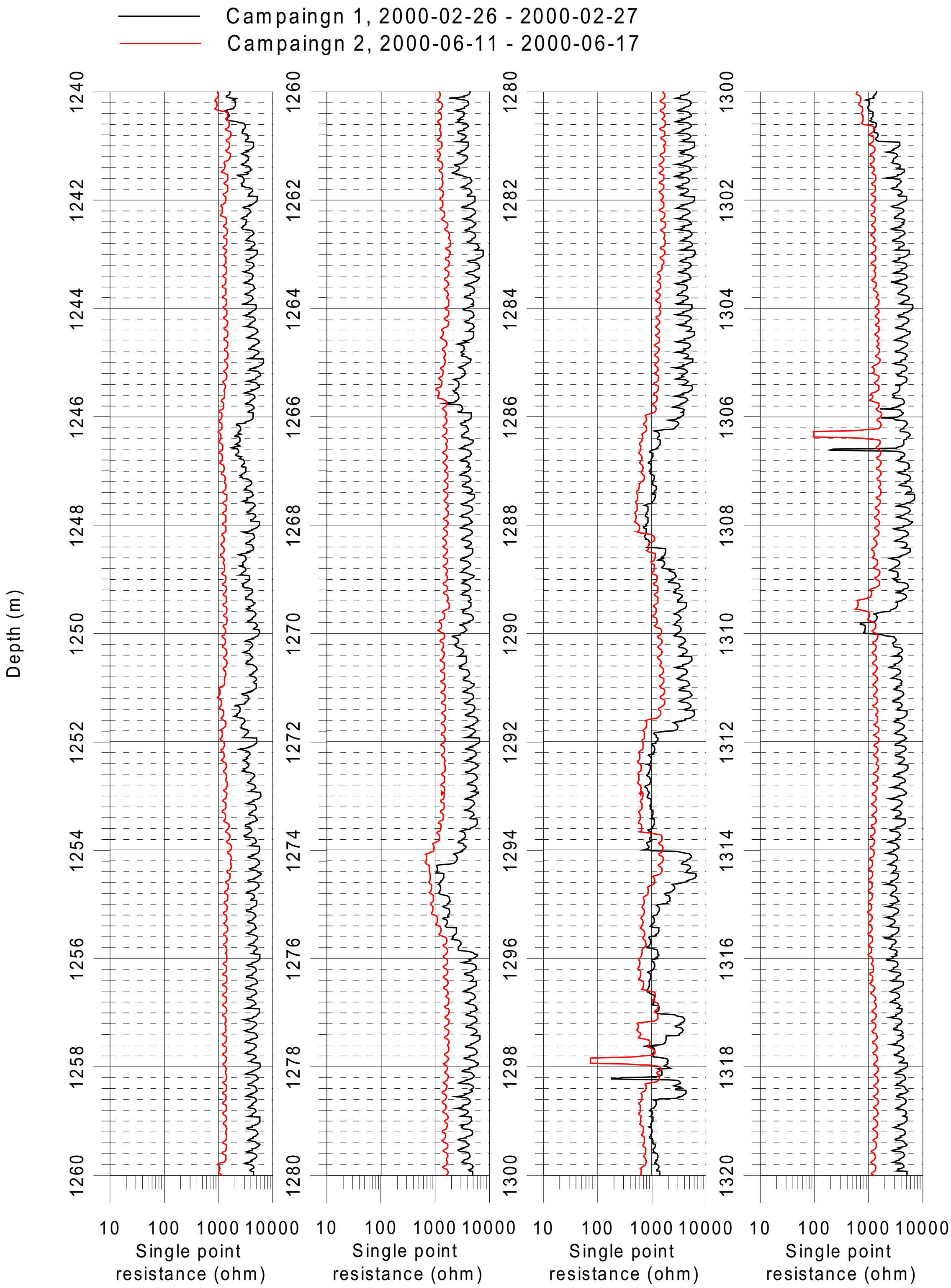

Laxemar, borehole KLX02
Single point resistance during detailed flow logging

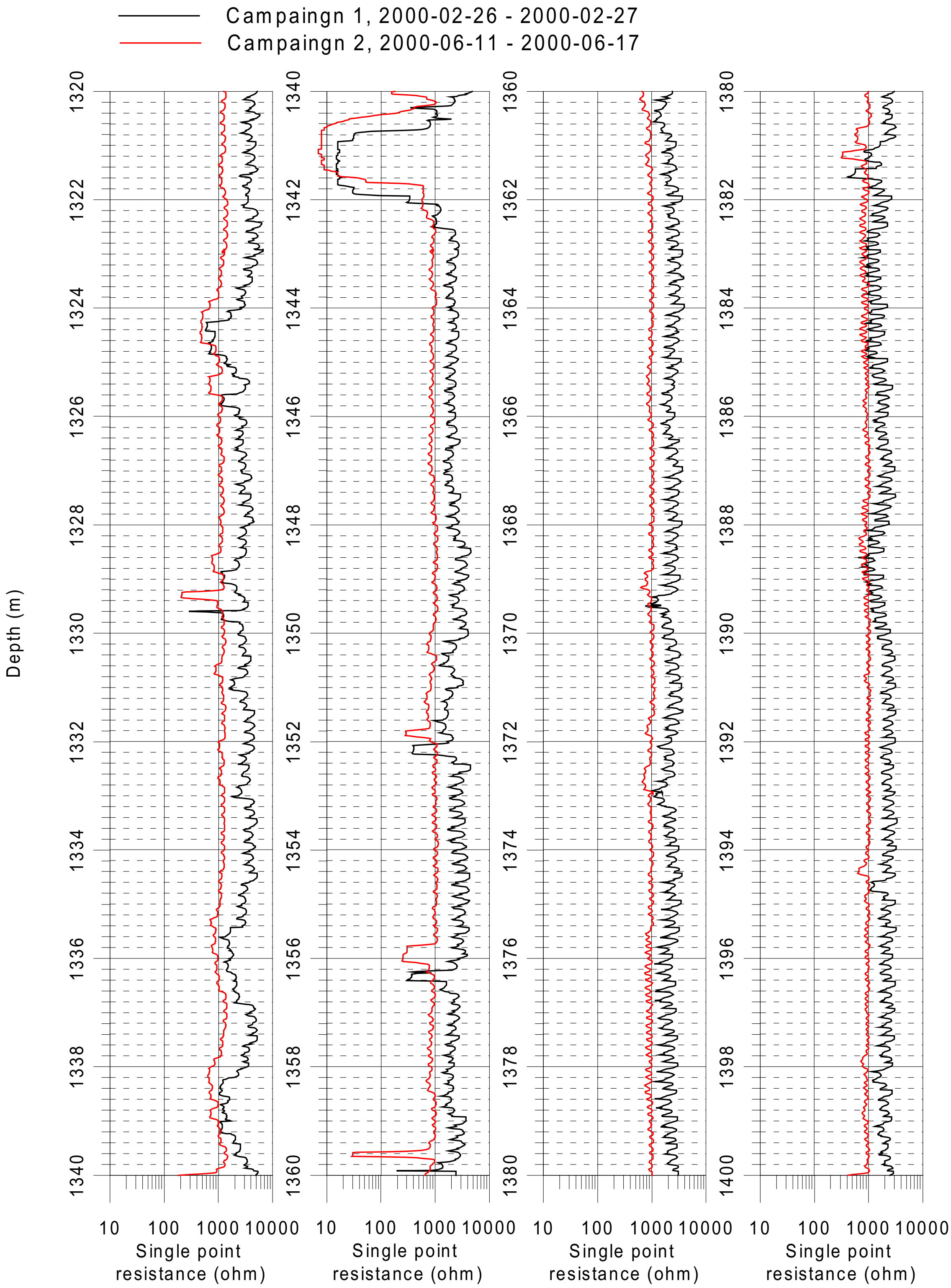

Laxemar, borehole KLX02
Single point resistance logs

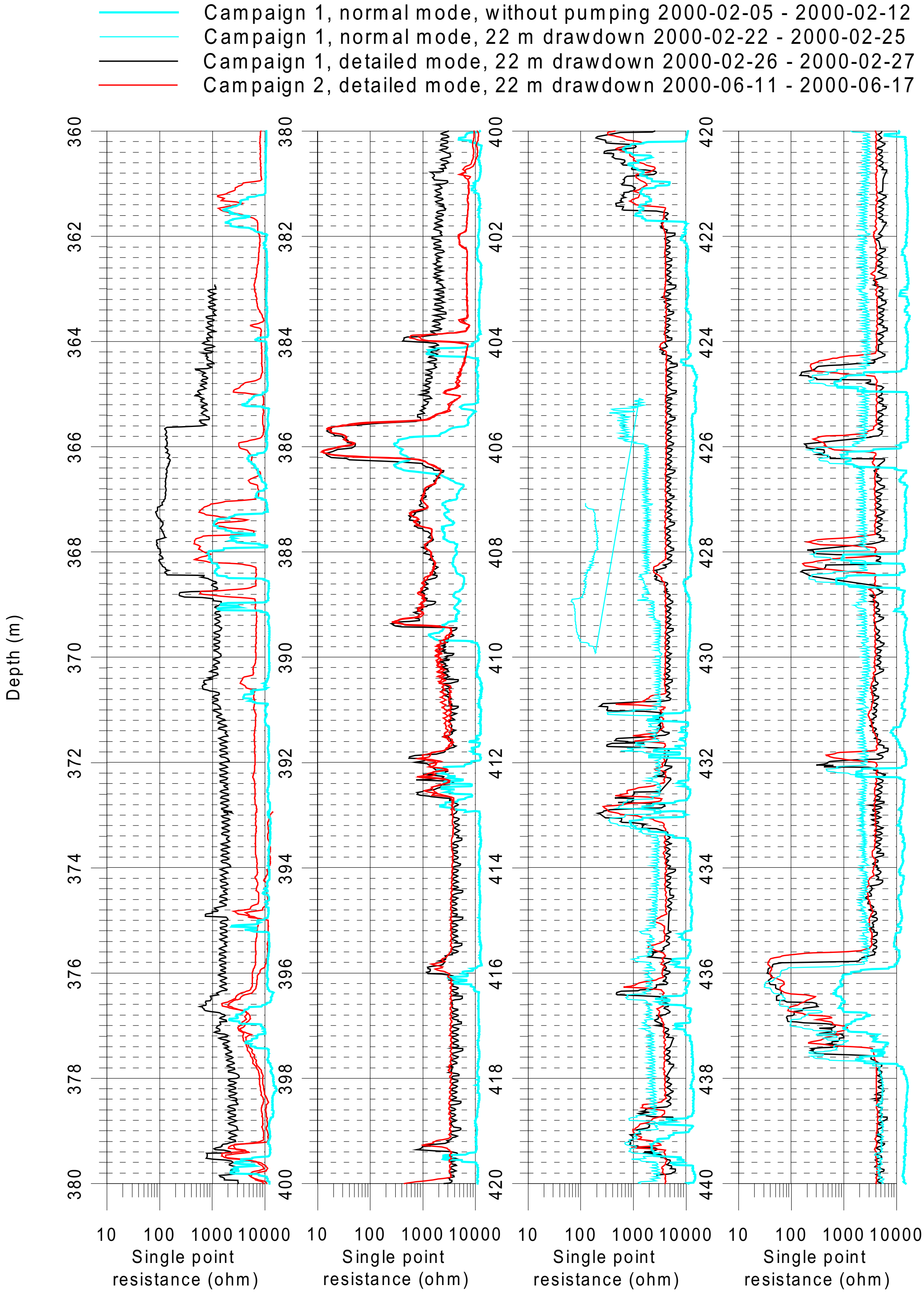

Laxemar, borehole KLX02
Single point resistance logs

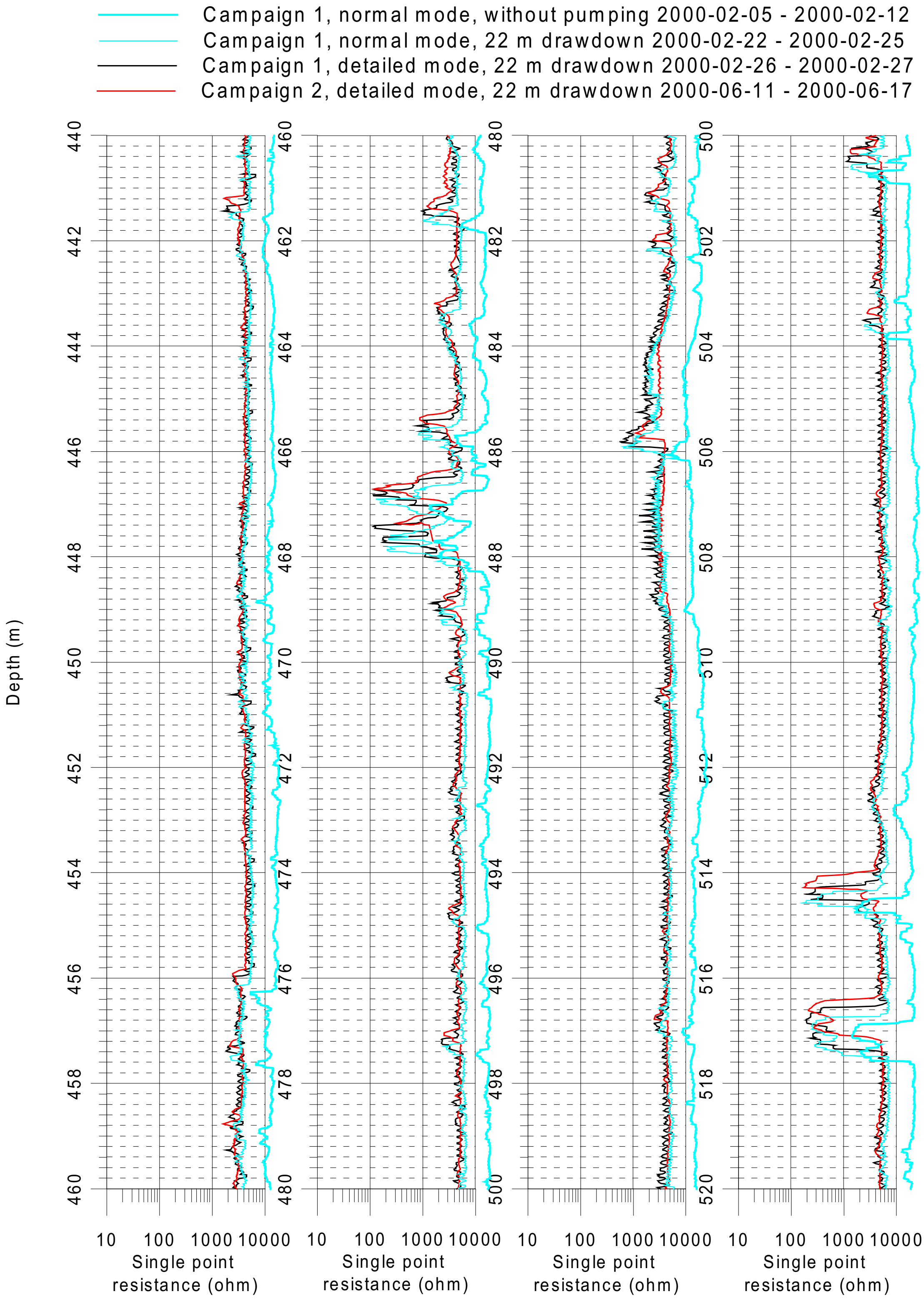

Laxemar, borehole KLX02
Single point resistance logs

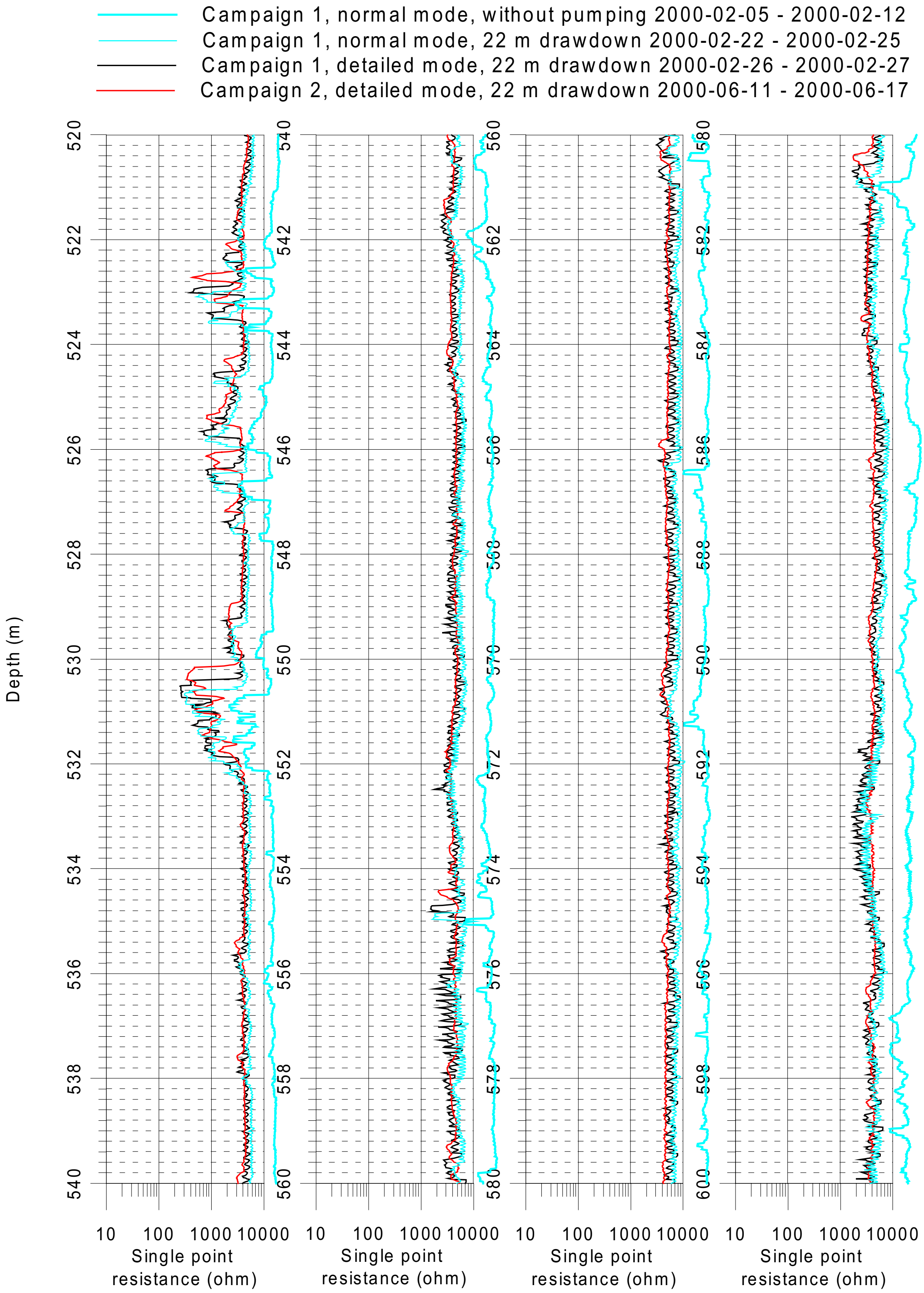

Laxemar, borehole KLX02
Single point resistance logs

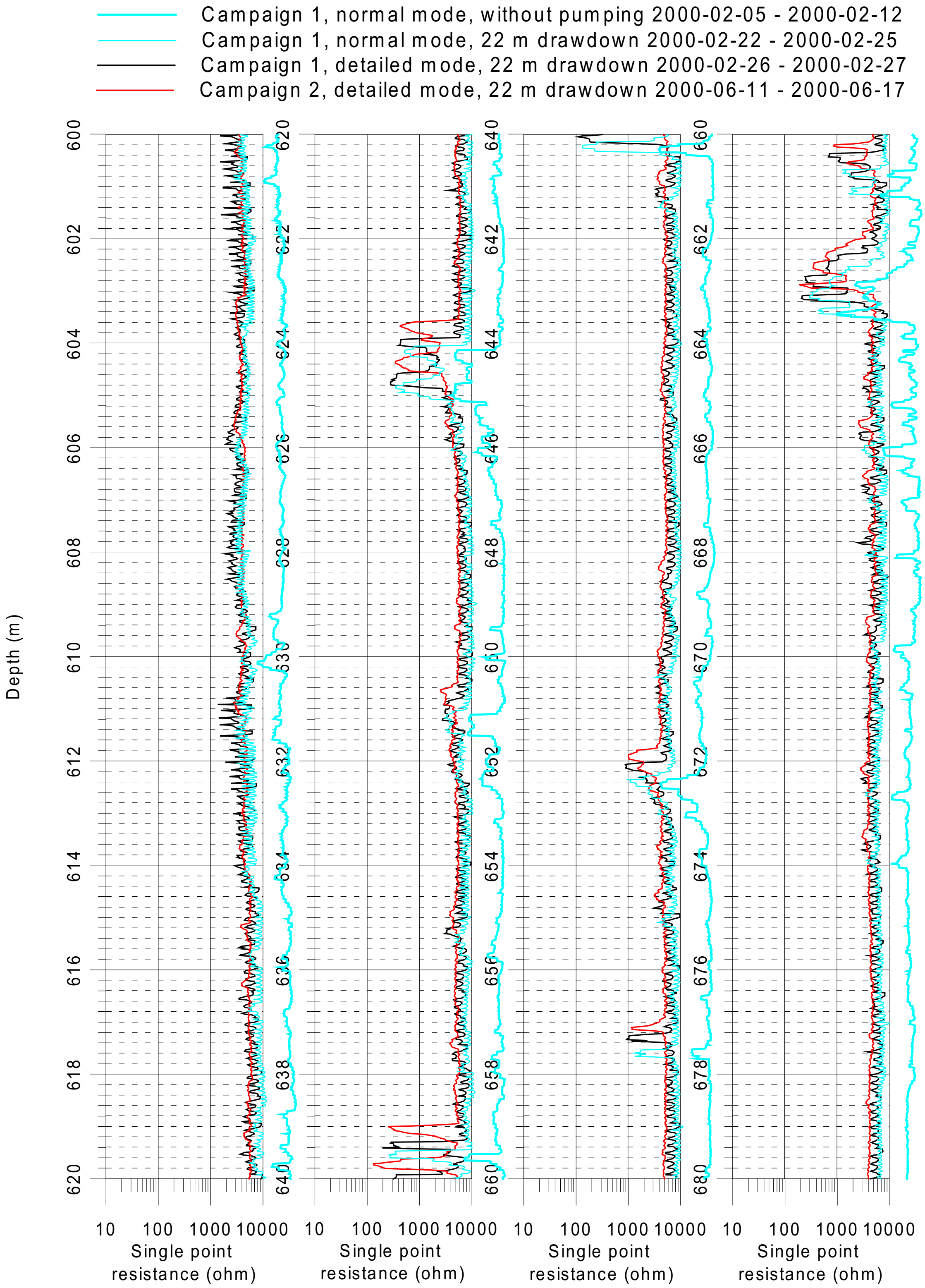

Laxemar, borehole KLX02
Single point resistance logs

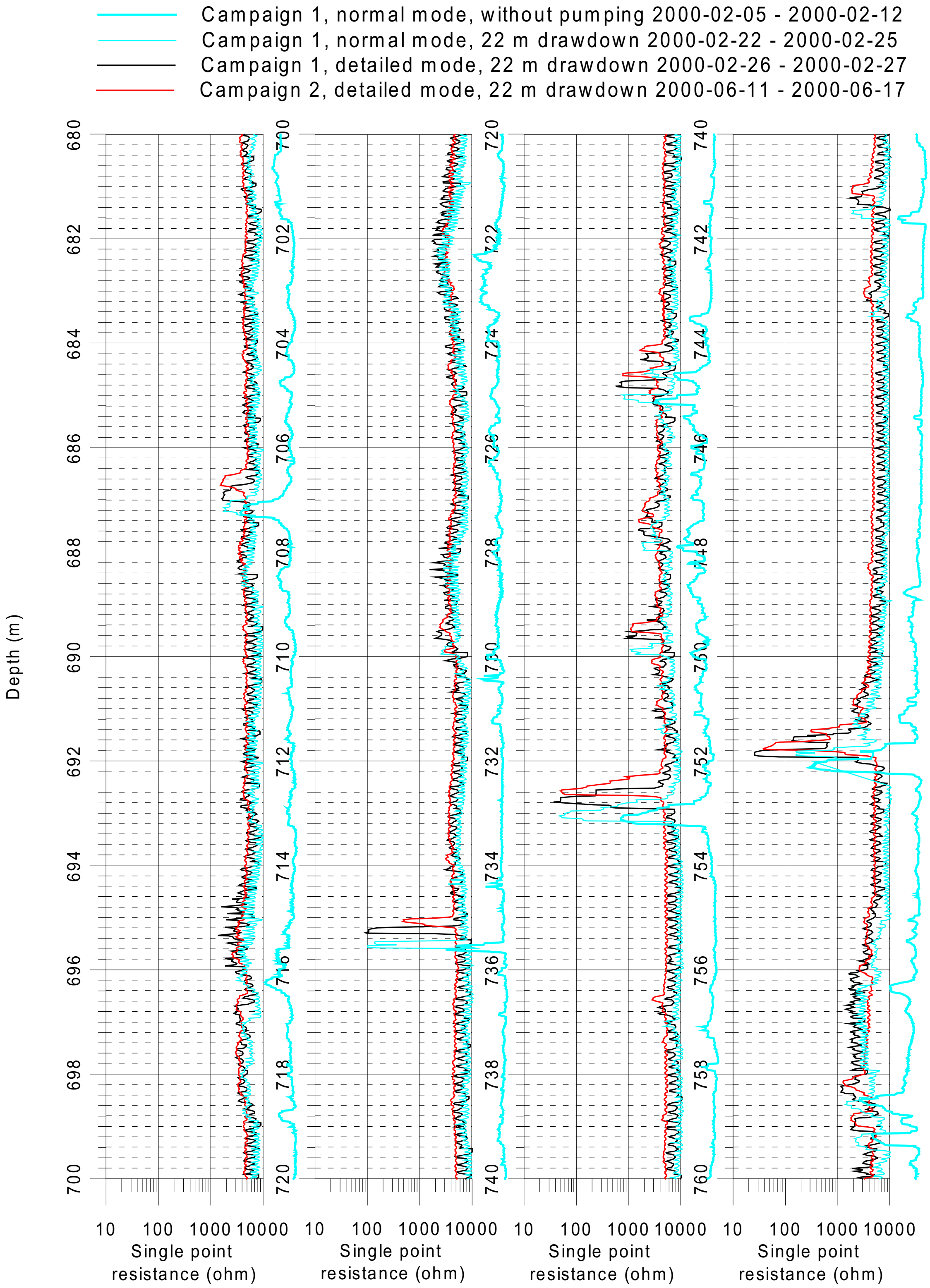

Laxemar, borehole KLX02
Single point resistance logs

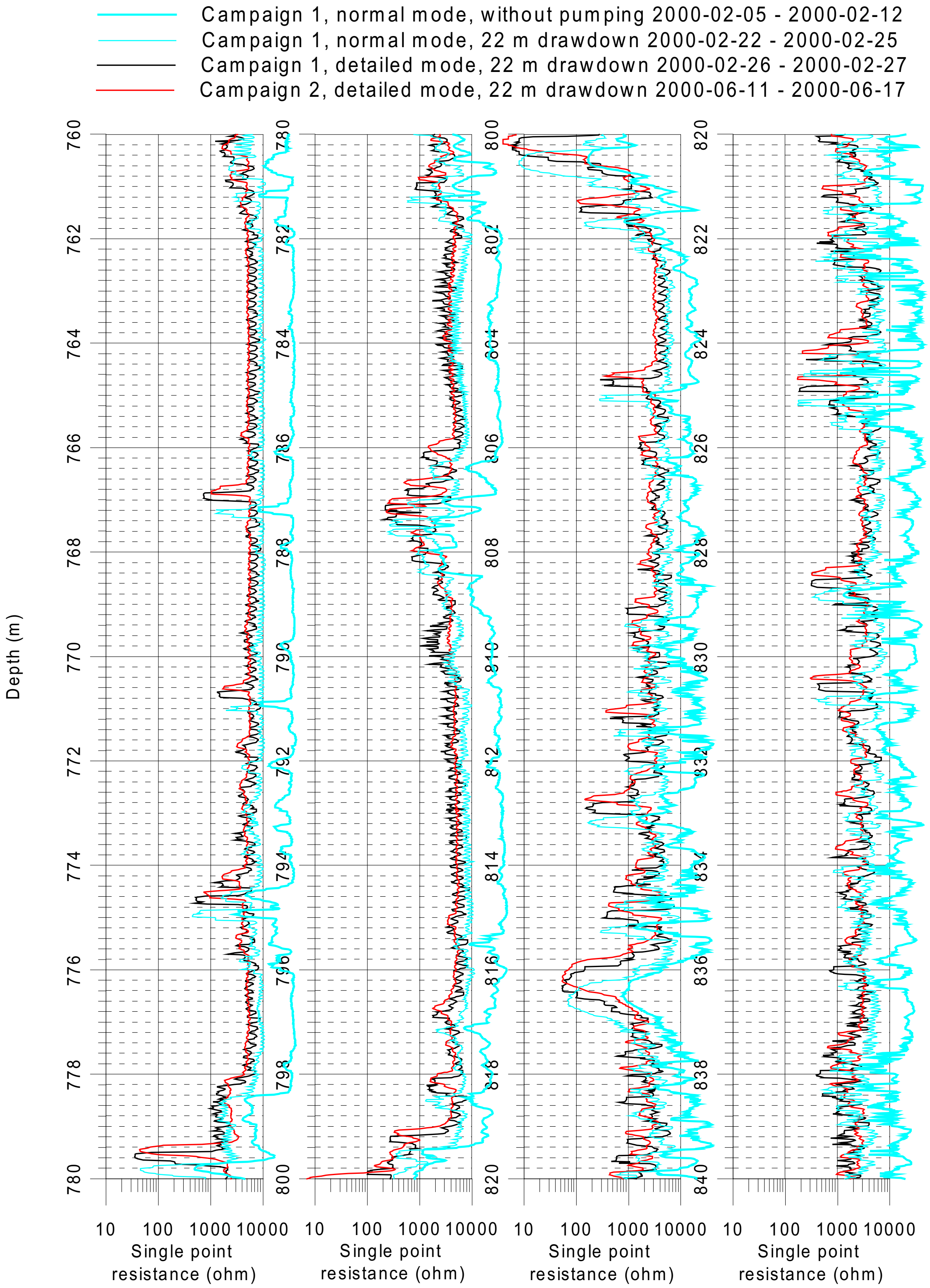

Laxemar, borehole KLX02
Single point resistance logs

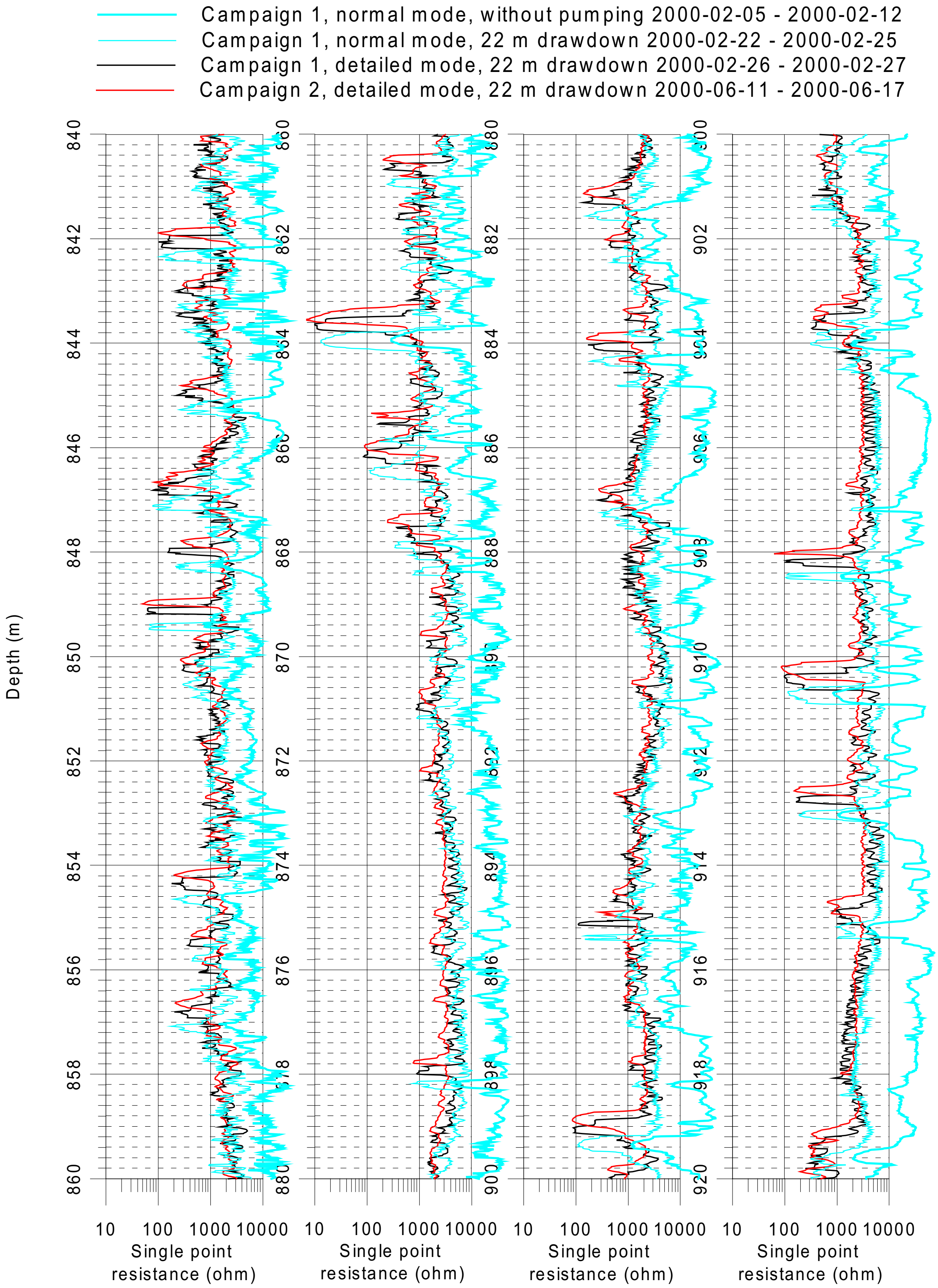

Laxemar, borehole KLX02
Single point resistance logs

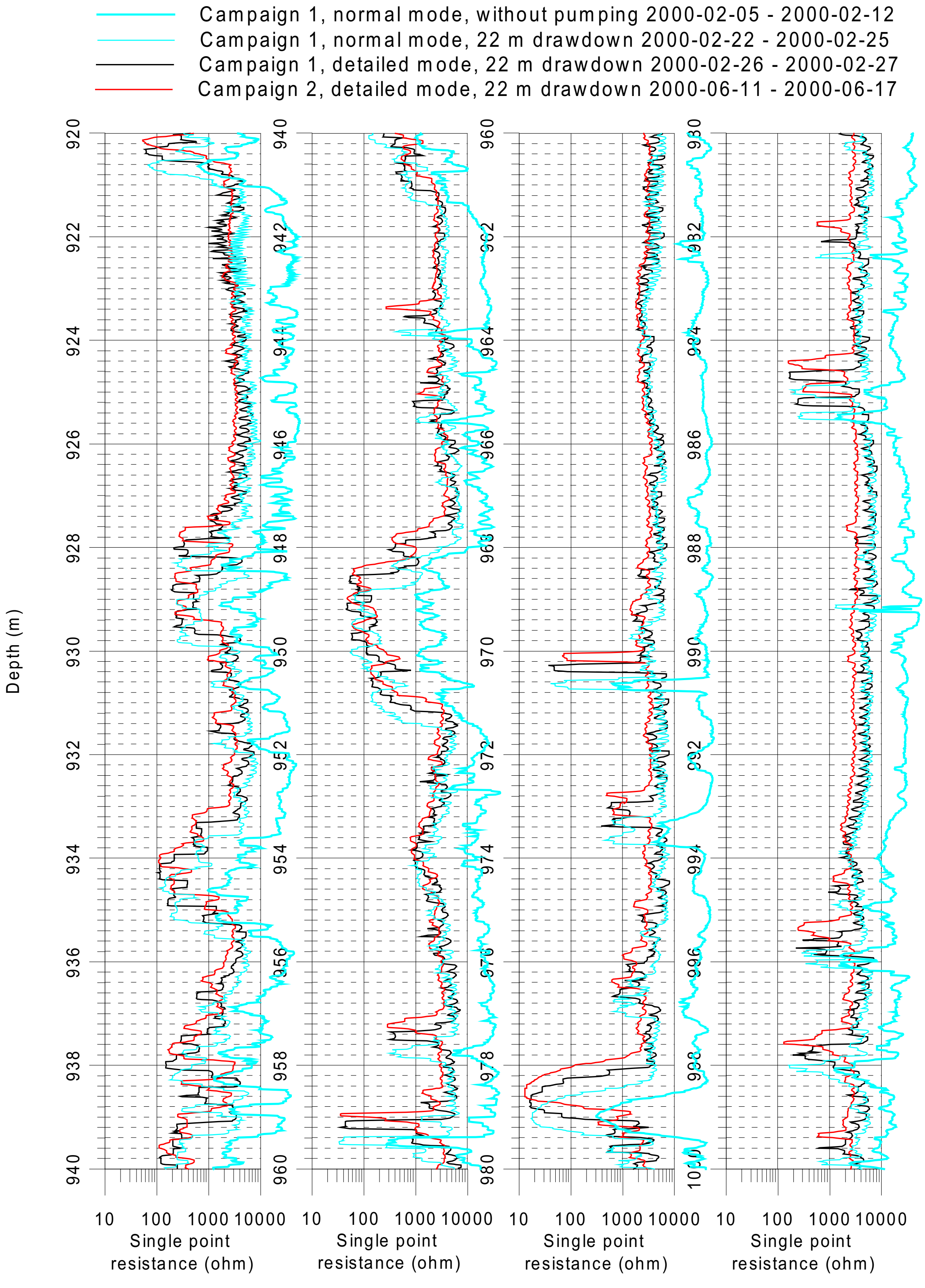

Laxemar, borehole KLX02
Single point resistance logs

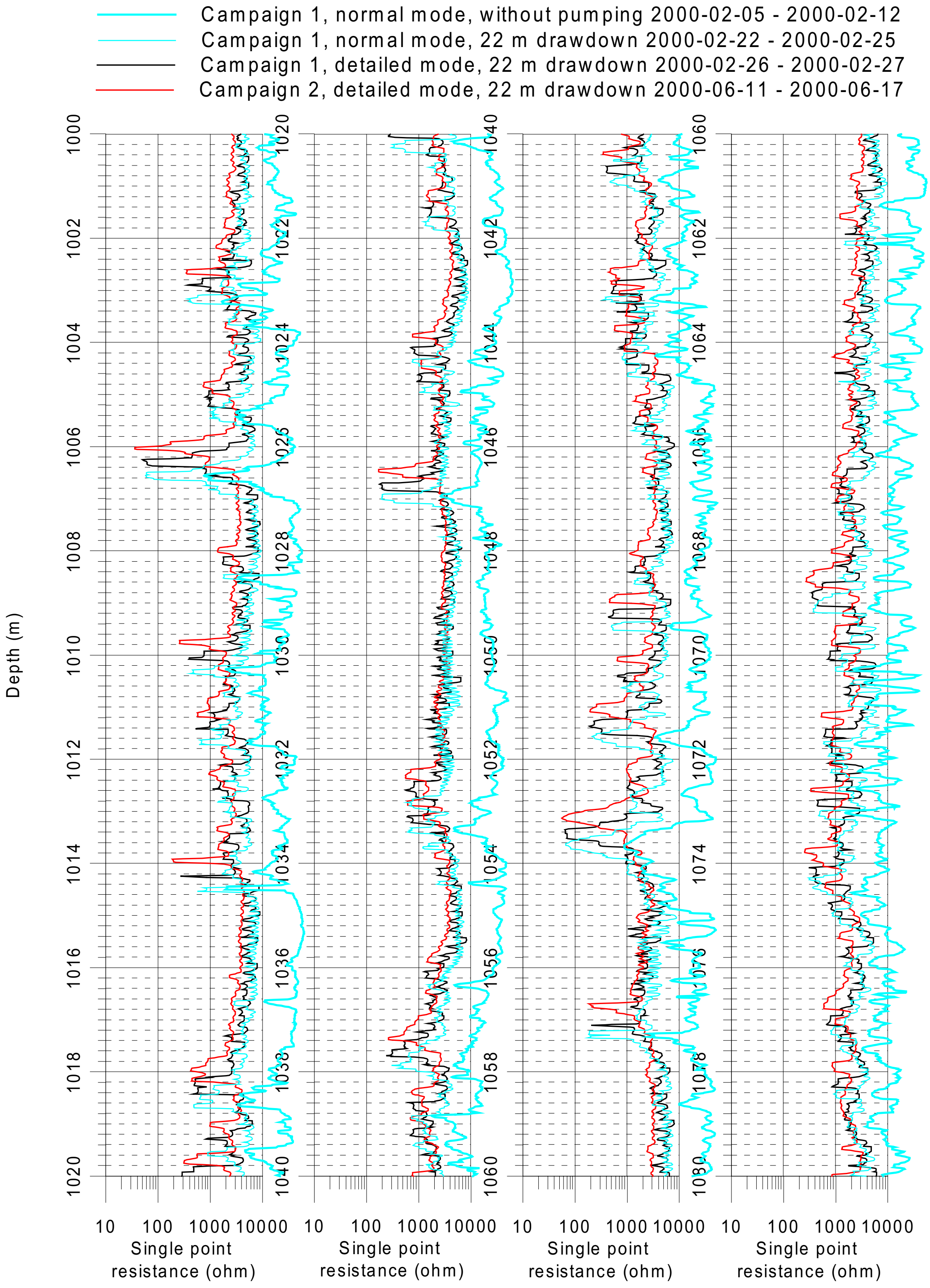

Laxemar, borehole KLX02
Single point resistance logs

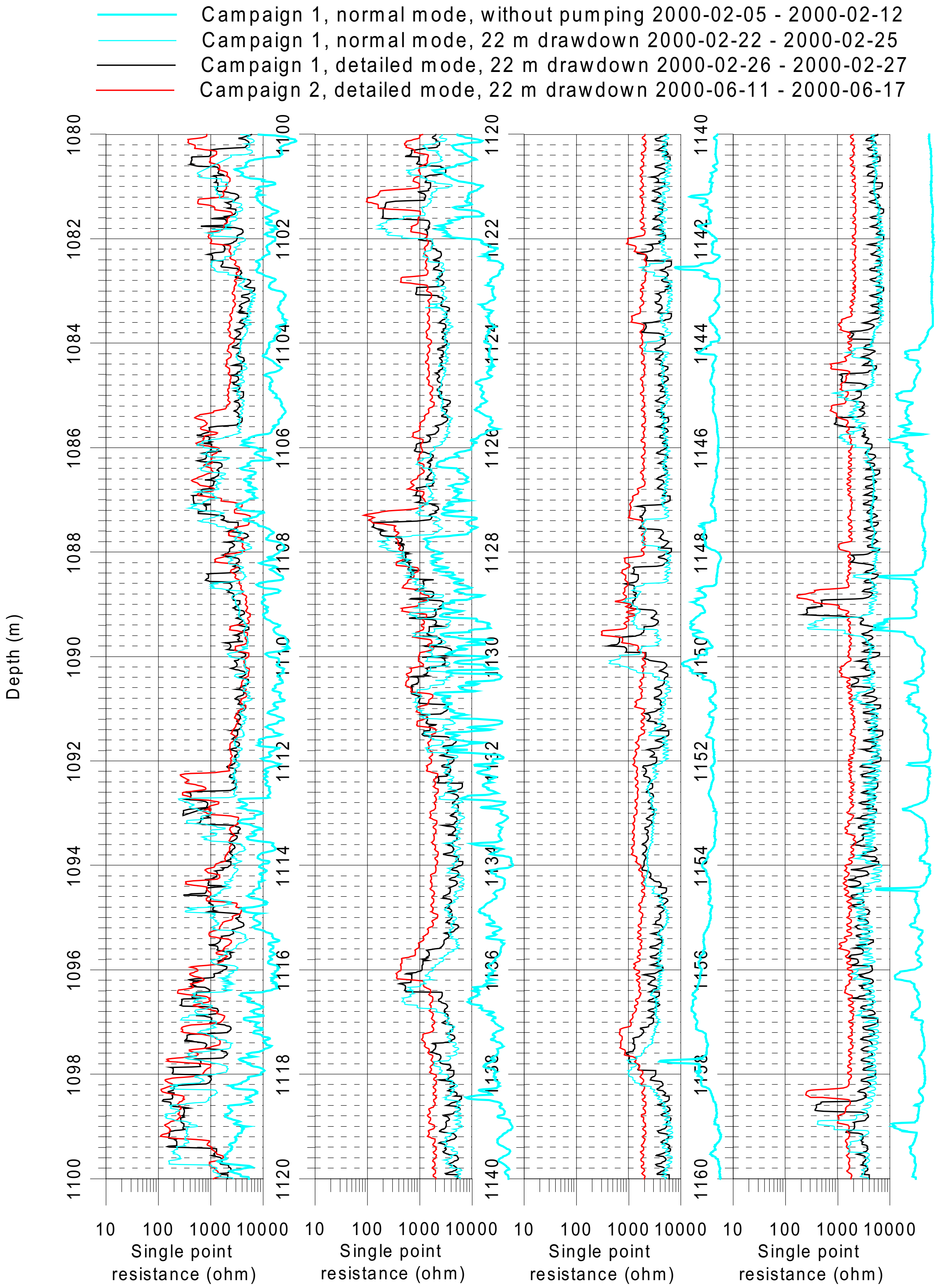

Laxemar, borehole KLX02
Single point resistance logs

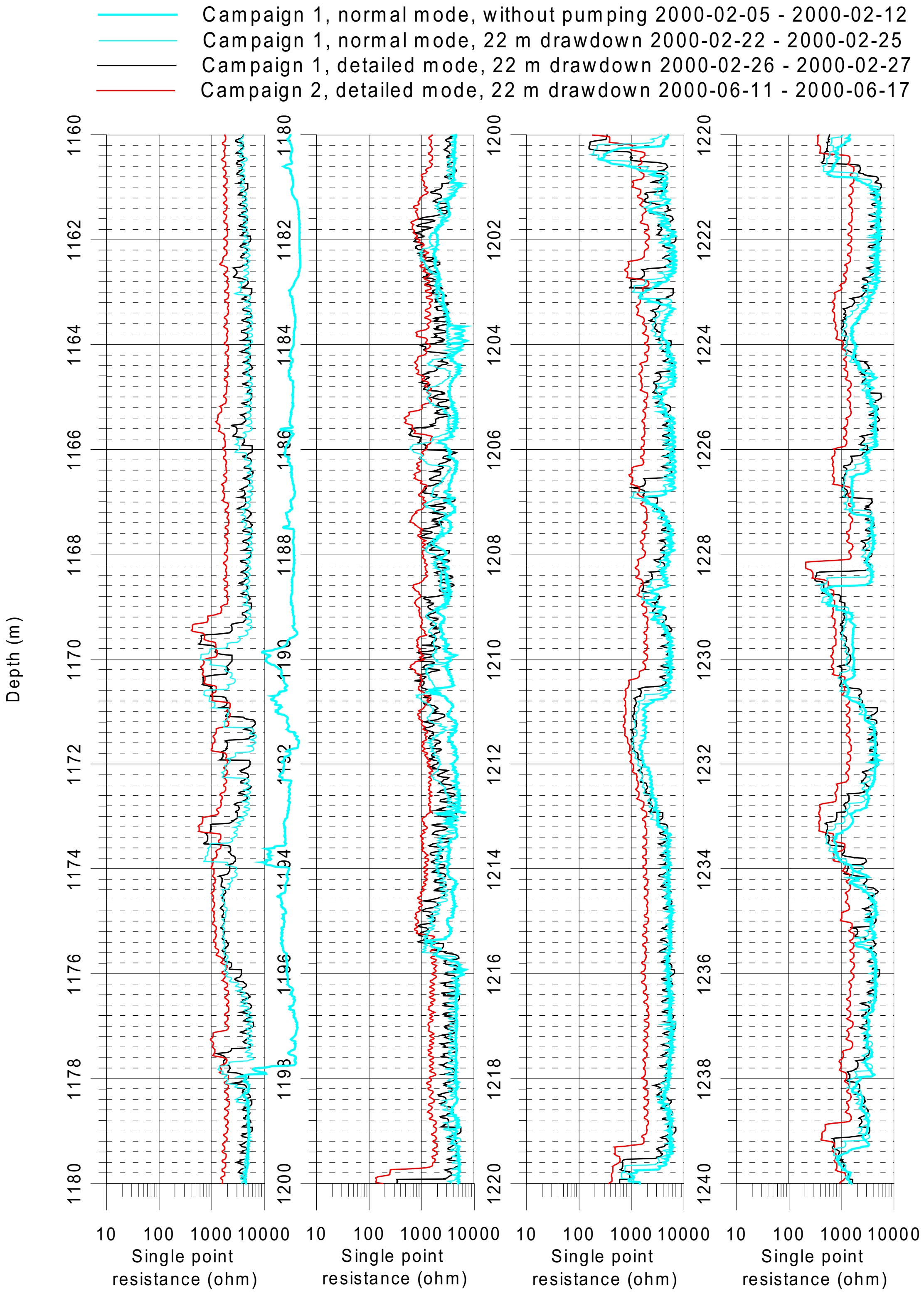

Laxemar, borehole KLX02
Single point resistance logs

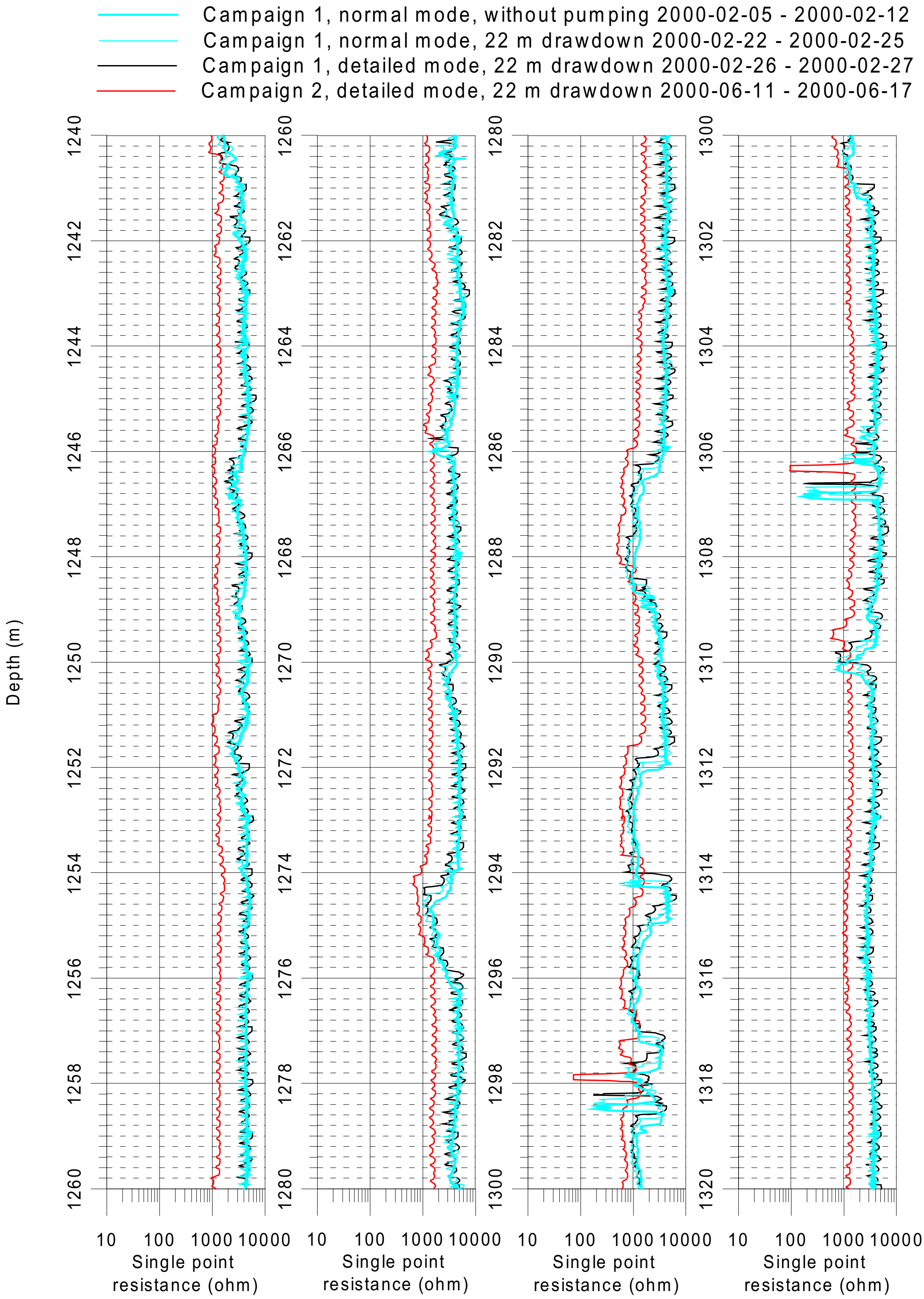

Laxemar, borehole KLX02
Single point resistance logs